2018

Spatial learning and memory in brain-injured and non-injured mice: investigating the roles of diacylglycerol lipase-α and -β.

Lesley D. Schurman
Virginia Commonwealth University

Spatial learning and memory in brain-injured and non-injured mice:

investigating the roles of diacylglycerol lipase-α and -β.

A dissertation submitted in partial fulfillment of the requirements for the degree of

Doctor of Philosophy at Virginia Commonwealth University

by

Lesley D. Schurman

Bachelor of Science, University of Guelph – Ontario, 2012

Master of Science, University of Guelph – Ontario, 2013

Advisor: Aron H. Lichtman, PhD

Professor of Pharmacology and Toxicology

Virginia Commonwealth University

Virginia Commonwealth University

Richmond, VA

December, 2018

Acknowledgements

I am profoundly grateful for every moment of the last 5+ years. Words will be entirely insufficient to explain the depth of the importance those with whom I have walked this path hold in my heart, but what follows will be my clumsy, earnest, unabashed attempt.

First and foremost I am forever changed because of the years of working with Dr. Aron Lichtman. You are not only an inspiring scientist, but a man of genuine character. My progress as a scientist is largely because of you. You have challenged my thinking, encouraged my ideas, and provided opportunities (through conferences, writing, collaborations etc. etc.) that have always been a crucible for my growth. Your ability to adapt your mentoring style to my unique needs and personality are not only impressive, but endlessly appreciated. You have taught me how to disagree well (and I enjoy few things more than talking with you about science and everything in between) and I have learned new things about myself simply because of who you are. I shall likely have to stop calling you *Boss* soon; but not, just, yet. Scienc-ing will not be the same without you.

To previous mentors; I would not be where I am today if it were not for two people who have, from the moment they met me, unreservedly believed in me, supported and encouraged me. That is Dr. Linda Parker, with whom I completed my Undergraduate thesis and Master thesis work; and Craig O'Brien, my brother. Linda you have my continuing gratitude for the foundation in, and love of, science you fostered in me. It is not an exaggeration to say that meeting and working with you forever changed the trajectory of my life. Craig, I have always brought my struggles and triumphs to you because you always walk me through them with grace and love. You are my guardian angel, my inspiration, and my soft place to land. And I love you. You are THE BEST big brother.

To my family; though some of you are far away, I carry you with me always. Mum, you consistently show up for me, every week on our Sunday chats and visiting me in every place I have ever lived. I try to remember your example and pass it along to others in little ways whenever I can. Dad your tenacity, work ethic, and your love of joyfulness is an inspiration I try to emulate! I know you are always there if I need anything. To my sister Marissa, I miss you every day! I'm so grateful for your encouragement. To my husband Brook, I am so grateful for your unwavering support during my PhD training. Meeting you has challenged the way I look at many things, and has brought me closer to the God of my understanding. I love you, and I am so grateful to have walked this path with you.

To my committee members; Dr. Linda Phillips, Dr. Steve Negus, Dr. Laura Sim-Selley, and Dr. Joseph Porter. I have learned so much from each of you. You all provided such valuable input to my dissertation research and my progress as a scientist. Particularly, to Dr. Phillips, thank you for welcoming me into your lab as if I were one of your own students, I have enjoyed immensely all my time working with you and all your lab group! Also, to Dr. Negus, thank your for acting almost as a second mentor. I have valued immensely our frequent one on one discussions, you are a voice of reason and wisdom which I greatly respect and admire.

To colleagues; Dr. Thomas Reeves your support as a collaborator, particularly opening up the resources of your lab group to me, has been a source of gratitude and joy these years. I

have enjoyed immensely working with you, and value and respect all your feedback. I also want to convey my deep gratitude to Terry Smith. You have the ability to make any task fun! You are diligent, and detailed, with a wicked sense of humor that I particularly appreciate! You have always made time for me whenever I need help. You are a genuinely wonderful woman and it has been my great joy and honor working with you! Thank you to all the Lichtman and Scholsburg lab members during this time: Dr. Laura Wise, Brittany Mason, Dr. Travis Grimm, Mohammed Mustafa, Dr. Allen Owens, Dr. Jenny Wilkerson, Dr. Giulia Donvito, Zach Curry, Julien Dodu, Lauren Moncayo, Moriah Carper, Kennedy Goldsborough, Roz Goodson, and Erica Golden. You have all, in different ways, contributed to my growth either scientifically or personally, or both. I am grateful to have been part of a remarkable department here at VCU, I want to particularly thank Pharmacology and Toxicology Department Chair Dr. William Dewey, and faculty Dr. Jennifer Wolstenholme, Dr. Jill Bettinger, Dr. Joel Scholsburg, and Dr. Matthew Banks; who have freely given mentoring support/advice/time.

To my friends; you are my chosen family. To Christine, my sister and my soul mate. Life is Technicolor with you in it. Knowing you is a highlight of my life, let alone my PhD! To Jen, my old friend, you are wise as you are strong. Your hugs are the best in Maryland, and your couch has always felt like home away from home to me. Cathy, my oldest friend! I spend years looking forward to seeing you next… you are always in my heart and the voice in the back of my head, cheering me on! To the friends I have met here at VCU; Amy, Jacy, Giulia, and Clare. You are my Band of Sisters. You who “know”. You are each a special kind of woman, but also each of you knows and practices what it means to lift each other up whilst walking in Theodore’s arena. You women who dare greatly, my heart belongs to you!

To my Friends of Lois; I have no understanding of how anyone completes a PhD without you! Week after week you listen. You share your experience, strength, and hope. And your wisdom, honesty, and friendships humble me… There are so many too numerous to mention, just a few are; Shirley H., Brooke D., Kara B., Teresa D., Amanda S., Stephanie P., Julie S., Christi M., Scott A., George H., Jannequin B., Kris N., and Dianne B.

To my sweet Hurley, please stop stealing my socks.

“We grow not better or worse as we get old, but more like ourselves”

– Mary Lamberton Becker

Table of Contents

List of Tables

List of Figures

List of Abbreviations

µL = Microliter

2-AG = 2-Arachidonoyl glycerol

2-LG = 2-linoleoyl-glycerol

2-PG, 2-palmitoyl-glycerol

AA = Arachidonic acid

ABHD6 = α/β-hydrolase domain-6

ABHD12 = α/β-hydrolase domain-12

AEA = Anandamide

ANOVA = Analysis of Variance

APP = Amyloid precursor protein

ATM = Atmospheres

ATP = Adenosine triphosphate

BBB = Blood brain barrier

CCI = Controlled cortical impact model of TBI

CDTA = Calcium-dependent transacylase enzyme

CHI = Closed head injury model of TBI

cm = Centimeter

COX-2 = Cyclooxygenase-2

CNS = Central nervous system

cPLA2 = Cytosolic phospholipase A2

DAGL-α = Diacylglycerol lipase-α

DAGL-β = Diacylglycerol lipase-beta

DAPI = 4′,6-Diamidino-2-phenylindole dihydrochloride

eCB = Endocannabinoid

EPSC = Excitatory post-synaptic current

FAAH = Fatty acid amide hydrolase

FPI = Fluid percussion injury model of TBI

GFAP = Glial fibrillary acidic protein

h = Hour

Iba-1 = Ionized calcium-binding adapter molecule 1

IHC = Immunohistochemistry

IP = Intraperitoneal

Kg = Kilogram

LTP = Long term potentiation

MAGL = Monoacylglycerol lipase

Mg = Milligram

MWM = Morris water maze

NArPE = *N*-arachidonoyl phosphatidylethanolamine

NBS = Neurological behavioral score

nM = Nanomolar

NMDA = N-methyl-D-aspartate

NPE = Neurogenic pulmonary oedema

NSS = Neurological severity score

pM = Picomolar

PLA2 = Phospholipase A2 enzyme

PLC = Phospholipase C enzyme

p-tau = Hyperphosphorylated tau

ROS = Reactive oxygen species

SEM = Standard error of the mean

TBI = Traumatic brain injury

TDP-43 = TAR DNA-binding protein

THC = Δ^9-Tetrahydrocannabinol

UCH-L1 = ubiquitin C-terminal hydrolase L1

ABSTRACT

SPATIAL LEARNING AND MEMORY IN BRAIN-INJURED AND NON-INJURED MICE: INVESTIGATING THE ROLES OF DIACYLGLYCEROL LIPASE-α AND -β.

Lesley D. Schurman, Master of Science

A dissertation submitted in partial fulfillment of the requirements for the degree of Doctor of Philosophy at Virginia Commonwealth University

Virginia Commonwealth University, 2018

Advisor: Aron H. Lichtman, PhD Professor of Pharmacology and Toxicology

A growing body of evidence implicates the importance of the endogenous cannabinoid 2-arachidonyl glycerol (2-AG) in memory regulation. The biosynthesis of 2-AG occurs primarily through the diacylglycerol lipases (DAGL-α and -β), with 2-AG serving as a bioactive lipid to both activate cannabinoid receptors and as a rate limiting precursor for the production of arachidonic acid and subsequent pro-inflammatory mediators. Gene deletion of DAGL-α shows decrements in synaptic plasticity and hippocampal neurogenesis suggesting this biosynthetic enzyme may be important for processes of normal spatial memory. Additionally, 2-AG is elevated in response to pathogenic events such as traumatic brain injury (TBI), suggesting its regulatory role may extend to conditions of neuropathology. As such, this dissertation investigates the *in vivo* role of DAGL-α and -β to regulate spatial learning and memory in the healthy brain and following neuropathology (TBI).

The first part of this dissertation developed a mouse model of learning and memory impairment following TBI, using hippocampal-dependent tasks of the Morris water maze (MWM). We found modest, but distinct differences in MWM performance between left and right unilateral TBI despite similar motor deficits, histological damage, and glial reactivity. These findings suggest that laterality in mouse MWM deficit might be an important consideration when modeling TBI-induced functional consequences. The second part of this dissertation work evaluated DAGL-β as a target to protect against TBI-induced learning and memory deficit given its selective expression on microglia and the role of 2-AG as a precursor for eicosanoid production. The gene deletion of DAGL-β did not protect against TBI-induced MWM or motor deficits, but unexpectedly produced a survival protective phenotype. These findings suggest that while DAGL-β does not contribute to injury-induced memory deficit, it may contribute to TBI-induced mortality. The third and final set of experiments investigated the role of DAGL-α in mouse spatial learning and memory under physiological conditions (given the predominantly neuronal expression of DAGL-α). Complementary pharmacological and genetic manipulations produced task specific impaired MWM performance, as well as impaired long-term potentiation and alterations to endocannabinoid lipid levels. These results suggest that DAGL-α may play a selective role in the integration of new spatial information in the normal mouse brain.

Overall, these data point to DAGL-α, but not DAGL-β, as an important contributor to hippocampal-dependent learning and memory. In contrast, DAGL-β may contribute to TBI-induced mortality.

Chapter I

General Introduction

How our brains acquire, store, and later retrieve representations of our experience influence not only our behavior and basic survival, but fundamentally contribute to our sense of who we are. Our ability to learn impacts our perceived usefulness and in part enables us to imagine our future. Our ability to remember connects us to our past. The following body of work examines critical components of a neuromodulatory system, the endocannabinoid system; one key feature of which is its action on the neurobiology of learning and memory. The examination of two endocannabinoid biosynthetic enzymes was conducted in the context of memory pathology produced as a result of traumatic brain injury in a mouse model organism.

A historical perspective of memory pathology. At the end of the nineteenth century, French psychologist Théodule Ribot studied clinical cases of brain pathology in an attempt to understand the normal organization of memory. His classic work *Diseases of Memory* (Ribot, 1882) proposed that the dissolution of memory which accompanies pathology follows an orderly temporal progression. Ribot proposed that older memories are most resistant to dissolution, followed by habits and emotional memories, with more recent memories being the first to be lost (now referred to as Ribot's Law). His insights, though now may seem obvious, were ground breaking for their implications toward the existence of different categories of memory, and in turn the possibility that they be

supported by different neural systems. He described various clinical cases of what might now be referred to as traumatic brain injuries (the most common causes of which in the 1880s seemed to be gentlemen being thrown out of carriages and thrown from horses) with descriptions of subsequent memory impairments mirroring deficits commonly familiar in the current century. A detailed description of the learning and memory deficits arising from traumatic brain injuries are presently described in detail in the Chapter Introduction for Chapter 2 (pages 39-40).

The endocannabinoid system as a memory modulator. Our basic understanding of the endocannabinoid system (as well as its name) arose from research investigating the pharmacological properties of the *cannabis* plant. *Cannabis* use has been recorded in China since 2727 BCE as medicinal (Booth, 2003), though *cannabis* has been widely used for centuries as a psychoactive drug. Most notably, Δ^9-tetrahydrocannabinol (Δ^9-THC, the major psychoactive component of the cannabis plant) shares a pharmacophore with the primary endocannabinoid ligands; anandamide (AEA) and 2-arachidonyl glycerol (2-AG, the most abundant endocannabinoid ligand) in that they bind and activate cannabinoid receptors. While a detailed description of the endocannabinoid system, its components and functional characteristics, is contained in the subsequent Chapter 1 “Endocannabinoids: A Promising Impact for Traumatic Brain Injury” pages 5-9, the endocannabinoid system can be most succinctly understood as a neuromodulator, a braking system used to restore physiology to states of homeostasis. The evidence which links the endocannabinoid system to the regulation of memory comes primarily from the ability of cannabinoid receptors to inhibit synaptic transmission (Kano *et al*, 2009) through the inhibition of neurotransmitter release. The understanding

specifically of 2-AG as a biologically active lipid in its own right, is however only part of a complicated memory story in which 2-AG also participates as an intermediate in a pathway which ultimately releases inflammatory mediators (Nomura *et al*, 2011). States of inflammation being intimately linked to impairments of learning and memory, 2-AG and its biosynthetic pathways are therefore the primary focus of the present work.

Summary. In the present dissertation, the enzymes responsible for 2-AG biosynthesis, the diacylglycerol lipases (DAGLs) are explored as targets to further understand the role this endocannabinoid system plays in learning and memory regulation. While Chapter 2 presents work completed to establish a mouse model of brain injury induced deficits, Chapter 3 explores considerations of 2-AG biosynthesis disruption (DAGL-β disruption) on mouse memory pathology as a result of traumatic brain injury. Finally, Chapter 4 examines 2-AG biosynthesis disruption (DAGL-α disruption) on mouse memory under conditions of normal physiology. First, a review of the present literature, concerning manipulations of the endocannabinoid system following traumatic brain injury, is evaluated.

Endocannabinoids: A Promising Impact for Traumatic Brain Injury

(Front Pharmacol 8:69, 2017)

Introduction

Traumatic brain injury (TBI) accounts for approximately 10 million deaths and/or hospitalizations annually in the world, and approximately 1.5 million annual emergency room visits and hospitalizations in the US (Langlois et al., 2006). Young men are consistently over-represented as being at greatest risk for TBI (Langlois et al., 2006). While half of all traumatic deaths in the USA are due to brain injury (Mayer et al., 2010), the majority of head injuries are considered mild and often never receive medical treatment (Corrigan et al., 2010). Survivors of TBI are at risk for lowered life expectancy, dying at a 3.2 times more rapid rate than the general population (Baguley *et al*, 2012). Survivors also face long term physical, cognitive, and psychological disorders that greatly diminish quality of life. Even so-called mild TBI without notable cell death may lead to enduring cognitive deficits (Niogi *et al*, 2008; Rubovitch *et al*, 2011). A 2007 study estimated that TBI results in $330,827 of average lifetime costs associated with disability and lost productivity, and greatly outweighs the $65,504 estimated costs for initial medical care and rehabilitation (Faul *et al*, 2007b), demonstrating both the long term financial and human toll of TBI.

The development of management protocols in major trauma centers (Brain Trauma Foundation, 2007) has improved mortality and functional outcomes (Stein *et al*, 2010). Monitoring of intracranial pressure is now standard practice (Bratton *et al*, 2007), and advanced MRI technologies help define the extent of brain injury in some cases

(Shah *et al*, 2012). Current treatment of major TBI is primarily managed through surgical intervention by decompressive craniotomy (Bullock et al., 2006) which involves the removal of skull segments to reduce intracranial pressure. Delayed decompressive craniotomy is also increasingly used for intractable intracranial hypertension (Sahuquillo and Arikan, 2006). The craniotomy procedure is associated with considerable complications, such as hematoma, subdural hygroma, and hydrocephalus (Stiver, 2009). At present, the pathology associated with TBI remains refractive to currently available pharmacotherapies (Meyer *et al*, 2010) and as such represents an area of great research interest and in need of new potential targets. Effective TBI drug therapies have yet to be proven, despite promising preclinical data (Lu *et al*, 2007; Mbye *et al*, 2009; Sen and Gulati, 2010) plagued by translational problems once reaching clinical trials (Mazzeo *et al*, 2009; Tapia-Perez *et al*, 2008; Temkin *et al*, 2007).

The many biochemical events that occur in the hours and months following TBI have yielded preclinical studies directed toward a single injury mechanism. However, an underlying premise of the present review is an important need to address the multiple targets associated with secondary injury cascades following TBI. A growing body of published scientific research indicates that the endogenous cannabinoid (endocannabinoid; eCB) system possesses several targets uniquely positioned to modulate several key secondary events associated with TBI. Here we review the preclinical work examining the roles that the different components of the eCB system play in ameliorating pathologies associated with TBI.

The Endocannabinoid (eCB) System

Originally, “Cannabinoid” was the collective name assigned to the set of naturally occurring aromatic hydrocarbon compounds in the *Cannabis sativa* plant (Mechoulam and Goani, 1967). Cannabinoid now more generally refers to a much more broad set of chemicals of diverse structure whose pharmacological actions or structure closely mimic that of plant-derived cannabinoids. Three predominant categories are currently in use; plant-derived phytocannabinoids (reviewed in Gertsch et al., 2010), synthetically produced cannabinoids used as research (Wiley *et al*, 2014) or recreational drugs (Mills et al., 2015), and the endogenous cannabinoids, N-arachidonoylethanolamine (anandamide) (Devane et al., 1992) and 2-arachidonyl glycerol (2-AG) (Mechoulam *et al*, 1995; Sugiura *et al*, 1995).

These three broad categories of cannabinoids generally act through cannabinoid receptors, two types of which have so far been identified, CB_1 (Devane *et al*, 1988) and CB_2 (Munro *et al*, 1993). Both CB_1 and CB_2 receptors are coupled to signaling cascades predominantly through $G_{i/o}$-coupled proteins. CB_1 receptors mediate most of the psychomimetic effects of cannabis, its chief psychoactive constituent Δ^9-tetrahydrocannabinol (THC), and many other CNS active cannabinoids. These receptors are predominantly expressed on pre-synaptic axon terminals (Alger and Kim, 2011), are activated by endogenous cannabinoids that function as retrograde messengers, which are released from post-synaptic cells, and their activation ultimately dampens pre-synaptic neurotransmitter release (Mackie, 2006). Acting as a neuromodulatory network, the outcome of cannabinoid receptor signaling depends on cell type and location. CB_1 receptors are highly expressed on neurons in the central nervous system (CNS) in areas such as cerebral cortex, hippocampus, caudate-

putamen (Herkenham *et al*, 1991). In contrast, CB_2 receptors are predominantly expressed on immune cells, microglia in the CNS, and macrophages, monocytes, CD4+ and CD8+ T cells, and B cells in the periphery (Cabral *et al*, 2008). Additionally, CB_2 receptors are expressed on neurons, but to a much less extent than CB_1 receptors (Atwood and Mackie, 2010). The abundant, yet heterogeneous, distribution of CB_1 and CB_2 receptors throughout the brain and periphery likely accounts for their ability to impact a wide variety of physiological and psychological processes (e.g. memory, anxiety, and pain perception, reviewed in Di Marzo, 2008) many of which are impacted following TBI.

Another unique property of the endocannabinoid (eCB) system is the functional selectivity produced by its endogenous ligands. Traditional neurotransmitter systems elicit differential activation of signaling pathways through activation of receptor subtypes by one neurotransmitter (Siegel, 1999). However, it is the endogenous ligands of eCB receptors which produce such signaling specificity. Although several endogenous cannabinoids have been described (Chu et al., 2003; Heimann et al., 2007; Porter et al., 2002) the two most studied are anandamide (Devane et al., 1992) and 2-AG (Mechoulam *et al*, 1995; Sugiura *et al*, 1995). 2-AG levels are three orders of magnitude higher than those of anandamide in brain (Béquet et al., 2007). Additionally, their receptor affinity (Pertwee and Ross, 2002; Reggio, 2002) and efficacy differ, with 2-AG acting as a high efficacy agonist at CB_1 and CB_2 receptors, while anandamide behaves as a partial agonist (Hillard, 2000a). In addition, anandamide binds and activates TRPV1 receptors (Melck *et al*, 1999; Smart *et al*, 2000; Zygmunt *et al*, 1999), whereas

2-AG also binds $GABA_A$ receptors (Sigel *et al*, 2011). As such, cannabinoid ligands differentially modulate similar physiological and pathological processes.

Distinct sets of enzymes, which regulate the biosynthesis and degradation of the eCBs and possess distinct anatomical distributions (see Figure 1), exert control over CB_1 and CB_2 receptor signaling. Inactivation of anandamide occurs predominantly through fatty acid amide hydrolase (FAAH) (Cravatt *et al*, 1996, 2001), localized to intracellular membranes of postsynaptic somata and dendrites (Gulyas *et al*, 2004), in areas such as the neocortex, cerebellar cortex, and hippocampus (Egertová *et al*, 1998). Inactivation of 2-AG proceeds primarily via monoacylglycerol lipase (MAGL) (Blankman *et al*, 2007; Dinh *et al*, 2002), expressed on presynaptic axon terminals (Gulyas *et al*, 2004), and demonstrates highest expression in areas such as the thalamus, hippocampus, cortex, and cerebellum (Dinh *et al*, 2002). The availability of pharmacological inhibitors for eCB catabolic enzymes has allowed the selective amplification of anandamide and 2-AG levels following brain injury as a key strategy to enhance endocannabinoid signaling and to investigate their potential neuroprotective effects.

Finally, 2-AG functions not only as a major cannabinoid receptor signaling molecule, but also serves as a major precursor for arachidonic acid (AA), and therefore plays a role in inflammatory pathways (see Figure 2). Although AA is a degradative product of both 2-AG (Bell *et al*, 1979) and anandamide (Deutsch *et al*, 1997), MAGL represents a rate-limiting biosynthetic enzyme of this highly bioactive lipid in brain, liver, and lung (Nomura *et al*, 2011). Historically, cytosolic phospholipase A2 (cPLA2) was considered to be the primary rate-limiting enzyme in AA production (reviewed in

Buczynski et al., 2009). However, MAGL contributes ~80% and cPLA2 ~20% of LPS-stimulated eicosanoids in mouse brain. In contrast, cPLA2 is the dominant enzyme to control AA production in spleen (Nomura *et al*, 2011). Therefore, MAGL and cPLA2 appear to play differential roles in AA production, and concomitantly its eicosanoid metabolites in a tissue-specific manner (Nomura *et al*, 2011). As such, 2-AG functions not only as an endogenous CB1 and CB2 receptor ligand, but also an immunomodulator by virtue of its being a major precursor for AA, making it a versatile target for the treatment of TBI related pro-inflammatory pathologies. Understanding the biosynthesis mechanisms of eCBs may prove useful in modulating their entry into pro-inflammatory pathways. While 2-AG is known to be synthesized by diacylglycerol lipase-α and –β (DAGL-α and DAGL-β) (Bisogno *et al*, 2003b), the mechanisms mediating anandamide production are incompletely understood (Blankman and Cravatt, 2013).

Traumatic Brain Injury Pathology

Traumatic brain injuries are heterogeneous in their etiology, clinical presentation, severity, and pathology. The sequelae of molecular, biochemical, and physiological events that follow the application of an external mechanical force produce interacting acute and delayed pathologies, described as primary and secondary injuries. The initial insult produces an immediate mechanical disruption of brain tissue (Reilly, 2001). This primary injury consists of contusion, blood vessel disruption and brain oedema, localized necrotic cell death, as well as diffuse axonal injury producing degeneration of cerebral white matter (Adams et al., 1989; Gaetz, 2004).

Secondary injury mechanisms are initiated within minutes, in which necrotic and apoptotic cell death in contused areas and pericontusional penumbra continue over a period of days to months (Raghupathi, 2004). Neuronal disruption spills excitatory amino acids into the interstitial space, producing glutamate-mediated excitotoxicity (Bullock *et al*, 1998). Massive influx of Ca^{2+} into cells (Floyd *et al*, 2010) produce mitochondrial dysfunction and the release of reactive oxygen species (ROS) which lead to further apoptosis (Zhao *et al*, 2005). Injury-induced activation of CNS resident glial cells, microglia, as well as recruitment of circulating inflammatory cells, e.g. macrophages, then produce secretion of inflammatory mediators, cytokines and chemokines (reviewed in Woodcock and Morganti-Kossmann, 2013). Increased intracranial pressure leads to reductions in cerebral blood flow (Shiina *et al*, 1998), while injury-induced breakdown of the cerebrovascular endothelium contributes to dysfunction of the blood brain barrier (BBB) (Chodobski *et al*, 2012). Extracranial pathologies are also evident following TBI with pulmonary complications being the most common (Pelosi *et al*, 2005). Neurogenic pulmonary oedema often develops early after brain injury, producing hypoxemia and further aggravating secondary brain injury (Brambrink and Dick, 1997; Oddo et al., 2010). These varied and interacting disease processes highlight the necessity to address the multiple targets associated with secondary injury cascades following TBI.

While there are many types of CNS injury models (e.g. spinal cord injury, lesion studies, focal and global ischemic injury etc. (Arai and Lo, 2009; Titomanlio *et al*, 2015), this review will focus primarily on the work investigating manipulations of the eCB system in preclinical models of traumatic brain injury.

Pre-Clinical Evaluation of Cannabinoids to Treat TBI

While basal anandamide and 2-AG levels differ within various structures in the CNS, levels increase on demand in response to a given stimuli (e.g. the induction of nausea [Sticht et al., 2016] or pain states [Costa et al., 2008]). eCBs are lipid messengers not stored in synaptic vesicles (likely due to their hydrophobicity) but rather synthesized in an activity-dependent manner from membrane phospholipid precursors (Alger and Kim, 2011). Consequently, endocannabinoid signaling is enhanced by a stimulus-response synthesis and release mechanism.

eCB levels increase in selected CNS tissue following neuronal damage, which may reflect a self-neuroprotective response. NMDA excitotoxicity produces elevations of anandamide in ipsilateral cortex of rats by 4-fold at 4 h, and 14-fold at 24 h, but with no changes in 2-AG levels (Hansen *et al*, 2002). Concussive head trauma in rats produces a similar pattern of findings in which modest increases of anandamide levels occur in ipsilateral cortex, and again with no change in 2-AG levels (Hansen *et al*, 2002). This pattern was replicated by Tchantchou et al., 2014, who found a 1.5 fold increase of anandamide levels at three days post-TBI in ipsilateral mouse brain, and with no change in 2-AG. In contrast, Panikashvili et al., 2001 reported that TBI in mice led to increases of 2-AG in ipsilateral brain from 1 h to 24 h with elevations as high as 10-fold. Thus, further research is needed to discern whether species differences, the model used to elicit neurotrauma, and/or other procedural considerations contribute to the differential elevation of these eCBs (Mechoulam and Lichtman, 2003).

A lack of studies systematically investigating the consequences of TBI on changes in eCB levels in specific brain regions perhaps point to the difficulty in

measuring changes in the volatile eCBs, prone to rapid degradation (Deutsch and Chin, 1993; Dinh *et al*, 2002). While pharmacological and genetic manipulations of the eCB system continue to be evaluated following TBI; full characterization of how eCB biosynthetic and degradative enzymes, receptors, and endogenous ligands, their precursors and catabolic products, change as a consequence of TBI remains to be fully illuminated.

Treatment of Cellular and Molecular Pathophysiology of TBI

In this section, we review preclinical studies of cannabinoids in the context of their potential to protect against cellular and molecular TBI pathology, (see Table. 1).

CNS Cell Death. TBI-induced neuronal loss occurs almost immediately as necrotic cell death and continues for months following the initial insult via both necrotic and apoptotic cell death (Raghupathi, 2004). From a traumatic insult, the initial contused area forms a regional primary lesion or infarct surrounding which is the pericontusional penumbra, the area immediately adjacent to the primary lesion and at risk for further neurodegeneration. The evolution of the pericontusional penumbra occurs largely due to secondary injury mechanisms and has long been considered a candidate for interventions to protect against, or salvage from, further injury (Wang *et al*, 2014). The investigation of cannabinoids on traumatic CNS cell death have thus far demonstrated efficacy in two areas; attenuated neurodegeneration and reduced lesion volume.

Neurodegeneration, commonly measured by reductions in the neuronal marker fluoro-jade C, has been found to be readily attenuated in mice by CB_2 receptor agonists (Amenta *et al*, 2012), as well as by inhibitors of FAAH (Tchantchou *et al*, 2014) and

MAGL (Zhang *et al*, 2014). Additionally, FAAH inhibitors produce reductions in lesion volume, and increased production of the heat shock proteins Hsp70, known to be structurally protective, and Hsp72, a negative regulator of apoptosis (Tchantchou *et al*, 2014). Tchantchou et al., 2014 also showed that FAAH inhibition increased expression of the anti-apoptotic protein Bcl-2.

Several enzymes hydrolyze 2-AG including MAGL, which accounts for an estimated 85% of its total hydrolysis, as well as α/β-hydrolase domain-6 (ABHD6) and ABHD12, which are responsible for much of the remaining 15% (Blankman *et al*, 2007). Tchantchou and Zhang, 2013 found that inhibition of ABHD6 also reduced lesion volume and lowered neurodegeneration in a mouse CCI model. A CB_1 receptor antagonist attenuated the protective effects on lesion volume, while CB_1 and CB_2 receptor antagonists prevented the protective effects on neurodegeneration (Tchantchou and Zhang, 2013).

Combined, this evidence suggests that inhibitors of eCB hydrolysis offer protection against TBI-induced cell death which involve CB_1 and CB_2 receptors, though the distinction between the eCBs remains to be clarified. Few studies have evaluated interactions between anandamide and 2-AG in laboratory models of TBI. One study using a model of cerebral focal ischemia found that exogenously administered anandamide and 2-AG in combination reduced infarct size in rats, but with no facilitatory effects beyond anandamide or 2-AG alone (Wang *et al*, 2009). Given the recent availability of dual FAAH/MAGL inhibitors (Long *et al*, 2009; Niphakis *et al*, 2012), simultaneous blockade of these enzymes following TBI may further reveal some insight into the relationship between anandamide and 2-AG on TBI-induced cell death.

Excitotoxicity. Previous efforts to attenuate the effects of excitotoxicity following brain injury focused on NMDA receptor antagonists, presumably with the understanding that the induction of depressed NMDA receptor function would counteract TBI-induced excitotoxicity. This class of drugs showed promise in laboratory animal models of TBI (Shohami *et al*, 1995), but failed to produce long-term beneficial outcomes in clinical trials, despite some acute benefits of improved intracranial pressure and cerebral perfusion pressure (Knoller *et al*, 2002; Maas *et al*, 2006). Research investigating manipulations of the eCB system on glutamatergic functioning following TBI have thus far focused primarily on 2-AG, and paradoxically, its effectiveness to protect the integrity of glutamate receptor function.

Several studies investigating the effects of cannabinoids in laboratory animal models of TBI have focused on expression changes of metabotropic ($mGluR_1$, $mGluR_5$), AMPA (GluA1, GluA2), and NMDA (GluN1, GluN2A, GluN2B) glutamatergic receptors. Specifically, post-injury administration of the MAGL inhibitor JZL184 reversed TBI-induced reductions of GluN2A, GluN2B, and GluA1 receptor expression, but with no impact on GluN1 or GluA2 receptors (Zhang *et al*, 2014). The CB_1 receptor antagonist Rimonabant did not alter injury-induced lowered expression of $mGluR_1$, but surprisingly reversed reduced $mGluR_5$ receptor expression six weeks following TBI (Wang *et al*, 2016). Both findings were completed 30 days post injury (Wang *et al*, 2016; Zhang *et al*, 2014), suggesting long term changes in glutamatergic function following acute administration of cannabinoids post-injury. However, little overlap is found between receptor expression endpoints across papers. In an example of contradictory patterns of GluA1 expression after injury, GluA1 expression was reduced in a study that subjected

mice to a daily mild closed head injury on three consecutive days (Zhang et al., 2014), and was increased in rats subjected to a single lateral fluid percussion brain injury (Mayeux et al., 2016). In these studies, MAGL inhibition ameliorated both the reduced (Zhang et al., 2014) and increased (Mayeux et al., 2016) GluA1 expression. As discussed above (see Section 4), systematic investigation of species (mice vs. rat), brain injury model, number of injuries, and other experimental variables are needed to understand the consequences of brain injury on glutamate receptor changes.

eCBs are known to depress glutamate release from pre-synaptic terminals, and in particular, 2-AG has been explored in its ability to influence the functioning of electrochemical neurotransmission. MAGL inhibition has been found to protect against injury-induced increases in frequency and amplitude of excitatory post-synaptic currents (EPSC) in pyramidal neurons at the site of injury (Mayeux *et al*, 2016), which may suggest changes in pre-synaptic transmitter release or post-synaptic strength (Zhang *et al*, 2005). MAGL inhibition has also protected against injury-induced long term potentiation (LTP) impairments at hippocampal CA3-CA1 synapses (Zhang *et al*, 2014), implicating the restoration of glutamate receptor function in protection against TBI-induced memory impairments.

Finally, the excitotoxicity resulting from TBI is part of the sequelae of events that lead to release of damaging ROS. Antioxidants are known to prevent oxidation of free radicals and thus protect against the cellular damage in response to sudden ROS elevation. Endocannabinoids have been linked to the neuroprotective production of antioxidants as the administration of exogenous 2-AG following injury has been found to increase levels of antioxidants (Panikashvili *et al*, 2006).

Combined, these data suggest that MAGL represents a promising target to reduce the damaging effects of injury-induced excitotoxicity through complementary molecular pathways.

Neuroinflammation. Hydrolytic enzymes of anandamide and 2-AG produce a shared metabolic product in the formation of free AA, the major substrate of the biosynthetic enzymes of pro-inflammatory eicosanoids (Nomura *et al*, 2011). Therefore, eCB oxidation not only produces inactivation at cannabinoid receptors, but also leads to the production of bioactive lipids involved in inflammatory responses during the early stages of injury. Manipulations of the endocannabinoid system have proved effective in downregulating inflammation in many experimental models, such as inflammatory pain (Ahn *et al*, 2009), and multiple sclerosis (Mestre *et al*, 2005). The use of cannabinoids following TBI have thus far been linked to two predominant features of inflammation; decreased inflammatory cell activation, and decreases in pro-inflammatory cytokine production.

Pro-inflammatory activated microglia are known to exacerbate TBI-induced neuroinflammation (Kigerl *et al*, 2009). Thus, decreasing TBI-inductions of inflammatory cell activation is an attractive treatment strategy. MAGL inhibition protects against TBI-induced microglial activation (Katz *et al*, 2015; Zhang *et al*, 2014), while ABHD6 inhibition promotes microglia/macrophage shift from a pro-inflammatory M1 to an anti-inflammatory M2 phenotype (Tchantchou and Zhang, 2013). A parsimonious explanation for these findings is that prevention of 2-AG hydrolysis leads to reduced levels of AA and concomitant reductions of pro-inflammatory mediators. Given the contribution of 2-AG catabolism to eicosanoid production, it is unsurprising that several

studies have reported eCBs as demonstrating pro-inflammatory roles, some examples of which include models of nephropathy (Mukhopadhyay *et al*, 2010a), cardiomyopathy (Mukhopadhyay *et al*, 2010b), and experimental dermatitis (Oka *et al*, 2006). Most of such pro-inflammatory effects are attributed to 2-AG and not anandamide, likely due to its considerable abundance over anandamide. However, FAAH inhibition, similarly has been found to protect against TBI-induced microglial activation (Katz *et al*, 2015), as too has activation of CB_2 receptors (Amenta *et al*, 2012). Thus, a need exists to disentangle the potential contributions of 2-AG to pro-inflammatory processes from its role as a substrate for AA production, versus anti-inflammatory effects through cannabinoid receptors, following TBI.

Inhibition of eCB degradative enzymes has also produced decreases in TBI-induced pro-inflammatory mediators. Reductions in the expression of inducible enzymes that trigger eicosanoid production following brain injury, COX-2 enzyme (which converts free AA to prostaglandins) and iNos (which produces the free radical nitric oxide in response to cytokine signaling), are seen in response to ABHD6 inhibition (Tchantchou and Zhang, 2013) and FAAH inhibition (Tchantchou *et al*, 2014). Reductions in TBI-induced pro-inflammatory cytokine mRNA (Il-1β, TNFα, and IL-6) have also been found following treatment with exogenous 2-AG (Panikashvili *et al*, 2006). These findings seem counter-intuitive given the possibility of the rapid oxidation of 2-AG and its consequent contribution to eicosanoid production. However, exogenous 2-AG has also been shown to ameliorate TBI-induced transactivation of the nuclear factor NF-kB (linked to cytokine production) in wild type mice, but not in CB_1 knockout mice,

suggesting that CB_1 receptors mediate the protective effects of exogenous 2-AG (Panikashvili *et al*, 2005).

Cerebrovascular Breakdown. The blood vessels which carry oxygen rich blood to the brain are lined by endothelial cells as well as astrocytes. These cells, combined with specific transport proteins and enzymes, strictly regulate movement between the general circulation and CNS extracellular fluid, and are collectively known as the blood brain barrier (BBB). TBI has been well documented in producing cerebral blood flow pathology (Kelly *et al*, 1997) as well as interfering with BBB integrity (Başkaya *et al*, 1997). Given that cannabinoids are known to exert vascular effects, producing vasodilation as well as hypotension (reviewed in Hillard, 2000b), their manipulation may hold promise as protectants against cerebrovascular damage. Below, we review studies examining the effects of cannabinoids on TBI-induced disruption of BBB integrity.

Exogenous administration of 2-AG (Panikashvili *et al*, 2006), as well as MAGL inhibition (Katz *et al*, 2015), and ABHD6 inhibition (Tchantchou and Zhang, 2013) administered post-injury protect against BBB breakdown. However, Panikashvili et al., 2006 found that the expression of proteolytic enzymes implicated in BBB breakdown were unaffected by exogenous 2-AG post-injury. These enzymes include matrix metallopeptidase-9 (MMP9) involved in extracellular matrix degradation, and tumor necrosis factor-α-converting enzyme (TACE), which cleaves membrane-bound proteins. The mechanism by which 2-AG acts as a protectant of BBB integrity following traumatic insult is yet to be resolved.

One study found that post-surgery administration of a FAAH inhibitor protected against BBB breakdown (Katz *et al*, 2015), suggesting that anandamide and/or other

substrates of this enzyme play a protective role. While the mechanism underlying the structural protection of the BBB was not explored following TBI, anandamide has been found to decrease BBB permeability in a model of ischaemic stroke by transient receptor potential cation channel, subfamily V, member 1 (TRPV1) (Hind *et al*, 2015). Given that activation of TRPV1 receptors disrupts BBB integrity (Hu *et al*, 2005), it is possible that anandamide, as a partial agonist at TRPV1 channels (Pertwee and Ross, 2002), maybe be acting as a functional antagonist against a high efficacy endogenous agonist to produce its structurally protective effects of the cerebral microvascular endothelium. The exploration of how anandamide may be exerting its protective effects of BBB integrity may yet yield further novel targets for the treatment of TBI.

In cerebral circulation, CB_1 receptor activation produces vasodilation. Indeed, the CB_1 receptor antagonist rimonabant inhibited hypotension induced by endotoxin shock and hemorrhagic shock, as well as increasing survival (Varga *et al*, 1998). Though cannabinoids are yet to be explored in the context of TBI-induced changes in cerebral blood flow, CB_1 receptor antagonism may prove to be a potential target for the treatment of TBI-induced hypotension.

Cell Structure/Remodeling. The key biological idea that structure dictates function also holds true for the neurophysiology of TBI. The shearing and tearing forces of TBI and subsequent secondary injury cascades produce changes in cell architecture, extracellular matrices, and the balance of fluid homeostasis, that impair neuronal function often both in a focal and/or diffuse manner throughout the brain (Gaetz, 2004). The use of cannabinoids has thus far been linked to protection against several of the

CNS structural changes associated with TBI, with 2-AG being the most frequently studied eCB in this area.

While a traumatic insult can result in the rapid onset of cerebral oedema, exogenously administered 2-AG protects against TBI-induced oedema (Panikashvili *et al*, 2001, 2005). The observation that no such oedema protection was found following 2-AG administration in CB_1 receptor$^{-/-}$ mice (Panikashvili *et al*, 2005) suggests that this protection requires CB_1 receptor activation. Changes in protein physiology have also been found to occur following TBI. Specifically, the presence of protein aggregates such as amyloid-β plaques (Johnson *et al*, 2010), hyperphosphorylated tau (p-tau) (Goldstein *et al*, 2012), and TAR DNA-binding protein 43 (TDP-43) (Smith et al., 1999), have been found within hours following TBI. These proteins are thought to accumulate from damaged axons and as a result of a disturbed balance between genesis and catabolism (Johnson *et al*, 2010). MAGL inhibitors decrease amyloid-β protein and its precursor molecule amyloid precursor protein (APP), as well as p-tau and TDP-43 (Zhang *et al*, 2014). MAGL inhibition also decreases astrocyte activation (Mayeux *et al*, 2016), while exogenous 2-AG following TBI reduces hippocampal CA-3 neuron loss (Panikashvili *et al*, 2001). These consistent protective effects of 2-AG across varied TBI-related structural pathologies point to its important role in maintaining cell structure and promoting remodeling.

Protective roles played by anandamide in injury-induced structural changes are yet to be ascertained. Though FAAH inhibition decreases APP expression post-injury, as well as increases synaptophysin (Tchantchou *et al*, 2014), a synaptic vesicle protein whose elimination impairs object recognition and spatial learning in mice (Schmitt *et al*,

2009). Furthermore, eCBs may not be working alone to offer protection from TBI-induced structural impairments. For example, estradiol decreased the number of TBI-induced immunoreacitve astrocytes, which was inhibited by CB_1 and CB_2 receptor antagonists, while also increasing cerebral cortex mRNA levels of CB_2 receptors (Lopez Rodriguez *et al*, 2011). These findings suggest that the regulatory activity of the eCB receptors in response to TBI may be mediated by endocrine as well as paracrine signaling mechanisms.

TBI is well described to increase CB_1 and CB_2 receptor expression, which includes disruption of diurnal rhythms of CB_1 receptor expression (Martinez-Vargas *et al*, 2013). Post-injury treatment with a CB_1 receptor antagonist reduces CB_1 receptor expression at 6 weeks following injury (Wang *et al*, 2016), whereas ABHD6 inhibition produces increased CB_1 and CB_2 receptor expression (Tchantchou and Zhang, 2013). As such, TBI-induced increases in cannabinoid receptor expression are perhaps facilitated by 2-AG.

Neurogenic Pulmonary Oedema. Pulmonary complications are reported in 20-25% of TBI patients (Holland *et al*, 2003), and its severity is related to brain injury magnitude (Alvarez *et al*, 2015). The exact CNS circuits involved in neurogenic pulmonary oedema (NPE) have yet to be identified, though a sudden rise in intracranial pressure, rapid sympathetic surge, increased systemic vascular resistance and increase in hydrostatic pressure in the pulmonary vasculature, as well as release of pro-inflammatory mediators may all contribute to interstitial pulmonary oedema formation (Brambrink and Dick, 1997). NPE rapidly occurs within hours of TBI onset in clinical populations (Alvarez *et al*, 2015), and within minutes in animal models (Atkinson et al.,

1998), producing CNS hypoxia (Oddo *et al*, 2010) which further contributes to secondary injury. NPE is a much needed area of interest in the study of TBI.

While at the present time there are no studies evaluating the contributions of, or protection by, the eCB system to NPE following TBI, this may prove an interesting area of future investigation. Specifically, the lung possesses a basal tone of 2-AG (Avraham *et al*, 2008; Nomura *et al*, 2008), and recently it has been shown that resident lung macrophages express major components of the eCB system, CB_1 and CB_2 receptors as well as anandamide and 2-AG (Staiano *et al*, 2015). Furthermore, MAGL inhibition has already been found to be protective against LPS-induced acute lung injury in mice, and attenuated with CB_1 and CB_2 receptor antagonists (Costola-de-Souza *et al*, 2013).

Treatment of Behavioral Deficits of TBI

The heterogeneous clinical presentation of TBI pathology in populations of survivors is reminiscent of its cellular and molecular pathophysiology described above. TBI patients report changes in mental health (depression, irritability, anxiety, and personality changes), sleep disturbance, post-traumatic headaches, persistent fatigue, epilepsy, learning and memory deficits (manifested also as impairments in attention and processing speed [Vakil, 2005]), and balance disorders (Stéfan *et al*, 2016). Most frequently investigated measures in the pre-clinical TBI literature include neurological motor, and learning and memory impairments, leaving a wide breadth of TBI clinical effects yet to be studied. Once again, components of the eCB system may become active to compensate for TBI symptomology given what is currently known of its

regulatory effects within these areas, two examples being pain, and anxiety and depression (Corcoran *et al*, 2015).

In this section, we review what is currently known of cannabinoids in the context of their ability to alter post-traumatic animal behavior (see Table. 2).

Learning and Memory. Learning and memory impairments are among the most frequently reported symptoms following TBI, and are slow to recover with deficiencies reported ten years later (Zec *et al*, 2001). The eCB system has been shown to play a well-documented role in memory regulation (reviewed in Mechoulam and Parker, 2011), and as such its manipulation holds considerable promise to address such a profound consequence of TBI.

Inhibition of the eCB hydrolytic enzymes FAAH (Tchantchou *et al*, 2014), MAGL (Zhang *et al*, 2014), and ABHD6 (Tchantchou and Zhang, 2013) have been shown to protect against TBI-induced memory impairments, suggesting that anandamide and 2-AG elevation post-TBI may offer protection from TBI-induced learning and memory deficits. The protective effects of 2-AG appear to be task specific, with ABHD6 inhibition showing learning and memory protection in a Y-maze task, but not a Morris water maze task. To date, only a Y-maze task has been used to evaluate the memory protective effects of FAAH inhibition, and this task-specific effect did not occur with a MAGL inhibitor. Mice are a well-used pre-clinical model organism to study the memory effects of TBI; however, they are known to perform behavioral tasks more readily, and with less error, when the task does not rely on aversive motivation (Stranahan, 2011). This attribute of mice may, in some part, contribute to the task-related differences seen between the Y-maze task (which uses exploratory behaviors associated with novelty)

and the aversively motivated escape behavior necessary in the Morris water maze. Regardless, in clinical populations the most common memory process vulnerable to TBI involves difficulties applying active or effortful strategies in the learning or retrieval process (Vakil, 2005). Moving forward, the use of behavioral tasks able to selectively assess such frontal lobe-type memory impairments might improve the translational capacity of eCB TBI pre-clinical assessments (one such example being the Morris water maze Reversal Task, which evaluates cognitive flexibility).

Neurological Motor. TBI-induced neurological motor impairments currently represent the most frequently studied behavioral outcome measure in the TBI-cannabinoid literature. In clinical populations, neurological motor impairments seen as a result of TBI show spontaneous improvement over time, but one third of patients continue to experience neuromotor abnormalities two years after injury (Walker and Pickett, 2007). A variety of eCB system manipulations have thus far been found to be protective against the neurological motor deficits associated with murine models of TBI.

Both 2-AG and anandamide elevation provide protection against TBI-induced neurological motor deficits. MAGL inhibitors (Katz *et al*, 2015; Mayeux *et al*, 2016; Zhang *et al*, 2014), ABHD6 inhibitors (Tchantchou and Zhang, 2013), and exogenous 2-AG administration (Panikashvili *et al*, 2001), improve Neurological Severity Score (NSS) in laboratory animal models of TBI. Moreover, ABHD6 inhibition also protects against TBI-induced rotarod deficits (Tchantchou and Zhang, 2013). Administration of exogenous 2-AG did not enhance NSS scores in CB_1 receptor knockout mice subjected to TBI (Panikashvili *et al*, 2005), suggesting a CB_1 receptor mechanism of action. FAAH inhibition has produced mixed findings in neurological motor tests, such as beam-walk

deficit protection (Tchantchou *et al*, 2014) but no improvement on TBI-induced NSS deficits (Katz *et al*, 2015). In support of anandamide being protective against TBI-induced motor deficits, exogenous anandamide has also produced improved NSS performance (Martinez-Vargas *et al*, 2013). Full reversal, and partial reversal, of FAAH inhibitor mediated beam-walk deficit protection by respective CB_2 and CB_1 receptor antagonists (Tchantchou *et al*, 2014), suggest a role of both of these receptors in anandamide's neuromotor deficit sparing effects. The involvement of the CB_2 receptor is further supported by rotarod deficit protection from a CB_2 receptor agonist (Amenta *et al*, 2012).

The role of entourage effects has also been evaluated in the area of TBI-induced neurological motor impairments. Co-release of endogenous fatty acid derivatives can potentiate 2-AG signaling, termed an entourage effect (Ben-Shabat *et al*, 1998; Lambert, D. M., Di Marzo, 1999; Lichtman *et al*, 2002). Administration of 2-AG with two related lipids that do not bind cannabinoid receptors, 2-linoleoyl-glycerol (2-LG) and 2-palmitoyl-glycerol (2-PG), enhances recovery from TBI-induced NSS deficits (Panikashvili *et al*, 2001). Given FAAH is responsible for the degradation of various fatty acid amides in addition to anandamide (Boger *et al*, 2000), its various substrates may work in concert to ameliorate pathologies related to TBI. Thus any inferences drawn about anandamide through the use of FAAH inhibition need to consider contributions of noncannabinoid fatty acid amides.

Anxiety and Post-Traumatic Seizures. The signs of post-traumatic anxiety have been difficult to replicate in murine models of TBI (Tucker *et al*, 2016). Also, as there is a limited number of studies evaluating eCBs in this area, no definitive

conclusions can be made. Thus far, only FAAH inhibition has been explored to address post-traumatic anxiety, and was found to protect against TBI-induced increases in anxiety-like behavior in mice (Tchantchou *et al*, 2014). This protection in the zero maze was unaffected by either CB_1 or CB_2 receptor antagonists, suggesting that these receptors are dispensable. Modeling post-traumatic epilepsy is time consuming and faces other challenges such as a low percentage of animals that develop epilepsy (Mazarati, 2006), however, recent models that produce consistent replication of spontaneous seizure activity following a TBI are available (Ping and Jin, 2016). Contrary to preclinical research demonstrating that the eCB system plays a protective roles against seizures (Marsicano et al., 2003; Wallace et al., 2001), a CB_1 receptor antagonist has protected against injury-induced seizure threshold deficits as well as lowered seizure mortality (Wang *et al*, 2016), potentially through the disinhibition of GABAergic terminals.

This nascent body of data suggests that eCB manipulations hold promise to treat injury-induced clinical symptoms outside of the more popular areas of learning and memory and neurological motor impairments.

Primary Phytocannabinoids and Traumatic Brain Injury

Although currently well over one hundred phytocannabinoids have been elucidated from the *Cannabis Sativa* plant (Elsohly *et al*, 2017), the most extensively studied of these are Δ^9-tetrahydrocannabinol (THC) and cannabidiol (CBD). The investigation of phytocannabinoids on TBI pathology not only holds topical relevance, but also holds promise as potential treatment for TBI and other disorders.

Without exception, all of the experimental work reviewed and listed in Tables 1 and 2 have used post-injury drug administration times ranging from 15 minutes to several days, clearly an attempt to simulate clinical intervention timing possibilities. However, clinical and pre-clinical findings provide evidence suggesting that the primary psychoactive constituent of *Cannabis Sativa*, THC, is neuroprotective when administered prior to a traumatic insult. In a three year retrospective study of patients who had sustained a TBI, urine toxicology screen results showed decreased mortality in individuals with a positive THC screen (Nguyen *et al*, 2014a). In two mouse models of CNS injury that yield cognitive deficits, pentylenetetrazole (an excitotoxic agent) and carbon monoxide induced hypoxic injury, prior administration of THC provided impairment protection (Assaf *et al*, 2011). Curiously, an extraordinarily low dose of THC (i.e. 0.002 $mg.kg^{-1}$) reduced injury-induced cognitive deficits in mice (Assaf *et al*, 2011). The authors explained this effect through the known biphasic effects of THC producing analgesia, acute hypothermia, and decreased locomotion at high doses (10 $mg.kg^{-1}$), and producing hyperalgesia, hyperthermia, and increased locomotion at a low dose (0.002 $mg.kg^{-1}$) (reviewed in Sarne et al., 2011). Such low dose effects of THC have been found to potentiate calcium entry into cells *in vitro* (Okada et al., 1992), increasing glutamate release, and thus may be mildly neurotoxic. Therefore, Assaf et al., 2011 hypothesized that low dose THC pre-treatment produced a pre-conditioning effect, where a mildly noxious stimulus becomes protective against a more severe subsequent insult, an effect known to occur in cardiology (Dirnagl *et al*, 2003) as well as cerebral ischaemia (kitagawa et al., 1991). Moreover, the molecular signalling cascades behind cardiac and cerebral ischaemia preconditioning include activation of ERK and Akt

(Dirnagl *et al*, 2003; Gidday, 2006), also shown to mediate the protective effects of ABHDB (Tchantchou and Zhang, 2013) and MAGL (Mayeux *et al*, 2016) inhibition following TBI.

Even though 80-90% of THC is excreted from individuals within five days of administration, the remaining slow release of lipophilic THC from lipid-storage compartments result in its long terminal half-life in plasma (Huestis, 2007). As such, individuals may experience very low plasma THC concentrations for prolonged periods after each application. Although the clinical study of TBI-induced mortality reported no data to quantify levels of THC in the THC positive individuals, the low dose THC in CNS injured mice may mimic the pharmacokinetics of THC in humans. This presumed prolonged exposure of THC due to its pharmacokinetics, as well as other potentially neuroprotective cannabinoids, such as CBD (Perez *et al*, 2013), may be responsible for the survival effects found in cannabis-exposed TBI patients. A finding of increased clinical relevance, is that post-conditioning (when the mildly noxious stimulus is applied after the insult) with low dose THC also produced cognitive sparing effects in mice (Assaf *et al*, 2011). These findings, however, remain controversial, and are yet to be replicated in animal models of TBI.

The phytocannabinoid CBD, currently being investigated in clinical trials for its seizure reduction potential in Tuberous Sclerosis Complex (GW Research Ltd, n.d.), has known anti-inflammatory properties. Although CBD does not bind CB_1 and CB_2 receptors, it activates the G-protein coupled receptor GPR55 (Ryberg *et al*, 2007), inhibits nucleoside transporter 1 (Carrier *et al*, 2006), inhibits sodium channels (Hill *et al*, 2014), and produces increased extracellular adenosine concentrations that

consequently downregulate inflammatory cells through the adenosine A_{2A} receptor (Hasko and Pacher, 2008; Ohta and Sitkovsky, 2001). While there are no studies at present which have investigated the anti-inflammatory effects of cannabidiol following TBI, cannabidiol has reduced FosB expression following cryogenic spinal cord injury (Kwiatkoski *et al*, 2012), and lowered iNos expression in a mouse model of tauopathy (Casarejos *et al*, 2013). As such cannabidiol may be a promising future avenue of investigation in the study of neuroinflammation in response to brain injury.

Concluding Remarks and Future Directions

The eCB system, through release of its endogenous ligands or by changes in cannabinoid receptor constitutive activity, possesses promise in the treatment of diverse TBI pathology. An important step forward in understanding the role that the eCB system plays in TBI pathology includes not only the full characterization of ligands targeting cannabinoid receptors and eCB regulating enzymes, but also changes in cannabinoid receptors, eCB levels, and eCB regulating enzymes as a consequence of TBI. Another future area of therapeutic interest is non-CB_1/CB_2 receptor targets, such as TRPV1 receptors, and their potential contribution to the protective effects following TBI. Furthermore, alternative activation of CB_1/CB_2 receptors, such as potential entourage effects from other fatty acid derivatives, antagonism, or allosteric modulation, might impact functional selectivity and thus TBI-related outcomes also warrants further investigation. So too do the plant-derived phytocannabinoids represent an understudied yet promising group of compounds given the neuroprotective results obtained from

other types of CNS injury. In particular, CBD as well as other phytocannabinoids which do not bind cannabinoid receptors, represent promising molecules to treat TBI.

To date, the only reported cannabinoid to be specifically evaluated for the treatment of TBI in patient populations is Dexanabinol, also known as HU211. While HU211 showed promise in animal models of TBI (Shohami *et al*, 1995), it failed to produce long term patient outcomes in one clinical trial despite some acute benefits (Knoller et al., 2002), and in a second study showed no short or long term benefits (Maas *et al*, 2006). Although HU211 has been described as a cannabinoid by virtue that it is an enantiomer of the potent synthetic cannabinoid agonist HU210, it does not bind or activate cannabinoid receptors. Instead, HU211acts as a non-competitive NMDA receptor antagonist (Feigenbaum *et al*, 1989). This therefore brings to light an important consideration of the classification of cannabinoids.

One consistently overlooked area across the study of TBI is the evaluation of the central penetration of systemically administered drugs. Pharmacological treatments will need to be assessed for their ability to cross the BBB. Also, it should be noted that TBI rapidly disrupts the BBB and lasts for three days post-injury (Başkaya *et al*, 1997). Furthermore, given the often biphasic nature of cannabinoid drugs, it is critical to move away from single dose pharmacology to full dose-response assessments, which may yield an increased understanding of the mechanism and potential of cannabinoids to treat TBI. Overall, the abundant and growing pre-clinical research suggests that the eCB system possesses many promising targets for new and existing drugs that may ameliorate diverse TBI pathology.

Table 1-1. **Effect of cannabinoids on TBI-induced cellular and molecular pathophysiology**. Drug targets; CB_2 receptor agonist (O-1966), FAAH inhibitor (PF3845), MAGL inhibitors (JZL184 & URB597), ABHD6 inhibitor (WWL70), and CB_1 receptor antagonist (Rimonabant). TBI Models; CCI (controlled cortical impact), CHI (closed head injury), and FPI (fluid percussion injury).

Compound / mutant	Dose	Species	TBI Model/ Severity	Effect	Receptor Mediated	References
CNS Cell Death						
O-1966	5 mg/kg, i.p.	mouse C57BL/6	CCI, moderate	↓ Neurodegeneration	CB_2	Amenta et al., 2012
PF3845	5 mg/kg, i.p.	mouse C57BL/6	CCI, severe	↓ Lesion volume ↓ Neurodegeneration ↑ Bcl-2, Hsp70 & 72	Not evaluated	Tchantchou et al., 2014
JZL184	10 mg/kg, i.p.	mouse C57BL/6	CHI, mild repetitive	↓ Neurodegeneration	Not evaluated	Zhang et al., 2014
WWL70	10 mg/kg, i.p.	mouse C57BL/6	CCI, severe	↓ Lesion volume ↓ Neurodegeneration	CB_1 CB_1 & CB_2	Tchantchou & Zhang, 2013
Excitotoxicity						
Rimonabant	2 mg/kg, i.p.	rat Sprague-Dawley	Lateral FPI, severe	$mGluR_5$ receptor recovery at 6 wks (no impact on $mGluR_1$)	CB_1	Wang et al., 2016
2-AG	5 mg/kg, i.p.	mouse Sabra	CHI, severe	↑ levels of weak antioxidants	Not evaluated	Panikashvili et al., 2006
JZL184	10 mg/kg, i.p.	mouse C57BL/6	CHI, mild repetitive	Glutamate receptor recovery Injury-induced ↓ in LTP protection	Not evaluated	Zhang et al., 2014
	16 mg/kg, i.p.	rat Wistar	Lateral FPI, mild	GluA1 expression protection Injury-induced ↑ in EPSC protection	Not evaluated	Mayeux et al., 2016
Neuroinflammation						
CB^1 -/-	N/A	mouse C57BL/6	CHI, severe	No effect on NF-κB transactivation	N/A	Panikashvili et al., 2005
CB^1 -/- + 2-AG	N/A	mouse C57BL/6	CHI, severe	No effect on NF-κB transactivation	N/A	Panikashvili et al., 2005
O-1966	5 mg/kg, i.p.	mouse C57BL/6	CCI, moderate	Microglial activation protection	CB_2	Amenta et al., 2012
PF3845	5 mg/kg, i.p.	mouse C57BL/6	CCI, severe	↓ COX-2 Expression ↓ iNos expression	Not evaluated	Tchantchou et al., 2014
URB597	0.3 mg/kg, i.p.	rat Sprague-Dawley	Lateral FPI, mild	Microglial activation protection	Not evaluated	Katz et al., 2015
2-AG	5 mg/kg, i.p.	mouse Sabra	CHI, severe	↓ TNFα mRNA ↓ IL-1β mRNA ↓ IL-6 mRNA	Not evaluated	Panikashvili et al., 2006

Table 1-1. Continued

Compound / mutant	Dose	Species	TBI Model/ Severity	Effect	Receptor Mediated	References
2-AG	5 mg/kg, i.p.	mouse C57BL/6	CHI, severe	↓ NF-κB translocation & transactivation	CB_1	Panikashvili et al., 2005
JZL184	10 mg/kg, i.p.	mouse C57BL/6	CHI, mild repetitive	↓ TNFα mRNA Microglial activation protection	Not evaluated	Zhang et al., 2014
	16 mg/kg, i.p.	rat Sprague-Dawley	Lateral FPI, mild	Microglial activation protection	Not evaluated	Katz et al., 2015
WWL70	10 mg/kg, i.p.	mouse C57BL/6	CCI, severe	↓ COX-2 Expression ↓ iNos expression M1 to M2 phenotype	Not evaluated	Tchantchou & Zhang, 2013
Cerebrovascular Breakdown						
URB597	0.3 mg/kg, i.p.	rat Sprague-Dawley	Lateral FPI, mild	BBB integrity protection	Not evaluated	Katz et al., 2015
2-AG	5 mg/kg, i.p.	mouse Sabra	CHI, severe	BBB integrity protection	Not evaluated	Panikashvili et al., 2006
JZL184	16 mg/kg, i.p.	rat Sprague-Dawley	Lateral FPI, mild	BBB integrity protection	Not evaluated	Katz et al., 2015
WWL70	10 mg/kg, i.p.	mouse C57BL/6	CCI, severe	BBB integrity protection	Not evaluated	Tchantchou & Zhang, 2013
CNS Cellular Structure/Remodeling						
Vehicle (saline-5% ETOH)	4 µL	rat Wistar	CHI, moderate	Diurnal CB_1 expression abolished ↑ contralateral CB_1 & CB^2 Expression		Martinez-Vargas et al., 2013
CB^1 -/-	N/A	mouse C57BL/6	CHI, severe	No effect on oedema	N/A	Panikashvili et al., 2005
CB^1 -/- + 2-AG	N/A	mouse C57BL/6	CHI, severe	No effect on oedema	N/A	Panikashvili et al., 2005
Rimonobant	2 mg/kg, i.p.	rat Sprague-Dawley	Lateral FPI, severe	↓ CB_1 Expression at 6 weeks post-TBI	CB_1	Wang et al., 2016
PF3845	5 mg/kg, i.p.	mouse C57BL/6	CCI, severe	↓ APP ↑ Synaptophysin	Not evaluated	Tchantchou et al., 2014
2-AG	5 mg/kg, i.v.	mouse Sabra	CHI, severe	↓ CA3 neuron loss Oedema protection	CB_1	Panikashvili et al., 2001
	5 mg/kg, i.p.	mouse C57BL/6	CHI, severe	Oedema protection	CB_1	Panikashvili et al., 2005
JZL184	10 mg/kg, i.p.	mouse C57BL/6	CHI, mild repetitive	↓ APP ↓ Amyloid-β peptide ↓ TDP-43 & p-tau	Not evaluated	Zhang et al., 2014
	16 mg/kg, i.p.	rat Sprague-Dawley	Lateral FPI, mild	↓ astrocyte activation	Not evaluated	Mayeux et al., 2016
WWL70	10 mg/kg, i.p.	mouse C57BL/6	CCI, severe	↑ CB_1 & CB_2 Expression	Not evaluated	Tchantchou & Zhang, 2013

Table 1-2. **Effect of cannabinoids on TBI-induced behavioral impairments**. Drug targets; CB_2 receptor agonist (O-1966), FAAH inhibitor (PF3845), MAGL inhibitors (JZL184 & URB597), ABHD6 inhibitor (WWL70), and CB_1 receptor antagonist (Rimonabant). TBI Model definitions; CCI (controlled cortical impact), CHI (closed head injury), and FPI (fluid percussion injury).

Compound/ mutant	Dose	Species	TBI Model/ Severity	Effect	Receptor Mediated	References
Learning and Memory						
PF3845	5 mg/kg, i.p.	mouse C57BL/6	CCI, severe	Y-maze deficit protection	CB_1 Partial CB_2	Tchantchou et al., 2014
JZL184	10 mg/kg, i.p.	mouse C57BL/6	CHI, mild repetitive	MWM deficit reduction	Not evaluated	Zhang et al., 2014
WWL70	10 mg/kg, i.p.	mouse C57BL/6	CCI, severe	Y-maze deficit protection No impact on MWM deficit	Not evaluated	Tchantchou & Zhang, 2013
Neurological Motor Deficits						
CB^1 -/-	N/A	mouse C57BL/6	CHI, severe	Impaired NSS score	CB_1	Panikashvili et al., 2005
CB^1 -/- + 2-AG	N/A	mouse C57BL/6	CHI, severe	Impaired NSS score	CB_1	Panikashvili et al., 2005
O-1966	5 mg/kg, i.p.	mouse C57BL/6	CCI, moderate	Rotarod deficit protection	Not evaluated	Amenta et al., 2012
Anandamide	1.25 µg/4 µL, ICV	rat Wistar	CHI, moderate	Improved NSS score	Not evaluated	Martinez-Vargas et al., 2013
PF3845	5 & 10 mg/kg, i.p.	mouse C57BL/6	CCI, severe	Beam-walk deficit protection	Partial CB_1 CB_2	Tchantchou et al., 2014
URB597	0.3 mg/kg, i.p.	rat Sprague-Dawley	Lateral FPI, mild	No impact on NSS or NBS	Not evaluated	Katz et al., 2015
2-AG	5 mg/kg, i.v.	mouse Sabra	CHI, severe	Improved NSS score	Not evaluated	Panikashvili et al., 2001
2-AG + 2-PG + 2-LG	1 mg/kg, i.v.	mouse Sabra	CHI, severe	Improved NSS score	Not evaluated	Panikashvili et al., 2001
JZL184	10 mg/kg, i.p.	mouse C57BL/6	CHI, mild repetitive	Improved NSS score	Not evaluated	Zhang et al., 2014
	16 mg/kg, i.p.	rat Sprague-Dawley	Lateral FPI, mild	Improved NSS & NBS score, out to 1 d	Not evaluated	Katz et al., 2015
	16 mg/kg, i.p.	rat Sprague-Dawley	Lateral FPI, mild	Improved NSS & NBS score, out to 14 d	Not evaluated	Mayeux et al., 2016
WWL70	10 mg/kg, i.p.	mouse C57BL/6	CCI, severe	Improved NSS score Rotarod deficit protection	Not evaluated	Tchantchou & Zhang, 2013

Table 1-2. Continued

Compound/ mutant	Dose	Species	TBI Model/ Severity	Effect	Receptor Mediated	References
Anxiety-Like Behavior						
PF3845	5 & 10 mg/kg, i.p.	mouse C57BL/6	CCI, severe	Zero-maze anxiety-like profile protection	No CB_1, CB_2 reversal	Tchantchou et al., 2014
Post-Traumatic Seizures						
Rimonabant	2 mg/kg, i.p.	rat Sprague-Dawley	Lateral FPI, severe	Protective against seizure threshold deficits Lowered seizure mortality	CB_1	Wang et al., 2016

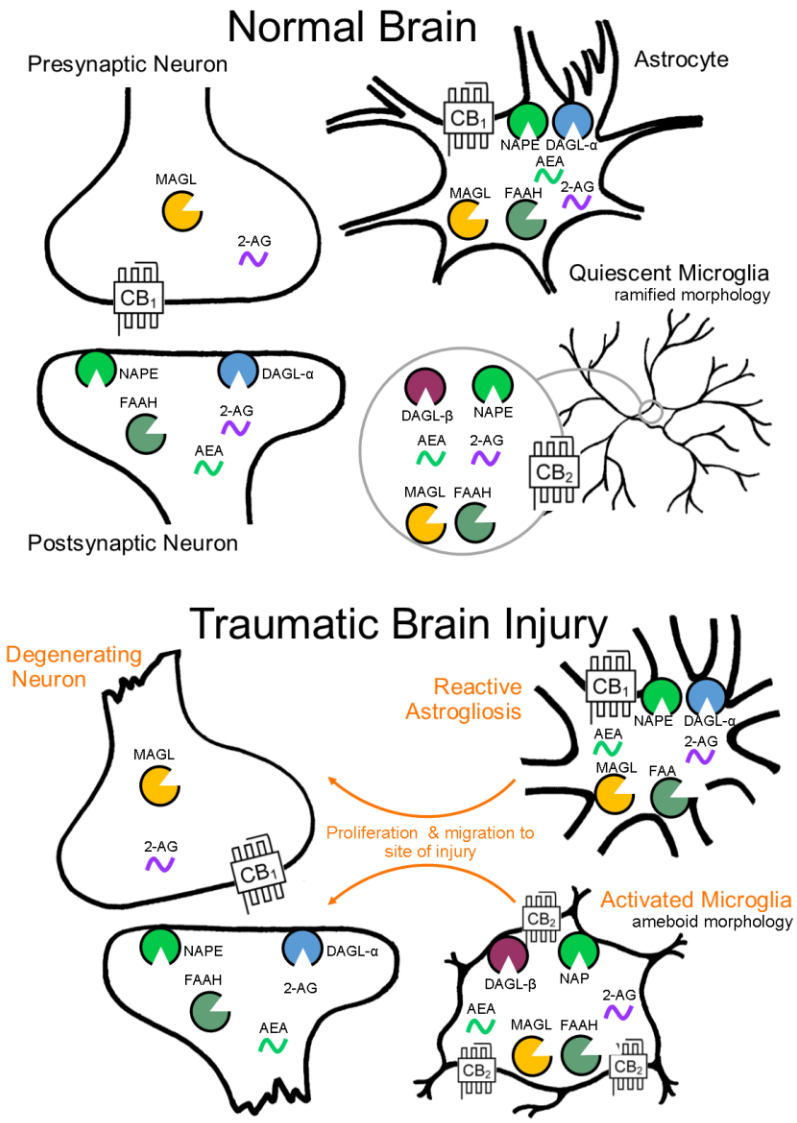

Figure 1-1. **Endocannabinoid System Cell Localization by CNS Cell Type**. Endocannabinoid functional specialization among CNS cell types is determined by the cellular compartmentalization of biosynthetic and catabolic enzymes (biosynthesis by NAPE and DAGL-α, -β, catabolism by FAAH and MAGL). Cellular level changes in eCB biosynthetic and catabolic enzymes as a result of brain injury have yet to be investigated, though morphological and molecular reactivity by cell type is well documented.

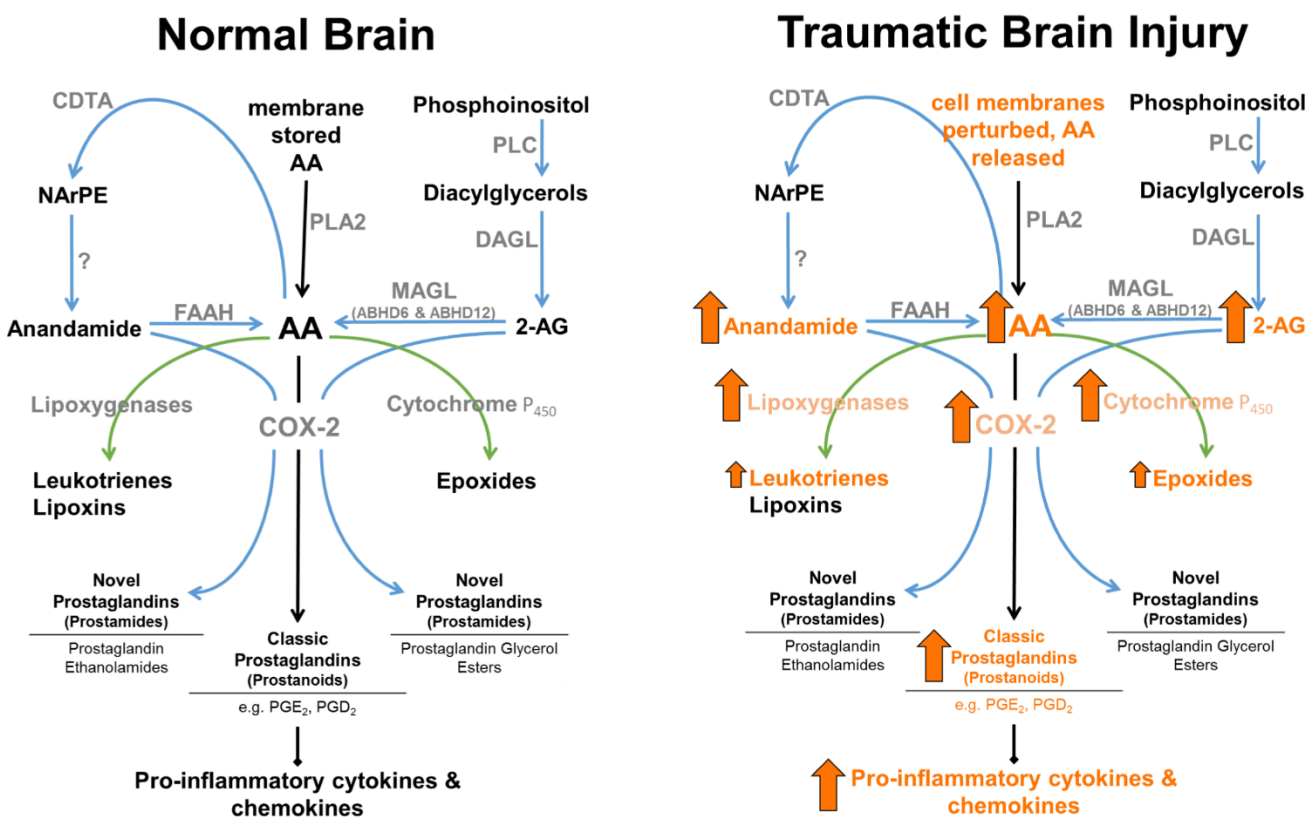

Figure 1-2. **Enzymatic regulation of anandamide and 2-AG in normal brain, and following traumatic brain injury**. 2-AG levels are approximately 1,000 fold higher than anandamide levels in brain. MAGL plays a rate-limited role in the production of AA in brain, lung, and liver (Nomura *et al*, 2008). Arrows represent known TBI-induced changes in eCBs, catabolic and downstream enzymes, and their metabolic products (arrow size has no relation to magnitude of change).

Dissertation Goals

In light of the evidence that endocannabinoids both regulate processes of learning and memory and are produced in response to pathogenic events, it is likely their important contributions to memory function extend to conditions of memory pathology. As such, the present dissertation project had three goals. The first goal being to establish a preclinical mouse model of TBI-induced cognitive deficit, second to target diacylglycerol lipase-β (DAGL-β) as a novel target for the reduction of TBI-induced cognitive impairment, and the third and final goal was to understand the role of diacylglycerol lipase-α (DAGL-α) in spatial learning and memory regulation under physiological conditions.

The initial method development investigated functional deficits following TBI in mice using the fluid percussion injury model, as measured by spatial memory tasks of the Morris water maze and tasks of neurological motor impairment, as well as cellular changes evaluated in both histological outcomes and morphological changes to resident immune cells of the CNS. The development of this procedure and evaluation of these outcome measure differences following a left or a right unilateral insult, are described and discussed in Chapter 2.

Manipulations of endocannabinoid biosynthetic pathways may further reveal their role in compensatory repair pathways. The selective expression of diacylglycerol lipase-β (DAGL-β) on resident immune cells of the CNS (microglia) and the role of 2-AG as a precursor for the production of pro-inflammatory eicosanoids, drove the consideration of this 2-AG biosynthetic production enzyme contribution to neuroinflammatory responses to TBI. Therefore a second goal of this dissertation was to focus on DAGL-β as a novel

target for the reduction of mouse TBI-induced cognitive impairment. Our working hypothesis was that disrupting DAGL-β activity would provide cognitive protection following brain injury by reducing pools of 2-AG metabolites (AA and pro-inflammatory eicosanoids) in microglia, and was funded by an F31 grant (1F31NS095628-01A1). These studies were conducted using the *in vivo* measures described in Chapter 2. An unexpected finding that DAGL-β disruption produced a survival phenotype following TBI, led us to continue the evaluation of this mortality protective effect. All of which is described in Chapter 3.

The neuronal expression of diacylglycerol lipase-α (DAGL-α), the second of two 2-AG biosynthetic enzymes, drove the consideration of this enzyme contribution to the normal regulation of learning and memory processes. Therefore the third and final goal of this dissertation was to understand the *in vivo* role of DAGL-α in spatial learning and memory regulation in mice. This set of studies used complementary genetic and pharmacological approaches to investigate the role of DAGL-α in various hippocampal-dependent memory processes. The dissertation concludes with a discussion of the overall implications of the entirety of these studies, as well as future directions.

Chapter II

Chapter Introduction

The first goal of this dissertation was to establish a preclinical mouse model of TBI-induced cognitive dysfunction using the fluid percussion injury model, and learning and memory evaluation by the Morris water maze.

Memory dysfunction following TBI. TBI frequently results in a heterogeneous range of persistent comorbidities, with symptoms ranging from psychological (e.g. personality changes, anxiety, irritability, depression), to physiological (e.g. epilepsy, sleep disturbance, headache), motor (e.g. balance disorders), and cognitive deficits (e.g. impaired learning and memory). Learning and memory specifically is one of the most commonly experienced, and quality of life impacting impairments, following brain injury. Both retrograde amnesia (loss of event memory prior to TBI onset) and deficits in prospective memory (remembering to perform previously planned actions) are commonly reported following brain injury (Carlesimo *et al*, 1997; Groot *et al*, 2002). While very few experience global amnesia (total disruption of short term memory and impaired access to long term memory) after a TBI, the most commonly reported vulnerable memory processes include difficulties applying effortful strategies in learning and retrieval (Vakil, 2005) reminiscent of deficits associated with frontal lobe damage (della Rocchetta, 1986). Explicit memory (conscious recollection) is widely affected by TBI, with deficits seen in working memory tasks (Christodoulou *et al*, 2001; Stablum *et*

al, 1994) (during which neural activity becomes more bilateral and dispersed (Christodoulou *et al*, 2001), verbal and visual memory deficits (Zec *et al*, 2001), impaired learning rate (Zec *et al*, 2001), and accelerated forgetting rate (Haut *et al*, 1990). Implicit memory (unconscious and procedural memory) is less consistently impacted, with well-practiced skills acquired prior to TBI being resistant to injury induced-impairments (Schmitter-Edgecombe and Nissley, 2000), whereas performance acquiring new skills post-TBI can be task and injury severity dependent (Vakil, 2005). Other cognitive domains which in turn affect learning and memory such as attention (Oddy *et al*, 1985) and processing speed (Ferraro, 1996) are also frequently negatively impacted by TBI.

While patients suffering from TBI are not an ideal group to study brain region-behavior relationships (given the widespread diffuse pathophysiology of TBI), there is a great need to further understand the selective memory processes affected, as well as identify novel treatments.

Spatial memory evaluation in mice. To evaluate our primary functional endpoint, TBI-induced learning and memory deficits, we chose to use spatial memory tasks of the Morris water maze (MWM). The MWM was first described over 30 years ago (Morris, 1981) as a model to investigate spatial learning and memory in rats. It has since been used extensively in behavioral neuroscience, but has also become a well characterized tool in the study of memory impairments following TBI. Mice have been repeatedly and successfully used in the MWM, an important adaptation from its original design using rats, given the utility of transgenic mouse models. However, MWM performance is affected by mice strain differences. Injured C57BL/6 mice have been

found to demonstrate deficits in learning compared to their sham controls, whereas sham controls for 129/SvEMS and FVB/N strains could not acquire the task (Fox *et al*, 1999). Thus C57BL/6 mice are a useful strain for the study of TBI-induced MWM impairments.

The MWM is considered a test of spatial memory given it is hippocampal-dependent, particularly sensitive to the effects of hippocampal lesions (Morris, 1984). While alternative hippocampal-dependent learning and memory tasks have been characterized (e.g. the object in place paradigm; Mitchnick *et al*, 2016), a unique utility of the MWM is the number of task variations that can be used to study distinct memory processes. The fixed platform task is used to assess the acquisition of memory, the reversal task evaluates cognitive flexibility (a form of fluid intelligence whereby inhibitory responses are required to explore alternative solution paths, increasing cognitive demands), and the cued task is used to control for sensory-motor and motivational confounds (Vorhees and Williams, 2006); are but some examples of such task variations. As such the MWM is a useful and adaptable tool to study the various types of memory impairments that brain injury can produce.

Neurological-motor evaluation in mice. Measures of neurological impairment can also be useful when administered following brain injury as a correlate of injury severity (Tsenter *et al*, 2008). We chose to utilize both the Neurological Severity Score (NSS) assessment and the Rotarod assay to corroborate injury severity between and within cohorts, but also as control measures to assess motor impairments during learning and memory assay conditions. The NSS is a neurological motor impairment assessment battery specifically for mice (Beni-Adani *et al*, 2001), widely used in pre-

clinical studies of TBI. The Rotarod is a measure of motor coordination with specific sensitivity to murine models of TBI (Hamm *et al*, 1994). While the Rotarod assay itself requires motor learning processes, the presently used accelerating schedule is designed to evaluate motor performance while minimizing motor skill learning (Jones and Roberts, 1968).

Traumatic brain injury induction. The fluid percussion injury (FPI) model of traumatic brain injury has been extensively used in murine pre-clinical models, where by an injury is induced by striking a fluid-filled column secured to the exposed dura of the animal. A FPI creates a mixed focal and diffuse axonal injury (Dixon *et al*, 1987), which replicates key features of clinical head injury, and produces motor and memory deficits commonly seen in clinical cases of TBI (Hamm, 2001).

A unique utility of the FPI is its adaptability in terms of scalable injury severity as well as injury location. The severity of a FPI can be manipulated by raising or lowering the height from which the mallet (which strikes the fluid-filled column) is released. Injury severity is measured by pressure transduction via an oscilloscope, as well as assessed using standardized outcome measures relating to the status of the animal, such as righting time, and the previously mentioned neurological motor assessments. The unit of pressure used to evaluate the injury magnitude (atmospheres (atm), with 1 atm = 14.70 pounds per square inch) is relatable to a category of injury severity (mild, moderate, severe), though no current standardization exists in the literature. For the purpose of the present work in mice, a mild FPI is considered <1.5 atm (Spain *et al*, 2010), a moderate FPI is considered 1.5 to 2.0 atm (Mukherjee *et al*, 2013), and a severe FPI is considered > 2.0 atm (Bolkvadze and Pitkanen, 2012). Further ways to adapt the FPI

include changing the position of the craniectomy, commonly positioned for either a central injury (directly over the sagittal suture and in between bregma and lambda) or as either a right or a left lateral injury (craniectomy positioned approximately 1 mm to the left or right of the sagittal suture, between bregma and lambda). The lateral FPI is commonly used (Van and Lyeth, 2016) and produces degenerative cascades in selectively vulnerable brain regions, including the ipsilateral hippocampus (Hicks *et al*, 1996). An initial central mild (1.4 atm) FPI produced no change in our mouse learning and memory assessment behaviors (data not included). This finding prompted an increase in injury severity, and due to concerns over survivability of a central moderate FPI, a change to a lateral injury. Both left and right lateral injuries were then evaluated at a moderate (1.92 atm) injury severity following which modest but distinct differences in learning and memory assessment performance was noted.

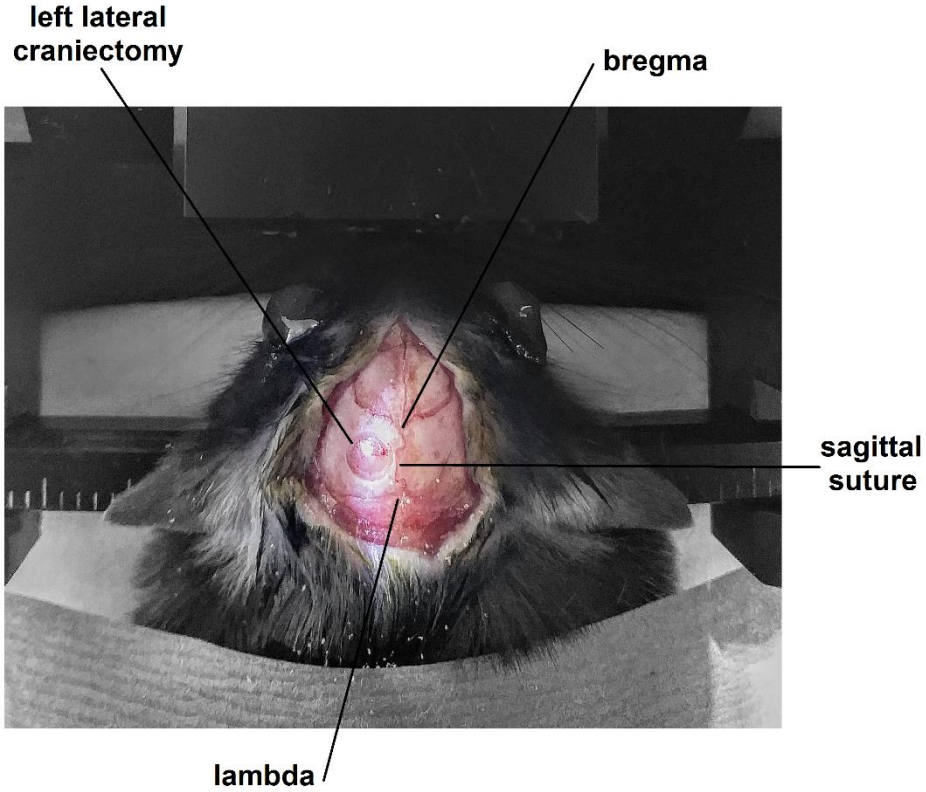

Figure 2-A: Example of a mouse left-lateral craniectomy position. Pictured is a DAGL-β transgenic mouse (mixed background), in a stereotaxic surgical frame under gaseous isoflurane anesthesia (2.7%, 250 mL/min). Ophthalmic ointment is applied to the eye area, and iodine and ethanol sterilized soft tissue prior to the surgical incision.

Lateralization of brain function. The medial longitudinal fissure separates the human brain into two distinct cerebral hemispheres with subcortical structures frequently occurring in duplicate "mirrored" in the left and right hemispheres. Accordingly, neural functions and cognitive processes (e.g. language; Gazzaniga and Sperry, 1967) are frequently more dominant in one hemisphere than the other; referred to as lateralization of brain function. It has long been posited that such functional lateralization is beneficial, and more recently greater functional lateralization has been associated with improved cognitive ability (Gotts *et al*, 2013). Indeed, lateralization of higher order brain functions has been well described in humans, with the left hemisphere being dominant for language processing and the right for visuospatial attention (Hutsler and Galuske, 2003). The hippocampus also demonstrates lateralization with increased left hippocampal activity occurring in response to task relevant semantic information, whereas increased right hippocampal activity occurs from spatial information (Motley and Kirwan, 2012). Left-right hippocampal structures also support complementary functions in human episodic memory (Iglói *et al*, 2010). These unilateral specializations have been speculated to increase efficiency in available circuitry (Shipton *et al*, 2014), though the mechanisms by which bilateral neural structures support differences in cognitive function across hemispheres remains unknown. Evidence continues to mount in favor of lateralization of function not being a uniquely human characteristic, with left-right differences in neural processing also being widespread among vertebrates (Halpern *et al*, 2005).

Summary. The following work evaluates differences in functional outcome following a left or a right unilateral insult in mice, specifically; spatial memory tasks of

the MWM and tasks of neurological motor impairment, as well as cellular changes evaluated in both histological outcomes and morphological changes to resident immune cells of the CNS. This initial method development of mouse spatial learning and memory deficits following TBI thus also investigates functional lateralization and considers its relevance to pre-clinical models of injury-induced cognition dysfunction.

Investigation of Left and Right Lateral Fluid Percussion Injury in C57BL6/J Mice: In Vivo Functional Consequences

(Neurosci Lett 653: 31-38, 2017)

Disclosure: all glial reactivity immunohistochemistry experiments were conducted in the laboratory of Dr. Linda Phillips, primarily by Dr. Linda Phillips and Nancy Lee.

Introduction

The fluid percussion injury model of traumatic brain injury (TBI) in laboratory animals elicits functional and pathophysiological hallmarks of human TBI, including cognitive dysfunction, intracranial haemorrhage, oedema, and progressive grey matter damage (Graham *et al*, 2000). Originally developed as a midline injury in cats (Hayes *et al*, 1987) and rabbits (Hartl *et al*, 1997), a lateral fluid percussion injury was used in rats (McIntosh *et al*, 1989), and further adapted for mice (Carbonell *et al*, 1998), now widely used given the utility of transgenic lines. Lateral fluid percussion injury produces a combined focal cortical contusion and diffuse subcortical neuronal injury in rats (Hicks *et al*, 1996), the extent and location of which is subject to small changes in craniotomy position (Vink *et al*, 2001). It is noteworthy that small alterations in craniotomy position in rats lead to differences in cognitive performance (Floyd *et al*, 2002). In mice, left (Tchantchou and Zhang, 2013; Fox *et al*, 1999) and right (Carbonell *et al*, 1998; Spain *et al*, 2010) craniotomy placement generally differs across research groups; however, there are no systematic studies investigating craniotomy position on measures of learning and memory or motor effects in mice.

Several lines of evidence suggest existence of left-right hemisphere molecular (Kawakami *et al*, 2003; Shinohara and Hirase, 2009), morphological (Kawakami *et al*, 2003; Shinohara *et al*, 2008), and functional differences (Kohl *et al*, 2011; Shipton *et al*, 2014) at hippocampal synapses in mice. Left-right morphological differences exist in the mouse hippocampus where left originating CA3 inputs innervate small spines, whereas inputs originating from the right CA3 innervate larger, mushroom-shaped spines (Kawakami *et al*, 2003; Shinohara *et al*, 2008). The molecular composition of these smaller spines also differ, exhibiting a higher density of GluN2B subunits in postsynaptic spines receiving left CA3 input (Kawakami *et al*, 2003; Wu *et al*, 2005). Morphological differences; size of left infrapyramidal mossy fiber projections, also positively correlate with precision in swimming navigation (Bernasconi-Guastalla *et al*, 1994). Furthermore, long-term potentiation (LTP) reveals hemispheric specialization in which LTP induction of CA3 synaptic inputs to CA1 when input originates from the left, but not the right CA3, using spike timing-dependent LTP (Kohl *et al*, 2011), or conventional high-frequency stimulation-induced LTP (Shipton *et al*, 2014). Similarly, in behaving mice silencing of left, but not right, CA3 pyramidal neurons resulted in Y-maze task deficits (Shipton *et al*, 2014), and *inversus viscerum* mice (bred to express only a right phenotype at CA3-CA1 synapses) exhibited dry maze task deficits (Goto *et al*, 2010).This evidence of structural and behavioral hemispheric differences raises the question of whether left versus right hemisphere TBI will reveal differing patterns of cognitive deficits.

The Morris water maze (MWM) is frequently used to assess TBI-induced spatial learning and memory impairments. Although hippocampal lesions (Gerlai *et al*, 2002) or TBI (Fox *et al*, 1999) severely impairs MWM performance, mice with bilateral

hippocampal lesions are still able to improve their performance (Gerlai *et al*, 2002). Accordingly, MWM performance may employ brain areas in addition to the hippocampus, such as the striatum (Whishaw *et al*, 1987), basal forebrain (Waite *et al*, 1994), insular cortex (Gutiérrez *et al*, 1999), etc. making this task a useful model to study the functional consequences of a lateralized brain injury in mice. MWM task variations are also used to infer the underlying processes affecting performance. Here, the Fixed Platform task assesses reference memory acquisition, and the reversal task; cognitive flexibility. Moreover, the Cued task, where the location of the hidden platform is made visible, infers sensorimotor and motivational influences. Based on the established left-right molecular and morphological asymmetry in the mouse hippocampus, we examine whether unilateral TBI of the left and right hemisphere will elicit differential patterns of spatial memory and motor deficits in mice.

Materials and Methods

Mice. All experiments used adult male C57BL/6J mice (Jackson Laboratories, Bar Harbor, Maine), left injury (n=10), left sham (n=10), right injury (n=8), right sham (n=7), (further described in the supplement), and complied with EC Directive 86/609/EEC, conducted in accordance with the National Institute of Health (NIH) Guide for the Care and Use of Laboratory Animals (NIH Publications No. 8023, revised 1978), and were approved by the Virginia Commonwealth University Institutional Animal Care and Use Committee.

Craniotomy and Induction of Lateral Fluid Percussion Injury (FPI). Under isoflurane anesthesia (2.5%, 250 mL/min) a sagittal scalp incision was made and a 2.7

mm trephine craniectomy performed over the left or right parietotemporal cortex, further description of which is included in the supplement. After a 2 h recovery period, mice were anesthetized with isoflurane (4%, 400 mL/min) and immediately subjected to a moderate lateral fluid percussion injury (1.94±0.1 atm left lateral, 1.92±0.1 atm right lateral injury), described in the supplement.

Neurological Motor Impairment Evaluation. Mice were evaluated in Rotarod and Neurological Severity Score, 2 days prior to injury, and 1, 2, 3, 7, 14 and 21 days post-injury (see Figure 2-1). Single Rotarod (IITC Life Science Rota-Rod, Woodland Hills, CA, with 3 cm diameter rotating drums) trials per day used an accelerating protocol, a description of which appears in supplementary information. A 10-point Neurological Severity Score (NSS) assessed the functional neurological status of mice based on the presence of reflexes and the ability to perform motor and behavioral tasks (see Supplementary Table 2-1). Further description appears in supplementary information.

Learning and Memory Assessment. The MWM consisted of a circular, galvanized steel tank (1.8 m in diameter, 0.6 m height) filled with opaque water (maintained at 20ºC±2ºC) with a submerged platform (10 cm diameter) and distal and proximal visual cues, further described in the supplement. A description of the Fixed Platform, Reversal, and Cued Tasks also appears in supplementary information, (see Figure 2-1).

Histology and Lesion Volume Quantification. Animals were anesthetized, transcardially perfused with paraformaldehyde and brains extracted. Brains were sectioned (50µm thickness) on a Leica VT1000S vibratome, Nissl stained using cresyl

violet acetate, and digitally imaged. Microscopy was performed at the VCU Department of Anatomy and Neurobiology Microscope Facility. Further detail and the lesion volume quantification description appears in supplementary information.

Qualitative Assessment of Glial Cell Response to Injury. Immunohistochemistry (IHC) was performed in left and right injured and sham animals (n=3/group) surviving for 3 days post-injury. Mice were perfused as described for histology and 40 µm coronal brain sections cut by vibratome were processed for IHC (Reeves *et al*, 2016) using antibodies for IBA1 (Wako, Abcam; 1:300), and GFAP (Dako, Encor Biotechnology; 1:20,000). Images were collected on a Zeiss 700 confocal microscope for qualitative assessment of each protein.

Statistical Analysis. Differences were considered significant when $P < 0.05$, and analyses were conducted using IBM SPSS Statistics 22 (IBM Software, New York, NY). To assess TBI-induced changes to MWM performance, mean latency-to-goal (seconds) in left and right injury was compared to left or right sham, respectively. To directly compare the effects of right vs. left injury, mixed-factor ANOVA analyses were also conducted on MWM latencies normalized as percent-of-sham-control (using the corresponding hemisphere right and left sham group: injured animal score / mean sham score * 100%). This normalization approach increases sensitivity to detect the effects of TBI and reduces the influence of minor sham control differences (Townend, 2013). Normalized data were also analyzed using a one sample t-test to compare left or right to sham performance (value of 100). Motor differences and MWM acquisition were analyzed using a mixed factor ANOVA, probe trial measures by independent group t-test, and righting times and lesion volume by 2-way ANOVA. Post hoc tests for MWM

acquisition (Fixed Platform and Reversal tasks) were conducted using a Bonferroni adjustment, and for NSS and Rotarod used a Tukey HSD adjustment.

Results

Left and right hemisphere injury produced neurological motor deficits. *NSS Measure.* NSS scores increased for left and right lateral injury on post-injury day one. A significant interaction for both left (Figure 2-2A), $F(6, 108) = 11.93$, $P < 0.001$; and right lateral (Figure 2-2C) NSS, $F(6, 78) = 2.39$, $P < 0.05$, revealed an increased NSS in both left and right lateral injured animals on post-injury day 1 ($P < 0.01$) compared to day -1, not present in both left and right lateral sham animals.

Rotarod measure. Both left and right lateral Injury produced impaired rotarod performance, with no left-right performance differences. A significant interaction for both left lateral (Figure 2-2B), $F(7, 126) = 2.47$, $P < 0.05$; and right lateral (Figure 2-2D) latency to fall, $F(7, 91) = 2.54$, $P < 0.05$, revealed a significant decrease in latency to fall compared to sham in left lateral injury on post-injury day 1 ($P < 0.01$), and in right lateral injured animals on post-injury days 1 ($P < 0.01$), 2 ($P < 0.05$), 3 ($P < 0.05$), day 7 ($P < 0.05$), and 14 ($P < 0.05$). Direct comparison of left and right cohorts on percent of sham control revealed no significant interaction (Figure 2-2E) $P = 0.10$, with no main effect of hemisphere $P = 0.47$ in latency to fall.

Both left and right lateral injury produced MWM task deficits, with modest left-right hemisphere differences. *Fixed Platform Task.* The right lateral injury group showed a small but significant delay in the acquisition of reference memory compared to sham; and poorer performance compared to left injured animals. Both left and right

lateral injured mice demonstrated reference memory expression impairments. The acquisition of reference memory showed no significant interaction for left lateral (Figure 2-3A) $P = 0.75$; or right lateral (Figure 2-3B) $P = 0.88$ injuries. A significant main effect of injury was found for the right lateral cohort, $F(1, 13) = 10.05$, $P < 0.01$, but not left ($P = 0.15$), where the right lateral injured animals demonstrated longer latencies to the platform than sham animals. A comparison of normalized left-right acquisition performance revealed a significant main effect of hemisphere, $F(1, 16) = 7.87$, $P< 0.05$, indicating greater acquisition deficits in the right lateral cohort compared to the left (Figure 2-3C), while the Injury X Day interaction was not significant (P=0.07). The fixed platform probe trial revealed significantly longer latencies to the platform location in injured mice compared to sham animals for both left (Figure 2-3D), $t(18) = 2.41$, $P < 0.05$, and right lateral injuries (Figure 2-3E), $t(13) = 3.17$, $P < 0.01$. Analyses of normalized probe trial measurements confirmed injury-induced increases in mean latency for both left, $t(9) = 3.16$, $P< 0.05$, and right, $t(7) = 3.74$, $P< 0.01$, cohorts relative to sham levels (one sample t-test), although normalized latencies did not differ between hemispheres (P=0.16, independent samples t-test).

Reversal Task. No left vs. right performance differences were found in reversal task learning, however left lateral injury demonstrated modest impairments relative to sham in reversal acquisition and expression. Reversal acquisition learning revealed no significant interaction for either left lateral (Figure 2-4A), $P = 0.92$; or right lateral (Figure 2-4B), $P = 0.39$; injury. However, a main effect of injury was found for the left lateral injury cohort, $F(1, 18) = 7.93$, $P < 0.05$, but not right, $F(1, 13) = 1.89$, $P = 0.19$, where left injured animals demonstrated longer latencies to the platform than sham animals.

Direct comparison of left and right injury revealed no significant interaction (Figure 2-4C) $P = 0.39$, and no significant main effect of hemisphere $P < 0.28$ on percent of sham control. The reversal probe trial revealed significantly longer latencies to the new platform location in left lateral injured mice compared to sham animals (Figure 2-4D), $t(18) = 2.75$, $P < 0.05$, and but not right (Figure 2-4E), $P = 0.37$. Direct comparison of left vs. right injury normalized reversal probe trial latencies, showed performance did not differ between these injury groups (P=0.17, independent samples t-test), although the left, $t(9) = 2.90$, $P< 0.05$, but not right (P=0.22), injury group differed from sham levels (one sample t-test) (Figure 2-4F).

Cued Task and Swim Speed. The injury-induced MWM performance impairments were likely not due to sensory-motor or motivational impairments measured by the Cued Task (Supplementary Figure 2-1), or swim speed (Supplementary Figures 2-2 and 2-3).

Injury severity and histological outcome in left and right hemisphere injury groups. The injury procedure produced a mortality rate of 20.8% for the left lateral cohort, and 22.7% for the right lateral cohort (dead mice were excluded from all subsequent measures).

Righting Time. Neither the interaction between hemisphere and injury (Figure 2-5A, 2-5D), $P = 0.84$, nor the main effect of hemisphere, $P = 0.79$, achieved significance; however, a main effect of injury, $F(1, 31) = 44.58$, $P < 0.001$, showed longer righting times in injured animals than shams.

Lesion Volume Percentage. Neither the injury by hemisphere interaction (Figure 2-5B, 2-5E), $P = 0.53$, nor main effect of hemisphere, $P = 0.86$, achieved significance;

however, there was a main effect of injury, $F(1, 12) = 23.08$, $P < 0.001$, in which lesion volumes were significantly larger in injured animals than in shams.

Hippocampal glial cell response to left and right hemisphere injury. Hippocampal IHC of microglial (IBA1) and astrocytes (GFAP) showed robust glial response to TBI. IBA1 imaging in the dentate gyrus revealed prominent shift from ramified microglial phenotype in sham brains (Figure 2-6A), to a reactive state with larger cell bodies and multiple lobular processes, a phenotype seen ipsilateral to both left and right hemisphere injury. Similarly, GFAP imaging revealed a reactive astrocyte response ipsilateral to both left and right hemisphere injury compared to sham (Figure 2-6B), with extensive hypertrophy of cellular processes. Contralateral left and right injured hippocampus also showed both microglial (Figure 2-6A) and astrocyte (Figure 2-6B) reactivity, but at a much reduced level.

Discussion

The present study revealed that both left and right hemisphere TBI produce cognitive deficits. During the Fixed Platform task probe trial, the expression of reference memory was impaired by both left and right lateral injury, though acquisition was delayed only in the right lateral injury. In contrast, cognitive flexibility deficits measured by reversal acquisition and the reversal probe trial did not differ between left and right hemisphere, yet modest left hemisphere impairments were seen relative to sham.

The left and right lateral injury deficits seen in the Fixed Platform probe trial are consistent with existing left (Chen *et al*, 1998) and right (Shinohara *et al*, 2012) lateral injury reference memory expression deficits. These results support findings that both

hippocampal hemispheres contribute to spatial learning (Shinohara *et al*, 2012). MWM Fixed Platform acquisition deficits (Carbonell *et al*, 1998; Spain *et al*, 2010) have been shown in right hemisphere injury, though contrary to the present findings, others have noted acquisition deficits also from left lateral injuries (Tchantchou and Zhang, 2013; Fox *et al*, 1999). Comparison of left-right hemisphere injury across studies is difficult due to methodological differences, such as post-injury training timing, injury magnitude and model, and varying numbers of training days or trials per day. Accordingly, one unique contribution of the present work was the identical experimental conditions under which left and right hemisphere injury was studied.

The reversal task finding where left lateral injury produced modest MWM performance impairments only relative to sham controls would be intriguing to further investigate at increased injury magnitudes to determine if unilateral injury would reveal a differential vulnerability to cognitive flexibility disruption. Although few rodent TBI studies have employed the MWM reversal task, a left lateral controlled cortical impact injury study reported deficits in a similar task in mice (Zhao *et al*, 2012). Furthermore, superior MWM reversal task accuracy was reported to correlate with larger left mossy fiber projections (Schöpke *et al*, 1991), also true in Collins High-lateralized mice known to exhibit larger left mossy fiber projections (Bernasconi-Guastalla *et al*, 1994). As such, the MWM reversal tasks ability to assess changes in cognitive flexibility may yet prove useful in the study of TBI.

Although the present study did not address mechanisms underlying left and right hemisphere TBI behavioral deficits, the observations reported are consistent with the El-Gaby et al. (2014) theoretical model which accounts for differential use of distinct left-

right hippocampal synapse populations during learning and memory in mice (El-Gaby *et al*, 2014). Specifically, pre-configured CA3-CA1 synapses attributed to stable cell assemblies of the right hippocampus function to facilitate rapid incorporation of spatial information (Nakashiba *et al*, 2008). Left hippocampal CA3-CA1 synapses, however, recruit new place cells to instruct the formation of de novo cell assemblies (Hollup *et al*, 2001) facilitating representation of salient new locations (Leutgeb *et al*, 2007). Consequently, the fixed platform acquisition impairments of right injured mice may reflect a heavier reliance on plastic but slower left CA3-CA1 hippocampal synapses. Whereas left lateral injury reversal task impairments could be explained by heavier reliance on right CA3-CA1 hippocampal assemblies still pre-assigned to the previous Fixed Platform location. An adaptive advantage of such anatomical dissociation could be an efficient division of labor between left and right hemisphere hippocampi.

Neurological motor behavior was also impaired by both left and right lateral injury, though neither the NSS nor Rotarod performance revealed differential left-right hemisphere motor vulnerability to TBI. Despite acute post-injury motor impairments, assessments of sensorimotor and motivational performance in the MWM cued task and MWM swim speeds revealed no impairment for either left or right lateral injuries. This suggests that left-right hemisphere injuries which produced cognitive impairments did not impact MWM sensorimotor performance or impair learning of MWM procedural components.

Left and right hemisphere injury elicited equivalent injury severity as measured by post-injury righting time. Also, neurodegeneration in response to injury measured by cortical lesion volume was not found to differ between left and right hemisphere injury.

Qualitative assessment of the glial response to left and right hemisphere injury demonstrated robust activation of hippocampal microglia and astrocytes ipsilateral to left and right hemisphere injury, reflecting a significant level of traumatic insult. Contralateral hippocampal structures in both left and right injured mice also evidenced modest glial reactivity, consistent with previous reports (Shitaka *et al*, 2012). These data indicate that left and right hemisphere injury generate a similar cellular response to trauma pathology, and suggest that variance in left-right behavioral outcome is not correlated with overt differences in glial reactivity.

Conclusions. Left and right lateral TBI both produced MWM performance deficits in mice, with modest left-right differences. The investigation of left versus right lateral injuries contributes to the understanding of the mouse TBI model. Consequently, laterality in mouse MWM learning and memory impairments may be worthy of consideration for future study design and interpretation in the investigation of TBI-induced cognitive consequences.

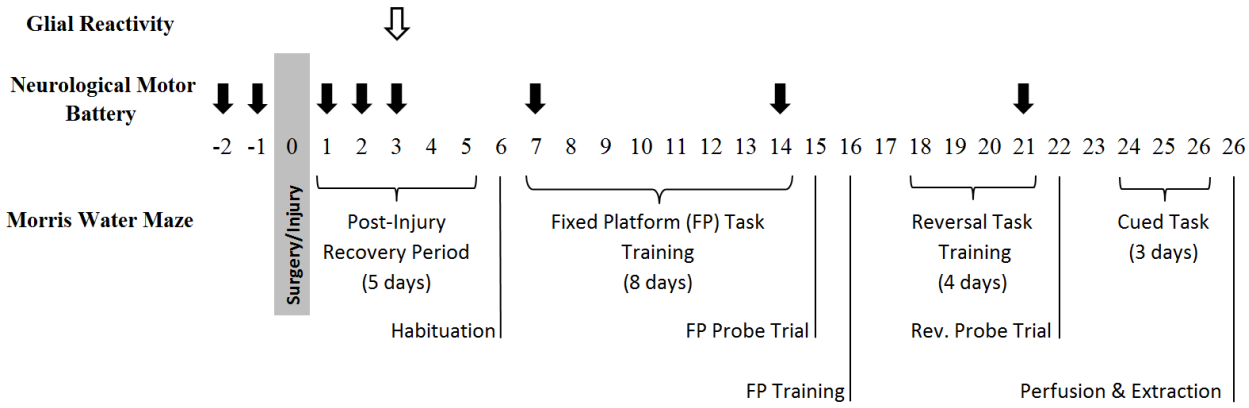

Figure 2-1. **Experimental timeline**. Experimental timeline (relative to injury) of neurological motor battery (indicated by down arrows) and spatial learning and memory tasks of the MWM, for left lateral and right lateral fluid percussion injuries.

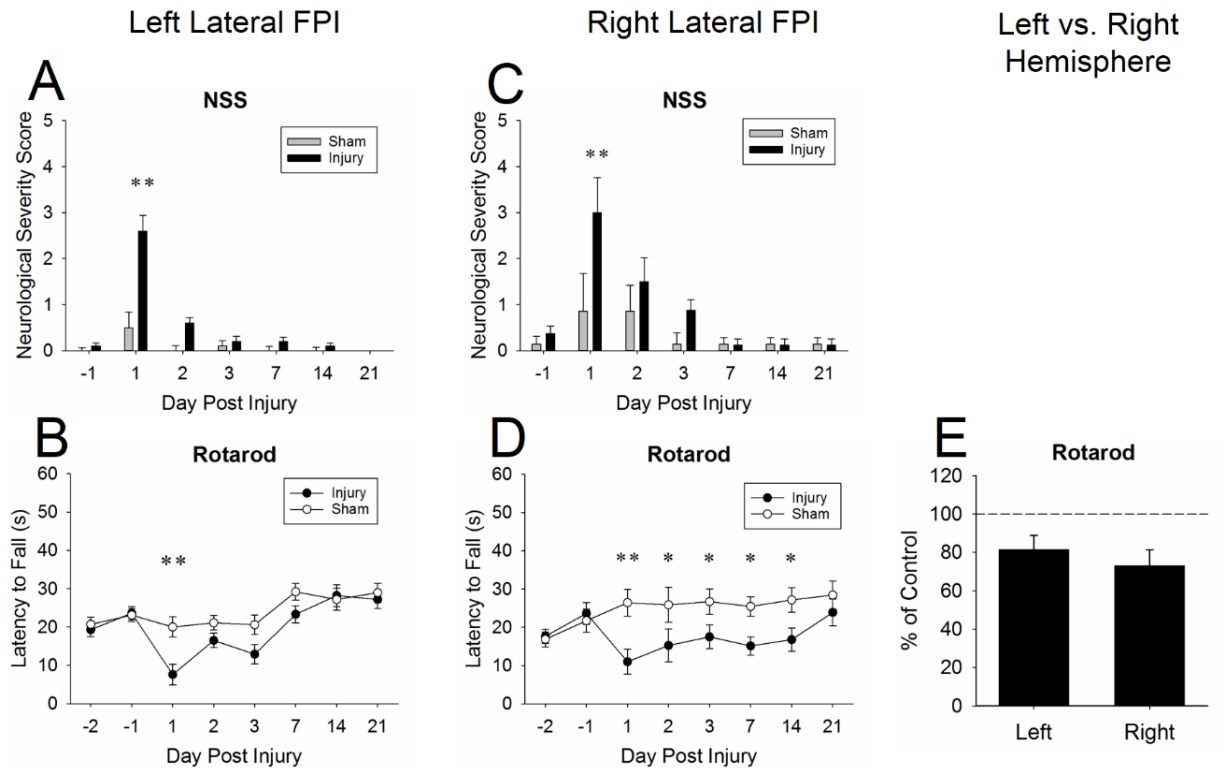

Figure 2-2. **Left and right hemisphere injury produced neurological motor deficits.** NSS scores increased for left (Panel A) and right (Panel C) lateral injury on post-injury day one. Injury also produced impaired rotarod performance in both left (Panel B) and right (Panel D) lateral hemispheres, with no significant difference in performance between hemispheres (Panel E, represents main effect of injury marginal means). Values represent means ±SEM; Panels A and C ***P*<0.01 vs. injury day -1. Panels B and D **P*<0.05, ***P*<0.01 vs. sham.

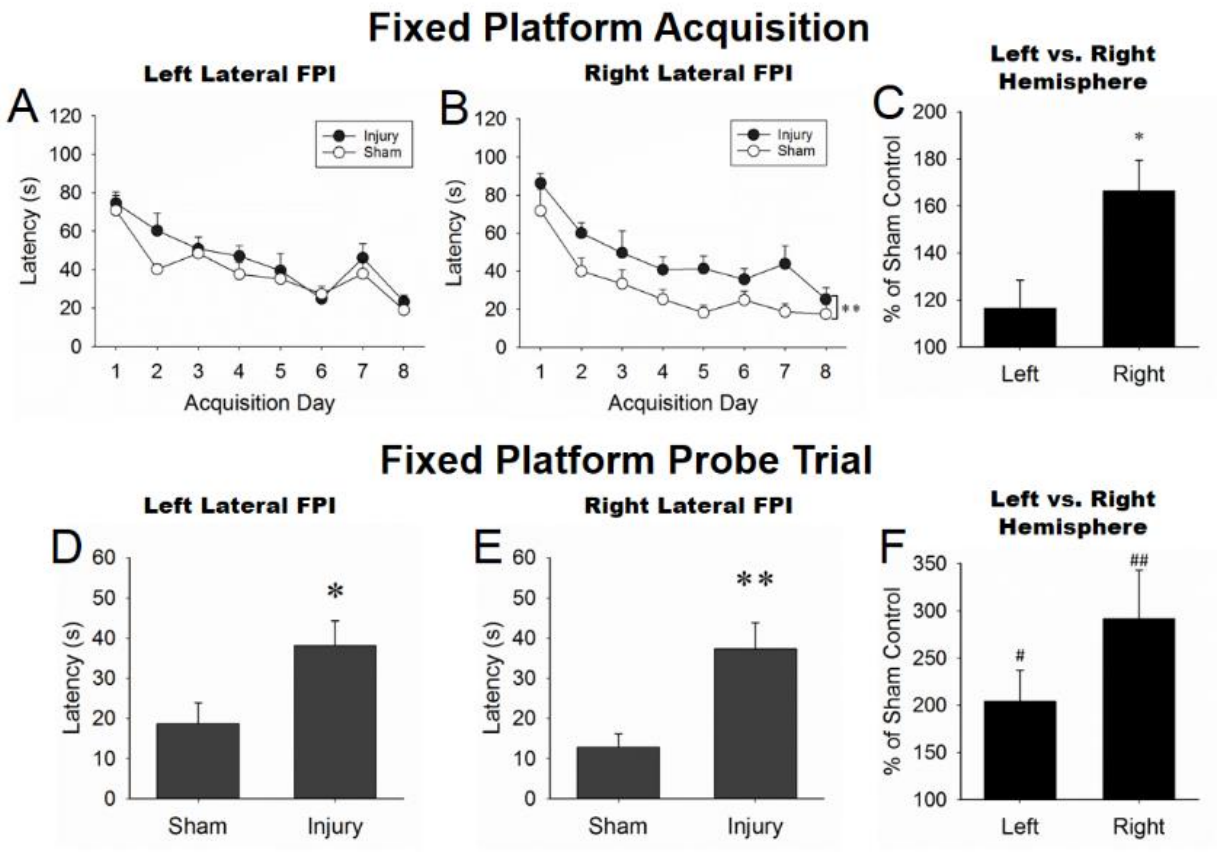

Figure 2-3. **Both left and right lateral injury produced MWM Fixed Platform task deficits.**

During Fixed Platform acquisition (Panels A, B, C) only the right lateral injury (Panel B) showed a small but significant delay in the acquisition of reference memory compared to sham; and compared to left injured animals (Panel C, represents main effect of injury marginal means). During the Fixed Platform Probe trial (Panels D, E, F), both left and right lateral injured mice demonstrated latency impairments relative to sham (Panels D, E, F), but with no left-right differences (Panel F). Values represent mean ±SEM; **P*<0.05, ***P*<0.01 vs. sham; #*P*<0.05, ##*P*<0.01 vs. 100 (sham performance).

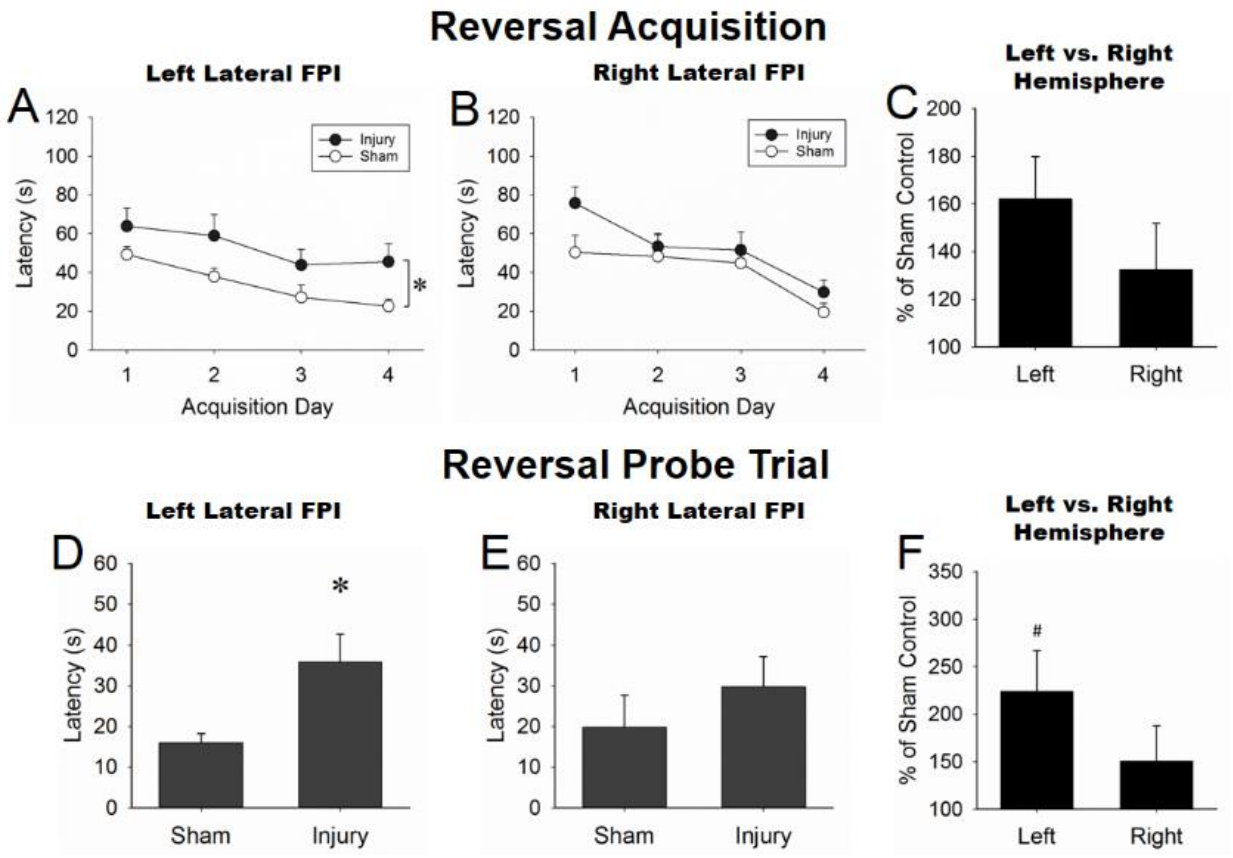

Figure 2-4. **The MWM Reversal Task did not reveal any left-right differential vulnerability to cognitive flexibility.**

Both reversal task acquisition (Panels A, B, C) and reversal probe trial (Panels D, E, F) produced no left-right performance differences in reversal task learning (Panels C [main effect of injury marginal means] and F). However left lateral injury demonstrated modest latency impairments relative to sham in both reversal acquisition (Panel A), and reversal probe trial (Panel D, F). Values represent mean ±SEM; *P<0.05 vs. sham; #P<0.05 vs. 100 (sham performance).

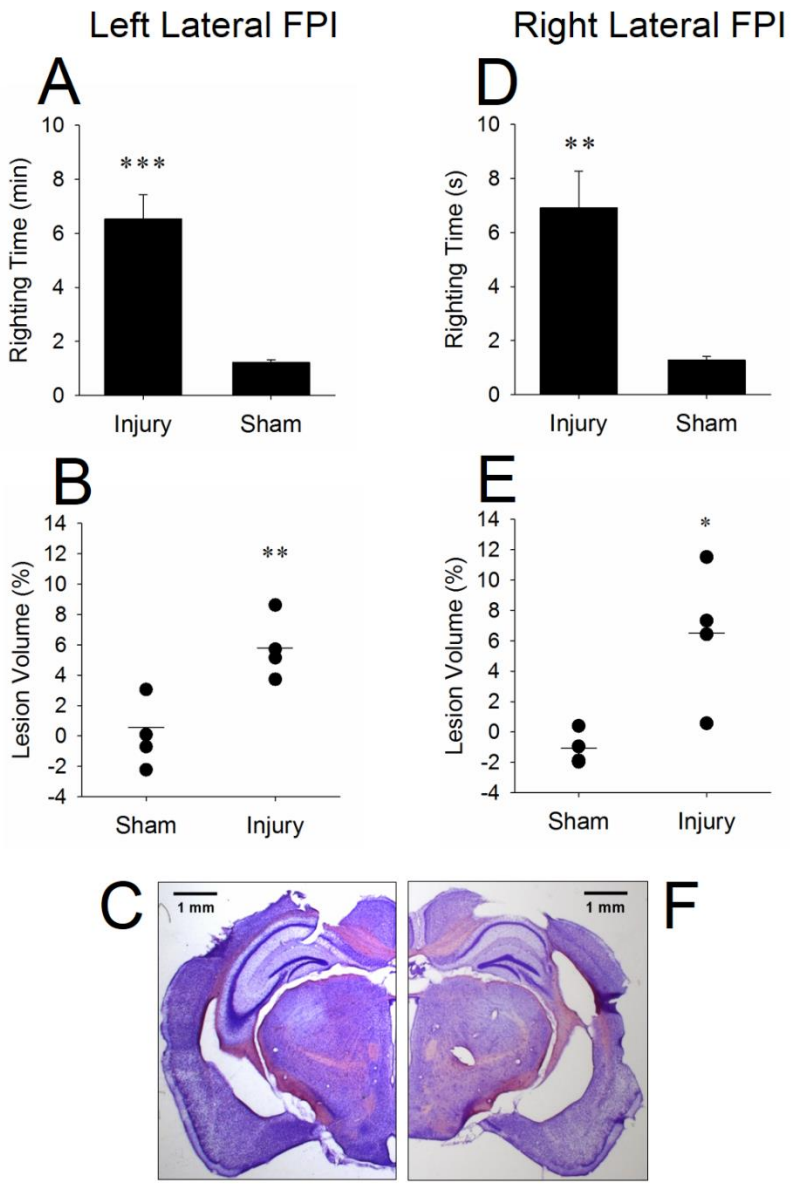

Figure 2-5. **Left and right hemisphere injury produced impaired righting time and histological outcome.**

Both left and right lateral injury produced significantly greater righting times (Panels A, D) and lesion volume %'s (Panels B, E) compared to sham animals. No left-right differences were found in righting time or lesion volume %. Representative coronal sections of left (Panel C) and right (Panel F) lateral injury-induced lesion are shown. Values represent mean ±SEM; *P<0.05, **P<0.01, ***P<0.001 vs. sham.

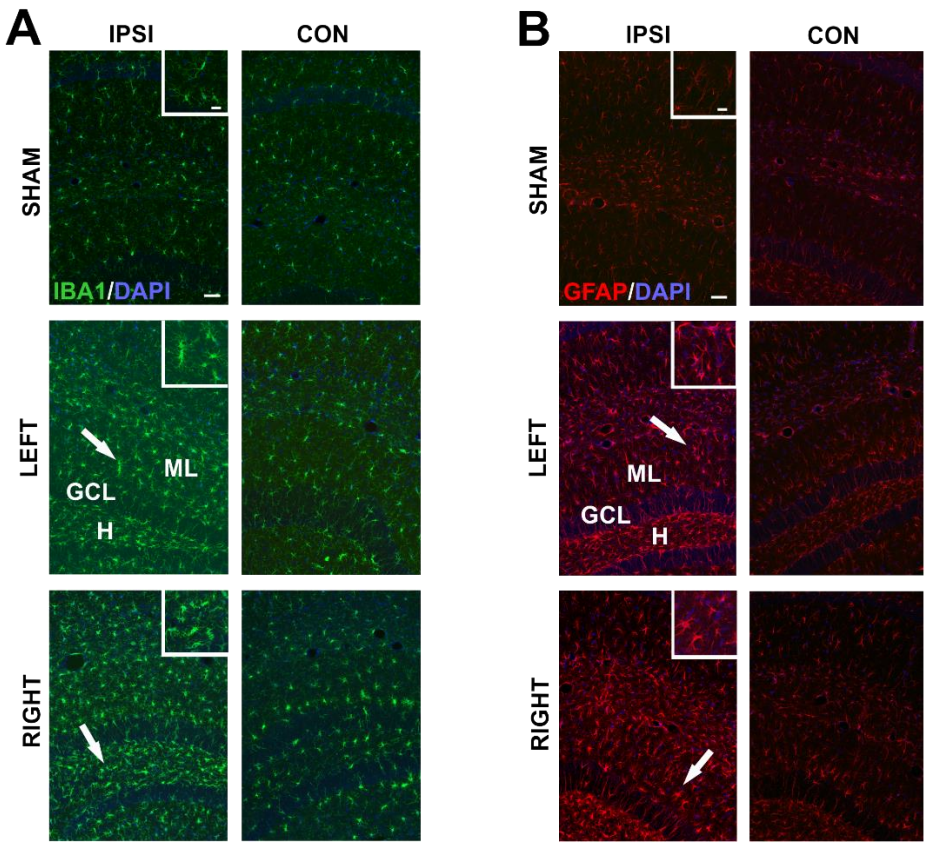

Figure 2-6. **Hippocampal glial cell response to left and right hemisphere injury.** Microglial (IBA1 +; green) morphology (Panel A) showed non-reactive, ramified state within the dentate gyrus of sham controls (see insets for cell detail). A robust reactive phenotype was observed in the dentate gyrus ipsilateral to both left and right hemisphere injury, where microglia exhibited enlarged, rounded cell bodies and lobular processes (arrows; inset). Astrocyte (GFAP +; red) morphology (Panel B) showed thin process bearing stellate cells within the dentate gyrus of sham controls (see insets for cell details). Reactive hypertrophic phenotype, with enlarged cell bodies and increased, thick cell processes (arrows; inset) was seen in the dentate gyrus ipsilateral to both left and right hemisphere injury. Cell nuclei co-stained with DAPI. IPSI= ipsilateral to injury; CON= contralateral to injury; H= hilus; GCL= granule cell layer; ML= molecular layer; Bar = 30 µm large images, 20 µm insets.

Appendix 2. Supplementary Material

Table 2-I. Neurological Severity Score (NSS) for mice

Task	Description	Points	
		Success/Failure	
Exit Circle	Ability & initiative to exit a circle of 30 cm diameter (2 min)	0	1
Mono-/Hemiparesis	Paresis of upper &/or lower limb of the contralateral side	0	1
Straight Walk	Alertness, initiative, & motor ability to walk straight	0	1
Startle Reflex	Innate reflex: mouse will bounce or wince to a loud hand clap	0	1
Seeking Behavior	Physiological behavior as exploration of the environment	0	1
Beam Balancing	Balance on a 7 mm width beam, 25 cm high (10 s)	0	1
Round Stick Balancing	Balance on a 5 mm diameter round stick, 25 cm high (10 s)	0	1
Beam Walk: 3cm	Cross a 30 cm long beam of 3 cm width, 25 cm high	0	1
Beam Walk: 2cm	Cross a 30 cm long beam of 2 cm width, 25 cm high	0	1
Beam Walk: 1cm	Cross a 30 cm long beam of 1 cm width, 25 cm high	0	1
	Maximal Score		10

Table 2-I. **Neurological Severity Score test battery items.**

The modified neurological severity score (NSS) battery of motor, sensory, reflex, and balance tests to assess neurological damage following closed head trauma in mice.

Materials and Methods

Mice. Adult male C57BL/6J mice weighed 24-29 g and age 10-11 weeks at the time of injury. Mice were pair-housed under a 12 h light/12 h dark cycle (0600 to 1800 h), at a constant temperature (22ºC) and humidity (50-60%), with food and water available *ad libitum*.

Craniotomy and Induction of Lateral Fluid Percussion Injury (FPI). The left or right parietotemporal craniectomy was performed between lambda and bregma, approximately 1 mm from the sagittal suture. A 3.5 mm (inside diameter) Leur-Loc syringe hub (modified from a 20G needle) was secured over the craniotomy and surrounded with dental acrylic. After a 2 h recovery period, mice were anesthetized with isoflurane (4%, 400 mL/min). The injury cap was attached to a Leur-Loc fitting and filled with 0.9% NaCl. Mice were then connected to transducer housing of the fluid percussion injury device (AmScien Instruments, Richmond, VA), and immediately subjected to a moderate lateral fluid percussion injury (1.94±0.1 atm left lateral, 1.92±0.1 atm right lateral injury).

The injury was produced by a metal pendulum that struck the piston, transiently injecting a small volume of saline into the cranial cavity and briefly deforming the brain tissue (20-millisecond pulse duration). Immediately following the delivery of the injury, mice were placed on their backs to assess the righting reflex, which was scored as the duration of time to right itself, and was used as an index of traumatic unconsciousness and a correlate of injury severity. In succession, mice were again anesthetized with isoflurane (4%, 400 mL/min), the hub removed, the injury site checked for intactness of

the dura, and the skin sutured. Mice were placed in a recovery cage atop a heating pad for 1 h, then returned to their home cage. Sham-injured controls underwent identical anesthetic and surgical procedures, as well as connection to the injury device, except that the intracranial pressure pulse was not applied.

Rotarod Assay. Each mouse was placed on the device facing the experimenter (forward direction), rotating the drum in the opposite direction. The mice were given one habituation trial to adapt to the testing equipment using a fixed speed of 4 rpm for 60 s. All subsequent single trials per day used an accelerating protocol, starting at 4 rpm and ending at 40 rpm ramping over 60 s, with a 120 s test period. Each trial ended prior to the 120 s cut-off if the mouse fell off the rod, or gripped the device and spun around one full revolution without attempting to walk on the drum.

Neurological Severity Score. In the 10-point Neurological Severity Score (NSS), one point is awarded for failing to perform a particular task, and no points for succeeding. The points of each of the 10 individual tasks are summed to achieve the NSS, in which a score of zero represents a naïve uninjured mouse, whereas a maximal score of 10 indicates severe neurological dysfunction. The NSS (Albert-WeiBenberger *et al*, 2012) has been shown to correlate with severity of brain damage as determined by *in vivo* magnetic resonance studies in mice (Tsenter *et al*, 2008).

Learning and Memory Assessment. The Morris water maze consisted of a circular, galvanized steel tank (1.8 m in diameter, 0.6 m height). The tank was filled with water (maintained at 20ºC±2ºC) with a white platform (10 cm diameter) submerged 1 cm below the water's surface. A sufficient volume of white paint (Valspar 4000 latex

paint, Lowe's Companies Inc., Mooresville, NC) was added to render the water opaque and the platform invisible. In addition to distal visual cues on the walls of the laboratory (shapes), five sheets of laminated paper with distinct black-and-white geometric designs were attached to the sides of the tank serving as proximal cues. Dependant measures were collected using an automated tracking system (ANY-maze, San Diego Instruments, Inc., San Diego, CA).

Fixed Platform Task. The Fixed Platform task was used to assess acquisition of reference memory to a spatial location in the water maze. On post-injury day 6, mice were given a pre-training acclimation session (habituation) during which they were allowed to swim in the pool for 4 min without the platform present. Beginning on post-injury day 7, mice were given eight daily acquisition sessions consisting of four-120 s duration trials per day with an inter-trial interval of 10±2 min. Throughout the course of this acquisition period the hidden platform remained in a fixed position for all mice. Mice were released facing the tank wall from four starting points along the perimeter of the maze arbitrarily designed as N, S, E, W, the order of which was counterbalanced across trials. Once a mouse located the hidden platform, it was allowed to remain there for 15 s before being removed from the tank. If a mouse failed to locate the platform within 120 s, it was manually guided to it and removed 15s later. On post-injury day 15 (i.e., one day following the eighth acquisition day), the platform was removed from the tank, and the mice were subjected to a 60 s probe trial to measure spatial bias for the previous platform location. The percentage of time spent in the target quadrant (where the platform used to be) and control quadrant (the quadrant directly opposite the target

quadrant) was measured, as well as latency to the prior platform location and the number of times the mouse traversed the prior platform location. Given that the Fixed Platform probe trial acts as an extinction trial for prior learning, on post-injury day 16 mice were given a further day of Fixed Platform training in which the hidden platform was returned to the same fixed position as during the acquisition procedure.

Reversal Task. The Reversal task assesses cognitive flexibility, in which the initiation of inhibitory responses is required to explore alternative solution paths. Beginning on post-injury day 18, mice were subjected to a reversal procedure in which the submerged platform was moved to the opposite side of the tank (now within the control quadrant of the Fixed Platform task). Mice were given four daily reversal sessions, with all other task parameters identical to the acquisition procedure. On post-injury day 22, the mice were subjected to another 60 s probe trial, with task parameters identical to the acquisition probe.

Sensorimotor-Motivational Procedure (Cued Task). The Cued task assesses the sensorimotor and motivational capacity of the mice to find the submerged platform irrespective of cognitive ability. Beginning on post-injury day 24, the location of the submerged platform was made known to the mice by the placement of a black cylinder (12 cm height; 4 cm diameter) which extended approximately 11 cm out of the water. Mice were given three cued sessions, during which the location of the submerged platform was changed daily. The first two daily cued sessions consisted of four-120 s length trials each, with an inter-trial interval of 10±2 min, and release was counterbalanced across the four possible start positions (N, S, E, W). The third cued

session consisted of two-120 s length trials, with start positions counterbalanced across the two start positions furthest from the cued platform location.

An automated tracking system (ANY-maze, San Diego Instruments, Inc., San Diego, CA) analyzed the swim path of each subject and calculated escape latencies (the time between being placed in the water and finding the hidden platform), average swim speed, number of platform crossings, and percentage of time spent in each quadrant.

Histology and Lesion Volume Quantification. Animals were anesthetized with sodium pentobarbital, 360 mg/kg, i.p. (administered at 6 ml/kg [60 mg/ml]), and then transcardially perfused with 0.9% saline followed by 4% paraformaldehyde in 0.1 M $NaHPO_4$, pH=7.4. Immediately following, brains were extracted and placed in 4% paraformaldehyde for 24 h before transfer to storage in 0.03% NaN_3 (Sigma Chemical Co., St. Louis, MO, USA) in 1.0 M phosphate-buffered saline (PBS).

Brains were sectioned (50μm thickness) in PBS on a Leica VT1000S vibratome in the coronal plane throughout the rostro-caudal extent of the lesion, extending from approximately -0.5 to -3.5 relative to bregma, and mounted on bovine gelatin and chromium potassium sulfate-treated Superfrost slides (ThermoFisher Scientific, Waltham, MA). Every fifth section was processed with a Nissl stain using cresyl violet acetate and digitally imaged with a Zeiss Discovery V20 StereoZoom microscope using AxioVision.

The area of normal staining (lacking necrosis, cavitation, or hemorrhage), was measured in each section using NIH ImageJ software and a Wacom Intuos4 Digitizing

Tablet. The lesion area was calculated as the area of normal staining on the contralateral side minus that of the ipsilateral side, and then used to calculate the full lesion volume as previously described (Dash *et al*, 2010) using; $(A_1+A_2)*0.5 + (A_2+A_3)*0.5 + \ldots + (A_6+A_7)*0.5$; in which A is the lesion area (mm^2) for each slice and 0.5 (mm) is the distance between two sequential slices. Lesion volume was then expressed as a percentage of remaining normal staining (contralateral + ipsilateral) within whole brain using; [(C-I) / (C+I)] * 100%.

Results

Neurological Motor Deficits: Rotarod main effect of day. The non-significant Mixed-factor ANOVA (2x8) investigating percent of sham control in latency to fall between left and right cohorts also revealed a significant main effect of day $F(7, 112) = 9.82$, $P < 0.001$, with a Bonferroni adjustment revealing significant differences from day -1 to day 1 ($P < 0.01$), day 2, 3, and 7 ($P < 0.05$), and significant differences from day -2 to day 1 ($P < 0.001$), day 2 and 3 ($P < 0.01$), and day 7 ($P < 0.05$).

Fixed Platform Task: main effect of day. In the non-significant Mixed-factor ANOVA (2x8) investigating the acquisition of reference memory, main effects of day were found for left lateral, $F(7, 126) = 13.90$, $P < 0.001$, and right lateral injury, $F(7, 91) = 16.07$, $P < 0.001$. Left and right cohorts demonstrated significantly faster latencies to the platform on days 4-8 than on day 1 (*P value*s < 0.01). The non-significant Mixed-factor ANOVA (2x8) investigating percent of sham control in latencies to the platform between left and right cohorts also did reveal a significant main effect of day $F(7, 112) =$

2.31, $P < 0.05$, despite a Bonferroni adjustment revealing no significant differences between days.

Reversal Task: main effect of day. In the non-significant Mixed-factor ANOVA (2x4) investigating the acquisition of reversal learning, Left lateral, $F(3, 54) = 5.24$, $P < 0.01$, and right lateral, $F(3, 39) = 12.27$, $P < 0.001$, injury cohorts showed a significant main effect of day, with the left cohort demonstrating significantly shorter latencies to the platform on days 3 and 4 compared to day 1 ($P < 0.05$), and the right cohort demonstrating significantly shorter latencies to the platform on day 4 compared to day 1 ($P < 0.001$).

Search strategy. Also, a visual inspection of swim paths suggests that injured animals utilized a looping rather than spatial swim strategy (Zhao *et al*, 2012), though they did not appear to differ between unilateral injury cohorts (left; Supplemental Figure 4G and 5G, right; Supplemental Figure 4H and 5H).

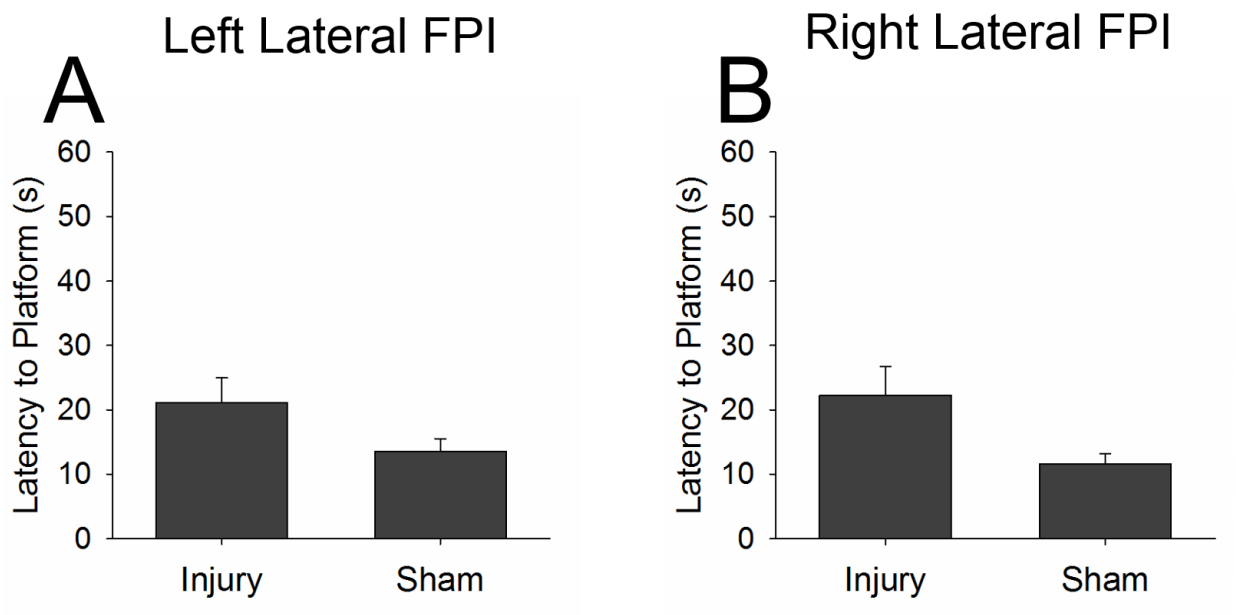

Supplementary Figure 2-1. **MWM Cued task.**

Left and right hemisphere injury produced no difference in sensorimotor and/or motivational performance in the Cued Task of the MWM, as measured by latency to a cued platform location. An independent groups t-test demonstrated no significant difference in latency between either left lateral (Panel 3A; *P = 0.10)*, or right lateral injury (Panel 3B; *P = 0.06)*, and their respective sham controls. Also, when analyzed using a 2 x 2 ANOVA no significant interaction, *P = 0.40*, and no main effects of lateralization, *P = 0.22*, and injury, *P = 0.80* were found. Values represent mean ±SEM.

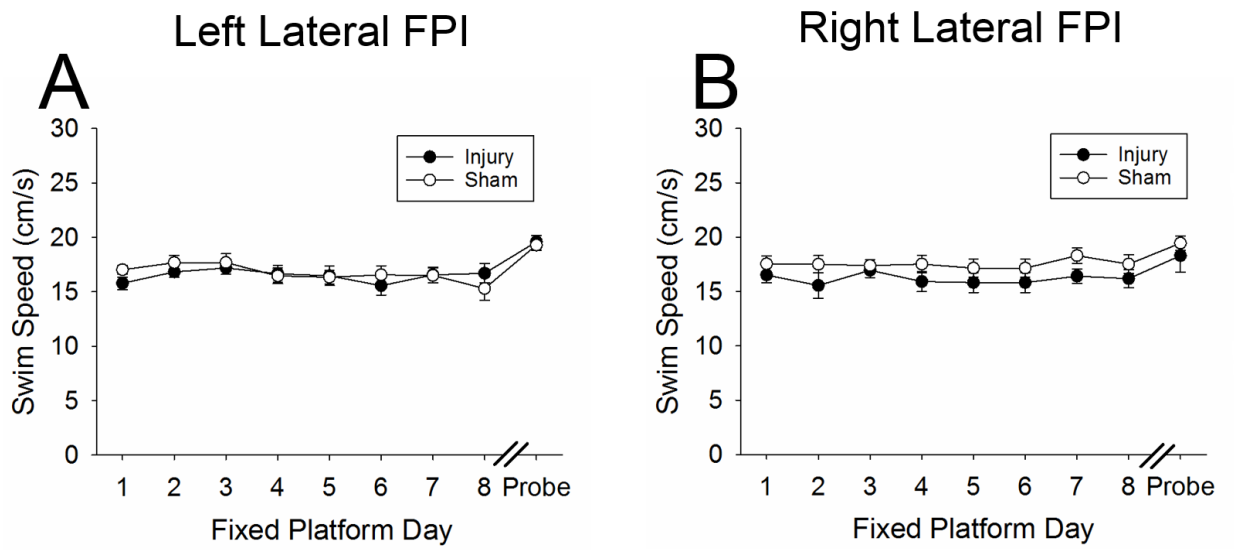

Supplementary Figure 2-2. **Swim speed during the Fixed Platform task.**

Left and right hemisphere injury produced no difference in swimming ability in the Fixed Platform Task of the MWM, as measured by swim speed. Both left lateral injury (Panel 4A) and right lateral injury (Panel 4B) produced no significant difference in swim speed between injured and sham animals across any of the Fixed Platform acquisition days or probe trial. Specifically, in a 2 x 8 mixed factor ANOVA left lateral injury (Panel 4A) had no effect on swim speed during Fixed Platform acquisition, as the interaction between day and injury, $F(7, 126) = 1.39$, $P = 0.21$, main effect of day, $F(7, 126) = 2.02$, $P = 0.06$, and main effect of injury, $F(1, 18) = 0.08$, $P = 0.78$, failed to achieve significance, revealing no difference in swim speed between left lateral injury and sham groups. An independent groups t-test was used to analyze the Fixed Platform probe trial where no difference was found in swim speed between a left lateral injury and sham controls, $t(18) = 0.24$, $P = 0.81$. The right lateral cohort (Panel 4B) also showed no swim speed

differences during Fixed Platform acquisition. In a 2 x 8 mixed factor ANOVA the interaction, $F(7, 91) = 0.41$, $P = 0.89$, main effect of day, $F(7, 91) = 0.83$, $P = 0.56$, and main effect of injury, $F(1, 13) = 2.44$, $P = 0.14$, failed to achieve significance. An independent groups t-test found no difference in swim speed between a right lateral injury and sham controls during the Fixed Platform probe trial, $t(13) = 0.68$, $P = 0.51$. Values represent mean ±SEM.

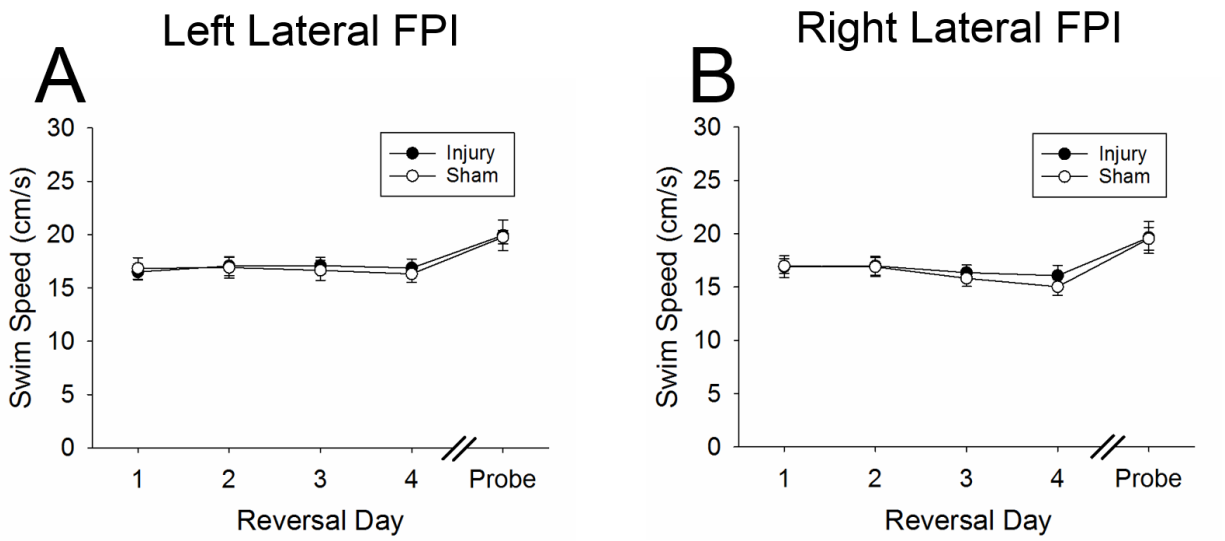

Supplementary Figure 2-3. **Swim speed during the Reversal task.**

Left and right hemisphere injury produced no difference in swimming ability in the Reversal Task of the MWM, as measured by swim speed. Both left lateral injury (Panel 5A) and right lateral injury (Panel 5B) produced no significant difference in swim speed between injured and sham animals during the Reversal acquisition days or probe trial. Specifically, A left lateral injury (Panel 5A) had no effect on swim speed during Reversal acquisition, as the interaction between day and injury, $F(3, 54) = 0.56$, $P = 0.65$, main effect of day, $F(3, 54) = 0.46$, $P = 0.71$, and main effect of injury, $F(1, 18) = 0.03$, $P = 0.86$, failed to achieve significance, revealing no difference in swim speed between left lateral injury and sham groups. An independent groups t-test also found no difference in swim speed between a left lateral injury and sham controls during the Reversal probe trial, $t(18) = 0.11$, $P = 0.91$. In contrast, the right lateral injury group (Panel B) demonstrated a significant main effect of day, $F(3, 39) = 7.68$, $P < .001$, but the

interaction, $F(3, 39) = 1.02$, $P = 0.39$, and main effect of injury, $F(1, 13) = 0.12$, $P = 0.73$, failed to achieve significance. Post-hoc tests did not detect significant differences across Reversal acquisition days (day 1, $P = 0.96$; day 2, $P = 0.95$; day 3, $P = 0.61$; day 4, $P = 0.43$). An independent groups t-test also found no difference in swim speed between a right lateral injury and sham control groups during the Reversal probe trial, $t(13) = 0.06$, $P = 0.95$. Values represent mean ±SEM.

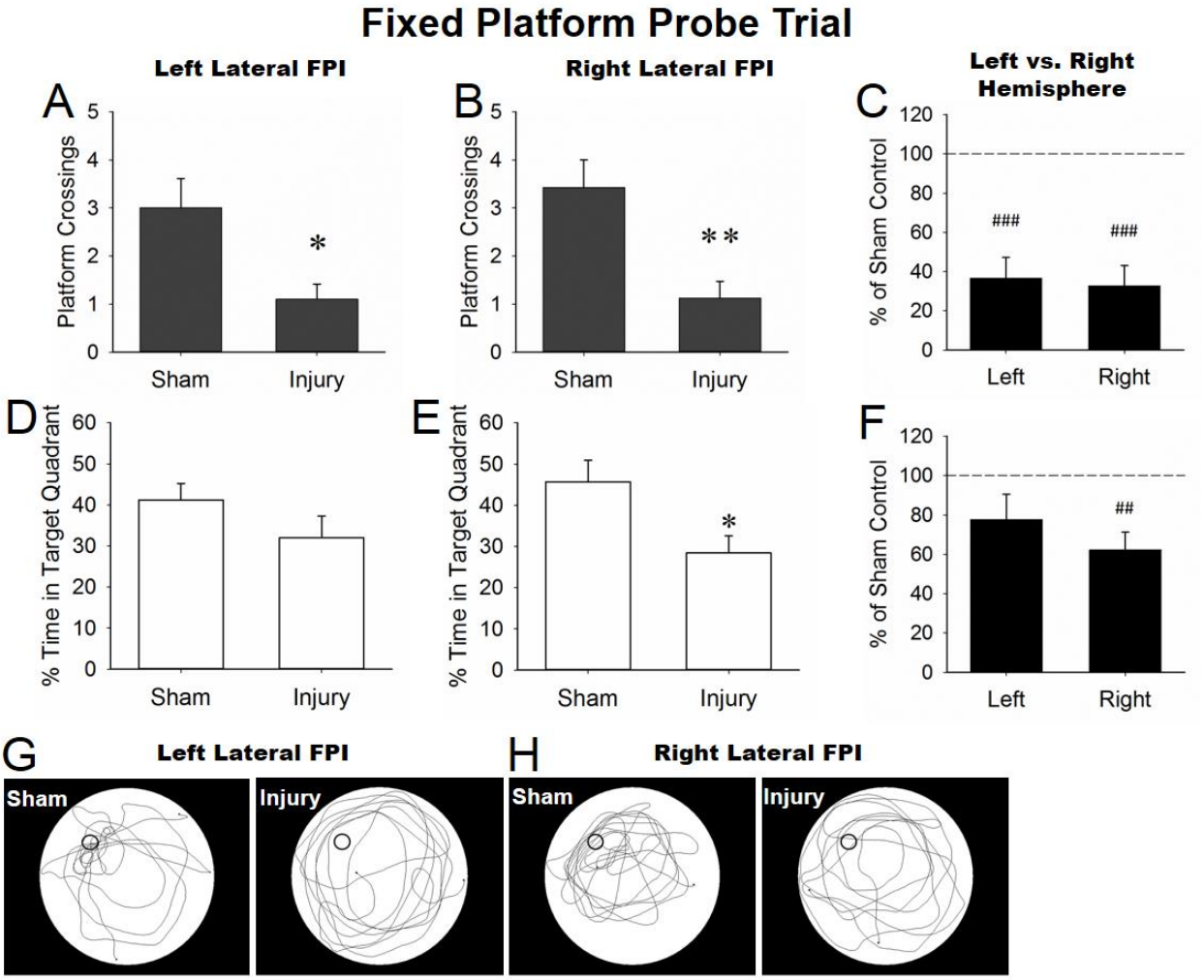

Supplementary Figure 2-4. **Fixed Platform Probe task additional measures.** Independent samples t-tests showed significantly fewer platform crossings in injured animals than sham animals for both left lateral (Panel 1A), $t(18) = 2.75$, $P < 0.05$, and right lateral injuries (Panel 1B), $t(13) = 3.54$, $P < 0.01$. When directly comparing left and right cohorts (Figure 1C), an independent samples t-test revealed no significant percent of sham control difference for platform crossings between left and right hemisphere injury ($P = 0.80$), and a one sample t-test confirmed that both left, $t(9) = 6.04$, $P < 0.001$,

and right, $t(7) = 6.58$, $P < 0.001$, lateral injuries showed significantly poorer performance to their sham controls.

Independent sample t-tests revealed a spatial preference for the target quadrant by sham animals through an increase in percent time spent in the target quadrant in the right (Panel 1E) lateral injury cohort, $t(13) = 2.63$, $P < 0.05$, but not the left lateral (Panel 1D; $P = 0.70$). When directly comparing left and right cohorts (Figure 1F), an independent samples t-test revealed no significant percent of sham control difference in preference for the target quadrant between left and right hemisphere injury ($P = 0.36$), though a one sample t-test found that right, $t(7) = 4.17$, $P < 0.01$, but not left, ($P = 0.12$), lateral injuries showed significantly less of a target quadrant preference to their sham controls. Values represent mean ±SEM; *P<0.05, **P<0.01 vs. respective control; ##P<0.01, ###P<0.001 vs. 100 (sham performance).

A visual inspection of swim paths suggests that injured animals (left; Figure 1G, right; Figure 1H) utilized a looping rather than spatial swim strategy, though they did not appear to differ between unilateral injury cohorts.

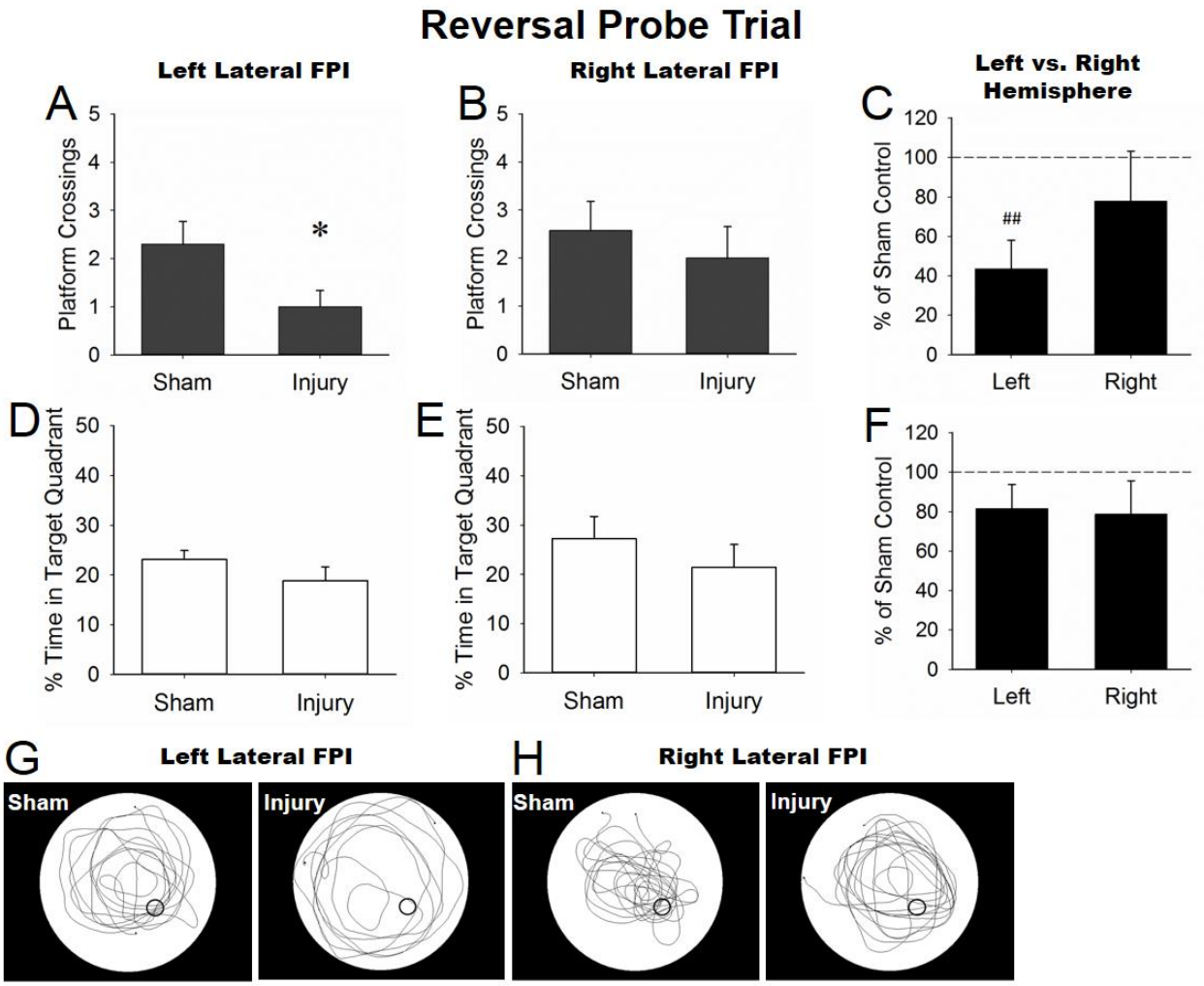

Supplementary Figure 2-5. **Reversal Probe task additional measures.**

Independent samples t-tests showed significantly fewer platform crossings in left injured animals than sham animals (Panel 2A), $t(18) = 2.75$, $P < 0.05$, but not right (Panel 2B), ($P = 0.54$). When directly comparing left and right cohorts (Figure 2C), an independent samples t-test revealed no significant percent of sham control difference for platform crossings between left and right hemisphere injury ($P = 0.13$), yet a one sample t-test showed that left, $t(9) = 3.90$, $P < 0.01$, but not right, ($P = 0.41$), lateral injuries showed significantly poorer performance to their sham controls.

Independent sample t-tests revealed no spatial preference for the target quadrant by sham animals over right (Panel 2E) lateral injury cohort, (P = 0.39), or left (Panel 2D; P = 0.22). When directly comparing left and right cohorts (Figure 2F), an independent samples t-test revealed no significant percent of sham control difference in preference for the target quadrant between left and right hemisphere injury ($P = 0.89$), also, a one sample t-test found that neither right, (P = 0.25), nor left, (P = 0.17), lateral injuries were significantly different in target quadrant preference to their sham controls. Values represent mean ±SEM; *P<0.05 vs. respective control; ##P<0.01 vs. 100 (sham performance).

A visual inspection of swim paths suggests that injured animals (left; Figure 2G, right; Figure 2H) utilized a looping rather than spatial swim strategy, though again they did not appear to differ between unilateral injury cohorts.

Chapter III

Chapter Introduction

The second goal of this dissertation was to investigate the 2-AG biosynthetic production enzyme, DAGL-β, as a novel target for the reduction of TBI-induced cognitive impairment, using DAGL-$\beta^{-/-}$ mice.

Endogenous cannabinoids and inflammatory signaling. The biological processes that drive inflammation act as a protective mechanism in response to pathology (through debris clearing etc), yet they can also lead to tissue damage and neurodegeneration if chronic and self-perpetuating. The eCB system plays important dual roles in inflammation; indirectly through the production of precursors for soluble immunoactive molecules, as well as directly through synaptic cannabinoid receptor signaling. It is possible that the eCB system may possess biphasic roles; resolution of inflammation through cannabinoid receptors, yet perpetuate chronic states of inflammation (often still present years following a TBI) through pro-inflammatory downstream eCB metabolites. While the biological role played by the eCB system has frequently been described as pro-homeostatic, the full implications of the interaction between inflammatory mechanisms and the eCB system are thus still unfolding.

One of the main mediators of the eCB-eicosanoid signaling pathway is the endogenous cannabinoid ligand 2-arachidonoylglycerol (2-AG), which serves as a major precursor for the formation of free arachidonic acid (AA) in brain. 2-AG is formed from

diacylglycerol lipase (DAGL) (Nomura *et al*, 2011) and hydrolyzed to AA predominantly by monoacylglycerol lipase (MAGL) (Nomura *et al*, 2011) but also to a lesser extent by serine hydrolase α-β-hydrolase domain 6/12 (ABHD6/12) (Blankman *et al*, 2007). In turn, AA is a major substrate for the biosynthetic enyzmes of pro-inflammatory prostanoids (e.g. prostaglandins), which play a role in cytokine release (Nomura *et al*, 2011). Cytokines further regulate inflammation, influence microglial activation sates, induce the activation of neurotoxic astrocytes, as well as contribute to neurodegeneration following TBI, one such example being that IL-1β release stimulates glutamate-mediated synaptic transmission (Viviani *et al*, 2003) and limits GABA-mediated inhibitory transmission (Rossi *et al*, 2012), resulting in hyperexcitation and potential excitotoxic neurodegeneration. Although the second main endogenous cannabinoid ligand anandamide (AEA) is also metabolized to AA, it does not account for appreciable free AA in brain, likely due to its being 1000 times less abundant than 2-AG (Blankman and Cravatt, 2013; Sugiura *et al*, 1995).

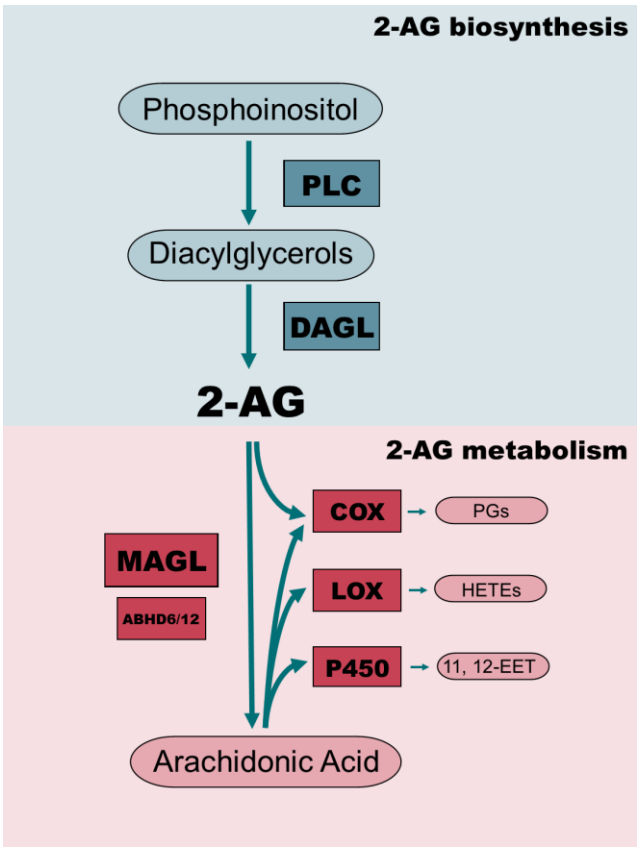

Figure 3A: 2-AG-Eicosanoid Signaling Pathway

The prostanoids produced by eCB catalysis exist under physiological conditions in almost trivial amounts, their biological importance being marginal (Ricciotti and

FitzGerald, 2011). However, in response to acute inflammation as occurs immediately following neurotrauma, prostanoid levels rapidly increase prior to the infiltration of immune cells – perhaps a consequence of 2-AG's dynamic production capacity, e.g. increases being found two minutes following an inflammatory challenge (Liu *et al*, 2003). Therefore, this eCB-eicosanoid signaling pathway can also be understood as a primed homeostatic rapid-response system.

DAGL-β: 2-AG biosynthesis and localization. Compelling evidence suggesting that the eCB system plays a distinct immunomodulatory role outside of receptor signaling, is the expression of DAGL in species that do not express cannabinoid receptors (e.g. Drosophila) (Elphick and Egertova, 2005). The DAGL enzyme is a multi-domain serine hydrolase, the family of which consists of approximately 200 enzymes. Two DAGL isoforms exist, both of which produce 2-AG, DAGL-α and DAGL-β, and are found in a wide range of species including rodents and man (Bisogno *et al*, 2003a). Both DAGL-α and DAGL-β have 4-transmembrane domains and are expressed at the plasma membrane in ordered microdomains. A great deal of structural conservation exists between these isoforms, with the main difference being the substantial carboxy-terminal tail of DAGL-α.

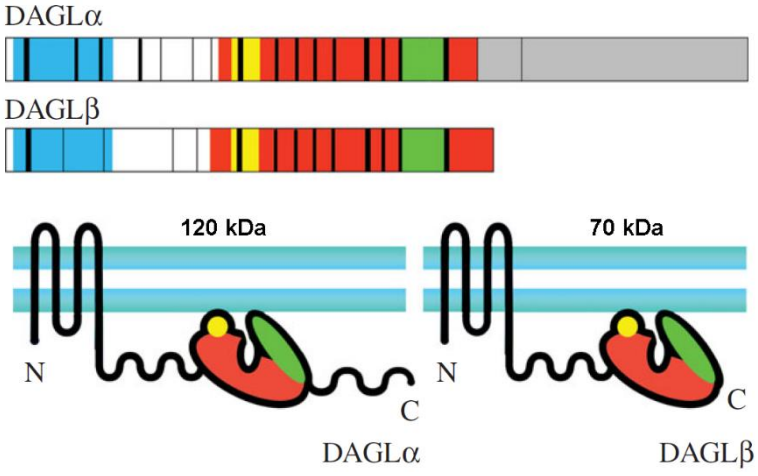

Figure 3B: The exon structure and schematics of DAGL-α and DAGL-β. The transmembrane domain is in blue, the catalytic domain in red (with a cysteine rich area in yellow), the regulatory loop in green, and the C-terminal tail in grey. (Adapted from Reisenberg et al, 2012).

The relative contribution of each isoform to 2-AG production

is determined by their respective cellular location. DAGL-α is found predominantly on neurons (with a major role in synaptic plasticity (Gao *et al*, 2010) and DAGL-β is most highly expressed on CNS microglia and peritoneal macrophages (playing an important role in inflammatory responses (Hsu *et al*, 2012). While DAGL-α is expressed on neurons and especially in areas important for learning and memory (hippocampus, striatum, and prefrontal cortex (Katona *et al*, 2006; Lafourcade *et al*, 2007), the expression pattern of DAGL-β is less well understood (Oudin *et al*, 2011), though DAGL-β mRNA has been found to be high in hippocampus (Gao *et al*, 2010) and the cerebellar granular layer (Yoshida *et al*, 2006).

Microglia: function, and the endocannabinoid system. The term "microglia" was first coined by Pio del Río-Hortega early in the 20th century (Del Río-Hortega, 1932). Unlike other CNS resident cells such as neurons and astrocytes (which are derived from CNS resident progenitor cells), microglia arise from hematopoietic stem cells in blood islands of the yolk sac during early embryogenesis, and then migrate through the embryo vascular system to the brain (Naito *et al*, 1990). As such, microglia share a common myeloid progenitor cell lineage with monocytes/macrophages and have common properties, such as expression of similar markers (e.g. CD11b) (Perry *et al*, 1985). Classified as mononuclear phagocytes, microglia act under the protection of the BBB in response to neuroinflammation, moderating CNS damage and favoring tissue repair, as well as participating in the resolution of inflammation. In the healthy CNS, microglia also control neuronal proliferation and differentiation, as well as the formation of new synapses (Graeber, 2010; Hughes, 2012).

To perform their assorted functions, microglia adopt various phenotypic activation states characterized by changes in morphology, cytokine secretion, and marker expression, largely depending on local environmental cues (Martinez and Gordon, 2014). The M0 phenotype is that of the surveillant microglia, ramified in morphology and present under homeostatic conditions. In CNS pathology, microglia become activated to an M1 pro-inflammatory/phagocytic phenotype in which the cell acquires an ameboid morphology with diminished number and length of processes and enlarged soma (Stence *et al*, 2001). M2a and M2b phenotypes are used to describe alternatively activated microglia, associated with tissue remodeling and immunoregulation

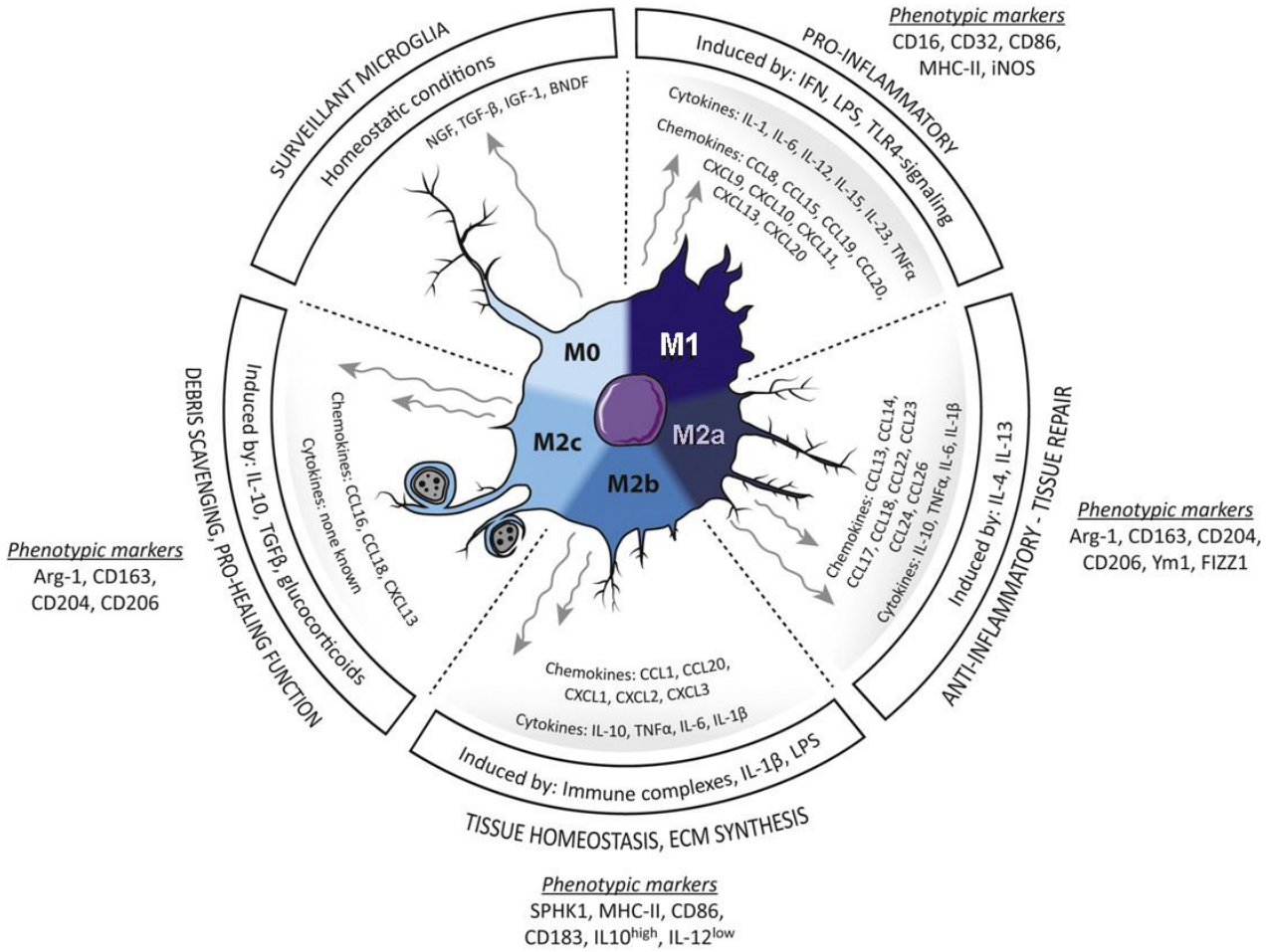

Figure 3C: Microglial phenotypes, markers, and actions (Adapted from Mecha et al, 2016)

(Ponomarev *et al*, 2007). The acquired deactivated phenotype of M2c is induced by immunosuppressive cytokines and further contributes to inflammation resolution (Mecha *et al*, 2016).

Microglia express functional components of the eCB system: cannabinoid receptors (CB_1 and CB_2) and machinery for the biosynthesis and degradation of 2-AG and AEA (Mecha *et al*, 2016), suggesting novel functions of eCBs in autocrine and/or paracrine control of neuroinflammation. Specifically, microglial 2-AG increases 2- to 3-fold in response to calcium ionophore exposure, and increases microglial proliferation via the CB_2 receptor (Carrier *et al*, 2004). Other components of the eCB system also change with microglial activation states. CB_2 receptors, which in healthy brain tissue are present only in trace amounts (Maresz *et al*, 2005), show increased expression during M2 polarization with IL-4 (Mecha *et al*, 2015). Also, some evidence suggests that DAGL-β may be a dynamically regulated enzyme. Mecha *et al*, 2015 found that DAGL-β expression showed non-significant decreases during M1 phenotypes, and elevations during M2c (acquired deactivated) phenotypes in primary cell culture. However, the contributions eCB microglial expression have on processes of neuroinflammation remains to be determined. This avenue of inquiry is of particular interest following TBI given the potential for increased intracellular pools of 2-AG to act as substrate for microglial eicosanoid production.

Microglia and neurotrauma. A rapid and controlled activation of the immune system following TBI is necessary to minimize injury and repair damage. The phenotypes and subsequent functional profiles of microglia change in response to signals detected in the brain parenchyma. Release of adenosine triphosphate (ATP)

(Davalos *et al*, 2005) and extracellular calcium wave propagation (Sieger *et al*, 2012) following injury promote polarization from surveillant (M0) to pro-inflammatory (M1) microglia, as well as proliferation and migration to the site of injury. At the lesion site, microglia fuse to form a barrier between healthy and damaged cells (microgliosis), perform cell debris removal (phagocytosis), and release various effector substances including nitric oxide, proteases, and cytokines. Microglia play a central role in secondary injury processes when a shift to the anti-inflammatory M2 phenotype (of angiogenesis, extracellular matrix reconstruction etc) is not prompted, perpetuating pro-inflammatory responses associated with further CNS damage, compromised BBB, enhanced peripheral macrophage infiltration, and chronic release of further cytokines, cytotoxic superoxide, nitric oxide, and proteases. Increased microglia activation can be present for decades following a TBI (Donat *et al*, 2017; Ramlackhansingh *et al*, 2011), and has been associated with increased risk of neurodegenerative disease such as Alzheimer's Disease (Plassman *et al*, 2000).

Targeting DAGL-β to treat TBI. Studies of enzyme inhibition downstream of 2-AG production have thus far produced mixed results in attenuating TBI functional deficits. Inhibition of 2-AG degradative enzymes has shown both improvement and a lack of improvement in neurological motor (Katz *et al*, 2015; Zhang *et al*, 2014) and learning and memory assessments (Tchantchou and Zhang, 2013; Zhang *et al*, 2014). This contradictory evidence is perhaps attributable to the direct oxidation of 2-AG by COX-2 (Straiker *et al*, 2011), which produces prostaglandin glycerol esters (Hu *et al*, 2008; Sang *et al*, 2007). COX inhibition has also shown both improvement and a lack of improvement in neurological motor assessments (Cernak *et al*, 2002; Girgis *et al*, 2013)

and learning and memory assessments (Cernak *et al*, 2002; Dash *et al*, 2000), perhaps a consequence of the availability of alternative AA metabolism pathways such as the lipoxygenases (Maccarrone *et al*, 2000) and cytochrome P450 enzymes (Chen *et al*, 2008). Given the complex degradation pathways of 2-AG, we propose that targets upstream of production, specifically the biosynthetic enzymes of 2-AG synthesis, warrant further investigation as to their injury-protective potential when disrupted.

The spatial specificity of 2-AG production provided by the distinct cellular expression of DAGL-α and -β might be particularly useful following traumatic brain injury. We anticipated that disruption of DAGL-β would not significantly impede neuronal 2-AG production. Indeed, DAGL-α deletion leads to profound adverse phenotypic consequences such as memory impairment and changes in neuronal excitability in mice (Sugaya *et al*, 2013), as well as impairing AA signaling and function, such as membrane fluidity and regulation of ion channels (Piomelli, 1996). However, deactivating 2-AG production specifically in microglial cells through DAGL-β could reduce the capacity for pro-inflammatory signaling by 2-AG in its role as metabolic intermediate thus affording cognitive deficit protection following TBI. As such, DAGL-β inactivation could reduce inflammatory processes in microglial cells, without disrupting other adaptive functions of 2-AG and its downstream pathways.

Summary. The following work evaluates DAGL-β as a novel target for the reduction of TBI-induced cognitive deficit, using the working hypothesis that disrupting DAGL-β activity will provide cognitive protection from brain injury by reducing pools of 2-AG pro-inflammatory metabolites, specifically in microglia. An unexpected finding that DAGL-β deletion produced a survival protective phenotype prompted further

investigation into the extent of this mortality protective effect. This investigation of the neuroprotective effects of DAGL-β following TBI thus considers the unexpected and provocative possibility that DAGL-β contributes to acute brain injury pathology.

Targeting diacylglycerol lipase-β to treat traumatic brain injury

Introduction

A rapid and controlled immune response to traumatic brain injury (TBI) is necessary to minimize further injury and initiate repair processes. The increase of brain endogenous cannabinoid (eCB) levels following TBI (Panikashvili *et al*, 2001) suggests the eCB system may play a role in such essential repair mechanisms. Shortly following an initial injury, acute neuroinflammatory processes are triggered as part of a cascade of secondary injury mechanisms. The acute neuroinflammatory response includes activation of resident central nervous system (CNS) immune cells, microglia, to an M1 profile and the release of proinflammatory mediators (as well as proliferation and migration to the injury site (microgliosis), and cell debris removal (phagocytosis).

TBI can be thought of not only in terms of an acute event, but fundamentally as a chronic disease. Adaptive inflammatory immune responses to TBI can be perpetuated over time by high levels of pro-inflammatory eicosanoids (prostaglandins and cytokines) in damaged tissue, prompting a continued state of chronic inflammation. An unsuccessful resolution of inflammation is frequently seen following TBI in which persistent and dysfunctional inflammation promotes a failure to shift microglia from a pro-inflammatory M1 phenotype to an anti-inflammatory M2 phenotype (which would prevent angiogenesis, and promote extracellular matrix integrity resolution and tissue repair, Sica and Mantovani, 2012; Mantovani et al., 2013). An increase in neuroinflammation accompanied by activated microglial phenotypes has been observed in humans for years after injury (Johnson *et al*, 2013), as well as chronically in murine

TBI models (Holmin and Mathiesen, 1999). The prolonged nature of chronic neuroinflammation is then linked to further neurodegeneration through synaptic alterations (Centonze *et al*, 2009) as well as a compromised blood brain barrier (enhancing CNS infiltration of peripheral macrophages further promoting inflammation). Neuroinflammation is widely linked to learning and memory deficits, producing changes in expression and composition of AMPA receptors (Stellwagen *et al*, 2005), promoting neuronal hyperexcitability (Rossi *et al*, 2012), and impairing long-term potentiation induction and maintenance (Murray and Lynch, 1998). The learning and memory deficits commonly seen in clinical TBI cases can persist for decades after injury, consistent with such neuroinflammatory temporal profiles.

Understanding of the eCB system has recently evolved to include important contributions toward inflammatory eicosanoid production. The most abundant eCB in brain, 2-arachidonyl glycerol (2-AG), serves not only as a signaling molecule during neurotransmission (Hillard, 2000a), but also as an intermediate during lipid metabolism (Nomura *et al*, 2011). The hydrolysis of 2-AG by its predominant catabolic enzyme monoacylglycerol lipase (MAGL) provides the major pool of arachidonic acid (AA) for the generation of inflammatory eicosanoids in brain (Nomura *et al*, 2011). 2-AG production is regulated by two distinct enzymes in a cell specific manner. Diacylglycerol lipase-α (DAGL-α) is responsible for 2-AG biosynthesis in neurons and astrocytes whereas diacylglycerol lipase-β (DAGL-β) regulates 2-AG predominantly on immune cells (microglia in brain and peritoneal macrophages in the periphery) (Bisogno *et al*, 2003a). DAGL-β regulates pro-inflammatory responses in mammalian macrophages, with DAGL-β disruption attenuating pro-inflammatory responses in peripheral tissues

(Hsu *et al*, 2012; Wilkerson *et al*, 2016). Given DAGL-β is readily expressed in brain (Gao *et al*, 2010; Yoshida *et al*, 2006), and its disruption perturbs microglia eCB-eicosanoid crosstalk (Viader *et al*, 2015a), this enzyme is also likely to play a role in CNS neuroinflammation. Bulk levels of brain 2-AG are controlled predominantly via DAGL-α, as DAGL-$\alpha^{-/-}$ mice show a 90% reduction of brain 2-AG (Gao *et al*, 2010; Tanimura *et al*, 2010), whereas DAGL-$\beta^{-/-}$ mice show either a 50% reduction (Gao *et al*, 2010) or no change (Hsu *et al*, 2012; Tanimura *et al*, 2012; Viader *et al*, 2015a). DAGL-β likely plays a smaller role in establishing bulk 2-AG levels than DAGL-α as microglia compose only 5-12% of CNS cells (Lawson *et al*, 1990). As such, DAGL-β could represent a target to attenuate neuroinflammation given its unique expression profile on microglia in brain without producing global CNS alterations of 2-AG tone.

We hypothesize that DAGL-β participates in TBI-induced neuroinflammation contributing towards subsequent learning and memory deficits. We therefore investigated DAGL-β as a novel target for the reduction of TBI-induced spatial learning and memory impairments in mice, predicting that disruption of DAGL-β activity would provide cognitive protection from TBI by reducing pools of microglial 2-AG pro-inflammatory metabolites. Given that selectivity and brain permeability of subtype selective DAGL inhibitors are yet to be optimized (Janssen and van der Stelt, 2016), we utilized DAGL-$\beta^{-/-}$ and -$\beta^{+/+}$mice in the present studies. We also investigated if blocking 2-AG production on other cell types would offer protection from TBI functional deficits. DAGL-α is primarily expressed on neurons (and also astrocytes) (Katona *et al*, 2006), therefore we conducted an experiment to assess if DAGL-$\alpha^{-/-}$ mice would be protected

against TBI-induced spatial memory deficit, however high mortality rates precluded systematic investigation.

Materials and Methods

Animals. Subjects consisted of adult male DAGL-$\beta^{-/-}$, and -$\beta^{+/+}$ mice (females were included in the mortality experiment only) and male DAGL-$\alpha^{-/-}$, and -$\alpha^{+/+}$ mice, on a mixed 99% C57BL/6 (50% J [Jackson Laboratories, Bar Harbor, Maine], 50% N [Charles River, Wilmington, Massachusetts]) and 1% 129/SvEv background, as previously described (Hsu *et al*, 2012). DAGL-$\beta^{+/-}$ and -$\alpha^{+/-}$ mouse breeding pairs were originally generated in the Cravatt laboratory and transferred to Virginia Commonwealth University. All mice (age 8-10 weeks) were pair-housed under a 12 h light/12 h dark cycle (0600 to 1800 h), at a constant temperature (22ºC) and humidity (50-60%), with food and water available *ad libitum*. All experiments were conducted in accordance with the National Institute of Health (NIH) Guide for the Care and Use of Laboratory Animals (NIH Publications No. 8023, revised 1978), and were approved by the Virginia Commonwealth University Institutional Animal Care and Use Committees.

Craniectomy and induction of lateral fluid percussion injury (FPI). Mice were anesthetized with isoflurane (2.7%, 250 mL/min) and inserted into a stereotaxic frame. A sagittal incision was made in the scalp and a 2.7 mm craniotomy was performed with a trephine over the left parietotemporal cortex between lambda and bregma and approximately 1 mm from the sagittal suture, keeping the dura intact. A 3.5 mm (inside diameter) luer-Lok syringe hub (modified from a 20G needle) was secured over the

craniotomy and surrounded with dental acrylic. Mice were then placed in a recovery cage atop a heating pad.

After a 2 h recovery period, mice were anesthetized with isoflurane (4%, 400 mL/min). An injury cap was attached to the Leur-Lock fitting and filled with 0.9% NaCl. Mice were then connected to transducer housing of the FPI device (AmScien Instruments, Richmond, VA), and immediately subjected to lateral FPI (behavioral assessment experiment; 1.94±0.1 atm, mortality experiments; 2.0±0.1 atm and 2.17±0.1 atm). The injury was produced by a metal pendulum that struck the piston, transiently injecting a small volume of saline into the cranial cavity and briefly deforming the brain tissue (20-millisecond pulse duration). The pressure pulse force was measured extracranially with a transducer, recorded on a storage oscilloscope, (expressed in atmospheres of pressure). In succession, mice were again anesthetized with isoflurane (4%, 400 mL/min), the hub removed, the injury site checked for intactness of the dura, and the skin sutured. Mice were placed in a recovery cage atop a heating pad for 1 h, after which they were returned to their home cage. Sham-injured controls underwent identical anesthetic and surgical procedures, as well as connection to the injury device, except that the intracranial pressure pulse was not applied.

Physiological Measures. Immediately following the delivery of the injury, mice were placed on their backs to assess the righting reflex, which was scored as the duration of time to right itself, and was used as an index of traumatic unconsciousness. When mortality occurred it did so within 2 min following the initial injury, otherwise mice survived until the end of the 34 day experiment. Therefore, during the separate mortality experiments at increased injury severity, mortality was considered acute mortality and a

2 min post-injury cut off was applied. Body weight was taken prior to craniectomy surgery (day 0) and considered baseline, and then recorded daily for the duration of the MWM assessments (until day 30 post-TBI). On day 34 post-TBI, rectal temperature was taken to evaluate body temperature by inserting a thermocouple probe (2 cm) into the rectum. A baseline rectal temperature was recorded, then further assessments were made at 1, 3, 10, and 30 min post-2 min MWM swim.

Morris water maze assessments. The MWM consisted of a circular, galvanized steel tank (1.8 m in diameter, 0.6 m height). The tank was filled with water (maintained at 20º C ± 2º C) with a white platform (10 cm diameter) submerged 1 cm below the water's surface. A sufficient volume of white paint (Valspar 4000 latex paint, Lowe's Companies Inc., Mooresville, NC) was added to render the water opaque and the platform invisible. In addition to distal visual cues (shapes) on curtains surrounding the tank (30 cm from the tank wall), five sheets of laminated paper with distinct black-and-white geometric designs were attached to the sides of the tank serving as proximal cues. An automated tracking system (ANY-maze, San Diego Instruments, Inc., San Diego, CA) analyzed the swim path of each subject and calculated distance (path length between being placed in the water and finding the hidden platform), average swim speed, number of platform crossings, and percentage of time spent in each quadrant as well as in the outer ring.

After induction of the FPI, mice were given a five day post-injury recovery period prior to commencing learning and memory assessment (see Fig. 1A). On post-injury day 6, mice were given a pre-training acclimation session (habituation) during which they were allowed to swim in the pool for 4 min without the platform present. To assess

reference memory DAGL-$\beta^{-/-}$ and -$\beta^{+/+}$ mice received 8 MWM Fixed Platform acquisition training days (i.e. a submerged platform remained in the same location across days) each day consisting of four-120 s duration trials separated by 10±2 min inter-trial intervals. Four points along the perimeter of the maze arbitrarily designed as N, S, E, W, served as starting points from where the mice were released, facing the tank wall. The order of release location was counterbalanced across trials with each point used only once per acquisition day. Once a mouse located the hidden platform, it was allowed to remain there for 15 s before being removed from the tank. If a mouse failed to locate the platform within 120 s, it was manually guided to it.

Assessment for the expression of spatial memory occurred the next day (post-injury day 17) in a single MWM Fixed Platform Probe Trial (to measure spatial bias for the previous platform location where the submerged platform was removed from the tank). Given that the Fixed Platform probe trial acts as an extinction trial for prior learning, on post-injury day 18 mice were given a further day of Fixed Platform training in which the hidden platform was returned to the same fixed position as during the acquisition procedure.

Reversal learning and cognitive flexibility were assessed using a Reversal task in which the submerged platform was moved to a new location. Thus, mice first must inhibit responses swimming to the original platform location before exploring alternative solution paths. In the Reversal training task, mice were given four daily reversal sessions, with all other task parameters identical to the acquisition procedure, followed again by a 2 min probe trial on day 25 post-injury.

A cued task assessed mice for potential sensori-motor/motivational deficits. The platform location was made visible by placing a 10 cm high, 4 cm diameter black cylinder on the submerged platform (assessing the capacity of the mice to find the submerged platform irrespective of reliance on spatial cues). Mice were given three cued sessions, during which the location of the submerged platform was changed daily. On two Cued training days mice were given four-120 s trials separated by 10±2 min inter-trial intervals (release counterbalanced across the four possible start positions N, S, E, and W). On the third cued session, mice were given two-120 s trials separated by 10±2 min inter-trial intervals (released from the farthest two release points).

Neurological motor assessments. Mice were trained in assays of neurological motor impairment, Rotarod and Neurological Severity Score (NSS), 2 days prior to injury, and 1, 2, 3, 7, 14 and 21 days post-injury (see Fig. 1A).

The Rotarod assay used an IITC Life Science Rota-Rod (Woodland Hills, CA) with 3 cm diameter rotating drums. Each mouse was placed on the device facing the experimenter (forward direction), rotating the drum in the opposite direction. The mice were allowed to remain stationary for 10 s at 0 rpm prior to the start of the test. Mice were given one habituation trial to adapt to the testing equipment using a fixed speed of 4 rpm for 60 s. All subsequent trials used an accelerating protocol, starting at 4 rpm and ending at 40 rpm ramping over 60 s, with a 2 min test period. Each trial ended prior to the 2 min cut off if the mouse fell off the rod, or gripped the device and spun around two full revolutions without attempting to walk on the drum. Mice were given one test per day.

The NSS is a 10-point task battery assessment to evaluate the functional neurological status of mice based on the presence of reflexes and the ability to perform motor and behavioral tasks (see Schurman et al., 2017 for NSS task battery description). One point is awarded for failing to perform a particular task, and no points for succeeding. The points of each of the 10 individual tasks are summed to achieve the NSS, in which a score of zero represents a naïve uninjured mouse, whereas a maximal score of 10 indicates severe neurological dysfunction.

Tests of Affective Behavior. Mice were assessed for affective behavior using the light-dark box and the elevated plus maze on day 32 and 33 post-injury respectively (see Fig. 1A).

The light-dark box consisted of a small enclosed dark box (36 x 10 x 34 cm) with an opening (6 x 6 cm) to a larger brightly lit area (36 x 21 x 34 cm). Mice spent 1 h acclimatization to the testing room, then were placed in the light side of the apparatus to explore freely for 5 min. An automated tracking system (ANY-maze, San Diego Instruments, Inc., San Diego, CA) recorded time spent in the light area for each subject, number of entries into the light side, and the total distance travelled.

The elevated plus maze (Hamilton-Kinder, Poway, CA) consisted of a plus-shaped platform elevated 60 cm above the floor, with a central platform (5 x 5 cm) allowing access to each of the four arms. Two opposing arms (35 x 5 cm) were enclosed by 15 cm high walls, the further two arms had no walls. Mice were acclimatized to the testing room for 1 h, then placed on the central platform facing an open arm and allowed to explore the apparatus for 5 min. An array of photocells

connected to a MotorMonitor® system (Hamilton-Kinder, Poway, CA) recorded time in the open arms, number of open arm entries, and the total distance travelled.

Experimental design and statistical analysis. Behavioral data are presented as mean + SEM, The criterion for significance in all experiments was set at $p < 0.05$, and all analyses were conducted using IBM SPSS Statistics 22 for Windows (IBM Software, New York, NY).

All changes in body temperature, % baseline weight, MWM Fixed Platform and Reversal acquisition, MWM swim speed, Rotarod, and NSS data were analyzed using a mixed factor ANOVA (°C, grams, distance, cm/s, and latency measures). All probe trial and cued task analyses, righting time, baseline temperature, light-dark box, and elevated plus maze data were analyzed using a two-way ANOVA (% time in quadrant, % time in outer ring, cm/s, temperature, time, entries, and distance measures). Baseline weight was analyzed by an independent groups t-test. All survival analyses were conducted using a Chi Square analyses by each injury severity.

Results

Figure 1: DAGL-β deletion increased FPI survival and injury-induced righting times, with no impact on body temperature or TBI-induced weight loss. Per the experimental timeline (Figure 1A), DAGL-$\beta^{-/-}$ mice were significantly spared from FPI-induced mortality (day 0) compared to DAGL-$\beta^{+/+}$ mice, ($X^2_{(1, N=28)} = 4.53$, $p = 0.033$, Chi Square, Figure1B). However, a significant righting time interaction ($F_{(1,51)} = 4.63$, $p = 0.036$, ANOVA, Figure 1C) revealed that TBI-DAGL-$\beta^{-/-}$ mice took longer to recover from post-traumatic unconsciousness than TBI-DAGL-$\beta^{+/+}$ mice ($p = 0.003$). DAGL-$\alpha^{-/-}$ mice,

approximately 30-60 min post-surgery, exhibited tonic-clonic seizure-like movements followed by spontaneous death. Of eight mice tested (DAGL-$\alpha^{+/+}$ n=1, DAGL-$\alpha^{-/-}$ n=7), only three lived to receive a TBI (one DAGL-$\alpha^{+/+}$ and two DAGL-$\alpha^{-/-}$ mouse, all of which survived) (data not graphed).

No differences in body temperature were seen between DAGL-$\beta^{+/+}$ and DAGL-$\beta^{-/-}$ mice at baseline (non-significant 3-way interaction; $F_{(1,51)} = 0.004$, $p = 0.953$, ANOVA, Figure 1D), and no main effect of injury ($F_{(1,51)} = 0.532$, $p = 0.469$, ANOVA). However, a significant main effect of time ($F_{(3,153)} = 795$, $p = 0.000$, ANOVA, Figure 1E) revealed that body temperature recovery (following a 2-min MWM swim) changed over time, with greater Δ body temperature at 1 min ($p = 0.000$), 3 min ($p = 0.000$), and 10 min ($p = 0.000$) post-swim compared to 30 min. Although a significant 2-way Δ body temperature time by injury status interaction occurred ($F_{(3,153)} = 2.95$, $p = 0.035$, ANOVA), sidak post-hoc testing revealed no significant difference between sham and injured mice at any time point (1 min; $p = 0.957$, 3 min; $p = 0.364$, 10 min; $p = 0.088$, 30 min; $p = 0.527$), suggesting no relevant effect of injury on body temperature recovery.

Post-injury weight evaluation revealed a main effect of injury ($F_{(1,51)} = 16.4$, $p = 0.000$, ANOVA, Figure 1F) in that TBI lowered percent baseline weight, though a main effect of day showed that all mice increased their percent baseline weight by day 13 through day 30 (consecutively; $p = 0.009$, $p = 0.000$, $p = 0.001$, $p = 0.000$, $p = 0.001$, $p = 0.002$, $p = 0.000$, $p = 0.000$, $p = 0.000$, $p = 0.038$, $p = 0.002$) compared to day 1 post-injury. No pre-existing phenotypic weight differences were seen between DAGL-$\beta^{+/+}$ and DAGL-$\beta^{-/-}$mice at baseline ($t_{(53)} = 1.14$, $p = 0.2605$, T-test, Figure 1G).

Figure 2: DAGL-β deletion did not protect against TBI-induced reference memory deficits or altered search strategy. In MWM Fixed Platform acquisition, a main effect of injury showed that TBI mice had longer swim distances to the platform than sham mice ($F_{(1,51)}$ = 0.237, p = 0.000, ANOVA, Figure 2A). This TBI-induced deficit also occurred in DAGL-$\beta^{-/-}$ mice (non-significant 3-way interaction; $F_{(7,357)}$ = 0.613, p = 0.745, ANOVA) with no main effect of genotype ($F_{(1,51)}$ = 0.730, p = 0.397, ANOVA), demonstrating that TBI produced reference memory deficits are irrespective of DAGL-β deletion. A significant main effect of day ($F_{(7,357)}$ = 32.2, p = 0.000, ANOVA) showed that all mice had significantly reduced swim distances on Fixed Platform days 2 through 8 (all p = 0.000) compared to day 1. In the evaluation of swim speed, a significant main effect of injury ($F_{(1,51)}$ = 8.69, p = 0.005, ANOVA, Figure 2B) showed that TBI mice swam slower than sham mice during Fixed Platform acquisition trials.

The probe trial (Figure 2C, 2D, 2E) test also revealed significant performance deficits in TBI mice. Specifically, these mice spent a reduced percentage of time in the target quadrant (main effect of injury; $F_{(1,51)}$ = 8.33, p = 0.006, ANOVA, Figure 2C), a concomitantly increased percentage of time in the control quadrant (main effect of injury; $F_{(1,51)}$ = 12.2, p = 0.001, ANOVA, Figure 2C), and had reduced platform location entries (main effect of injury; $F_{(1,51)}$ = 6.25, p = 0.016, ANOVA, Figure 2E) compared to sham mice. DAGL-β deletion did not affect any of these indices. No impact of TBI was evident in probe trial distance to the prior platform location (non-significant main effect; $F_{(1,51)}$ = 2.42, p = 0.126, ANOVA, Figure 2D). TBI mice also demonstrated altered probe trial search strategy in which they spent significantly more time in the MWM outer ring than sham mice ($F_{(1,51)}$ = 5.87, p = 0.019, ANOVA, Figure 2F).

The absence of significant differences in cued task performance ($F_{(1,51)}$ = 0.323, p = 0.572, ANOVA; Figure 4H) or cued task swim speed ($F_{(1,51)}$ = 0.159, p = 0.692, ANOVA; Figure 4I) suggests that TBI mice did not produce overt sensorimotor or motivational alterations.

Figure 3: DAGL-β deletion did not protect against TBI-induced reversal task memory deficits or altered reversal search strategy. During MWM Reversal acquisition, TBI mice had longer swim distances to find the Reversal platform than sham mice (main effect of injury; $F_{(1,51)}$ = 4.64, p = 0.036, ANOVA, Figure 3A). This deficit in reversal acquisition was not spared in DAGL-$\beta^{-/-}$ mice (non-significant 3-way interaction; $F_{(3,153)}$ = 0.075, p = 0.973, ANOVA: non-significant main effect of genotype; $F_{(1,51)}$ = 3.64, p = 0.062, ANOVA), demonstrating that while TBI produces deficits in cognitive flexibility, DAGL-β deletion affords no such protection. A significant main effect of day ($F_{(3,153)}$ = 14.9, p = 0.000, ANOVA) showed that all mice had significantly reduced distances to the platform on Reversal days 2 (p = 0.003), 3 (p = 0.004), and 4 (p = 0.000) compared to day 1. In the evaluation of swim speed, a significant main effect of injury ($F_{(1,51)}$ = 5.72, p = 0.020, ANOVA, Figure 3B) showed that TBI mice swam slower than sham mice during Reversal acquisition trials. Although a significant 2-way Reversal swim speed day by genotype interaction occurred ($F_{(3,153)}$ = 4.20, p = 0.007, ANOVA), sidak post-hoc testing revealed no significant difference between DAGL-$\beta^{+/+}$ and DAGL-$\beta^{-/-}$ mice at any time point (day 1; p = 0.329, day 2; p = 0.708, day 3; p = 0.901, day 4; p = 0.691), suggesting that genotype did not relevantly affect Reversal swim speed.

The Reversal probe test (Figure 3C, 3D, 3E) also revealed that TBI elicited a significant performance deficit. Specifically, injury resulted in an increased distance to

the prior Reversal platform location (main effect of injury; $F_{(1,51)} = 6.13$, $p = 0.017$, ANOVA, Figure 3D), and a reduction in the number of Reversal platform location entries (main effect of injury; $F_{(1,51)} = 11.1$, $p = 0.002$, ANOVA, Figure 3E) compared to sham mice. Again, DAGL-$\beta^{-/-}$ mice did not differ from DAGL-$\beta^{+/+}$ mice. However, none of the factors affected the percentage of time spent in the target or control quadrants in the Reversal probe trial test (non-significant main effect of injury Target quadrant; $F_{(1,51)} = 0.782$, $p = 0.381$, non-significant main effect of injury Control quadrant; $F_{(1,51)} = 3.07$, $p = 0.086$, ANOVA, Figure 3C). TBI mice also demonstrated an increased duration of time spent in the MWM outer ring during the probe trial compared with the sham mice ($F_{(1,51)} = 4.61$, $p = 0.037$, ANOVA, Figure 3F).

Figure 4: DAGL-β deletion did not protect against TBI-induced neurological motor impairments. During Rotarod testing, a significant 2-way interaction of day by injury ($F_{(7,357)} = 6.20$, $p = 0.000$, ANOVA, Figure 4A), irrespective of genotype, revealed that TBI mice had reduced latencies to fall on post-injury days 1 ($p = 0.000$), 2 ($p = 0.000$), and 3 ($p = 0.000$) compared to sham mice, suggesting that TBI produced neurological motor Rotarod deficits, which resolved by day 7 post-injury. Similarly, DAGL-$\beta^{-/-}$ mice undergoing TBI mice showed Rotarod performance deficits (non-significant 3-way interaction; $F_{(7,357)} = 0.916$, $p = 0.494$, ANOVA: non-significant main effect of genotype; $F_{(1,51)} = 0.449$, $p = 0.506$, ANOVA), suggesting that DAGL-β deletion did not protect against neurological motor impairments as measured by the Rotarod.

A significant 2-way interaction of day by injury ($F_{(6,306)} = 8.04$, $p = 0.000$, ANOVA, Figure 4B) revealed increased NSS scores in TBI mice on post-injury days 1 ($p = 0.002$), 2 ($p = 0.028$), and 7 ($p = 0.010$) compared to sham mice, irrespective of

genotype. These findings suggest that TBI produced neurological motor NSS deficits resolved by day 14 post-injury. The finding that genotype did not affect NSS scores (non-significant 3-way interaction; $F_{(6,306)} = 0.243$, $p = 0.962$, ANOVA: non-significant main effect of genotype; $F_{(1,51)} = 1.20$, $p = 0.279$, ANOVA) suggests that DAGL-β deletion did not protect against neurological motor impairments as measured by the NSS.

Figure 5: Anxiety-like behavior was unaffected by DAGL-β deletion or TBI. In the light-dark box assay, neither TBI nor DAGL-β deletion produced any change in time spent in the light area (non-significant main effect of injury; $F_{(1,51)} = 0.002$, $p = 0.964$, ANOVA: non-significant main effect of genotype; $F_{(1,51)} = 2.69$, $p = 0.107$, ANOVA, Figure 5A), or entries into the light area (non-significant main effect of injury; $F_{(1,51)} = 0.137$, $p = 0.713$, ANOVA: non-significant main effect of genotype; $F_{(1,51)} = 0.005$, $p = 0.943$, ANOVA), suggesting that when evaluated at post-injury day 32 neither TBI nor DAGL-β deletion affected behavior in this assay. No changes in Light-Dark box activity were seen between groups as measured by total distance traveled (non-significant 2-way interaction; $F_{(1,51)} = 0.571$, $p = 0.453$, ANOVA).

Likewise, the elevated plus maze test failed to reveal effects of either TBI or DAGL-β deletion in time spent in the open arms (non-significant main effect of injury; $F_{(1,51)} = 2.90$, $p = 0.095$, ANOVA: non-significant main effect of genotype; $F_{(1,51)} = 0.046$, $p = 0.832$, ANOVA, Figure 5B), or entries into the light area (non-significant main effect of injury; $F_{(1,51)} = 0.422$, $p = 0.519$, ANOVA: non-significant main effect of genotype; $F_{(1,51)} = 0.355$, $p = 0.554$, ANOVA). These findings suggest that when evaluated at post-injury day 33 neither TBI nor DAGL-β deletion impacted performance in the elevated

plus maze, a common test used to infer anxiety-related behavior. No changes in elevated plus maze activity were seen between groups as measured by total distance traveled (non-significant 2-way interaction; $F_{(1,51)} = 1.63$, $p = 0.207$, ANOVA).

Figure 6: The survival protective phenotype of mouse DAGL-β deletion persisted at increased injury severity. Male DAGL-$\beta^{-/-}$ mice were significantly spared from FPI-induced mortality compared to male DAGL-$\beta^{+/+}$ mice when injury magnitude was increased to 2.0 atm, ($X^2_{(1, N=31)} = 4.31$, $p = 0.038$, Chi Square, Figure1A), as well as at 2.17 atm, ($X^2_{(1, N=28)} = 4.09$, $p = 0.043$, Chi Square), suggesting that the survival protective phenotype of DAGL-$\beta^{-/-}$ mice persists with increased injury severity. In contrast, female DAGL-$\beta^{-/-}$ and -$\beta^{+/+}$ mice showed high survival rates at either 2.0 atm ($X^2_{(1, N=30)} = 1.03$, $p = 0.309$, Chi Square) or 2.17 atm ($X^2_{(1, N=28)} = 2.15$, $p = 0.142$, Chi Square). The high survival rates of females (2.0 atm; DAGL-$\beta^{+/+}$ 93%, DAGL-$\beta^{-/-}$ 100%, 2.17 atm; DAGL-$\beta^{+/+}$ 86%, DAGL-$\beta^{-/-}$ 100%) suggest that being female was generally protective.

Discussion

TBI disrupted Fixed Platform and Reversal task performance accompanied by non-spatial search strategies, irrespective of genetic deletion of DAGL-β. Thus, contrary to our hypothesis, deletion of this enzyme did not provide protection from TBI-induced spatial learning and memory impairments. Injury also produced changes in neurological motor function and body weight, but without impacting temperature regulation or performance in common assays used to infer anxiety. In addition, no phenotypic differences from DAGL-β disruption were evident in these measures. Unexpectedly,

DAGL-β deletion produced a survival protective phenotype, which persisted at increased injury severities in male mice. However, female mice did not display injury-related mortality, regardless of genotype.

While the disease state following a TBI is composed of heterogeneous secondary injury mechanisms, chronic neuroinflammation has been a popular neuroprotective target, perhaps given the neuroinflammatory temporal profile providing intervention opportunities following the primary insult. Yet, thus far, all late phase clinical trials have failed to yield an effective anti-inflammatory neuroprotective treatment (Chakraborty *et al*, 2016; Narayan *et al*, 2002). The modulation of neuroinflammation in murine models of TBI have seen mixed success. While high dose anti-inflammatories (NSAIDs and glucocorticosteroids) can exacerbate learning and memory deficits (Brown *et al*, 2006; Chen *et al*, 2009, 2010b), isolated stand-alone drugs targeting neuroinflammation (antibiotics, COX-1 inhibitors, a plant-based alkaloid, and an apolipoprotein mimetic peptide) attenuate memory impairment (Ferguson *et al*, 2017; Laskowitz *et al*, 2007; Shang *et al*, 2014; Siopi *et al*, 2012). The mixed results of anti-inflammatory drug targets in preclinical research and the failed translation to clinical learning and memory protection is perhaps a consequence of the necessity to promote the beneficial effects of acute neuroinflammation, while minimizing detrimental chronic effects. The temporal profile of microglia activation phenotypes may also be of relevance. Specifically, increased 2-AG production during M2a (alternatively activated) and M2c (acquired deactivated) microglial phenotypes occurs in concert with increased CB_2 receptor expression, driving the acquisition of further M2 phenotypes and promoting inflammation resolution (Mecha *et al*, 2015). Furthermore, DAGL-β

expression is upregulated during an M2c phenotype (Mecha *et al*, 2015), suggesting that DAGL-β may play a temporal dependent role with regards to inflammation pathology. The current constitutive genetic deletion of DAGL-β may therefore mask time dependent protective effects of DAGL-β disruption. Future experiments using pharmacological tools would be valuable to manipulate the timing of DAGL-β disruption, but are currently challenging given the lack of availability of selective and brain penetrant DAGL-β inhibitors. Furthermore, 2-AG is a potent CB_2 receptor agonist (Hillard, 2000a), consequently DAGL-β gene deletion may also result in decreased activation of microglial CB_2 receptors. Such reduced CB_2 receptor signaling could offset any presumed beneficial effects of reduced AA metabolites.

The high mortality rates of DAGL-$\alpha^{-/-}$ mice following the craniectomy surgery precluded systematic investigation of neuronal DAGL disruption. DAGL-$\alpha^{-/-}$ mice are vulnerable to increased mortality in general (Powell *et al*, 2015) as well as being more susceptible to seizures (Sugaya *et al*, 2016) than DAGL-$\alpha^{+/+}$ mice. This pre-existing phenotype may be a consequence of alterations across ontogeny (e.g. decreased neurogenesis and altered inflammatory responses (Gao *et al*, 2010; Shonesy *et al*, 2014; Tanimura *et al*, 2010) and may lead to increased vulnerability to survival surgeries that compromise the integrity of the CNS.

The unexpected finding that DAGL-β disruption produced a survival protective phenotype, although not a frequently explored outcome measure in preclinical studies of TBI, might point to a surprising and novel understanding of DAGL-β as contributing towards acute TBI pathology. Despite otherwise susceptible DAGL-$\beta^{-/-}$ mice surviving the acute injury period (perhaps represented by the increased righting times of DAGL-β^{-}

$^{/-}$ mice compared to -$\beta^{+/+}$ mice), no potentiated learning and memory deficits in the DAGL-$\beta^{-/-}$ mice suggest these mice were not prone to increased functional impairment. Interestingly, a clinical study exploring the relationship of cannabinoids to TBI mortality used urine toxicology screen results and showed decreased mortality in individuals with a positive THC screen (Nguyen *et al*, 2014b), the primary psychoactive constituent of the *Cannabis sativa* plant. The authors hypothesized that chronic low-dose THC was mildly pro-inflammatory, producing a pre-conditioning effect where a mildly noxious stimulus proves to be protective against a more severe subsequent insult. Yet this logic seems contrary to DAGL-β disruption, found to be anti-inflammatory *in vitro* (Hsu *et al*, 2012). The observed mortality in the present study occurred within a 2-min post-injury window. Therefore, consideration of the processes responsible in terms of secondary injury mechanisms should also be relevant to such a time scale. Both reactive oxygen species (ROS) production (e.g. peroxynitrite, hydroxyl radical, etc.) and glutamate excitotoxicity occur within minutes following injury (Nilsson *et al*, 1990; Singh *et al*, 2006). Though few studies have examined injury-induced ROS production at time points earlier than 30 minutes, evidence suggests that TBI-induced ROS elevation magnitude is subject to injury force manipulations (Marklund *et al*, 2001), leaving the investigation of DAGL-β disruption on injury-induced ROS elevations at 2 min post-TBI as an interesting future experimental direction. Furthermore, a future avenue of investigation could include *in vivo* microdialysis measurement of extra-cellular glutamate at 2-min post injury.

Another mechanism of consideration, which may contribute towards the survival protective phenotype of DAGL-$\beta^{-/-}$ mice, includes ceramides, belonging to the family of

spingolipids. Spingolipids are essential constituents of all eukaryotic cell membranes, of which ceramide is composed of sphingosine and a fatty acid and its generation occurs within minutes through the hydrolysis of sphingomyelin by sphingomyelinases (Kolesnick and Kronke, 1998). Increases in ceramides have been linked to glutamate toxicity, mitochondrial dysfunction, and extrinsic apoptotic pathways (Novgorodov *et al*, 2018). In cancer, the reduction of ceramide accumulation is frequently observed (Morad and Cabot, 2013) and many chemotherapeutic drugs elevate ceramide (Radin, 2004) to promote cell death. While there is no reported link between DAGL-β activity and ceramide production, 2 to 3-fold increases in ceramide levels occur following TBI in rats (Barbacci *et al*, 2017; Roux *et al*, 2016). Of future interest would be to measure ceramide levels in TBI-DAGL-$\beta^{-/-}$ mice, which if contributing to the survival phenotype of these animals we would predict lower accumulation of ceramide in brain compared to TBI-DAGL-$\beta^{+/+}$ mice, providing a neurochemical lipid correlate of TBI survival and mortality.

A growing body of work implicates the importance of sex differences in response to TBI. While TBI frequently occurs in young males (Langlois *et al*, 2006) resulting from automotive accidents, war, etc., the elderly are also a highly vulnerable population (Thompson *et al*, 2006) due mostly as a result of falls, in which men and women are impacted equally. The present observation that female DAGL-$\beta^{-/-}$ and -$\beta^{+/+}$ mice showed survival phenotypes after injury is consistent with female mice and rats being generally protected from TBI-induced mortality compared to male mice/rats (Neese *et al*, 2010; Umeano *et al*, 2017). The high rates of survival in both genotypes of females is likely occurring through alternative mechanisms than DAGL-β gene deletion. The

mechanisms behind female protection from TBI mortality as of yet, remain unclear; here we consider several possibilities. Pre-clinical studies show female mice have differing inflammatory profiles than male mice following TBI. Female mice demonstrate a biphasic pro-inflammatory response, whereas male mice show a prolonged single phase increase in inflammatory mediators (Villapol *et al*, 2017). Inflammation resolution profiles also differ, with female mice showing a delayed peak of anti-inflammatory mediators, whereas male mice again show a single phase (Villapol *et al*, 2017). Pre-clinical studies also show a potential hormonal role driving sex differences in TBI mortality profiles. Umeano et al., 2017 using ovariectomized female mice showed similar mortality rates to males and concluded that female gonadal hormones may influence murine TBI mortality outcomes. While both estrogen and progesterone are neuroprotective when administered to male mice in functional and molecular endpoints (Lopez-Rodriguez *et al*, 2015; Meltser *et al*, 2008; Pascual *et al*, 2013; Schaible *et al*, 2014), no known work to date has shown a link to mortality protection by these hormones in murine studies. Future experiments to evaluate if survival phenotypes in DAGL-$\beta^{+/+}$ male mice could be rescued by estrogen/progesterone pre-treatment might prove a useful addition to our understanding of sex driven differences in mouse TBI mortality outcomes. However, female mortality in clinical populations differs to male only when cohorts are evaluated by age, with pubescent (Ley *et al*, 2013) and post-menopausal women (Berry *et al*, 2009; Davis *et al*, 2006) showing mortality protection, both being life cycle times of estrogen dominance unbalanced by progesterone. Furthermore, two large randomized clinical trials found no protection of progesterone (Skolnick *et al*, 2014; Wright *et al*, 2014). As such, the mechanisms by which females

are protected from TBI mortality compared to males strongly suggest the involvement of estrogen.

Despite the present finding that DAGL-β deletion was not protective against mouse spatial learning and memory deficits, continued investigation of neuroinflammation on TBI outcomes is arguably pertinent. The predisposition of TBI patients to develop other neurological pathologies such as Alzheimer's disease, thought to be a product of prolonged neuroinflammation, support the necessity of further investigation in this area. In sum, while DAGL-β deletion did not protect against TBI-induced learning and memory deficits nor motor deficits, these findings suggest the provocative possibility that DAGL-β activity contributes towards TBI-induced acute mortality in males, implicating this enzyme in acute TBI pathology.

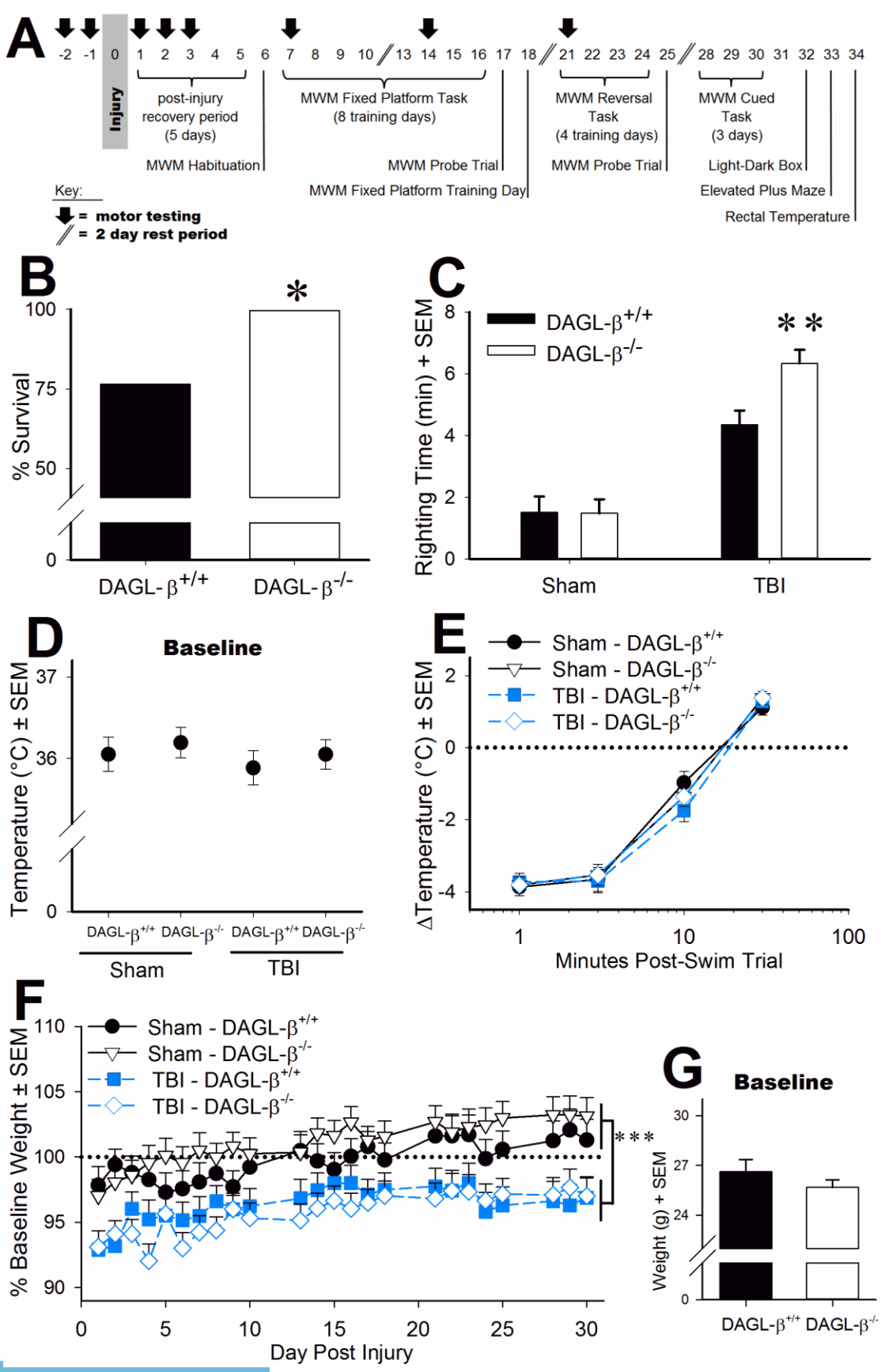

Figure 3-1. **Physiology: DAGL-β$^{-/-}$ mice showed increased survival and longer righting times**. **A,** Experimental timeline, days relative to injury (Sham-DAGL-β$^{+/+}$ n = 12, Sham-DAGL-β$^{-/-}$ n = 15, TBI-DAGL-β$^{+/+}$ n = 12, TBI-DAGL-β$^{-/-}$ n = 16). TBI lowered body weight and increased righting times, with no change in body temperature regulation. DAGL-β$^{-/-}$ mice showed increased survival and longer righting times with no change in weight loss. **B,** DAGL-β$^{-/-}$ mice showed increased survival from TBI compared to DAGL-β$^{+/+}$ mice (* $p < 0.05$, vs. DAGL-α$^{+/+}$ mice), as well as **C,** increased righting times (** $p < 0.01$, vs. TBI-DAGL-α$^{+/+}$ mice). No changes between experimental groups were seen in either **D,** baseline body temperature or **E,** body temperature recovery following a 2-min MWM swim. **F,** TBI produced lowered % baseline body weights with no effect of genotype (*** $p < 0.001$, TBI vs. Sham mice), and **G,** DAGL-β$^{-/-}$ mice showed no phenotypic body weight differences to DAGL-β$^{+/+}$ mice prior to TBI. Values represent mean + or ± SEM.

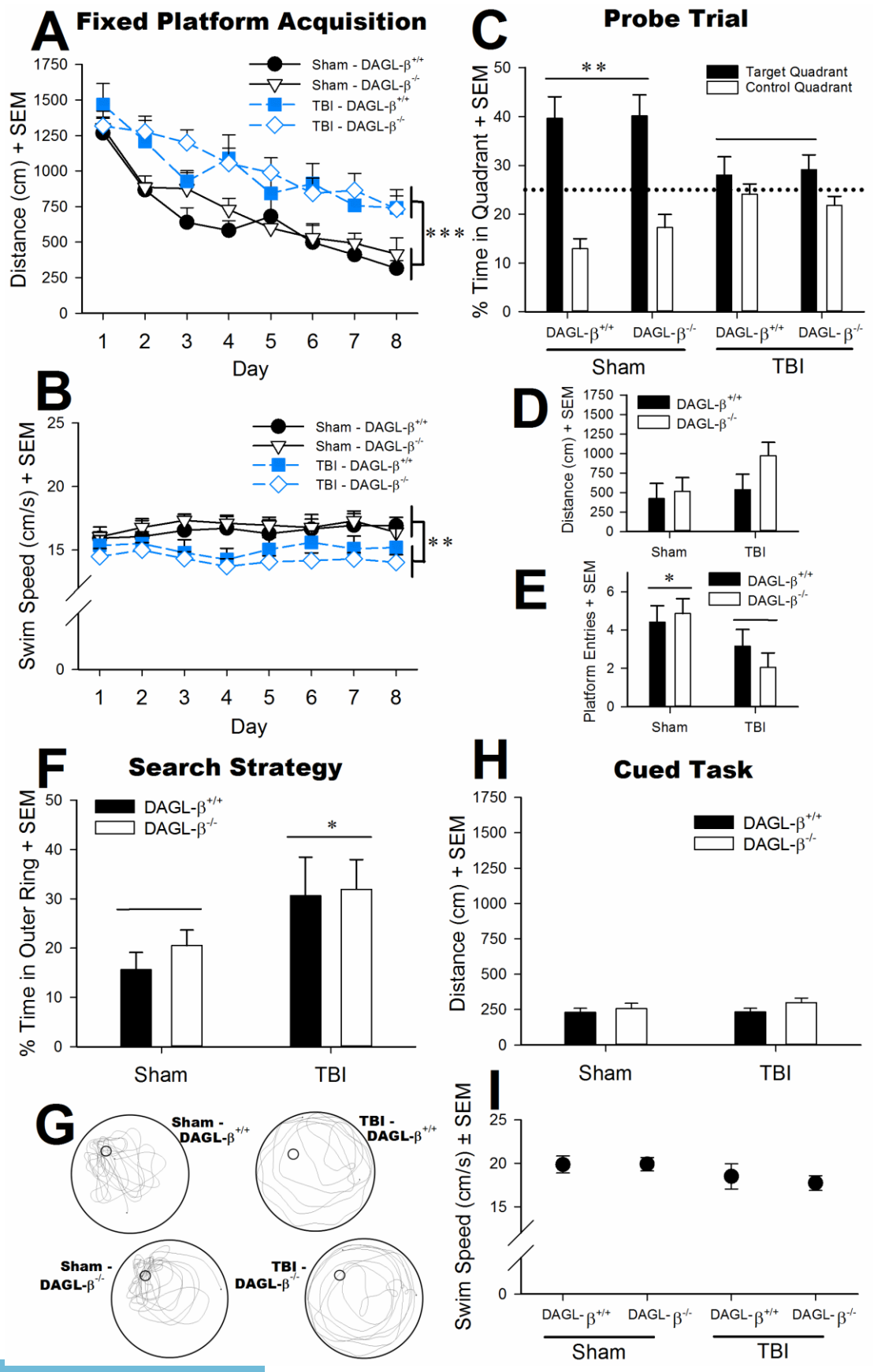

Figure 3-2. **DAGL-β$^{-/-}$ mice showed no TBI-induced reference memory deficit protection**. DAGL-β deletion did not protect against TBI-induced MWM Fixed Platform task impairments or altered search strategy (Sham-DAGL-β$^{+/+}$ n = 12, Sham-DAGL-β$^{-/-}$ n = 15, TBI-DAGL-β$^{+/+}$ n = 12, TBI-DAGL-β$^{-/-}$ n = 16). **A,** During MWM Fixed Platform acquisition TBI mice demonstrated greater distances to find the platform with no performance difference evident between genotype (*** $p < 0.001$, TBI vs. Sham mice) as well as **B,** slower swim speeds (** $p < 0.01$, TBI vs. Sham mice). During a MWM Fixed Platform probe trial **C,** TBI mice showed less spatial preference for the target quadrant with no performance difference evident between genotype (** $p < 0.01$, TBI vs. Sham mice), while **D,** no group differences were seen in distance to the prior platform location, but **E,** TBI mice showed fewer platform crossings of the prior platform location (* $p < 0.05$, TBI vs. Sham mice). During probe trial **F,** TBI mice also spent more time in the outer ring of the MWM (* $p < 0.05$, TBI vs. Sham mice) suggesting that TBI changes MWM search strategy, illustrated by also by **G,** representative swim paths of TBI and Sham, DAGL-β$^{+/+}$ and DAGL-β$^{-/-}$ mice, where TBI mice show circular search strategies. During a MWM Cued task **H,** no differences in distance to a cued platform were evident, or **I,** swim speed, suggesting no senori-motor or motivational confounds were present. Values represent mean + or ± SEM.

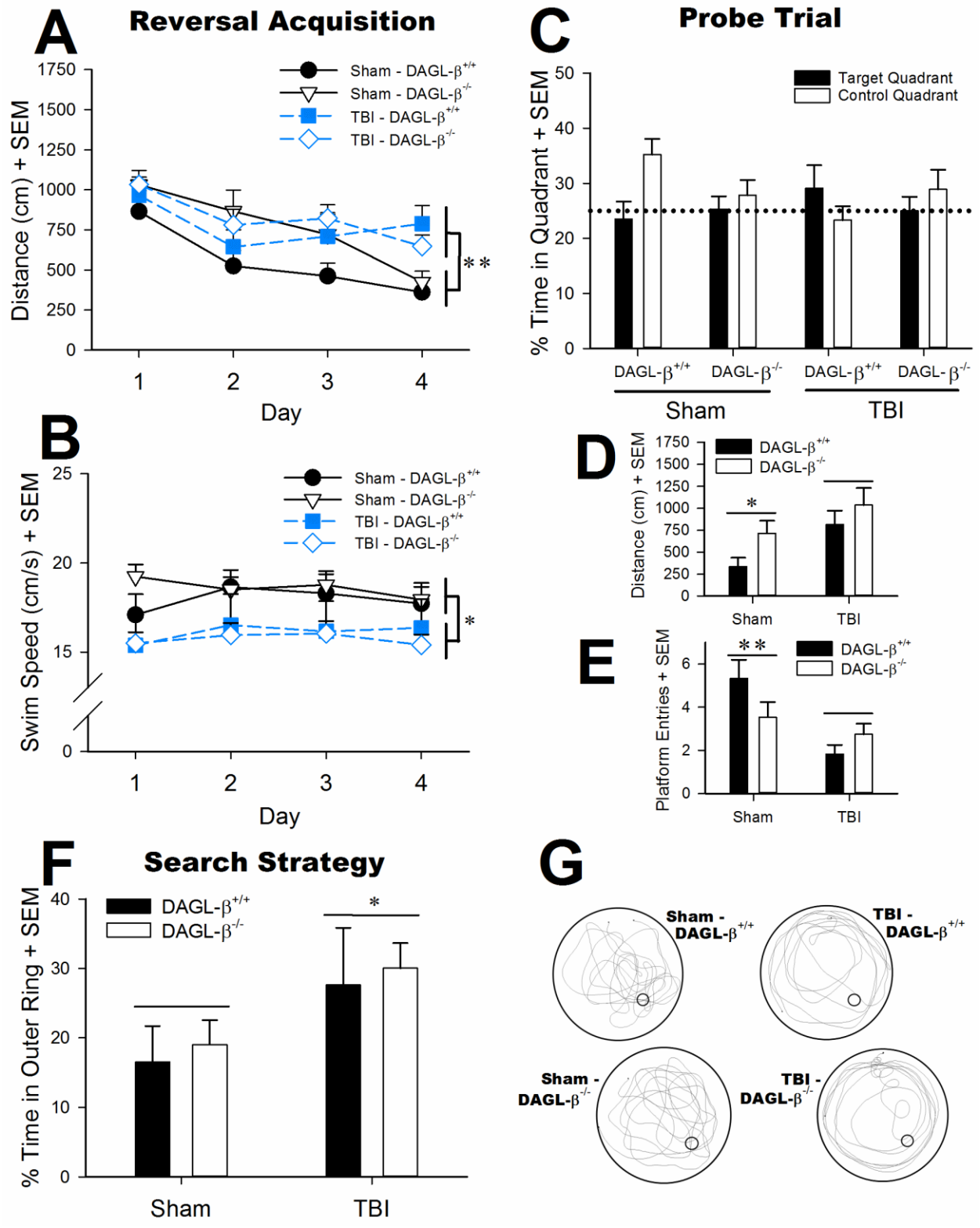

Figure 3-3. **DAGL-β$^{-/-}$ mice showed no TBI-induced cognitive flexibility deficit protection**. DAGL-β deletion did not protect against TBI-induced MWM Reversal task

impairments or altered Reversal search strategy (Sham-DAGL-$\beta^{+/+}$ n = 12, Sham-DAGL-$\beta^{-/-}$ n = 15, TBI-DAGL-$\beta^{+/+}$ n = 12, TBI-DAGL-$\beta^{-/-}$ n = 16). **A,** During MWM Reversal acquisition TBI mice demonstrated greater distances to find the platform with no performance difference evident between genotype (** $p < 0.01$, TBI vs. Sham mice) as well as **B,** slower swim speeds (* $p < 0.05$, TBI vs. Sham mice). During a MWM Reversal probe trial **C,** All groups showed no spatial preference for the Reversal target quadrant, while **D,** TBI mice showed greater distances to the prior Reversal platform location (* $p < 0.05$, TBI vs. Sham mice) **E,** as well as fewer platform crossings of the prior Reversal platform location (** $p < 0.01$, TBI vs. Sham mice). During Reversal probe trial **F,** TBI mice also spent more time in the outer ring of the MWM (* $p < 0.05$, TBI vs. Sham mice) suggesting that TBI changes MWM Reversal search strategy, illustrated by also by **G,** representative swim paths of TBI and Sham, DAGL-$\beta^{+/+}$ and DAGL-$\beta^{-/-}$ mice, where TBI mice show circular search strategies. Values represent mean + SEM.

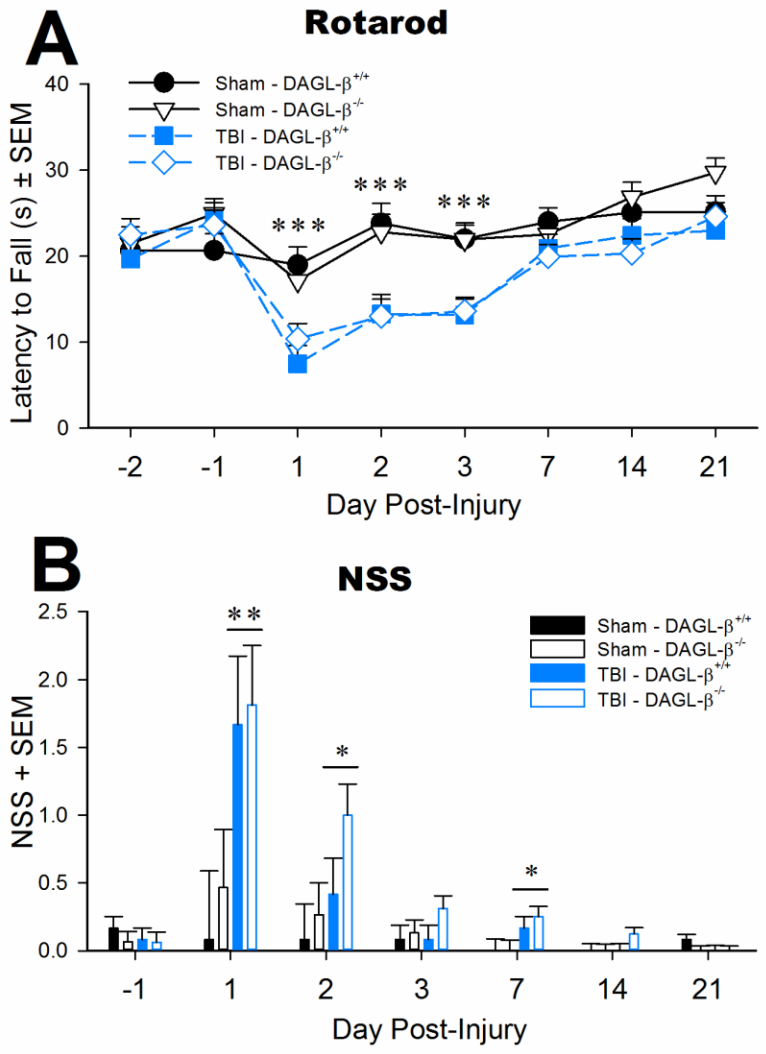

Figure 3-4. **DAGL-β$^{-/-}$ mice showed no TBI-induced neurological motor deficit protection**. DAGL-β deletion did not protect against TBI-induced neurological motor deficits (Sham-DAGL-β$^{+/+}$ n = 12, Sham-DAGL-β$^{-/-}$ n = 15, TBI-DAGL-β$^{+/+}$ n = 12, TBI-DAGL-β$^{-/-}$ n = 16). **A,** During the Rotarod assay, TBI mice demonstrated reduced latencies to fall on post-surgery days 1, 2, and 3, with no performance difference evident between genotype (*** $p < 0.001$, TBI vs. Sham mice days 1-3 post-injury). **B,** During NSS evaluation, TBI mice demonstrated greater NSS scores on post-injury days 1, 2, and 7 (** $p < 0.01$, TBI vs. Sham mice on day 1, and * $p < 0.05$, TBI vs. Sham mice on days 2 and 7). Values represent mean + SEM.

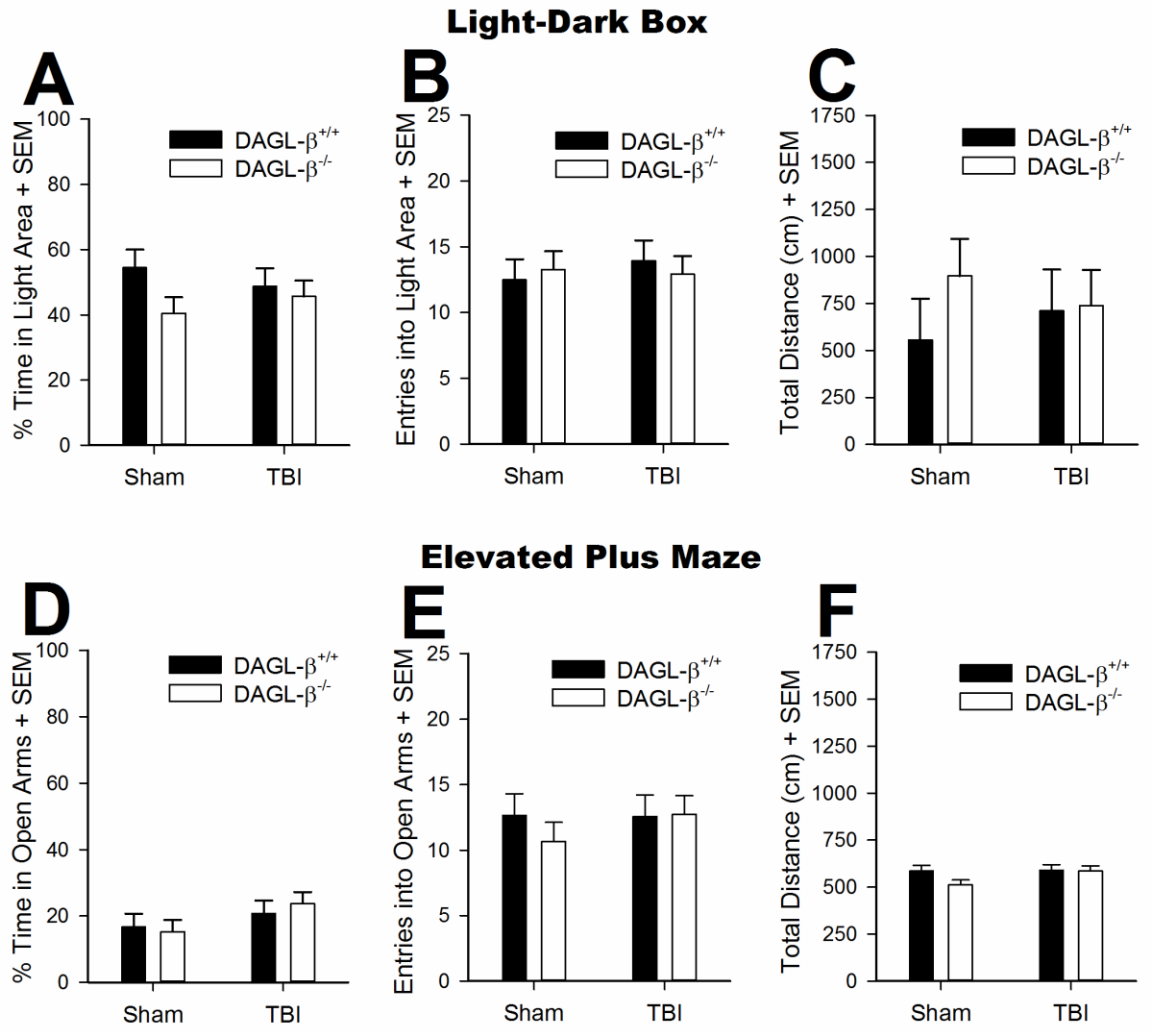

Figure 3-5. **Neither DAGL-β$^{-/-}$ deletion nor TBI altered performance on tests of affective behavior**. Both light-dark box and elevated plus maze performance was unaffected by DAGL-β deletion or TBI (Sham-DAGL-β$^{+/+}$ n = 12, Sham-DAGL-β$^{-/-}$ n = 15, TBI-DAGL-β$^{+/+}$ n = 12, TBI-DAGL-β$^{-/-}$ n = 16). In the light-dark box no performance difference was evident as a result of TBI or between genotype for either **A,** time spent in the light area, **B,** entries into the light area, or **C,** distance travelled. The elevated plus maze also saw no performance differences as a result of TBI or between genotype for either **D,** time spent in the open arms, **E,** entries into the open arms, or **F,** distance travelled. Values represent mean + SEM.

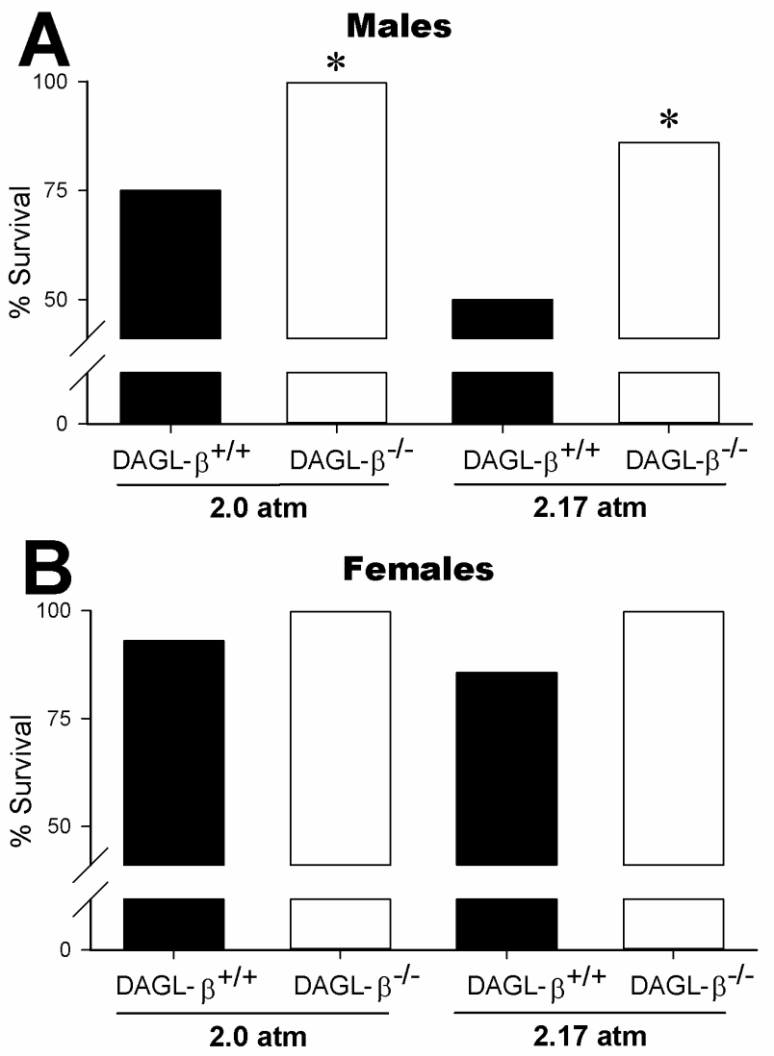

Figure 3-6. **DAGL-β$^{-/-}$ mice exhibit a survival protective phenotype**. The survival protective phenotype of DAGL-β$^{-/-}$ mice persisted at increased injury severity in male mice (male TBI mice; [2.0 atm]-DAGL-β$^{+/+}$ n = 16, [2.0 atm]-DAGL-β$^{-/-}$ n = 15, [2.17 atm]-DAGL-β$^{+/+}$ n = 14, [2.17 atm]-DAGL-β$^{-/-}$ n = 14), whereas being female was generally protective (female TBI mice; [2.0 atm]-DAGL-β$^{+/+}$ n = 15, [2.0 atm]-DAGL-β$^{-/-}$ n = 15, [2.17 atm]-DAGL-β$^{+/+}$ n = 14, [2.17 atm]-DAGL-β$^{-/-}$ n = 14). In male TBI mice **A,** at both 2.0 atm and 2.17 atm DAGL-β$^{-/-}$ mice demonstrated increased survival (* $p < 0.05$, DAGL-β$^{-/-}$ vs DAGL-β$^{+/+}$ mice). Whereas female TBI mice **B,** showed no significant difference in survival rates between DAGL-β$^{-/-}$ and DAGL-β$^{+/+}$ mice.

Chapter IV

Chapter Introduction

The third and final goal of this dissertation was to understand the *in vivo* role of diacylglycerol lipase-α (DAGL-α), the second of the two 2-AG biosynthetic enzymes, in hippocampal-dependent mouse learning and memory regulation under physiological conditions.

Hippocampal-dependent learning and memory. The hippocampus and its connection to other brain regions is fundamental to the memory of our experiences, their content, and our ability to re-play them. That is, episodic memory. The hippocampus specifically supports the storage and recollection of temporal-spatial contextual information. The study of several patients with selective damage to the hippocampus has helped provide insight into the function of this brain structure in learning and memory. One such patient, R.B., had complete loss of neurons from bilateral hippocampal CA1 region(see Figure 4-A) (where previously processed information by other hippocampal regions is sent out

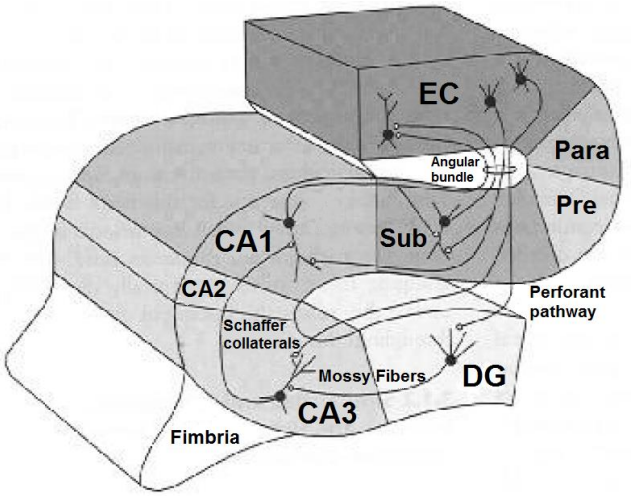

Figure 4-A. Hippocampal regional connectivity: DG; dentate gyrus, Sub; subiculum, Pre; presubiculum, Para; parasubiculum, EC; entorhinal cortex (adapted from publically available lecture slides by Dr. David S. Touretzky).

via the subiculum and entorhinal cortex and projects back to the neocortex, among other structures) as a result of complications from an artery bypass surgery (Zola-Morgan *et al*, 1986). R.B. experienced anterograde amnesia, with difficulty acquiring new information. Specifically R.B. had difficulty remembering word lists and story recall, and he reported loss of knowledge of events from a previous day such as talking to his children. A second example, V.C., is a patient who experienced loss of entire rostral-caudal length hippocampal volume as a result of an epileptic seizure (Cipolotti *et al*, 2001). V.C. also experienced severe anterograde amnesia, profoundly impairing his ability to acquire new information (story recall, word associations, newly experienced events and their contexts). While such selective and restricted brain damage to the hippocampus is rare, these cases support the assertion of Dr. Brenda Milner, who argued the critical importance of the hippocampus for episodic memory through her revolutionary work with H.M. (whose personal tragedy and removal of his bilateral temporal lobes led to testable hypotheses about what regions of the brain were critical for memory) (Milner, 1970; Scoville and Milner, 1957).

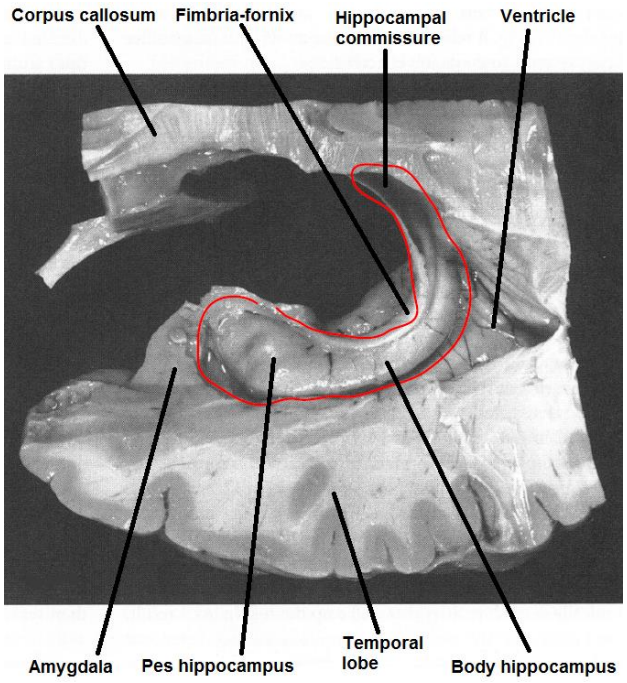

Figure 4-B. Structures adjacent to the Human Hippocampus (adapted from publically available lecture slides by Dr. David S. Touretzky).

The ways in which the hippocampus contributes toward memory storage and retrieval has been described by the indexing theory of memory (Teyler and

DiScenna, 1986), and since extensively supported by human and murine research (Teyler and Rudy, 2007). An experience activates patterns of neocortical activity which project to the hippocampus and responding hippocampal synapses are strengthened by long-term potentiation mechanisms (see next section). No memory content is stored in the hippocampus, but it acts as a system to retrieve neocortical stored information through activation of a hippocampal representation projecting back to the neocortex to activate patterns representing the entire experience. The neocortex alone is perhaps not well suited to the acquisition and retrieval of single memory episodes given its low associative connectivity (which might produce difficulty in distinguishing separate yet similar experiences) (Rudy, 2014).

Long-term potentiation. The tri-synaptic loop organization of the hippocampus makes it uniquely suited to the study of neuronal connections, where the stimulation of fibers known to synapse onto a particular subfield can be measured using a recording electrode placed near to neurons of that subfield. The original work by Bliss and Lomo, 1973 stimulated fibers in the perforant path, and then recorded from dentate gyrus neurons. They found that a strong stimulus applied after a weak stimulus produced an enduring increase in the synaptic response to the same weak stimulus, which they termed long-term potentiation (see Figure 4-C). It is now considered that experience is stored in the brain because it modifies the

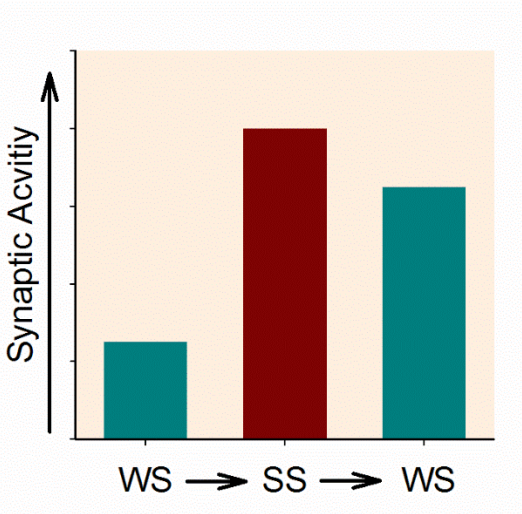

Figure 4-C. Graphical representation of long-term potentiation. A strong stimulus (SS) produced an enduring increase in the synaptic response to the weak stimulus (WS).

strength of synapses of connecting neurons. As such, Long-term potentiation is the idea that experience can be stored by altering the strength of neuron to neuron synaptic connections within networks of neurons, and is currently the best proposed molecular basis of memory.

DAGL-α and hippocampal-dependent learning and memory. The dominant production enzyme of 2-AG in brain is DAGL-α (Bisogno *et al*, 2003a; Jung *et al*, 2007), yet the biosynthetic pathways of 2-AG are almost as diverse as its catabolism. Two further biosynthetic pathways exist (see Figure 4-D), one through LPA phosphatase (Nakane *et al*, 2002) and the other through PLA1/lyso-PLC (Higgs and Glomset, 1994).

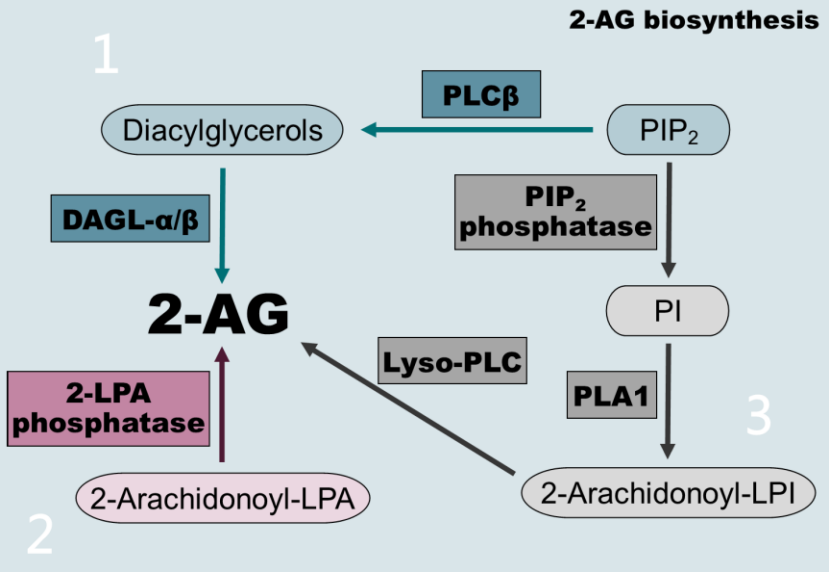

Figure 4-D. 2-AG biosynthetic pathways: 2-AG; 2-arachidonyl glycerol; 2-arachidonoyl-LPA; 2-arachidonoyl-lysophosphatidic acid, 2-arachidonoyl-LPI; 2-arachidonoyl lysophosphatidylinositol, 2-LPA phosphatase; 2-lysophosphatidic acid phosphatase, DAGL-α/β; diacyglycerol lipase-α/β; lyso-PLC; lyso-phospholipase C, PIP_2; phosphatidylinositol biphosphate, PIP_2 phosphatase; phosphatidylinositol biphosphate phosphatase, PI; phosphatidylinositol, PLA1; Phospholipase A1, PLCβ; phospholipase Cβ.

While the involvement of these latter and secondary pathways in the production of 2-AG is yet to be fully evaluated, they have been hypothesized as being responsible for some endocannabinoid-mediated synaptic plasticity found to be insensitive to DAGL inhibitors (Zhang *et al*, 2011), and perhaps are also responsible for low basal 2-AG levels

measurable in DAGL-$\alpha^{-/-}$ mice.

DAGLs are expressed in bacteria, fungi, plants, and animals. Mammalian DAGLs are widely expressed in the CNS, and specifically DAGL-α is abundantly expressed in the hippocampus (Katona *et al*, 2006; Yoshida *et al*, 2006). The distinct cellular expression patterns of DAGLs in part determine their physiological functions. DAGL-α is expressed on neurons, specifically hippocampal pyramidal cell dendritic spines (Yoshida *et al*, 2006), with a growing body of evidence to support its importance for the modulation of neurotransmission (Gao *et al*, 2010; Tanimura *et al*, 2010). While DAGL-$\alpha^{-/-}$ mouse models have pointed to the importance of this enzyme in a variety of physiological/psychological functions; anxiety, seizure activity, and sociability (Shonesy *et al*, 2014, 2018; Sugaya *et al*, 2016), the present work considers the importance of DAGL-α for hippocampal-dependent spatial memory in the mouse model organism.

Summary. The following work evaluates the hippocampal-dependent learning and memory contributions of DAGL-α, using pharmacological and genetic manipulations under the working hypothesis that DAGL-α is necessary for spatial learning and memory in mice under normal physiological conditions. The present chapter tests this hypothesis under three levels of investigation; cellular responses to LTP, *in vivo* spatial learning and memory deficits, and neurochemical correlates of behavior (eCB lipid levels) in brain areas important for learning and memory. The unique findings that DAGL-α disruption impairs acquisition and reversal tasks, but not expression, extinction or forgetting, implicates DAGL-α as being selectively important for the integration of new spatial information.

Diacylglycerol lipase-alpha regulates hippocampal-dependent learning and memory processes in mice

(Submitted for publication)

Disclosure: all electrophysiology experiments were conducted in the laboratory of Dr. Qing Song Lui, primarily by Laikang Yu and Xiaojie Liu, and Mass Spectrometry analysis was conducted by Justin Poklis.

Introduction

A growing body of evidence implicates the importance of 2-arachidonoyl glycerol (2-AG), the most highly expressed endogenous cannabinoid in brain, in regulating learning and memory. Diacylglycerol lipase (DAGL) forms 2-AG through the hydrolysis of diacylglycerols (Chau and Tai, 1981; Okazaki *et al*, 1981) and exists as two distinct biosynthetic enzymes, DAGL-α and DAGL-β (Bisogno *et al*, 2003a) that are expressed on distinct cell types, as well as in brain areas important for learning and memory (Katona *et al*, 2006; Lafourcade *et al*, 2007). Within the central nervous system, DAGL-β is highly expressed on microglia, while DAGL-α, expressed on synapse-rich plasma membranes of dendritic spines (Yoshida *et al*, 2006), serves as the principal synthetic enzyme of 2-AG on neurons (Viader *et al*, 2015a).

DAGL-α modulates neurotransmission through distinct processes of neurogenesis and endocannabinoid-mediated short-term synaptic plasticity, implicating it in learning and memory processes. Adult neurogenesis represents a form of cellular plasticity in the developed brain. Two prominent brain areas showing adult neurogenesis, the subventricular zone and the hippocampus, that express high levels of

DAGL-α (Goncalves *et al*, 2008) undergo marked reductions in the proliferation of neuronal progenitor cells in DAGL-$\alpha^{-/-}$ mice (Gao *et al*, 2010). Similarly, the non-selective DAGL inhibitors RHC80267 and tetrahydrolipstatin reduce proliferation of neuronal progenitor cells in the subventricular zone (Goncalves *et al*, 2008). DAGL-α also plays an essential role in endocannabinoid-mediated retrograde synaptic suppression in which 2-AG synthesized at post-synaptic terminals acts as a retrograde messenger to activate the pre-synaptic cannabinoid receptor type 1 (CB_1), which inhibits synaptic transmission. Tanimura et al. (2010) reported that deletion of DAGL-α, but not DAGL-β, annihilated two forms of endocannabinoid-mediated short-term synaptic plasticity, depolarization-induced suppression of excitation (DSE) and inhibition (DSI) in hippocampus, striatum, and cerebellum. Similarly, Gao et al. (2010) replicated these findings in hippocampus, and Yoshino et al. (2011) reported that DAGL-β plays a necessary role in DSI in prefrontal cortex (PFC). Furthermore, the DAGL inhibitor DO34, blocked DSE in cerebellar slices and DSI in hippocampal slices in a concentration dependent manner (Ogasawara *et al*, 2016).

The cell signaling events that occur after learning are frequently studied in terms of long-term potentiation (LTP). Carlson et al. (2002) demonstrated that transient release of endocannabinoids by depolarization facilitated the induction of LTP when preceded by DSI, suggesting that endocannabinoids may enhance plasticity at Schaffer collateral-CA1 synapses through a disinhibitory action. However, the role that the major 2-AG biosynthetic enzyme DAGL-α plays in the induction of LTP remains unknown. Here we hypothesize that this enzyme plays a necessary role in the induction of LTP.

Accordingly, we predict that pharmacological inhibition or genetic deletion of DAGL-α will disrupt LTP.

The present study also investigated the *in vivo* role of DAGL-α in learning and memory. Specifically, we evaluated whether endocannabinoid-regulated short-term synaptic plasticity disruption caused by deletion or inhibition of this enzyme translates to deficits in Morris water maze model (MWM) of learning and memory. Given the important role of hippocampal neurogenesis in the processing of spatial memory (Lieberwirth *et al*, 2016), we investigated the consequences of DAGL-α disruption on spatial memory processes of acquisition, expression, extinction, forgetting, and reversal in the MWM. To circumvent known pitfalls related to constitutive genetic deletions, such as the role of DAGL-α in axonal guidance during development (Williams *et al*, 2003), we utilized the DAGL-α/β inhibitor, DO34, and DAGL-$\alpha^{-/-}$ mice. Because DO34 also inhibits other serine hydrolases (i.e., ABHD2, ABHD6, CES1C, PLA2G7, PAFAH2), we also evaluated DO53, a structural analog of DO34 that cross-reacts with these off-targets but does not inhibit DAGL (Ogasawara *et al*, 2016).

In the present study, we ascertain the consequences of DAGL-α disruption at three levels of investigation; cellular responses to LTP, *in vivo* spatial learning and memory deficits, and alterations of endocannabinoid lipids, their substrates and metabolites, in hippocampus, prefrontal cortex, striatum, and cerebellum (brain areas important for learning and memory showing high DAGL-α activity [Baggelaar et al., 2017]).

Materials and Methods

Animals. Subjects consisted of adult male C57BL/6J mice (Jackson Laboratories, Bar Harbor, Maine), and DAGL-$\alpha^{-/-}$,-$\alpha^{+/-}$, and -$\alpha^{+/+}$ mice on a mixed 99% C57BL/6 (30% J, 70% N) and 1% 129/SvEv background, as previously described (Hsu *et al*, 2012). DAGL-$\alpha^{+/-}$ mouse breeding pairs were originally generated in the Cravatt laboratory and transferred to Virginia Commonwealth University. All mice (age 8-10 weeks) were pair-housed under a 12 h light/12 h dark cycle (0600 to 1800 h), at a constant temperature (22ºC) and humidity (50-60%), with food and water available *ad libitum*. All experiments were conducted in accordance with the National Institute of Health (NIH) Guide for the Care and Use of Laboratory Animals (NIH Publications No. 8023, revised 1978), and were approved by the Virginia Commonwealth University and Medical College of Wisconsin Institutional Animal Care and Use Committees.

Electrophysiology. For LTP experiments, DAGL-$\alpha^{+/+}$, -$\alpha^{+/-}$, -$\alpha^{-/-}$ and C57BL/6J mice were anaesthetized under isoflurane inhalation and decapitated. Hippocampi were dissected (in C57BL/6J mice 2 h post vehicle [VEH], DAGL-α inhibitor DO34 (Cravatt Laboratory, La Jolla, CA) [30 mg/kg], or its control analog and ABHD6 inhibitor DO53 [30 mg/kg] administration) and were embedded in low-melting-point agarose (3%, Sigma-Aldrich A0701). Transverse hippocampal slices (400 μm thick) were prepared using a vibrating slicer (Leica VT1200s) (Pan *et al*, 2011; Zhang *et al*, 2015). Slices were prepared at 4-6°C in a solution containing (in mM): 68 sucrose, 2.5 KCl, 1.25 NaH_2PO_4, 5 $MgSO_4$, 26 $NaHCO_3$, and 25 glucose. The slices were transferred to and stored in artificial cerebrospinal fluid containing (in mM): 119 NaCl, 3 KCl, 2 $CaCl_2$, 1

$MgCl_2$, 1.25 NaH_2PO_4, 25 $NaHCO_3$, and 10 glucose at room temperature for at least 1 hour before use. All solutions were saturated with 95% O_2 and 5% CO_2.

Field excitatory postsynaptic potentials (fEPSPs) were recorded with patch clamp amplifiers (Multiclamp 700B) under infrared-differential interference contrast microscopy. The recordings were made blind to drug treatment and mouse genotype. Data acquisition and analysis were performed using digitizers (DigiData 1440A and DigiData 1550B) and the analysis software pClamp 10 (Molecular Devices). Signals were filtered at 2 kHz and sampled at 10 kHz. Field recordings were made using glass pipettes filled with 1 M NaCl (1-2 MΩ) placed in the stratum radiatum of the CA1 region of the hippocampal slices, and fEPSPs were evoked by stimulating the Schaffer collateral/commissural pathway at 0.033 Hz with a bipolar tungsten electrode (WPI). Stable baseline fEPSPs were recorded for at least 20 minutes at an intensity that induced ~40% of the maximal evoked response. LTP was induced by theta burst stimulation (TBS), which consisted of a series of 15 bursts, with 4 pulses per burst at 100 Hz with a 200 ms inter-burst interval. TBS is designed to mimic the *in vivo* firing patterns of hippocampal neurons during exploratory behavior (Larson *et al*, 1986). All recordings were performed at 32 ± 1°C by using an automatic temperature controller.

Morris water maze (MWM) assessments. The MWM consisted of a circular, galvanized steel tank (1.8 m in diameter, 0.6 m height). The tank was filled with water (maintained at 20º C ± 2º C) with a white platform (10 cm diameter) submerged 1 cm below the water's surface. A sufficient volume of white paint (Valspar 4000 latex paint, Lowe's Companies Inc., Mooresville, NC) was added to render the water opaque and the platform invisible. In addition to distal visual cues (shapes) on curtains surrounding

the tank (30 cm from the tank wall), five sheets of laminated paper with distinct black-and-white geometric designs were attached to the sides of the tank serving as proximal cues. An automated tracking system (ANY-maze, San Diego Instruments, Inc., San Diego, CA) analyzed the swim path of each subject and calculated distance (path length between being placed in the water and finding the hidden platform), average swim speed, number of platform crossings, and percentage of time spent in each quadrant.

To assess MWM acquisition DAGL-$\alpha^{+/+}$, -$\alpha^{+/-}$, -$\alpha^{-/-}$ mice received 10 Fixed Platform training days (i.e. a submerged platform remained in the same location across days), and then were assessed for expression of spatial memory on day 11 in a single MWM Fixed Platform Probe Trial (i.e. the submerged platform was removed). C57BL6/J Mice received a 2 h pretreatment of the DAGL-α inhibitor DO34 (0.3, 3, and 30 mg/kg (Wilkerson *et al*, 2017), or its inactive analog and ABHD6 inhibitor DO53 (30 mg/kg), or VEH on each of 10 Fixed Platform training days. A cued task test assessed sensori-motor/motivational confounds by placing a 10cm high black cylinder on the submerged platform and mice were released from the farthest two release points. In order to assess whether DO34 affects the expression of spatial memory, separate groups of mice were given 10 days of drug-free Fixed Platform training. On day 11, each subject was administered 30 mg/kg DO34 or VEH, and 2 h later underwent a single 2 min MWM Fixed Platform Probe Trial. The extinction of spatial memory was assessed in drug-naïve acquisition trained mice, which received injections of 30 mg/kg DO34 or VEH (2 h pretreatment) and tested in 2 min probe trials at 1, 2, 3, 4 and 6 weeks post-acquisition. To assess forgetting, a group of drug-naïve acquisition trained mice were administered 30 mg/kg DO34 or VEH on day 11 and then returned to their home cage, given DO34 or

VEH at 6 weeks post-acquisition and administered a probe trial 2 h later. Reversal learning was assessed in drug-naïve acquisition trained mice, which received injections of 30 mg/kg DO34 or VEH (2 h pretreatment) and trained in reversal task trials where the submerged platform was moved to the opposite side of the tank over 5 days post-acquisition, followed by a 2 min drug-free probe trial on day 6 post-acquisition.

Lipid extraction and mass spectrometry. DAGL-$\alpha^{+/+}$, -$\alpha^{+/-}$, -$\alpha^{-/-}$ mice, and C57BL6/J mice receiving a 2 or 24 h pretreatment of DO34 (30 mg/kg) or VEH, were anaesthetized under isoflurane inhalation and decapitated. Hippocampi, prefrontal cortex, striatum, and cerebellum were dissected out from brain, flash frozen in liquid nitrogen, and stored at −80°C until assay. On the day of lipid extraction, as previously described (Kwilasz *et al*, 2015), the pre-weighed mouse brains were homogenized with 1.4 ml chloroform:methanol (containing 0.0348 g PMSF/ml). Six point calibration curves ranged from 0.078 pmol to 10 pmol for AEA, 0.125 nmol to 16 nmol for 2-AG, AA, and SAG, a negative control and blank control were also prepared. Internal standards (Cayman Chemicals, Michigan, USA) (50 µl of each of 8 nmol SAG-d8, 1 pmol AEA-d8, 1 nmol 2-AG-d8, 1 nmol AA-d8) were added to each calibrator, control, and sample, except the blank control. Each calibrator, control, and sample was then mixed with 0.3 ml of 0.73% w/v NaCl, vortexed, and centrifuged (10 min at 4000 × *g* and 4°C). The aqueous phase plus debris were collected and extracted again twice with 0.8 ml chloroform, the organic phases were pooled and organic solvents were evaporated under nitrogen gas. Dried samples were reconstituted with 0.1 ml chloroform, mixed with 1 ml cold acetone, and centrifuged (10 min at 4000 × *g* and 4°C) to precipitate

proteins. The upper layer of each sample was collected and evaporated to dryness and reconstituted with 0.1 ml methanol and placed in auto-sample vials for analysis.

An Ultra performance liquid chromatography-tandem mass spectrometer (*UPLC-MS/MS*) was used to identify and quantify the DAGL-α substrate 1-Stearoyl-2-Arachidonoyl-sn-Glycerol (SAG, a nuclear diacyglycerol [Deacon et al., 2001] preferentially used by DAGLs [Balsinde et al., 1991; Allen et al., 1992]), the DAGL-α metabolites 2-AG and arachidonic acid (AA), and anandamide (AEA, a biosynthetically distinct endogenous cannabinoid ligand), in brain. Sciex 6500 QTRAP system with an IonDrive Turbo V source for TurbolonSpray® (Ontario, Canada) attached to a Shimadzu UPLC system (Kyoto, Japan) controlled by Analyst software (Ontario, Canada). Chromatographic separation was performed on a Discovery® HS C18 Column 15cm x 2.1mm, 3µm (Supelco: Bellefonte, PA) kept at 25°C with an injection volume of 10 µL. The mobile phase consisted of A: acetonitrile and B: water with 1 g/L ammonium acetate and 0.1% formic acid. The following gradient was used: 0.0 to 2.4 minutes at 40% A, 2.5 to 6.0 minutes at 40% A, hold for 2.1 minutes at 40% A, then 8.1 to 9 min 100% A, hold at 100% A for 3.1 min and return to 40% A at 12.1 min with a flow rate was 1.0 mL/min. The source temperature was set at 600°C and had a curtain gas at a flow rate of 30 ml/min. The ionspray voltage was 5000 V with ion source gases 1 and 2 flow rates of 60 and 50 ml/min, respectively. The mass spectrometer was run in positive ionization mode for AEA and 2-AG and in negative ionization mode for AA, and the acquisition mode used was multiple reaction monitoring. The following transition ions (m/z) were monitored with their corresponding collection energies (eV) in parentheses: AEA: 348>62 (13) and 348>91 (60); AEA-d8: 356>63 (13); 2-AG: 379>287 (26) and

379>296 (28); 2-AG-d8: 384>287 (26); AA: 303>259 (-25) and 303>59 (-60); AA-d8: 311>267 (-25). The total run time for the analytical method was 14 min. Chromatographic analysis of SAG was performed on a Hypersil Gold® 3 X 50mm, 5 µ column (Thermo Scientific, Waltham, MA) kept at 25°C with an injection volume of 2 µL. The mobile phase consisted 10:90 mM ammonium formate: methanol mobile with a flow rate of 0.5 mL/min. The source temperature, curtain gas at a flow rate, ionspray voltage and source gas flow rates were the same as indicated above. The mass spectrometer was run in positive ionization mode. The following transition ions (m/z) were monitored with their corresponding collection energies (eV) in parentheses: SAG: 646>341 (34) and 646>287 (38); SAG-d8: 654>341 (34). The total run time for the analytical method was 5 min. Calibration curves were analyzed with each analytical batch for each analyte. A linear regression ratio of the peak area analyte counts with the corresponding deuterated internal standard versus concentration was used to construct the calibration curves.

Experimental design and statistical analysis. Electrophysiological data are presented as mean ± SEM. The magnitude of LTP (%) was calculated as follows: 100 × [mean fEPSP slope during the final 10 min of recording/mean baseline fEPSP slope]. Post-tetanic potentiation was calculated as the magnitude of the fEPSP slope relative to baseline for the first 5 min after TBS. Results were analyzed with one-way ANOVA followed by Tukey's *post hoc* analysis.

Behavioral data are presented as mean + SEM. All MWM acquisition, extinction, forgetting, reversal, and swim speed data, were analyzed using a mixed factor ANOVA (distance, percent time in outer ring, and cm/s measures). All probe trial analyses

focused on the first minute of exploration, with all gene deletion measures analyzed by one-way ANOVA and Sidak post hoc test, and DO34 measures analyzed by independent groups t-test. All MWM cued task data were analyzed by one-way ANOVA. MWM swim path selection metrics were assigned per Wagner et al., 2013 into three categories; spatial (direct, indirect, and self-orienting), non-spatial (scanning, circling, and random) and thigmotaxic, and were analyzed for gene deletion using a Chi Square analysis with pairwise comparisons and Bonferroni corrections (MacDonald and Gardner, 2000), and for drug-treatments using a Kruskall Wallis analysis. From the sample sizes, power was calculated using G*power 3 (Faul *et al*, 2007a) and was found, with alpha at .05, to range from 0.67 to 0.84 for mixed factor ANOVAs, from 0.45 to 0.99 for one-way ANOVAs, and from 0.34 to 0.51 for independent group t-tests.

Prior to data analysis, brain level data were transformed to pmol/g of brain tissue for AEA, and nmol/g of brain tissue for SAG, 2-AG and AA, and AEA. Drug and gene manipulations on brain endocannabinoids were evaluated by one-way ANOVA, for each lipid in each brain area, followed by a Sidak post hoc test. The criterion for significance in all experiments was set at $p < 0.05$, and all analyses were conducted using IBM SPSS Statistics 22 for Windows (IBM Software, New York, NY).

Results

Experiment 1: Genetic deletion or pharmacological blockade of DAGL-α attenuates LTP in CA1 region of the hippocampus. In hippocampal slices prepared from DAGL-$\alpha^{+/+}$ and DAGL-$\alpha^{+/-}$ mice (n = 9-11), TBS induced robust LTP that remained stable during the 60 min recording period (Figure 4-1A). The fEPSP slope in hippocampal slices from DAGL-$\alpha^{-/-}$ mice (n = 8) subjected to the same TBS stimulation

slowly decayed toward baseline. The magnitude of LTP as measured between 50-60 min after TBS stimulation significantly differed among the three groups ($F_{(2,27)} = 5.37$, $p = 0.011$, ANOVA), and *post hoc* tests indicated that TBS-induced LTP was significantly greater in DAGL-$\alpha^{+/+}$ and DAGL-$\alpha^{+/-}$ mice than in DAGL-$\alpha^{-/-}$ mice (DAGL-$\alpha^{+/+}$ vs. DAGL-$\alpha^{-/-}$, $p = 0.039$; DAGL-$\alpha^{+/-}$ vs. DAGL-$\alpha^{-/-}$, $p = 0.013$). However, the magnitude of LTP did not differ between DAGL-$\alpha^{+/+}$ mice and DAGL-$\alpha^{+/-}$ mice ($p = 0.926$).

Hippocampal slices from C57BL/6J mice treated with VEH, DO34 (30 mg/kg), or DO53 (30 mg/kg) showed significant differences in the magnitude of LTP ($F_{(2,23)} = 7.90$, $p = 0.003$, ANOVA; Figure 4-1B). *Post hoc* tests indicated that TBS induced similar LTP in hippocampal slices prepared from VEH-treated (n = 9) and DO53-treated mice (n = 8; $p = 0.514$ vs. vehicle), but slices prepared from DO34-treated mice displayed a significantly decreased magnitude of LTP (n = 7; $p = 0.002$ vs. vehicle; $p = 0.031$ vs. DO53). Moreover, the magnitude of post-tetanic potentiation (PTP) during the first 5 min of LTP induction significantly differed among the three treatment groups ($F_{(2,23)} = 7.17$, $p = 0.004$, ANOVA), in which DO34 administration produced a significant decrease in the PTP compared with vehicle ($p = 0.007$) and DO53 ($p = 0.011$).

Experiment 2.1: DAGL-$\alpha^{-/-}$ mice display profound phenotypic MWM spatial memory deficits and altered MWM search strategies. Per the experimental timeline (Figure 4-2A), the first acquisition day of fixed platform training (extended data Figure 4-2-1A) yielded no significant differences among groups and across trials ($F_{(6,114)} = 1.67$, $p = 0.135$, ANOVA). However, across the ten days of MWM fixed platform acquisition training (Figure 4-2B), a significant interaction ($F_{(18,342)} = 2.48$, $p = 0.001$, ANOVA) revealed DAGL-$\alpha^{-/-}$ mice (n = 13) had longer distances to the platform than DAGL-$\alpha^{+/+}$ (n

= 15) or DAGL-$\alpha^{+/-}$ mice (n = 15) on acquisition days 2 (p = 0.001, p = 0.005), 3 (p = 0.000, p = 0.000), 4 (p = 0.000, p = 0.000), 5 (p = 0.000, p = 0.000), 6 (p = 0.000, p = 0.000), 7 (p = 0.000, p = 0.001), 8 (p = 0.001), 9 (p = 0.000, p = 0.001), and 10 (p = 0.000, p = 0.000) respectively. Also, DAGL-$\alpha^{+/+}$ mice and DAGL-$\alpha^{+/-}$ mice, respectively, showed significant reductions in distances to the platform on days 4 (p = 0.005, p = 0.014), 5 (p = 0.000, p = 0.025), 6 (p = 0.001, p = 0.004), 7 (p = 0.000, p = 0.000), 8 ($\alpha^{+/+}$; p = 0.000), 9 (p = 0.000, p = 0.007), and 10 (p = 0.000, p = 0.001) compared to day 1. In contrast, DAGL-$\alpha^{-/-}$ mice showed no significant difference in distance compared to day 1 across subsequent fixed platform acquisition days (2; p = 1.000, 3; p = 1.000, 4; p = 1.000, 5; p = 1.000, 6; p = 1.000, 7; p = 0.625, 8; p = 0.399, 9; p = 0.373, and 10; p = 0.0670). Furthermore, during the fixed platform probe trial (Figure 4-2C,D,E) DAGL-$\alpha^{-/-}$ mice demonstrated significantly longer distances to the platform location ($F_{(2,38)}$ = 5.81, p = 0.006, ANOVA) than DAGL-$\alpha^{+/+}$ mice (p = 0.022) and DAGL-$\alpha^{+/-}$ mice (p = 0.011), significantly fewer platform entries ($F_{(2,38)}$ = 7.40, p = 0.002, ANOVA) than DAGL-$\alpha^{+/+}$ mice (p = 0.001), and a lower spatial preference for the target quadrant ($F_{(2,38)}$ = 7.73, p = 0.002, ANOVA) than DAGL-$\alpha^{+/+}$ mice (p = 0.002) and DAGL-$\alpha^{+/-}$ mice (p = 0.016). No significant difference in cued task performance (Figure 4-2F), ($F_{(2,38)}$ = 0.926, p = 0.405, ANOVA), or swim speed (Figure 4-2G), ($F_{(18,342)}$ = 0.648, p = 0.860, ANOVA), suggest the DAGL-$\alpha^{-/-}$ mice performance deficits were unaffected by sensorimotor or motivational impairments. Also, no significant differences in body weight (extended data Figure 4-2-2A,C) at baseline ($F_{(2,38)}$ = 3.08, p = 0.057, ANOVA) or during fixed platform acquisition ($F_{(2,38)}$ = 2.84, p = 0.071, ANOVA) were evident among the genotypes.

On Fixed Platform day 10 (Figure 4-3A), DAGL-$\alpha^{-/-}$ mice used significantly more non-spatial and thigmotaxic swimming strategies than DAGL-$\alpha^{+/+}$ or DAGL-$\alpha^{+/-}$ mice, ($X^2_{(4, N=41)}$ = 21.9, p = 0.000, Chi Square). The change in DAGL-$\alpha^{-/-}$ mice strategy proportion was indicated by pairwise comparisons (p = 0.001). Furthermore, during Fixed Platform acquisition (Figure 4-3B) a significant main effect of genotype ($F_{(2,38)}$ = 7.29, p = 0.002, ANOVA) indicated that DAGL-$\alpha^{-/-}$ mice spent more time in the MWM outer ring than DAGL-$\alpha^{+/+}$ mice (p = 0.002) and DAGL-$\alpha^{+/-}$ mice (p = 0.028). A significant main effect of day ($F_{(9,342)}$ = 13.9, p = 0.000, ANOVA) also showed that collectively DAGL-$\alpha^{+/+}$, -$\alpha^{+/-}$, and -$\alpha^{-/-}$ mice spent a decreased proportion of their time in the outer ring on days 4 (p = 0.015), 5 (p = 0.034), 6 (p = 0.001), and 7-10 (p = 0.000) compared to day 1.

Experiment 2.2: Pharmacological inhibition of DAGL-α produces impaired MWM spatial acquisition. Per the experimental timeline (Figure 4-4A), fixed platform day 1 (extended data Figure 4-2-1B), yielded no significant differences among groups and across trials ($F_{(12,171)}$ = 1.65, p = 0.082, ANOVA). During MWM fixed platform acquisition (Figure 4-4B) a significant main effect of drug ($F_{(4,57)}$ = 8.77, p = 0.000) revealed 30 mg/kg DO34-treated mice (n = 12) required longer swim path distances to the platform than mice in the VEH (n = 15, p = 0.000), 0.3 mg/kg DO34 (n = 12, p = 0.002), and 30 mg/kg DO53 (n = 12, p = 0.000) conditions, However, these mice did not statistically differ from mice in the 3 mg/kg DO34 group (n = 11, p = 0.103). Also, mice treated with VEH ($F_{(9,126)}$ = 12.7, p < 0.001, repeated measures ANOVA), 30 mg/kg DO34 ($F_{(9,99)}$ = 12.3, p = 0.000, repeated measures ANOVA), 3 mg/kg DO34 ($F_{(9,90)}$ = 8.01, p = 0.000, repeated measures ANOVA), 0.3 mg/kg DO34 ($F_{(9,99)}$ = 8.48, p = 0.000,

repeated measures ANOVA), and 30 mg/kg DO53 ($F_{(9,99)}$ = 15.8, p = 0.000, repeated measures ANOVA) showed significantly reduced distances to the platform days 3 (VEH p = 0.022), 4 (VEH p = 0.000), 5 (VEH p = 0.005; 30 mg/kg DO34 p = 0.021; 3 mg/kg DO34 p = 0.019; 30 mg/kg DO53 p = 0.005), 6 (VEH p = 0.001; 30 mg/kg DO34 p = 0.004; DO53 p = 0.003), 7 (VEH p < 0.001; 30 mg/kg DO34 p = 0.003; 3 mg/kg DO34 p = 0.008; DO53 p = 0.002), 8 (VEH p = 0.003; 30 mg/kg DO34 p = 0.034; 3 mg/kg DO34 p = 0.038; DO53 p = 0.001), 9 (VEH p = 0.001; 30 mg/kg DO34 p = 0.000; 3 mg/kg DO34 p = 0.002; DO53 p = 0.000), and 10 (VEH p = 0.000; 30 mg/kg DO34 p = 0.000; 3 mg/kg DO34 p = 0.024; 0.3 mg/kg DO34 p = 0.011; DO53 p = 0.000) compared to day 1.

In order to test whether DO34 affects memory of the platform location (Figure 4-4C), a probe trial revealed similar distances to the platform location ($t_{(15)}$ = 0.0880, p = 0.931, independent t-test; Figure 4-4D) in DO34-treated and VEH-treated mice, similar number of platform entries ($t_{(15)}$ = 1.17, p = 0.260, independent t-test; Figure 4-4E), and similar percentages of time spent in the target quadrant ($t_{(15)}$ = 1.28, p = 0.220, independent t-test; Figure 4-4F). The absence of significant differences in cued task performance ($F_{(4,57)}$ = 1.09, p = 0.368, ANOVA; Figure 4-4G), suggests that DO34 does not elicit sensorimotor or motivational impairments.

During fixed platform acquisition, a significant swim speed interaction ($F_{(36,513)}$ = 1.60, p = 0.016, ANOVA; Figure 4-4H), showed that mice administered 30 mg/kg DO34 swam faster than VEH-treated mice on days 1 (p = 0.019), 2 (p = 0.010), 4 (p = 0.042), 5 (p = 0.009), and 8 (p = 0.003), but 0.3 mg/kg DO34-treated mice swam slower than VEH-treated mice on days 7 (p = 0.026), 9 (p = 0.044), and 10 (p = 0.022). Also, while

no significant difference in body weight was evident at baseline ($F_{(4,57)}$ = 2.03, p = 0.103, ANOVA; extended data Figure 4-2-2B,D), a significant interaction between drug and day for this measure occurred throughout acquisition training ($F_{(56,798)}$ = 7.06, p = 0.000, ANOVA). DO34 elicited body weight reductions compared to VEH at 30 mg/kg DO34 (days 2 through 15, p = 0.000), 3 mg/kg DO34 (days 4, p = 0.006; 8, p = 0.032; and 13, p = 0.015), 0.3 mg/kg DO34 (day 4, p = 0.001), and 30 mg/kg DO53 (days 2, p = 0.000; 3, p = 0.000; days 4, p = 0.041; 5, p = 0.003; 7, p = 0.008; and 13, p = 0.000).

On Fixed Platform day 10, DO34-treated mice showed no significant change in swim path strategy ($X^2_{(3, N=49)}$ = 7.0;97, p = 0.069, chi square; Figure 4-5A). However, a significant main effect of drug was found for time spent in the outer ring of the MWM throughout the ten acquisition sessions ($F_{(4,57)}$ = 2.96, p = 0.027, ANOVA; Figure 4-5B). DO34 (30 mg/kg) produced a modest increase in the time spent in the MWM outer ring compared with VEH-treated mice (p = 0.035). A significant main effect of day ($F_{(9,513)}$ = 59.4, p = 0.000, ANOVA) also showed that mice spent a smaller proportion of their time in the outer ring on all subsequent days, 2, 3, 4, 5, 6, 7, 8, 9, and 10 (p < 0.001) than on day 1.

Experiment 2.3: Pharmacological inhibition of DAGL-α impairs MWM reversal, but not extinction or forgetting. The next experiments examined the effects of DO34 (30 mg/kg; n = 8) vs. VEH (n = 9) on extinction (Figure 4-6A), forgetting (Figure 4-6B), and reversal learning (Figure 4-6D, 30 mg/kg; n = 15, VEH; n = 15). As shown in Figure 6C, subjects displayed evidence of extinction following fixed platform day 10 and exposure to six sessions (including probe trial) in the MWM without the hidden platform present via a main effect of day ($F_{(5,75)}$ = 3.08, p = 0.014, ANOVA). Subjects had

significantly longer distances to the previous platform location on extinction weeks 4 (p = 0.047), and 6 (p = 0.027) compared to probe trial. The lack of a statistical interaction between drug and day ($F_{(5,75)}$ = 0.292, p = 0.916, ANOVA) and lack of significant main effect of drug ($F_{(1,15)}$ = 1.98, p = 0.180, ANOVA) indicate that DO34 did not affect extinction. In the probe trial assessment of forgetting (Figure 4-6C), the lack of a statistically significant interaction between drug and day ($F_{(1,10)}$ = 0.638, p = 0.443, ANOVA) or a main effect of drug ($F_{(1,10)}$ = 2.50, p = 0.145, ANOVA) indicates DO34 did not impact forgetting performance. In the evaluation of reversal learning (Figure 4-6E), the statistically significant interaction between drug and day ($F_{(5,140)}$ = 4.43, p = 0.001, ANOVA) indicates that DO34 delayed reversal, specifically on days 1 (p = 0.007), 2 (p = 0.007), and 5 (p = 0.016). Yet all subjects displayed evidence of reversal learning after exposure to five reversal sessions (and probe trial) via a main effect of day in VEH ($F_{(5,70)}$ = 6.05, p = 0.000, repeated measures ANOVA) and DO34 ($F_{(5,70)}$ = 13, p = 0.000, repeated measures ANOVA) mice. VEH-treated subjects had significantly reduced distances to the new platform location on reversal days 2 (p = 0.011), 3 (p = 0.0005) and 5 (p = 0.000) compared to day one. Similarly, DO34-treated subjects showed reduced distance to the platform on days 2 through probe (2, p = 0.033; 3, p = 0.000; 4, p = 0.008; 5, p = 0.010; and probe p = 0.001) compared to day one.

Experiment 3.1: Genetic deletion of DAGL-α produces profound alterations to eCB and related lipid profiles. DAGL-$\alpha^{-/-}$ mice (n = 8) possessed elevated levels of the DAGL-α substrate, SAG, across all four brain regions; hippocampus, ($F_{(2,21)}$ = 174, p = 0.000, ANOVA; Figure 4-7A), PFC ($F_{(2,21)}$ = 753, p = 0.000, ANOVA; Figure 4-7B), striatum ($F_{(2,21)}$ = 52, p = 0.000, ANOVA; Figure 4-7C), and cerebellum ($F_{(2,21)}$ = 32, p =

0.000, ANOVA; Figure 4-7D), compared to both DAGL-$\alpha^{+/+}$ (n=8, p = 0.000) and DAGL-$\alpha^{+/-}$ mice (n=8, p = 0.000). DAGL-$\alpha^{-/-}$ mice also showed profound reductions of 2-AG and its metabolite AA, respectively, across each brain region: hippocampus, ($F_{(2,21)}$ = 246, p = 0.000, ANOVA; Figure 4-7E; $F_{(2,21)}$ = 156, p = 0.000, ANOVA; Figure 4-7M), PFC ($F_{(2,21)}$ = 29, p = 0.000, ANOVA; Figure 4-7F; $F_{(2,21)}$ = 207, p = 0.000, ANOVA; Figure 4-7N), striatum ($F_{(2,21)}$ = 48, p = 0.000, ANOVA; Figure 4-7G; $F_{(2,21)}$ = 126, p = 0.000, ANOVA; Figure 4-7O), and cerebellum ($F_{(2,21)}$ = 70, p = 0.000, ANOVA; Figure 4-7H; $F_{(2,21)}$ = 155, p = 0.000, ANOVA; Figure 4-7P), compared to both DAGL-$\alpha^{+/+}$ (p = 0.000) and DAGL-$\alpha^{+/-}$ mice (p = 0.000). DAGL-$\alpha^{+/-}$ mice showed only modest reductions in striatal (p = 0.04), hippocampal (p = 0.002), and cerebellar (p < 0.002) 2-AG compared to DAGL-$\alpha^{+/+}$ mice. Also, region selective reductions of AEA were found in DAGL-$\alpha^{-/-}$ mouse hippocampus ($F_{(2,21)}$ = 51, p = 0.000, ANOVA; Figure 4-7I), and cerebellum ($F_{(2,21)}$ = 10.2, p = 0.001, ANOVA; Figure 4-7L), but not in PFC (Figure 4-7J) or striatum (Figure 4-7K) compared to both DAGL-$\alpha^{+/+}$ and DAGL-$\alpha^{+/-}$ mice.

Experiment 3.2: Pharmacological inhibition of DAGL produces brain region selective alterations in eCB and related lipid profiles. DO34-treated mice possessed elevated levels of SAG at 2 h post-injection (n = 5) across all four brain regions; hippocampus, ($F_{(2,15)}$ = 7.48, p = 0.006, ANOVA; Figure 4-8A), PFC ($F_{(2,15)}$ = 30, p = 0.000, ANOVA; Figure 4-8B), striatum ($F_{(2,15)}$ = 5.46, p = 0.017, ANOVA; Figure 4-8C), and cerebellum ($F_{(2,15)}$ = 6.83, p = 0.008, ANOVA; Figure 4-8D) compared to VEH (n = 5, p = 0.005, p = 0.000, p = 0.038, and p = 0.006 respectively), but not at 24 h post-injection (n = 8) compared to VEH (p = 0.232, p = 0.992, p = 0.999, p = 0.145). PFC and striatal SAG was also lower at 24 h compared to 2 h (p = 0.000, p = 0.027 respectively). DO34-treated

mice also showed consistent reductions of 2-AG in hippocampus ($F_{(2,15)}$ = 37, p = 0.000, ANOVA; Figure 4-8E), PFC ($F_{(2,15)}$ = 11.6, p = 0.001, ANOVA; Figure 4-8F), striatum ($F_{(2,15)}$ = 4.82, p = 0.024, ANOVA; Figure 4-8G), and cerebellum ($F_{(2,15)}$ = 94, p = 0.000, ANOVA; Figure 4-8H) at 2 h (p = 0.000, p = 0.001, p = 0.036, p = 0.000 respectively), and hippocampus and cerebellum at 24 h (p = 0.000, p = 0.000). PFC and cerebellar 2-AG was also higher at 24 h compared to 2 h (p = 0.008, p = 0.013 respectively).While no significant change in AEA was found in hippocampus ($F_{(2,15)}$ = 0.92, p = 0.421, ANOVA; Figure 4-8I), PFC ($F_{(2,15)}$ = 3.04, p = 0.078, ANOVA; Figure 4-8J), striatum ($F_{(2,15)}$ = 2.70, p = 0.099, ANOVA; Figure 4-8K), or cerebellum ($F_{(2,15)}$ = 2.44, p = 0.121, ANOVA; Figure 4-8L), reductions of AA following DO34-treatment were seen in all brain regions; hippocampus ($F_{(2,15)}$ = 13.8, p = 0.000, ANOVA; Figure 4-8M) at 2 h (p = 0.005) and 24 h (p = 0.000), PFC ($F_{(2,15)}$ = 65, p = 0.000, ANOVA; Figure 4-8N) at 2 h (p = 0.000) and 24 h (p = 0.000), striatum ($F_{(2,15)}$ = 145, p = 0.000, ANOVA; Figure 4-8O) at 2 h (p = 0.000) and 24 h (p = 0.000), and cerebellum ($F_{(2,15)}$ = 59, p = 0.000, ANOVA; Figure 4-8P) at 2 h (p = 0.000) and 24 h (p = 0.000). AA levels were also significantly greater at 24 h than 2 h in PFC (p = 0.000) and striatum (p = 0.000).

Discussion

The present study makes the novel observations that either genetic deletion or pharmacological inhibition of DAGL-α profoundly disrupts hippocampal LTP accompanied by varying magnitudes of learning and memory deficits in the mouse MWM Fixed Platform and Reversal tasks. Specifically, DAGL-$\alpha^{-/-}$ mice display non-spatial search strategies and concomitantly disrupted Fixed Platform acquisition,

whereas DO34-treated mice show significantly delayed MWM acquisition and reversal learning but performance is spared in probe trial memory, extinction, and forgetting tasks. Additionally, these alterations in LTP and *in vivo* learning and memory paradigms occur in concert with distinct altered patterns of endocannabinoids and related lipids, across brain areas integral to learning and memory.

The observation that DAGL-α disruption decreases CA1 LTP is consistent with non-selective DAGL inhibitors blocking CA1 pairing-induced potentiation in rats (Xu *et al*, 2012). The lowered production of 2-AG following DAGL-α disruption implicates 2-AG as a possible LTP facilitator, corroborated also by 2-AG catabolism inhibition facilitating CA1 LTP (Silva-Cruz *et al*, 2017). Given that endogenously produced endocannabinoids facilitate LTP at CA1 hippocampal synapses through stimulation of astrocyte-neuron signaling (Gomez-Gonzalo *et al*, 2015), as well as when preceded by DSI (Carlson *et al*, 2002), suggests that endocannabinoids enhance plasticity by disinhibition. 2-AG is well recognized as an integral retrograde modulator of short-term CB_1 receptor-mediated synaptic plasticity (i.e., DSE/DSI), (Tanimura et al., 2010; Yoshino et al., 2011). Furthermore CB_1 receptor activation correlates with enhanced CA1 LTP (Chevaleyre and Castillo, 2004). Thus, reducing 2-AG production decreases CB_1 receptor signaling and thereby disrupting LTP. However, CB_1 receptor deletion or antagonism leads to a different pattern of behavioral impairments compared with analogous DAGL-α disruption in the present study. Specifically, wild type mice administered the CB_1 receptor antagonist Rimonabant or $CB_1^{-/-}$ mice acquired MWM Fixed Platform at a similar rate as control mice, but showed impaired MWM extinction (Varvel *et al*, 2005; Varvel and Lichtman, 2002). In the case of DAGL-α, its close spatial

localization to excitatory CB_1 receptor synapses (and adjacent to group I metabotropic glutamate receptors) and distance from inhibitory synapses (Katona *et al*, 2006; Yoshida *et al*, 2006), may account for the resilience of DAGL-α compromised mice in the MWM extinction task.

Contrary to the present work, Sugaya et al., 2013 found DAGL-$\alpha^{-/-}$ mice show no change in CA1 LTP, while facilitating entorhinal cortex-dentate gyrus LTP. The lack of CA1 LTP change was observed in DAGL-$\alpha^{-/-}$ mice with in-dwelling electrodes *in vivo,* where lipid profile disruption interacts with on-going milieu changes in an awake brain, suggesting the possible involvement of model system differences with the present work. The impairment by DO34 of post-tetanic potentiation within minutes of TBS suggests that pharmacological inhibition of DAGL-α reduced Ca^{2+} buildup in presynaptic axon terminals (Zucker and Regehr, 2002). Furthermore, off-target effects of DO34 (e.g. ABDH6) are unlikely to be responsible for the observed decrease in LTP magnitude given DO53 did not impact SC-CA1 LTP, consistent with its inability to alter hippocampal DSI (Ogasawara *et al*, 2016). As DO34 also inhibits DAGL-β, a contribution of this 2-AG biosynthetic enzyme cannot be ruled out. Yet its low expression on neurons and high expression on microglia (Hsu *et al*, 2012) argues against its involvement in the present study.

The phenotypic MWM deficits displayed by DAGL-$\alpha^{-/-}$ mice and impaired acquisition and reversal learning performance in DO34-treated mice, represent the first evidence supporting a role of DAGL-α in a laboratory animal model of spatial learning and memory, specific to the integration of new information, but not memory retrieval, extinction, or forgetting. The findings show deletion of DAGL-α profoundly disrupt fixed

platform MWM learning, compatible with the body of evidence highlighting the necessity of hippocampal neurogenesis for spatial memory processing (Snyder et al., 2005; Sahay et al., 2011), to which this enzymes significantly contributes (Gao *et al*, 2010; Goncalves *et al*, 2008). The altered search strategy may reflect a stress-induced shift from utilizing hippocampal-cognitive to striatal-habit learning (Wirz *et al*, 2017). The anxiety-like phenotype of DAGL-$\alpha^{-/-}$ mice (Jenniches *et al*, 2016; Shonesy *et al*, 2014) as well as the stress-inducing component of the MWM may drive a heavier reliance on non-spatial circular search strategies after DAGL-α disruption.

The difference in behavioral impairment magnitude between DAGL-$\alpha^{-/-}$ and DO34-treated mice warrants discussion. Previous DSI/DSE disparities between DAGL-α inhibition and gene deletion have been explained by insufficient inhibitor slice penetration (Ohno-Shosaku and Kano, 2014), yet DO34 is brain penetrant (Ogasawara *et al*, 2016), and both inhibitor and gene deletion led to impaired LTP. The relatively modest 2-AG lipid profile differences between DO34-treated mice and DAGL-$\alpha^{-/-}$ mice may contribute, in part, to the profound disruption of spatial learning in DAGL-$\alpha^{-/-}$ mice compared with the delay-related deficits observed following DO34 treatment. However, developmental alterations in the brains of the DAGL-$\alpha^{-/-}$ mice across ontogeny may also be a contributing factor. In the developing brain DAGL-α is expressed at presynaptic terminals (Bisogno *et al*, 2003a), participating in the control of axonal growth and guidance (Brittis *et al*, 1996; Williams *et al*, 1994), but is expressed on post-synaptic neurons in the adult brain. As such, DAGL-α switches roles from growth and guidance during development, to a modulator of synaptic signaling. The present phenotypic

learning and memory deficits and altered search strategy in DAGL-α$^{-/-}$ mice, may therefore be influenced by both roles of this enzyme.

The unique finding that DAGL-α inhibition selectively impairs acquisition and reversal learning, but not expression, extinction, or forgetting, suggests that DAGL-α is selectively important for the integration of new spatial information. While DAGL-α disruption has not previously been evaluated in reversal learning, contrary to the present findings DAGL-α disruption by DO34 (Cavener *et al*, 2018) and in DAGL-α$^{-/-}$ mice (Cavener *et al*, 2018; Jenniches *et al*, 2016) produces extinction, but not acquisition, deficits in fear memory. While DAGL-α is expressed in areas important during fear conditioning such as the basolateral amygdala (Yoshida *et al*, 2011), stress reduces amygdala-hippocampal connectivity (Wirz *et al*, 2017). Accordingly, DAGL-α may yet differentially modulate memory processes based on brain region or neuronal type.

The spatial memory impairments of DAGL-α$^{-/-}$ mice were accompanied by profound lipid profile changes, specifically reductions of 2-AG across all four brain areas. Likewise, other lines of DAGL-α$^{-/-}$ mice show 80% reductions in whole brain 2-AG (Gao et al., 2010; Tanimura et al., 2010), as well as in PFC, amygdala, striatum (Shonesy *et al*, 2014), and hippocampus (Jenniches *et al*, 2016). Yet the modest DAGL-α$^{+/-}$ mice reductions in striatal, hippocampal, and cerebellar 2-AG did not translate to fixed platform acquisition or probe trial deficits. Previous studies showed that DO34 produces large reductions in whole brain 2-AG (Ogasawara *et al*, 2016; Wilkerson *et al*, 2017), consistent with the current finding that DO34 reduced 2-AG in all four brain regions evaluated. Given the region dependent reductions of AEA in DAGL-α$^{-/-}$ mice,

DAGL-α substrates and metabolites may also play a more complex role in the biosynthetic pathway of AEA. Similarly, reduced AEA levels in DAGL-$\alpha^{-/-}$ mice were seen in forebrain (Shonesy *et al*, 2014) and hippocampus, but not striatum (Jenniches *et al*, 2016). Unexpectedly, DO34 did not significantly reduce AEA levels in any brain region investigated, despite 50% reductions of AEA in whole brain (Ogasawara *et al*, 2016; Wilkerson *et al*, 2017). Reductions of AEA in hippocampi of DAGL-$\alpha^{-/-}$ mice must be considered, given elevations of AEA impair LTP (Basavarajappa *et al*, 2014) and enhance acquisition in aversively motivated spatial memory tasks (Varvel *et al*, 2007). As inhibiting the primary hydrolytic AEA enzyme fatty acid amide hydrolase (FAAH) elevates brain levels of this endocannabinoid and concomitantly accelerates extinction rates (Varvel *et al*, 2007), we might expect that region specific reductions of AEA in DAGL-$\alpha^{-/-}$ mice would manifest with impaired MWM extinction learning phenotype. However, this outcome is not observed, and furthermore FAAH inhibition failed to reverse fear extinction deficits in DAGL-$\alpha^{-/-}$ mice (Cavener *et al*, 2018). To fully exclude the role of lowered AEA after DAGL-α deletion, future experiments to evaluate the administration of a FAAH inhibitor to DAGL-$\alpha^{-/-}$ mice prior to MWM assessment and LTP would be necessary.

Another consideration for the present results is the impact of DAGL-α blockade on downstream and upstream lipid signaling molecules. The expression of DAGL in invertebrate species without cannabinoid receptors (e.g. *Drosophila*; Elphick and Egertova, 2005) underscores the important role of this enzyme in regulating lipid signaling molecules independent of substrate production for cannabinoid receptor activation. As anticipated, both DAGL-$\alpha^{-/-}$ mice and DO34-treated mice showed

consistent elevations of the DAG substrate for DAGL-α, SAG, across all four brain areas, previously seen in forebrain of DAGL-$\alpha^{-/-}$ mice (Shonesy *et al*, 2014) and whole brain following DO34 (Ogasawara *et al*, 2016). Diacylglycerols such as SAG are known protein kinase C (PKC) activators (Hindenes *et al*, 2000), and while PKC activation facilitates memory (Bonini *et al*, 2007) little is known of the effects following sustained activation through elevated SAG. The dramatically reduced levels of AA across all four brain regions in DAGL-$\alpha^{-/-}$ mice and after DO34 suggest DAGL-α is an important intermediate for the maintenance of basal AA levels in brain, previously seen in whole brain (Gao *et al*, 2010) and forebrain (Shonesy *et al*, 2014). DO34-induced reductions of AA were often still evident at 24 h (consistent with 24 h partial DAGL-α activity recovery following DO34 (Ogasawara *et al*, 2016). Given hippocampal neurons also activate PKC through AA cascades (Hama *et al*, 2004), the DAGL-α disruption-induced AA reductions may also contribute to the observed learning and memory deficits.

Collectively this work supports the importance of DAGL-α in modulating hippocampal learning and memory. Thus, reductions in DAGL-α expression or function may contribute to cognitive pathologies, consistent with this idea are correlations between decreased DAGL-α expression and impaired verbal memory (Bioque *et al*, 2016). Age-related decreases in DAGL-α expression (Piyanova *et al*, 2015), and decreased neurogenesis in DAGL-α rich areas (Goncalves *et al*, 2008; Knoth *et al*, 2010), suggest DAGL-α dysregulation may be a fruitful area of study, particularly with respect to age-related cognitive decline (Bilkei-Gorzo *et al*, 2017). In sum, the present findings that DAGL-α disruption lead to learning and memory impairments at cellular

and selective behavioral levels implicate this enzyme as playing a key role in spatial learning and memory.

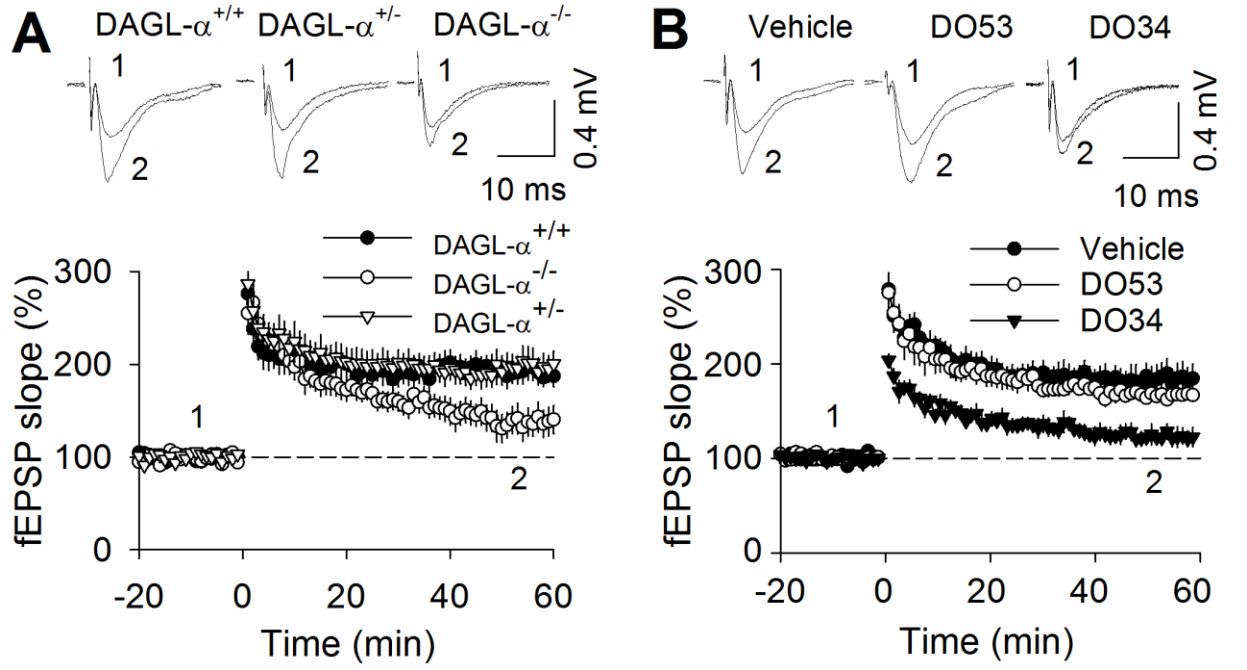

Figure 4-1. **DAGL-α$^{-/-}$ mice and C57BL/6 mice treated with the DAGL inhibitor DO34 show disrupted TBS-induced LTP in CA1 of the hippocampus**. The magnitude of LTP was significantly decreased in both **A,** DAGL-α$^{-/-}$ mice (n = 8) compared to DAGL-α$^{+/+}$ (n = 9) and DAGL-α$^{+/-}$ mice (n = 11), as well as in slices from **B**, DO34-treated C57BL/6J mice (n = 7) compared with VEH-treated (n = 9) or DO53-treated mice (n = 8). The magnitude of PTP during the initial induction phase was also significantly decreased in the DO34 group compared with VEH or DO53. Values represent mean ± SEM.

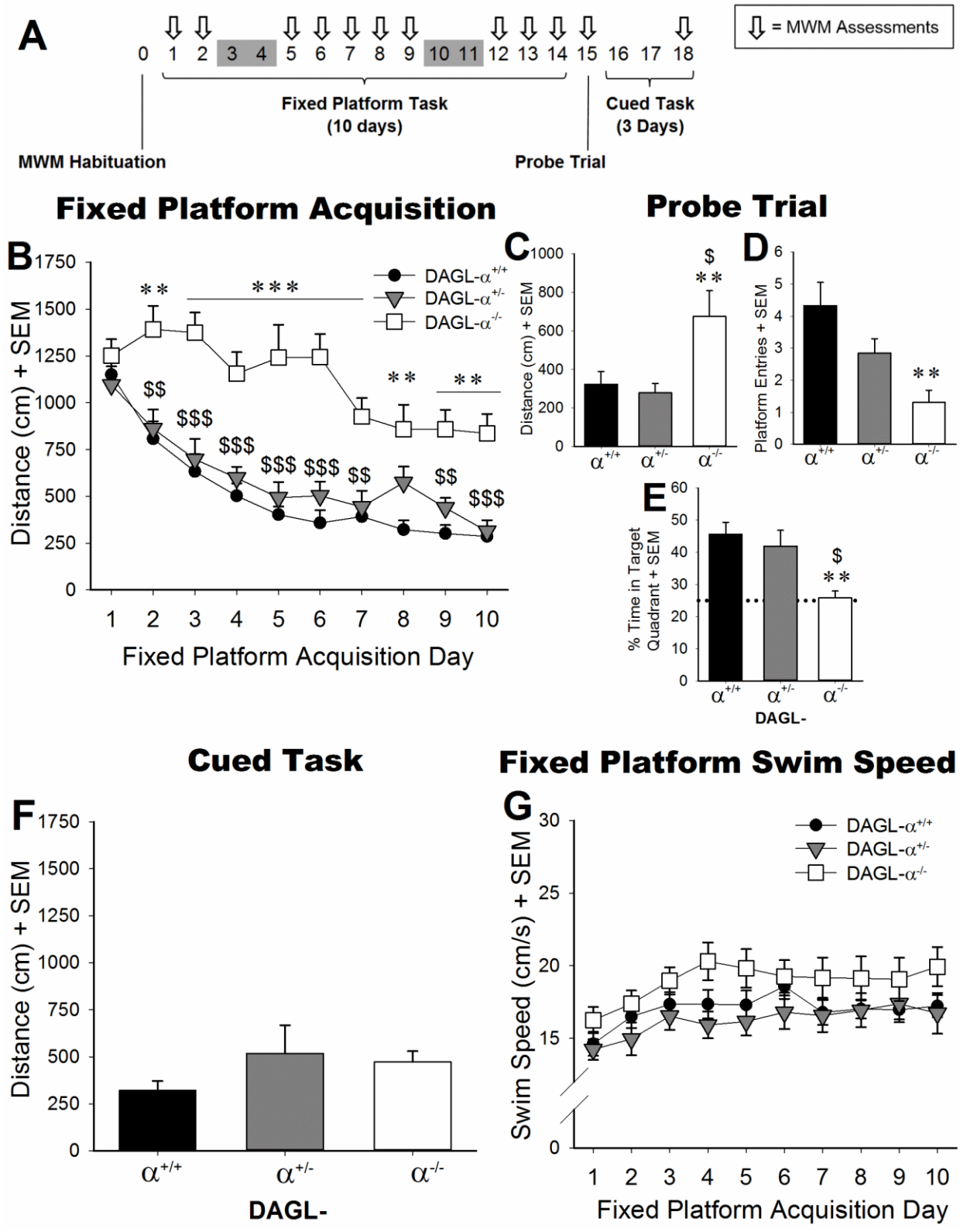

Figure 4-2. **DAGL-α $^{-/-}$ mice are profoundly impaired in MWM fixed platform task performance**. **A,** Fixed platform task experimental timeline (days). **B**, During MWM fixed platform acquisition, DAGL-$\alpha^{-/-}$ mice (n = 13) exhibited longer distances to the platform than both DAGL-$\alpha^{+/+}$ mice (n = 15) and DAGL-$\alpha^{+/-}$ mice (n = 13), as well as showed probe trial performance deficits of **C**, longer distances to the prior platform position **D**, fewer platform entries and **E**, a lower spatial preference for the target quadrant. No significant difference in **F**, cued task performance or **G**, swim speed suggest the DAGL-$\alpha^{-/-}$ mice performance deficits were unaffected by sensorimotor or motivational impairments. No significant differences were evident between genotype on fixed platform training day one across trials (extended data Figure 2-1A), or in body weight at either baseline or during fixed platform acquisition (extended data Figure 2-2A,C). Values represent mean +SEM; * $p < 0.05$, ** $p < 0.01$, *** $p < 0.001$ vs. DAGL-$\alpha^{+/+}$ mice, and *$ $p < 0.05$, *$$ $p < 0.01$, *$$$ $p < 0.001$ vs. DAGL-$\alpha^{+/-}$ mice.

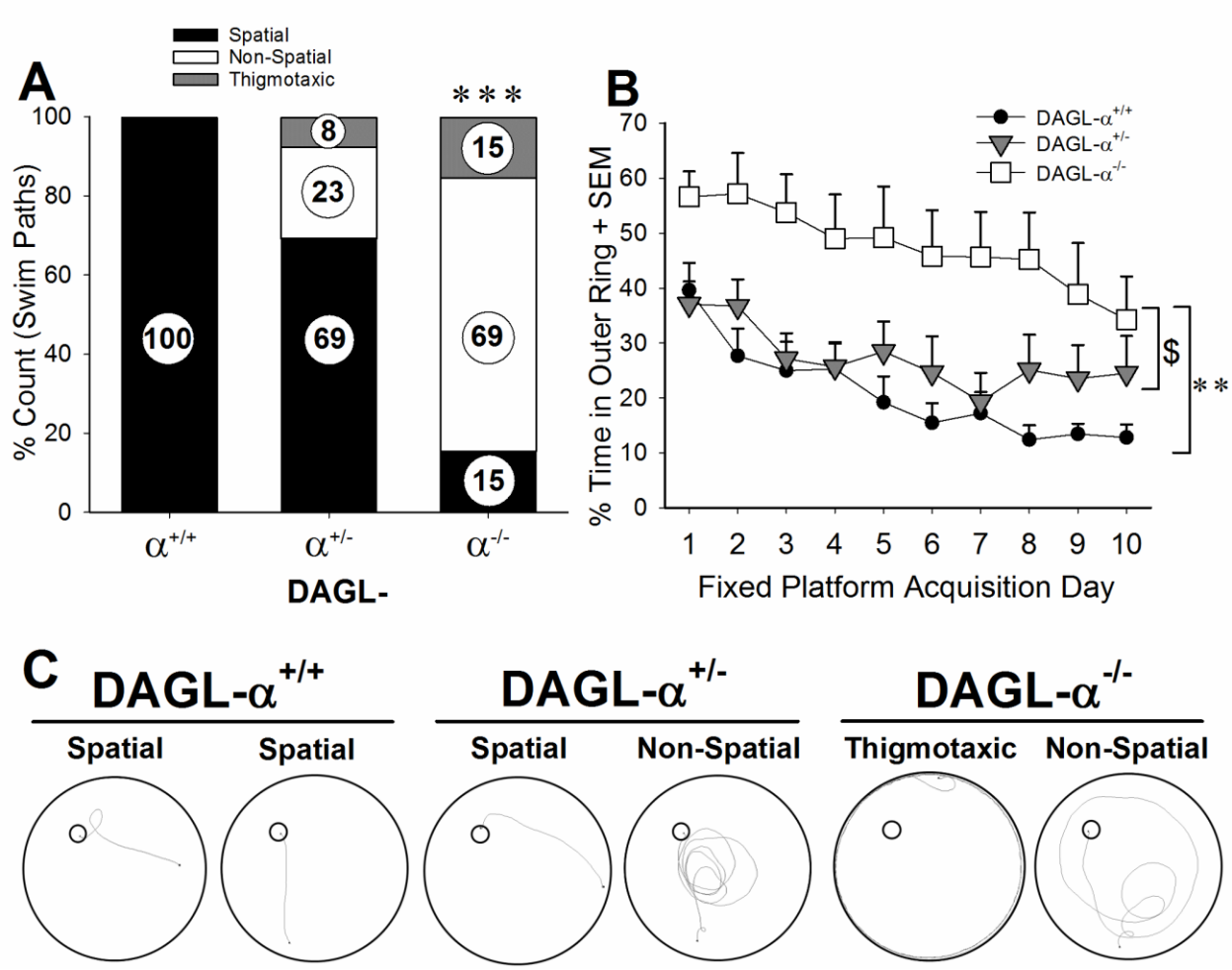

Figure 4-3. **DAGL-α $^{-/-}$ mice exhibit altered MWM search strategy**. DAGL-α$^{-/-}$ mice (n = 13) **A,** used more non-spatial and thigmotaxic swim paths than DAGL-α$^{+/+}$ mice (n = 15) on fixed platform day 10, as well as **B**, spent more time in the MWM outer ring than both DAGL-α$^{+/+}$ and DAGL-α$^{+/-}$ mice (n = 13) during fixed platform acquisition. **C**, Fixed platform day 10 representative swim traces show spatial (direct and self-orienting) swim paths in DAGL-α$^{+/+}$ mice, spatial (direct) and non-spatial (circling) swim paths in DAGL-α$^{+/-}$ mice, and non-spatial (circling and thigmotaxic) swim paths in DAGL-α$^{-/-}$ mice. Values represent mean +SEM; ** $p < 0.01$, *** $p < 0.001$ vs. DAGL-α$^{+/+}$ mice, and *$ $p <$ 0.05 vs. DAGL-α$^{+/-}$ mice.

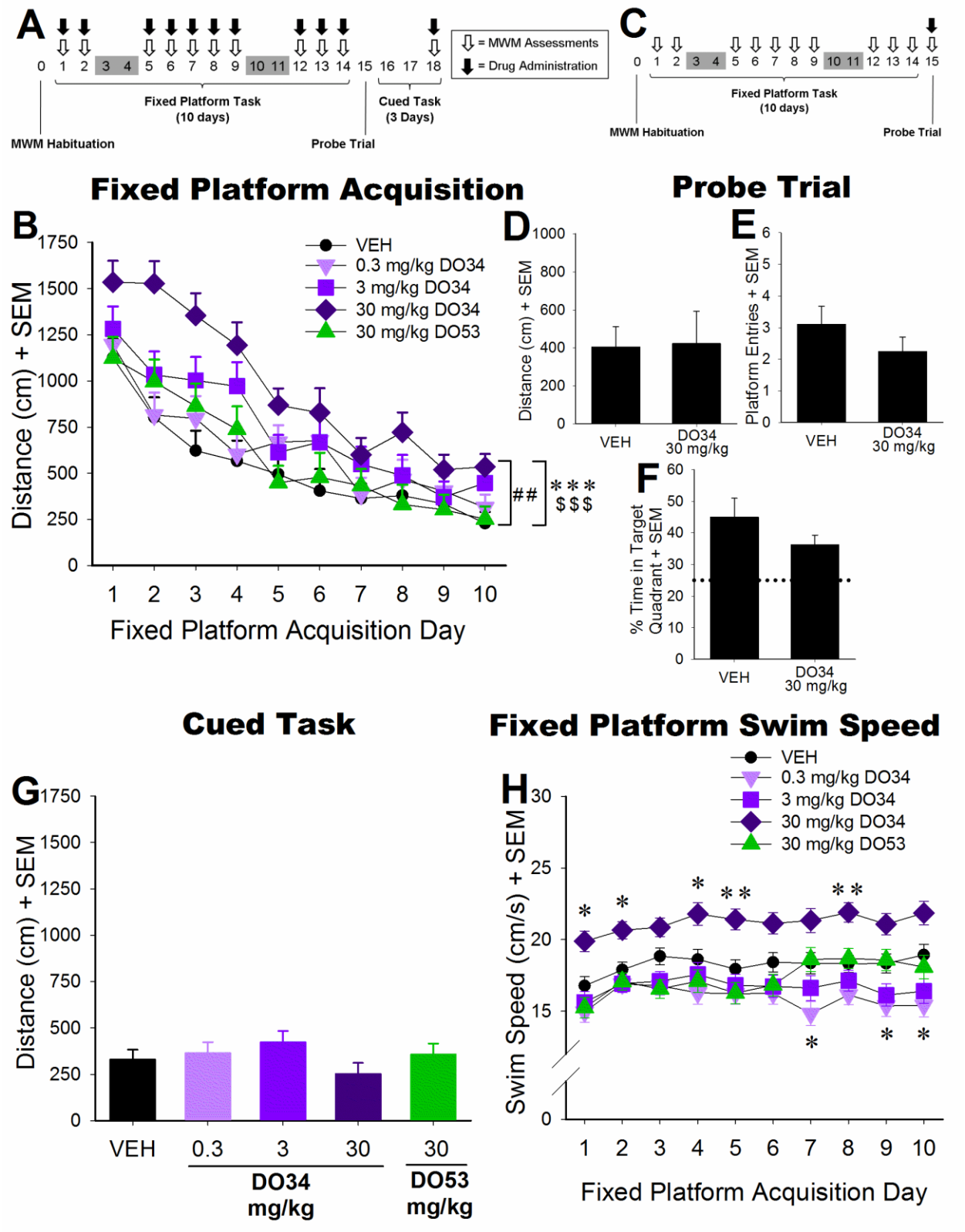

Figure 4-4. **DO34 delays MWM fixed platform acquisition, but does not affect probe trial performance**. **A,** Fixed platform task acquisition experimental timeline (days). **B**, During MWM fixed platform acquisition, mice treated with 30 mg/kg DO34 (n = 12) exhibited longer distances to the platform than VEH (n = 15), 0.3 mg/kg DO34 (n = 12), and 30 mg/kg DO53 (n = 12). **C,** Fixed platform task probe trial (expression) experimental timeline (days). Following drug-free MWM fixed platform acquisition training, no change in performance was seen at probe trial between drug treatments (VEH n = 9 or 30 mg/kg DO34 n = 8) for any measure; **D**, distances to the prior platform position **E**, platform entries or **F**, spatial preference for the target quadrant. No difference in **G**, cued task performance suggest the high dose DO34 did not affect sensorimotor or motivational components of MWM performance. **H**, Mice administered 30 mg/kg DO34 showed increased swim speeds during fixed platform acquisition compared to VEH-treated mice on days 1, 2, 4, 5, and 8, but 0.3 mg/kg DO34 reduced swim speeds on days 7, 9, and 10. No significant differences were evident between groups on fixed platform training day 1 across trials (extended data Figure 2-1A), or in body weight at baseline, yet a significant interaction between drug and day on body weight throughout acquisition training showed reductions compared to VEH at 30 mg/kg DO34 (days 2 through 15), 3 mg/kg DO34 (days 4, 8,13), 0.3 mg/kg DO34 (day 4), and 30 mg/kg DO53 (days 2, 3, 4, 5, 7, 13) (extended data Figure 2-2A,C). Values represent mean +SEM; * $p < 0.05$, ** $p < 0.01$, *** $p < 0.001$ vs. VEH; *$$$* $p < 0.001$ vs. 0.3 mg/kg DO34; and ## $p < 0.01$ vs. 30 mg/kg DO53.

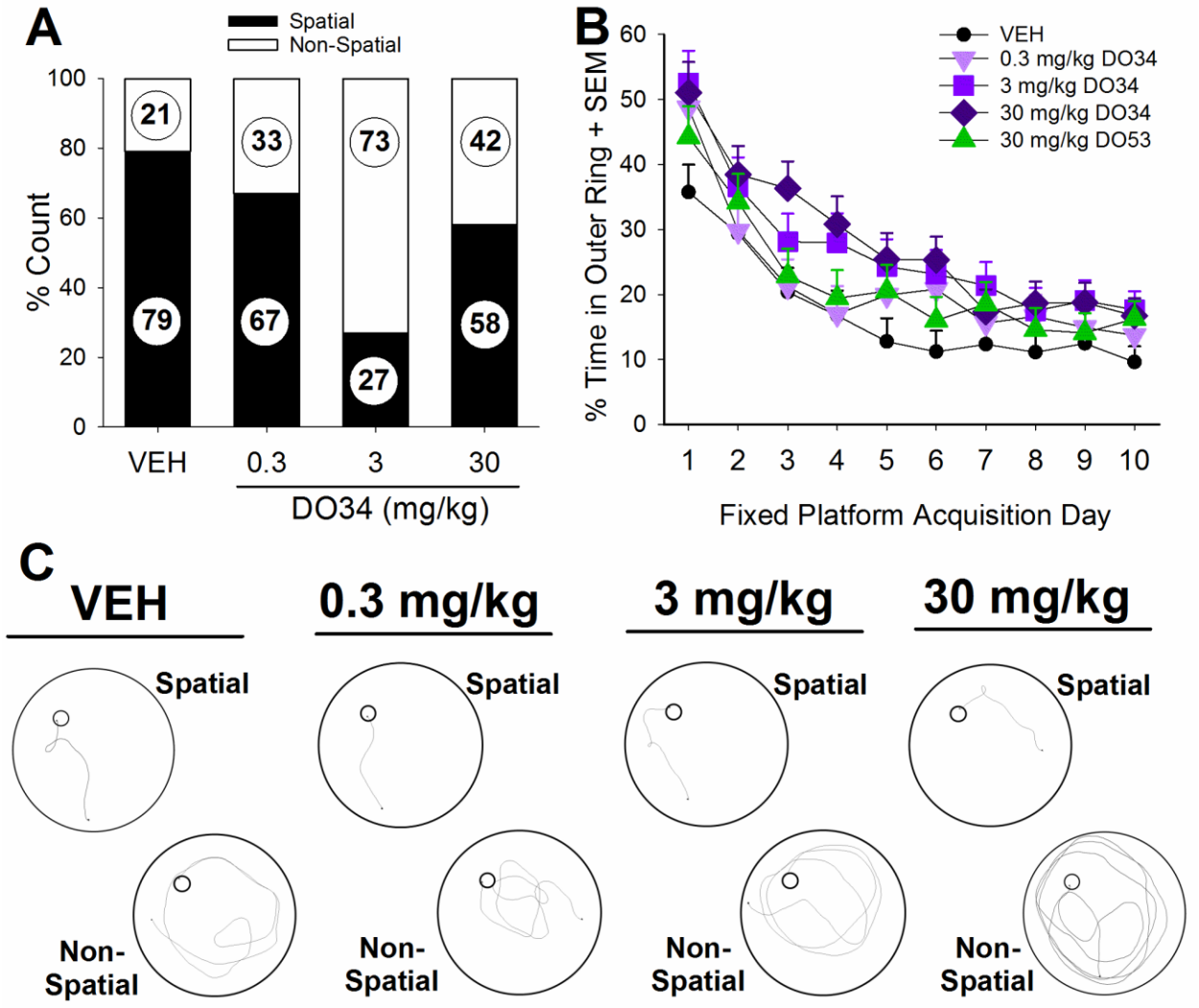

Figure 4-5. **DO34 produces modest and selective changes to MWM search strategy**. DO34-treated mice (0.3 mg/kg; n = 12, 3 mg/kg; n = 11, 30 mg/kg; n = 12) **A,** showed no significant change in swim path strategy than VEH-treated mice (n = 15) on fixed platform day 10 **B,** but mice administered 30 mg/kg DO34 showed a modest increase in the time spent in the MWM outer ring during fixed platform acquisition, than VEH-treated mice. **C**, Fixed platform day 10 representative swim traces show spatial (self-orienting and direct) and non-spatial (circling and scanning) swim paths in VEH, and DO34-treated (0.3, 3, 30 mg/kg) mice. Values represent mean +SEM; * $p < 0.05$ DO34 (30 mg/kg) vs VEH-treated mice.

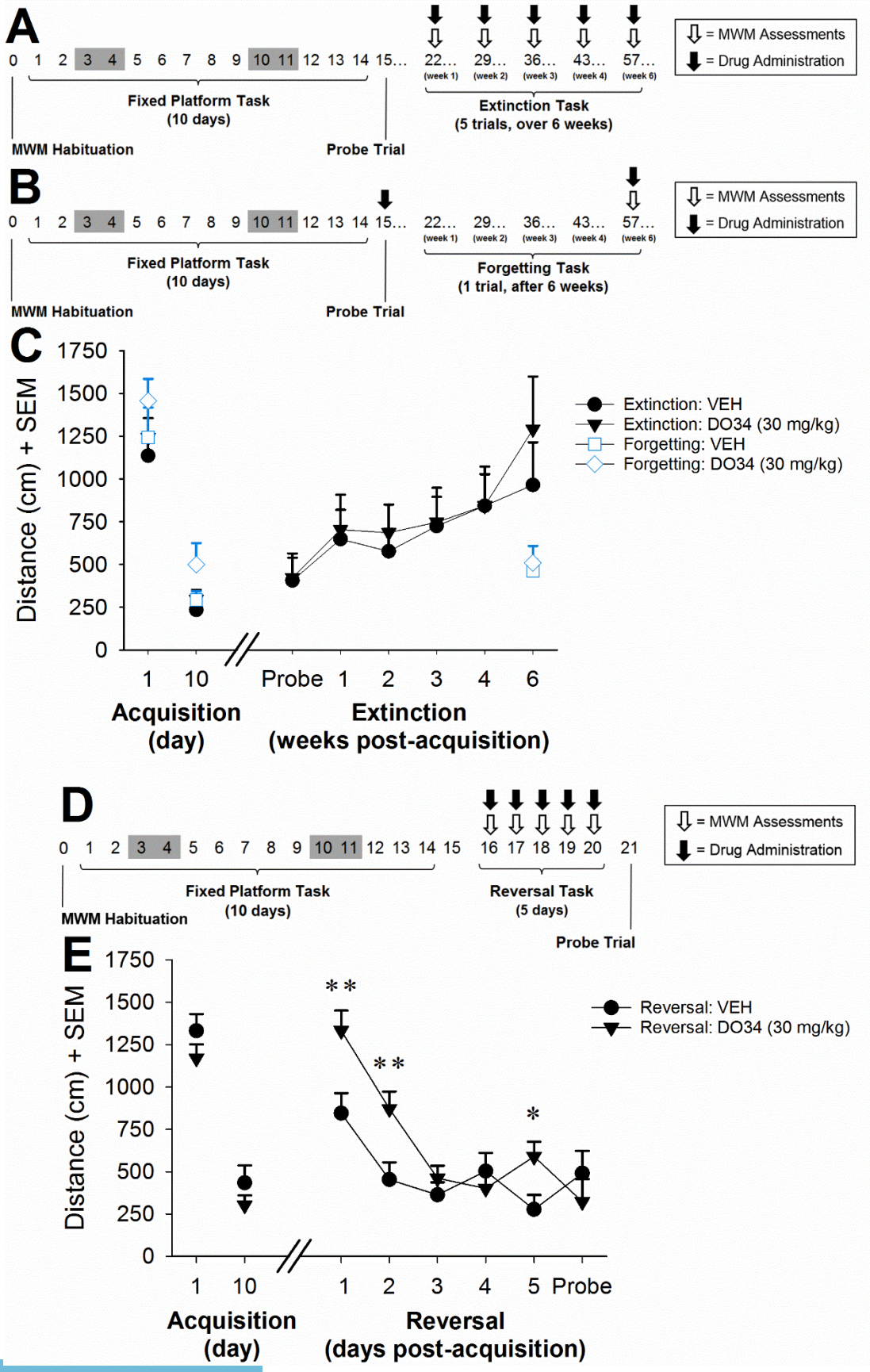

Figure 4-6. **DO34 delays reversal learning but does not affect extinction or forgetting MWM tasks**. **A,** Experimental timeline for the extinction (days/weeks) of mice trained drug-free in fixed platform task (same cohort as per probe trial [expression] Figure 4). **B**, Experimental timeline for additional mice trained drug-free in fixed platform task prior to a forgetting task (days/weeks). **C**, No change in either the extinction of the fixed platform task, or forgetting performance, was seen between VEH (n = 9 and n = 6 respectively) and 30 mg/kg DO34-treated mice (n = 8 and n = 6 respectively), (MWM fixed platform acquisition day 1 and 10 of VEH and 30 mg/kg DO34 for both extinction and forgetting tasks included for comparison). **D,** Experimental timeline for mice trained in a reversal task (days) following drug-free fixed platform training. **E,** During MWM reversal, mice treated with 30 mg/kg DO34 (n = 15) exhibited longer distances to the platform than VEH (n = 15) on reversal days one, two, and five (MWM fixed platform acquisition day 1 and 10 of VEH and 30 mg/kg DO34 included for comparison). Values represent mean +SEM; * $p < 0.05$, ** $p < 0.01$.

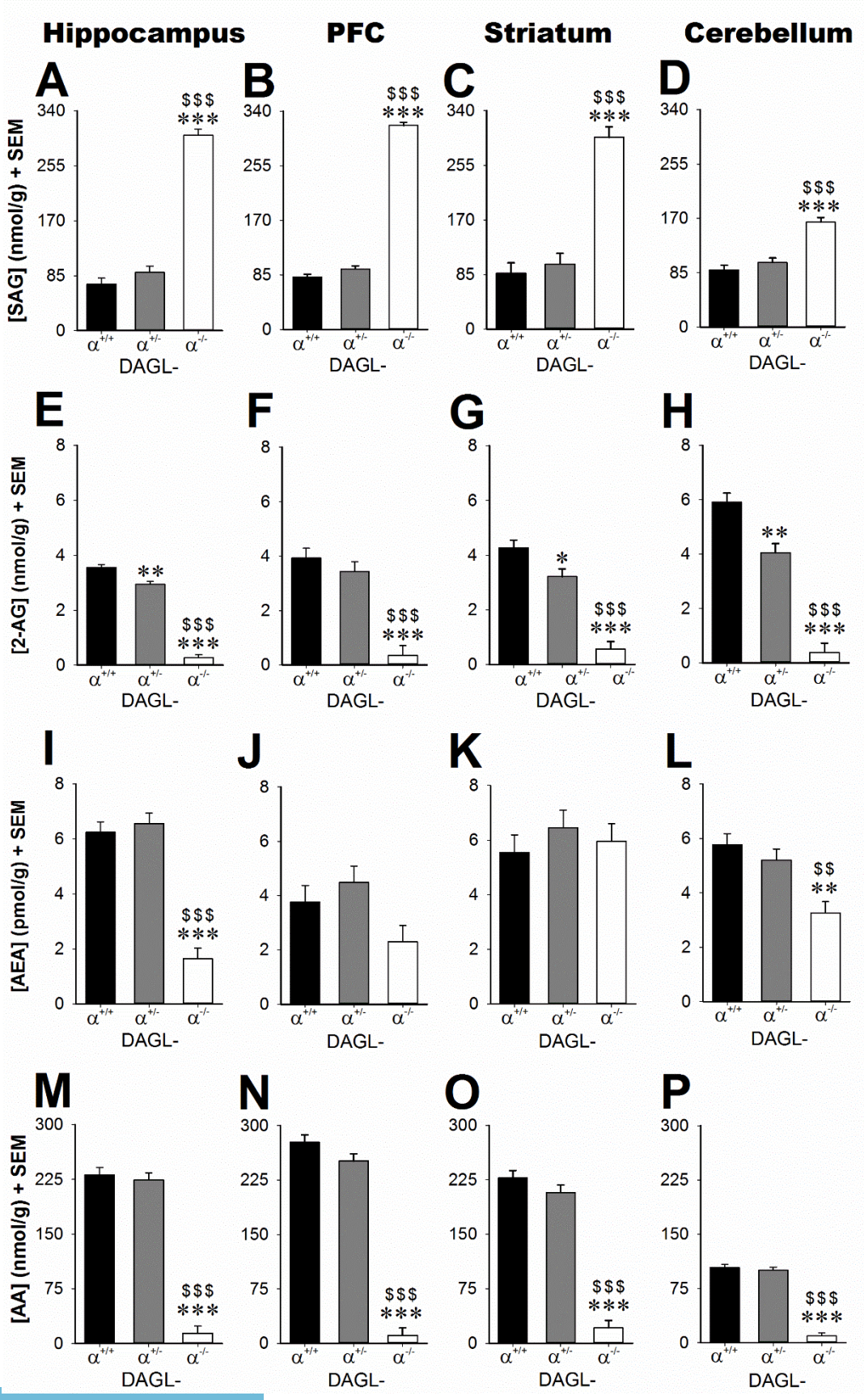

Figure 4-7. **Lipid profile changes in DAGL-α $^{-/-}$ mice show consistently elevated SAG, and lowered 2-AG and AA across all four brain regions**. **A, B, C, D,** The DAGL-α substrate SAG, was elevated in all four brain regions in DAGL-α$^{-/-}$ mice (n = 8) compared to both DAGL-α$^{+/+}$ (n = 8) and DAGL-α$^{+/-}$ mice (n = 8). DAGL-α$^{-/-}$ mice possessed decreased levels of 2-AG and AA, respectively in, **E** and **M,** hippocampus, **F** and **N,** PFC, **G** and **O,** striatum, and **H** and **P,** cerebellum. DAGL-α$^{+/-}$ mice showed modest 2-AG reductions in striatum, hippocampus, and cerebellum compared to DAGL-α$^{+/+}$ mice. AEA levels of DAGL-α$^{-/-}$ mice were significantly reduced in **I,** hippocampus, and **L,** cerebellum, but not in **J,** PFC, or **K**, striatum. Values represent mean +SEM; * $p < 0.05$, ** $p < 0.01$, *** $p < 0.001$ vs DAGL-α$^{+/+}$ mice, and $$ $p < 0.01$, $$$ $p < 0.001$ vs DAGL-α$^{+/-}$ mice.

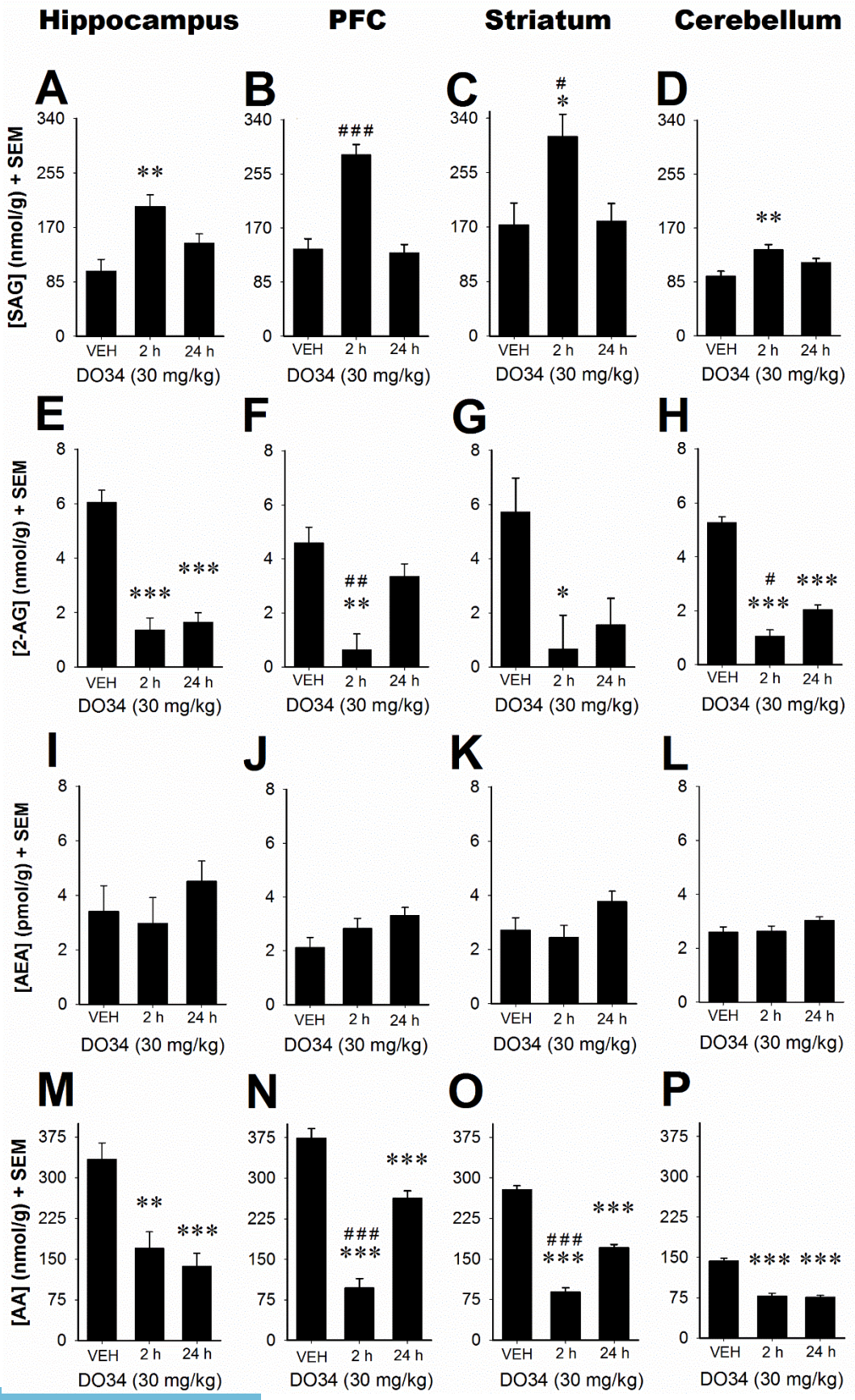

Figure 4-8. **Lipid profile changes in DO34-treated mice show consistently elevated SAG, and lowered 2-AG and AA across all four brain regions. A, B, C, D,** The DAGL-α substrate SAG, was elevated in all four brain regions at 2 h post-DO34 injection (n = 5) compared to VEH (n = 5), and compared to 24 h (n = 8) in PFC and striatum. At 2 h post-DO34 injection, 2-AG and AA were reduced respectively in, **E** and **M,** hippocampus, **F** and **N,** PFC, **G** and **O,** striatum, and **H** and **P,** cerebellum, while at 24 h post-DO34 injection, 2-AG was reduced only in **E**, hippocampus and **H,** cerebellum, whereas AA showed reductions across **M, N, O, P**, all four brain areas. No changes in, **I, J, K, L**, AEA were evident compared to VEH. Values represent mean +SEM; * $p < 0.05$, ** $p < 0.01$, *** $p < 0.001$ vs VEH, and # $p < 0.05$ vs 24 h.

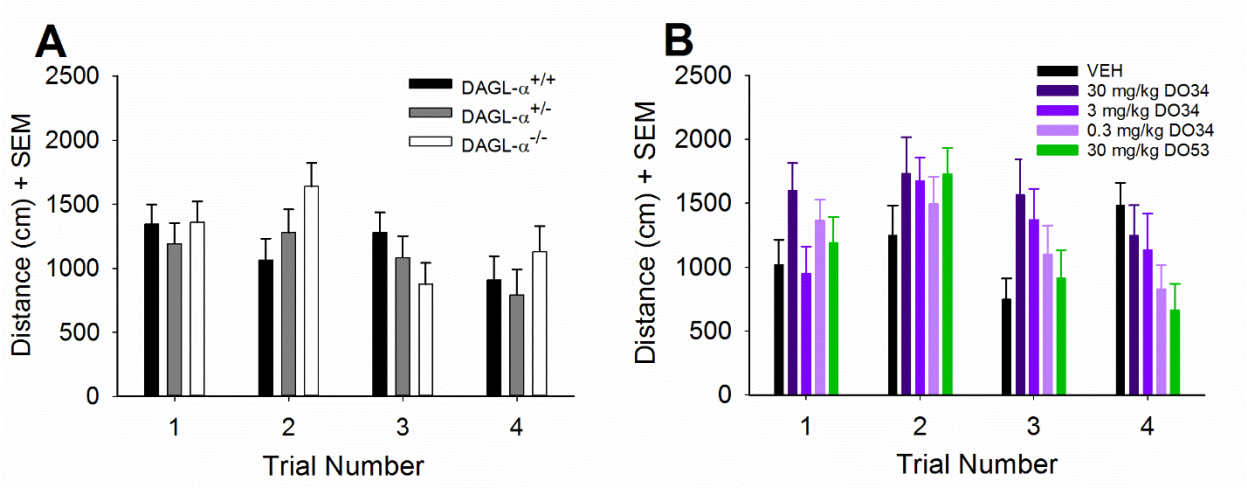

Extended Data Figure 4-2-1 **Both genetic deletion and pharmacological inhibition of DAGL-α produce no change in MWM fixed platform day one performance**. **A,** During MWM fixed platform day one, no performance difference was seen across the four acquisition trials between DAGL-$\alpha^{-/-}$ (n = 13), DAGL-$\alpha^{+/-}$ (n = 13), and DAGL-$\alpha^{+/+}$ mice (n = 15). **B,** Also during MWM fixed platform day one, no performance difference was seen across the four acquisition trials between DO34-treated mice (30 mg/kg DO34, n = 12; 3 mg/kg DO34, n = 11; 0.3 mg/kg DO34, n = 12), DO53 treatment (30 mg/kg, n = 12), and VEH (n = 15). Values represent mean +SEM.

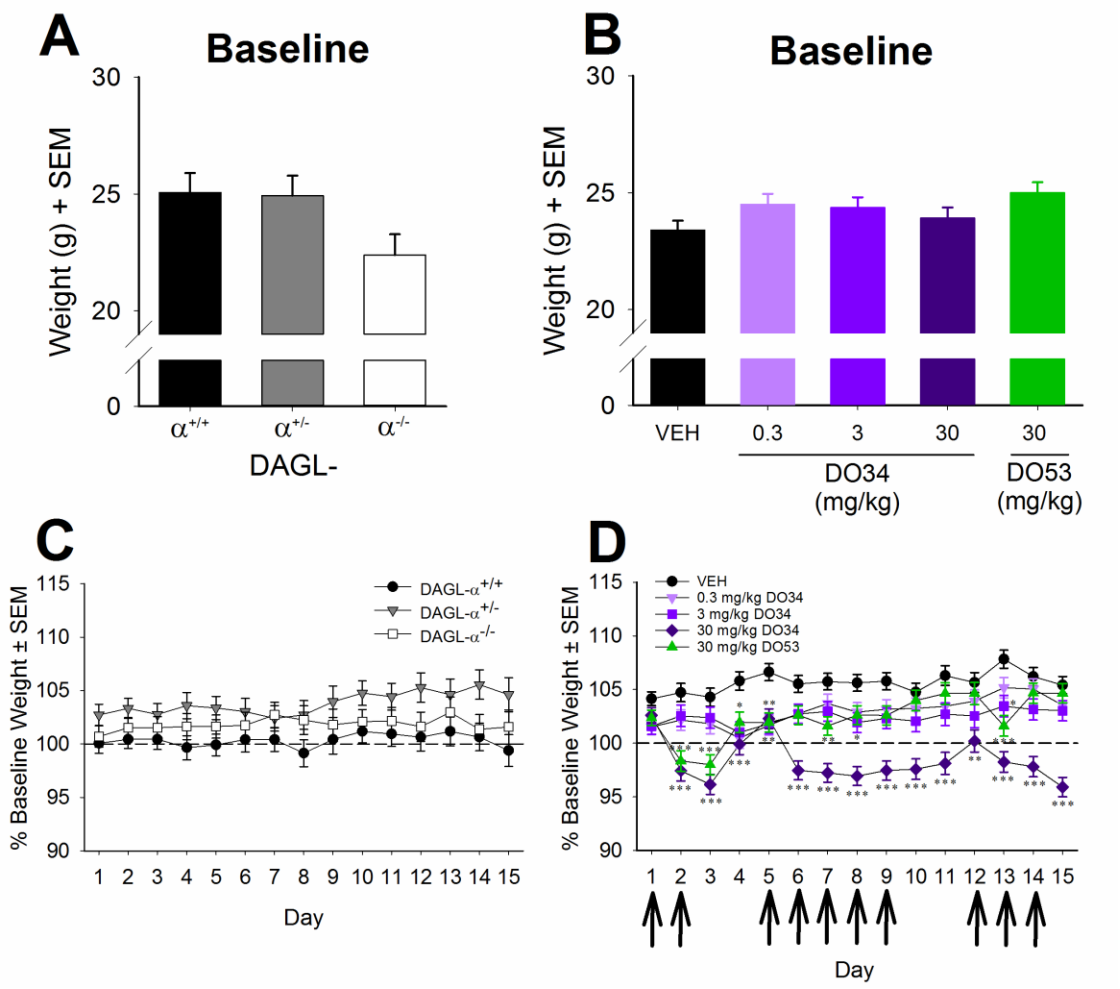

Extended Data Figure 4-2-2. **High dose DAGL-α inhibition produces body weight loss, not evident in mice with DAGL-α genetic deletion**. On day 0 prior to MWM habituation, baseline weight for naïve mice did not significantly differ between experimental groups for both **A,** DAGL-α genetic deletion, or **B**, pharmacological inhibition. During the MWM fixed platform task, **C,** no change in body weight was evident in DAGL-$\alpha^{-/-}$ (n = 13) and DAGL-$\alpha^{+/-}$ (n = 13) compared to DAGL-$\alpha^{+/+}$ mice (n = 15), whereas **D,** 30 mg/kg DO34 (n = 12) mice exhibited consistently lower body weight to VEH (n = 15). **D**, upright arrows indicate days of drug administration, and values represent mean +SEM or ±SEM; * $p < 0.05$, ** $p < 0.01$, *** $p < 0.001$ vs VEH.

Chapter V

General Discussion

Summary

The overall objective of this dissertation research was to understand the *in vivo* roles of DAGL-α and DAGL-β disruption on mouse learning and memory. The endocannabinoid (eCB) 2-arachidonyl glycerol (2-AG), produced by these enzymes, is elevated in response to pathogenic events such as traumatic brain injury (TBI) (Panikashvili *et al*, 2001). As such, we hypothesized that eCB biosynthetic enzyme contributions to learning and memory function may extend to conditions of memory pathology. Prior to evaluating this hypothesis, Chapter II focused on developing a mouse model of learning and memory impairment resulting from TBI, using spatial memory tasks of the Morris water maze (MWM). During the development of this mouse model of TBI-induced spatial memory deficit we found modest but distinct differences following a left vs a right unilateral insult. While both left and right lateral TBI impaired MWM Fixed Platform task probe performance, mild Fixed Platform acquisition differences were evident between left and right injuries despite similar motor deficits, histological damage, and glial reactivity. This finding suggests that laterality in mouse learning and memory deficits might be worthy of consideration when investigating TBI-induced functional consequences.

The experiments in Chapter III investigated the first of two biosynthetic production enzymes of 2-AG, diacylglycerol lipase-β (DAGL-β), as a target to protect against TBI-induced learning and memory deficits. The selective expression of DAGL-β on

CNS microglia and the role of 2-AG as a precursor for the production of pro-inflammatory eicosanoids led to the hypothesis that disrupting DAGL-β activity would provide protection from TBI-induced learning and memory impairments in mice (by reducing pools of 2-AG pro-inflammatory metabolites). Contrary to our hypothesis, DAGL-β deletion did not protect against TBI-induced spatial learning and memory impairments, nor did it protect against other functional assessments after injury such as neurological motor deficits. Unexpectedly, a survival protective phenotype was observed in male DAGL-$\beta^{-/-}$ mice, suggesting that while DAGL-β activity does not contribute towards injury-induced memory deficit, it may contribute to TBI-induced acute mortality.

Finally, Chapter IV investigated the role of the second biosynthetic production enzyme of 2-AG, diacylglycerol lipase-α (DAGL-α) in mouse spatial learning and memory under physiological conditions. The use of a pharmacological as well as a genetic approach facilitated the investigation of DAGL-α disruption in various MWM hippocampal-dependent memory assessments. Here, we show that DAGL-α gene deletion or inhibition disrupts CA1-hippocampal LTP and eCB lipid levels, but elicits varying magnitudes of deficits in behavioral learning and memory tasks. Specifically, DAGL-$\alpha^{-/-}$ mice display profound MWM acquisition deficits, whereas C57BL6/J mice treated with the DAGL-α inhibitor DO34 show impaired acquisition and reversal

learning, but no change in expression, extinction, or forgetting. These results suggest that DAGL-α may play a selective role in the integration of new spatial information in the normal mouse brain.

Functional lateralization and mouse models of TBI-induced memory deficit.

The investigation of learning and memory deficits in response to left vs right unilateral TBI, as well as utilization of the MWM reversal task, was an important contribution by the present work to the TBI preclinical literature. The reversal task models cognitive flexibility through increased task complexity in that mice suppress former spatial memory influences (inhibition as a result of non-reinforced trials) in order to explore alternative platform locations. The use of preclinical behavioral assessments that capture the variety and complexity of memory impairment seen in clinical populations could only benefit the translational potential of initial TBI mouse model work. Although presently, normalization of the reversal task dependent measures did not reveal significant left-right hemisphere injury differences, the finding that a left lateral injury produced MWM performance impairments compared to sham controls (not found after a right lateral injury) raises questions about functional lateralization in response to MWM task variation worthy of consideration.

The hippocampal molecular, morphological, and cellular signaling differences that exist between left and right hemispheres may influence MWM performance after TBI. Figure 5-A summarizes a conceptual model of the previously described left-right hippocampal molecular and morphological differences and how they may be impacted after a unilateral TBI. A left lateral TBI may perturb axons and projections ipsilateral to

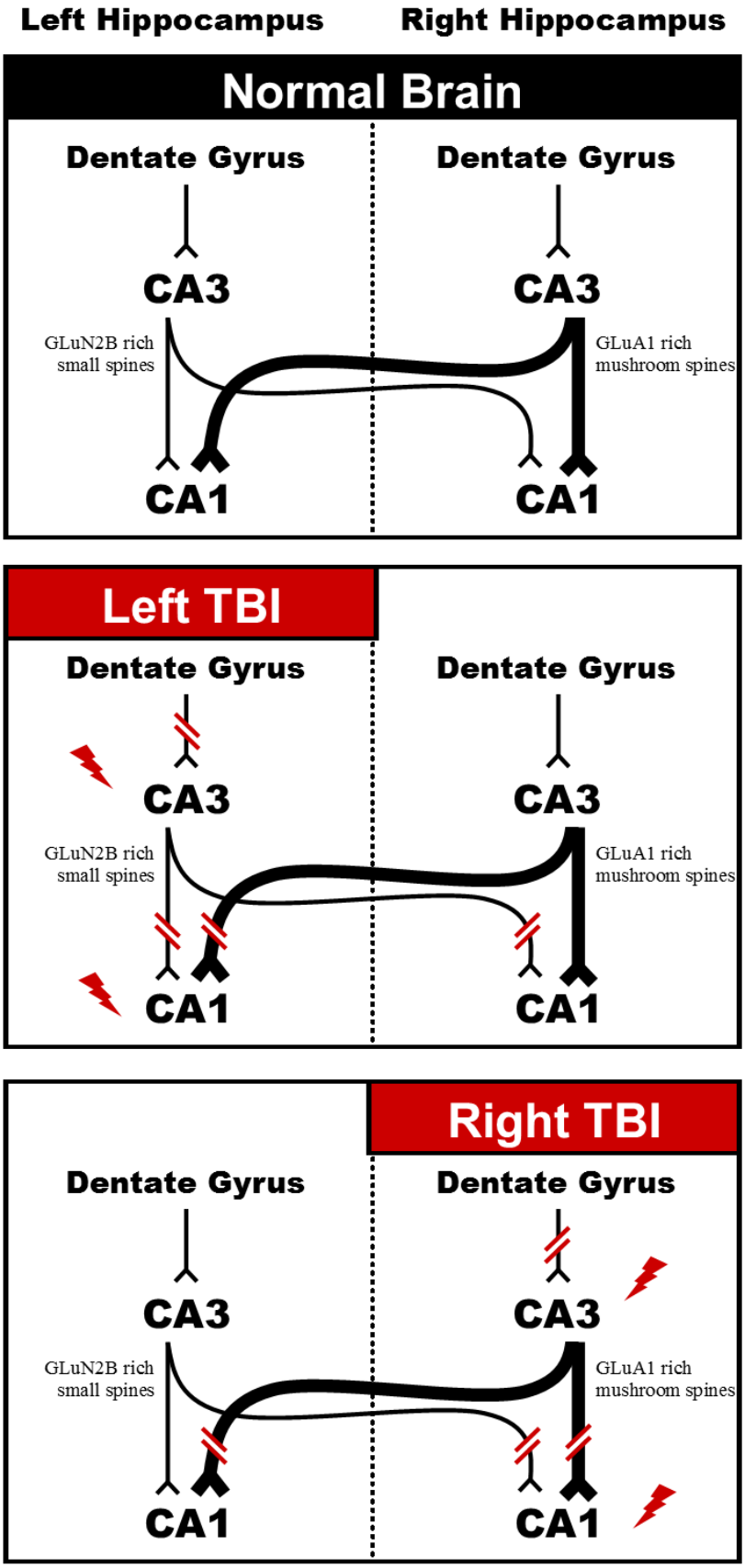

Figure 5-A. A conceptual model of how hippocampal molecular and morphological differences are impacted by TBI

the left injury as well as projections from the left CA3 to the contralateral right CA1, leaving perhaps a heavier reliance on right originating CA3-CA1 projections that are GLuA1 receptor subunit rich with mushroom-shaped spines. Conversely, a right lateral TBI may perturb axons and projections ipsilateral to the right injury as well as projections from the right CA3 to the contralateral left CA1, leaving perhaps a heavier reliance on left originating CA3-CA1 projections that are GLuN2B receptor subunit rich with smaller spines and intact CA3-CA1 LTP. The cognitive flexibility required by the reversal task might be facilitated by the molecular,

and functional asymmetry of the plastic left hippocampus, in which a higher density of GluN2B subunits exists in postsynaptic spines receiving left CA3 input (Kawakami *et al*, 2003; Wu *et al*, 2005), and LTP induction occurs only when the presynaptic input originates in the left, but not the right, CA3 (Kohl *et al*, 2011; Shipton *et al*, 2014). As such the reversal task deficits seen in left injured mice might be a consequence of heavier reliance on the stable right hippocampus. Left injured mice also demonstrated a spatial preference for the control quadrant during the reversal probe trial (data not shown), which might be interpreted as a deficit in their ability to inhibit the previously learned fixed platform location as well as an inability to integrate new spatial information, suggesting injury-induced perseverative behavior in left lateral TBI mice.

While Chapter 2 did not empirically address the molecular mechanisms of left and right hemisphere TBI MWM deficits, here I expand the discussion of the previously proposed theoretical model by El-Gaby *et al*, 2014 to account for the presently observed functional differences in left-right hemisphere injury. El-Gaby *et al*, 2014 proposed that the adult mouse hippocampus may use distinct left-right hippocampal synapse populations differentially during learning and memory. Specifically, pre-configured CA3-CA1 synapses are attributed to the right hippocampus where stable cell assemblies formed during post-natal development function to facilitate one-trial formation of spatial representations (Nakashiba *et al*, 2008). Such right hippocampal pre-configured synapses can be selected to represent a particular trajectory following a spatial learning event (Dragoi and Tonegawa, 2012, 2014), thus rapidly incorporating spatial information. In the left hippocampus, evidence suggests plastic CA3-CA1 synapses recruit new place cells throughout adulthood to instruct the formation of de novo cell

assemblies (Hollup *et al*, 2001) (potentially through LTP (El-Gaby *et al*, 2014), facilitating the accurate representative of a particularly salient location (Leutgeb *et al*, 2005, 2007). Applying this model to the present findings, the fixed platform deficits in right-injured mice could reflect the inability to rapidly incorporate a spatial location into pre-configured stable cell assemblies, yet the lack of performance impairments in the reversal task may reflect the continued functioning of plastic left CA3-CA1 hippocampal synapses. Whereas the reversal task impairments and perseverative behavior produced by a left hemisphere injury, may be exacerbated by a reliance on stable right CA3-CA1 hippocampal assemblies, already pre-assigned to a spatial representation and unable to integrate new salient information by plastic left CA3-CA1 synapses. The adaptive advantage of such anatomical dissociation between spatial learning processes in mice would produce efficient division of labor between left and right hemisphere hippocampi, while still being able to integrate these functions at the level of the CA1 through convergent left-right CA3 inputs (El-Gaby *et al*, 2014).

The composition of the hippocampal trisynaptic circuit, in addition to pyramidal cells in the CA3 and CA1, includes granule cells of the dentate gyrus. In this brain area, the mammalian hippocampus continues to be modified by additions of adult neurons (neurogenesis) (Altman and Das, 1965; Gage, 2000). Granule cells of the dentate gyrus are also distinct in that they are subject to a large degree of GABAergic inhibition (Jung and McNaughton, 1993), showing low levels of excitability. As such, the dentate gyrus is a predominantly silent network that incorporates new functional units. The specific functional role the dentate gyrus plays in hippocampal spatial learning and memory processes; however, remains unresolved. Recent studies suggest the integration of

adult-born neurons contribute to spatial learning and memory as pattern integrators, encoding the degree of similarity of events that occur closely in time (Deng *et al*, 2010a). Learning and memory tasks utilizing repeated trials such as used in the MWM produce similar events, which occur closely in time over a number of days, all of which could be encoded through dentate gyrus newborn neurons. The dentate gyrus has also been linked to spontaneous exploration of novel environments (Saab *et al*, 2009). In the present studies, while both left and right injured mice show altered MWM search strategies compared to their sham controls, no swim path lateralization differences were evident. This pattern of findings suggests that injury-induced MWM exploration differences were not subject to left-right hemisphere injury differences and likely did not drive the distinct left-right MWM Fixed Platform task behavioral impairments. The functionality of the dentate gyrus has been further linked to anterograde, not retrograde memory (Nanry *et al*, 1989); however, there is no evidence to suggest that there are left-right morphological, cellular, or functional differences in the hippocampal dentate gyrus. Therefore, while the dentate gyrus clearly plays important roles in spatial memory as assessed by MWM tasks, at present there is no evidence connecting any role to the lateralization of hippocampal function presently observed.

To understand the brain regions responsible for the presently observed functional asymmetry of the left and right lateral injuries, the structural and molecular asymmetry of the hippocampus are a logical first consideration given the MWM is a hippocampal-dependent learning task (Morris, 1984) particularly sensitive to the effects of hippocampal lesions (Gerlai *et al*, 2002). However, the neuronal loss and diffuse axonal injury from a lateral fluid percussion injury span beyond hippocampal regions. Cortical

neuron loss contributes greatly to trauma-induced MWM impairments, and others have found bilateral lesions of both the medial prefrontal cortex (Kosaki and Watanabe, 2012) and the medial striatum (Furtado and Mazurek, 1996) to result in reversal learning deficits. Interference with many other brain regions such as the cerebellum (Lalonde, 1994), insular cortex (Gutiérrez *et al*, 1999), thalamic structures (Mumby *et al*, 1999), and fimbria-fornix fibers (Eichenbaum *et al*, 1990), also impair MWM performance. As such, damage to any of these regions may also potentially contribute to the presently observed functional asymmetry.

Overall, the principle of functional asymmetry of learning and memory is invoked to account for differential MWM performance between mice subjected to left or right traumatic brain injury. Despite evidence in human research, which points to increased left hippocampal activity in response to task relevant semantic information, and increased right hippocampal activity from spatial information (Motley and Kirwan, 2012), the possible circuit basis and whether it is similar to that of the mouse remains unknown (El-Gaby *et al*, 2014). Drawing direct comparisons between mouse models and humans is inappropriate given the large number of functional differences. One such example being hippocampal neurogenesis, around which there is an extensive body of mouse model work in support. Recent evidence proposes that dentate gyrus neurogenesis, present in children, is extremely rate or complete absent in adult humans (Sorrells *et al*, 2018). Perhaps the disparity in such findings is a consequence of typical animal model work being performed on adolescent rodents. Nevertheless, left-right hemispheric asymmetry of spatial memory task deficits contributes to the understanding of the mouse model system of traumatic brain injury. Indeed, considerations of laterality in

MWM learning and memory impairments in mice are important for future study design and interpretation in the investigation of traumatic brain injury-induced cognitive consequences, as well as pharmacological and nonpharmacological treatments to mitigate the deficits.

The studies in this dissertation investigating DAGL-β as a target to protect against TBI-induced learning and memory deficits utilized a left lateral injury. A left FPI was chosen given it produced both a fixed platform probe trial performance deficit as well as reversal task performance deficit, suggesting a diverse model of the learning and memory impairments experienced in clinical populations after TBI. TBI mice of the DAGL-β experiments showed fixed platform acquisition deficits as well as probe trial deficits after a left lateral FPI, perhaps an artifact of an increased injury severity in these studies (1.96 atm compared to the previous 1.92 atm). This is perhaps then evidence to consider that changes in injury severity magnitude might reveal differential MWM deficit across tasks, possibly by left and right hemisphere injury.

Inflammation as a target to treat TBI-induced memory deficit.

The neuroflammatory processes that unfold following a TBI have been a popular target of interest to address TBI-induced functional deficits in pre-clinical studies. However, manipulation of TBI-induced neuroinflammation in murine models has seen mixed success in protecting against functional deficits. Moreover, no late phase clinical trials have yet yielded an effective anti-inflammatory neuroprotective treatment (Chakraborty *et al*, 2016; Narayan *et al*, 2002). It seems logical therefore to consider whether the continued exploration of neuroinflammation is a worthwhile avenue of investigation for

the treatment of learning and memory impairments brought about by TBI. In February 2018, the US Food and Drug Administration (FDA) authorized the first blood test to predict the presence of intracranial lesions resulting from mild TBI. The test assesses levels of two biomarkers of TBI, ubiquitin C-terminal hydrolase L1 (UCH-L1) and glial fibrillary acidic protein (GFAP). While UCH-L1 is involved in altering the function/fate of neurons and is associated with axonal health and stability (Chen *et al*, 2010a), GFAP is a protein important for the structural integrity of astrocytes which participate in astrogliosis and the formation of glial scars following CNS injury, one function of acute neuroinflammation. Therefore, the connection of the first FDA approved TBI biomarker to inflammation suggests this avenue of great interest has perhaps yet to be exhausted.

The current strategy of inhibiting upstream precursors of AA metabolism within microglial cells through DAGL-β does not account for the nuanced signaling of the various AA metabolism pathways (see Chapter 3, Figure 3-A, pg 82). In addition to inflammatory signaling through COX pathways, the cytochrome P450 epoxygenase enzymes (in liver, kidney, heart etc.) produce pro-inflammatory epoxides; epoxyeicosatrienoic acids (EETs) and dihydroxyeicosatrienoic acids (DHETs), and lipoxygenases (expressed in lung and CNS glial cells) produce pro-inflammatory leukotrienes, lipoxins, and hepoxilins (Brash, 2001). Specifically, epoxide products of cytochrome P450 epoxygenase play important roles in the regulation of cardiovascular inflammation (Deng *et al*, 2010b), pertinent given the frequent peripheral multisystem failure in heart, lungs, and peripheral vasculature that occurs following TBI. Furthermore, inhibition of spinal lipoxygenase enzymes have reversed NSAID-unresponsive inflammatory hyperalgesia (Gregus *et al*, 2018) through toll-like receptor 4

(TLR4) (Gregus *et al*, 2018) and transient receptor potential cation channel, subfamily V, member 1 (TRPV1) (Gregus *et al*, 2012) signaling in rats. These findings suggest that inhibition of alternative AA metabolic pathways outside of COX inhibition are worthy of investigation in the context of functional deficit protection following TBI.

The present results refuting our hypothesis that DAGL-β disruption would protect against TBI-induced memory deficit in mice, perhaps is a result of the global reduction of microglial arachidonic acid (AA) metabolites. While AA is the primary precursor for the production of pro-inflammatory prostaglandins, AA is also the precursor for the production of prostaglandins whose role contributes to the resolution of inflammation. Prostaglandins, while ubiquitously produced, are usually dominantly generated by cell type. Specifically, prostaglandin E_2 (PGE_2) is produced by microglia and macrophages (Tilley *et al*, 2001) and its effects are mediated through microglial EP2 and EP4 receptors (Ricciotti and FitzGerald, 2011). PGE_2 is one of the most abundant prostaglandins, and exhibits dual pro- and anti-inflammatory signaling roles. As a pro-inflammatory mediator PGE_2 contributes to the regulation of cytokine expression (Egan *et al*, 2004), whereas in its anti-inflammatory capacity PGE_2 blocks ATP-induced cytokine synthesis (Noda *et al*, 2007). Therefore, the global reduction of microglial prostaglandins may prevent some nuanced signaling involving the resolution of inflammation. Whether our mouse model of DAGL-β deletion reversed levels of PGE_2 we did not presently evaluate, however the importance of evaluating changes in prostaglandin levels following injury is discussed further in the Future Directions section at the end of this chapter.

An alternative approach to globally blocking 2-AG derived AA metabolites to achieve neuroprotection from TBI, would be to selectively block novel products of 2-AG oxidation (see figure 1-2, pg 36). Cyclooxygenase-2 (COX-2), both produces oxygenation products of AA (Xie *et al*, 1991); classic prostaglandins, as well as directly oxygenates 2-AG to produce prostaglandin glyceryl esters (PG-Gs) (Kozak *et al*, 2000); novel prostaglandins. Previously PG-Gs have only been observed *in vitro* (Kozak *et al*, 2002), though recently have been quantified *in vivo* in COX-2 overexpressing mice (Morgan *et al*, 2018). COX-2 is a dynamically regulated enzyme where CNS insults such as TBI lead to COX-2 induction (Lapchak *et al*, 2001), perhaps then also leading to increased PG-Gs after injury. COX-2 oxygenation of 2-AG has been implicated in glutamate-induced excitotoxicity (Sang *et al*, 2007), therefore the upregulation of COX-2 and production of PG-Gs after TBI may contribute towards TBI-induced neurotoxicity. The evaluation of COX-2 inhibitors that preferentially block the direct oxygenation of 2-AG (Duggan *et al*, 2011) after TBI might be useful in evaluating the neuroprotective potential of preventing PG-G production while not impacting the inflammation resolution capacities of classic prostaglandins such as PGE_2.

The idea that DAGL-β may play a temporal dependent role with regards to inflammation pathology is also worthy of further consideration. The current constitutive genetic deletion model of DAGL-β disruption may mask any time dependent protective effects of DAGL-β disruption. As such investigation of detailed intervention timing regarding DAGL-β disruption would be beneficial in future experiments. In a previous experiment (data not shown), administration of DAGL-β inhibitor KT109 (30 min, 24 h post-injury, i.p.) produced no change in TBI-induced MWM deficit. Since this work was

completed KT109 was found to show poor brain penetrance and low DAGL-β activity inhibition in brain when administered i.p. (Donvito et al, *in compilation*). Even though KT109 administration occurred at a time post-TBI when blood brain barrier integrity is presumably compromised, the extent to which KT109 penetrated the brain and inhibits DAGL-β was not quantified. A recurring challenge with currently available DAGL-β inhibitors is inadequate brain penetrance and only modest selectivity for DAGL-β over -α, making pharmacological investigation of DAGL-β inhibition after TBI not currently viable. The use of a mouse model of inducible DAGL-β genetic deletion may prove a valuable tool to study time-dependent inhibition of inflammation pathology through DAGL-β inactivation. However, the temporal resolution of a chemically inducible Cre-lox recombination system is relatively low, taking days to weeks for gene inactivation to complete.

The endocannabinoid system contains a rich source of targets to treat TBI-induced neuroinflammation. Therefore, the exploration of manipulating several endocannabinoid system signaling pathways at once might have advantages over a focus on a single target. One such example could be the combined activation of cannabinoid receptors with DAGL-β disruption. Microglial cells have most of the components of the endocannabinoid system, their receptors, and production and degradation enzymes, perhaps suggesting they participate in autocrine and paracrine signaling in response to neuroinflammation. Specifically, cannabinoid receptor 2 (CB_2) expression increases with the change in microglia activation state (Mecha *et al*, 2015). The activation of CB_2 receptors elicit a wide range of effects both within microglia (e.g. cell migration (Walter *et al*, 2003), induction of an anti-inflammatory M2 phenotype

(Mecha *et al*, 2015) as well as on their surroundings (e.g. induction of phagocytosis (Tolon *et al*, 2009), diminishing free radicals (Ribeiro *et al*, 2013) and reducing pro-inflammatory cytokines (Lu *et al*, 2015). Indeed after TBI CB_2 receptor activation reduces oedema, enhances cerebral blood flow, increases M2 polarization, and improves neurological motor deficits (Braun *et al*, 2018). One consideration for the lack of protection from TBI-induced MWM performance deficits may in part be due to a decrease in CB_2 receptor signaling because of reduced 2-AG levels in microglia. As such the administration of a CB_2 receptor agonist in a DAGL-$\beta^{-/-}$ mouse post-injury might be an interesting avenue to explore the dual effectiveness of CB_2 receptor inflammation resolution signaling combined with the inhibition of 2-AG into microglial eicosanoid production pathways on TBI-induced cognitive deficit. In support of this strategy of dual CB_2 receptor activation and reduced eicosanoid signaling, monoacylglycerol lipase (MAGL) inhibition (which increases 2-AG and lowers AA in a non-cell type specific manner) shows protection from the molecular and cellular damage inflicted by TBI (see Chapter I, Table 1-1, pg 31 & 32). However, given TBI-induced functional deficit protection was mixed following MAGL inhibition (see Chapter I, Table 1-2, pg 33 & 34), global reduction of AA production across all cell types might have wider reaching biological implications that in part mitigate the neuroprotective potential of reduced eicosanoid signaling.

TBI-induced memory deficit protection by cell type.

Despite our original hypothesis, that disrupting DAGL-β activity would provide protection from TBI-induced learning and memory impairments in mice (by reducing microglial

pools of 2-AG pro-inflammatory metabolites), complementary genetic and pharmacological approaches indicated that disrupting DAGL-β is not sufficient to ameliorate motor or cognitive deficits following TBI. A remaining question is whether blocking 2-AG production on other cell types would offer protection from TBI-induced memory deficit. DAGL-α, the other biosynthetic enzyme of 2-AG production, is primarily neuronal, as well as expressed on astrocytes in the CNS (Gao *et al*, 2010). As such, we conducted an experiment to assess if DAGL-$\alpha^{-/-}$ mice would be protected from TBI-induced spatial memory deficit (see Chapter 3). The DAGL-$\alpha^{-/-}$ mice responded poorly to the craniectomy surgery and approximately 30-60 min post-surgery exhibited tonic-clonic seizure-like movements followed by spontaneous death. Of the eight DAGL-α mice (DAGL-$\alpha^{+/+}$ n=1, DAGL-$\alpha^{-/-}$ n=7) undergoing surgery, only three survived to receive a TBI (one DAGL-$\alpha^{+/+}$ and two DAGL-$\alpha^{-/-}$, all of which survived). Constitutive DAGL-$\alpha^{-/-}$ mice have distinct phenotypes which include decreased survival (Powell *et al*, 2015) and seizure-susceptibility (Sugaya *et al*, 2016), and as such future experiments to investigate the role of neuronal/astrocyte 2-AG production inhibition following TBI might be conducted in an inducible mouse model of DAGL-α deletion. Pharmacological blockade of DAGL-α also has associated challenges. The DAGL-α inhibitor, DO34, lacks selectivity for this enzyme in that it is equipotent for DAGL-α and DAGL-β (Ogasawara *et al*, 2016). However, DO34 could yet prove a useful tool to answer questions about the role of 2-AG in neurons and astrocytes if administered to a DAGL-$\beta^{-/-}$ mouse (known to show no TBI memory protection) after TBI. We did however conduct an additional experiment administering DO34 to C57BL6/J mice daily for 2 days prior to injury and for 6 days post-injury. We found no significant change in MWM performance

in the DO34-treated TBI mice compared to the vehicle-treated mice, suggesting that disrupting DAGL-α (and therefore lowering neuronal and astrocytic 2-AG), is also not sufficient to ameliorate motor or cognitive deficits following TBI.

TBI Mortality protection by DAGL-β.

The survival protective phenotype observed in mice with a DAGL-β deletion suggests that DAGL-β activity may contribute to TBI-induced acute mortality. The expression pattern of DAGL-β in brain is not yet well understood; however, the brain areas responsible for autonomic function and basic life support such as cardiac, respiration, and blood pressure control are well understood and are predominantly located in the brain stem (medulla oblongata, pons) and hypothalamus (arcuate nucleus) (as well as other aspects of voluntary control occurring in higher motor cortices). Specifically, murine models of TBI have found respiratory dysfunction to occur within seconds post-injury (Dixon *et al*, 1987), frequently in proportion to the magnitude of the injury severity (Atkinson *et al*, 1998), and result in either transient or irreversible pulmonary oedema, hypoxemia, endothelial damage, and respiratory failure (Koutsoukou *et al*, 2016). The mortality that occurs from fluid percussion injury in mice is frequently attributed to acute lung failure. In clinical cases of TBI acute lung injury is also reported in as high as 30% of cases (Nicolls and Laubach, 2014), with a similar resulting pathology to that seen in mice and rats (Alvarez *et al*, 2015).

The pathophysiology behind TBI-induced lung injury is not well understood, though currently three mechanisms have been considered; an increase in intracranial pressure affecting pulmonary control centers in the brain, a sympathetic surge

producing increased plasma adrenaline driving capillary bed pressure and endothelial damage, and/or macrophage activation and migration increasing systemic production of inflammatory mediators (Koutsoukou *et al*, 2016). Increased numbers of macrophage in mouse lung occur post-TBI (Kalsotra *et al*, 2007) suggesting macrophage migration in response to injury. DAGL-β is highly expressed on intraperitoneal magcrophages in the periphery (Hsu *et al*, 2012), a possible population from which this migration occurs. A substantial population of lung resident macrophages are also present. This population of mouse and human lung resident macrophages has been found to express several components of the endocannabinoid system; CB_1 and CB_2 receptors, with basal levels of tonic lung 2-AG and anandamide (Avraham *et al*, 2008; Nomura *et al*, 2008; Staiano *et al*, 2015). Furthermore, increases in lung 2-AG occur in response to LPS-induced inflammation in mice (Staiano *et al*, 2015). Given the basal levels of 2-AG present in lung it is possible that DAGL-β may be expressed on lung resident macrophages, or that increased lung 2-AG (in response to an inflammatory challenge) might be in part a consequence of infiltrating intraperitoneal macrophages. Regardless, it is an interesting possibility that DAGL-β may play a role in acute lung injury and thus acute mortality after TBI. An avenue of future interest would be the investigation of whether DAGL-β is expressed on lung resident macrophages, and if 2-AG levels in lung increase following TBI in mice. In a model of LPS-induced acute lung injury the MAGL inhibitor JZL184 reduced lung leukocyte migration and cytokine levels (Costola-de-Souza *et al*, 2013), perhaps as a result of the prevention of 2-AG oxidation to AA pro-inflammatory metabolites. As such, evaluating outcome measures such as macrophage migration and levels of pro-inflammatory mediators after TBI in DAGL-$\beta^{-/-}$ and -$\beta^{+/+}$ mice may

provide answers as to whether the survival protective effect of DAGL-β deletion occurs concurrently with reduced inflammation in lung.

DAGL-α regulation of learning and memory: physiology to pathophysiology.

The varying magnitudes of behavioral learning and memory deficit evidenced between DAGL-$\alpha^{-/-}$ mice (displaying profound MWM acquisition deficits), versus DAGL-α inhibition (showing modestly impaired acquisition rate) could be a result of various factors; such as developmental alterations across ontogeny, off target engagement at high dose DO34, or the relative magnitude of lowered 2-AG and AA. The future use of inducible DAGL-$\alpha^{-/-}$ mice may prove useful in resolving this disparity. Should the MWM impairment profile of inducible DAGL-$\alpha^{-/-}$ mice mirror that of DO34-treated mice in acquisition deficit magnitude, or lack of expression impairment, then conclusions about DAGL-α also being important for normal neural development and its impact on future learning and memory could be drawn. Regardless, the impaired acquisition and reversal learning as a result of DAGL-α inhibition (with no effect on expression, extinction, or forgetting processes) suggests that DAGL-α may play a selective role in the integration of new spatial information in the normal mouse brain.

The varying magnitudes of lipid profile alterations between DAGL-$\alpha^{-/-}$ mice and wild type mice treated with a DAGL-α inhibitor could also be a consequence of developmental alterations across ontogeny. While 2-AG levels were lowered across all brain regions in both DAGL-$\alpha^{-/-}$ mice and DO34-treated mice, changes in anandamide (AEA) levels differed by intervention and brain area. Only DAGL-$\alpha^{-/-}$ mice showed reductions in AEA, and these changes were regionally dependent. Compensatory

changes to the production, metabolism, and signaling of AEA in response to the constitutive deletion of DAGL-α could be partly responsible for the lowered AEA in DAGL-$\alpha^{-/-}$ mice. While AEA has distinct biosynthetic and catabolic pathways from 2-AG, the metabolic product of both, AA, is also a substrate for one AEA production pathway (Izzo and Deutsch, 2011). Therefore, the large reduction of AA in DAGL-$\alpha^{-/-}$ mice (four-fold that of DAGL-α inhibition) may also contribute to lowered AEA. On the other hand, DAGL-$\alpha^{-/-}$ mice showed significant AEA decreases in hippocampus and cerebellum, but not in PFC or striatum, despite having profoundly decreased AA levels in all four brain regions evaluated. Thus, factors beyond AA reductions many also contribute to the phenotypic AEA decreases, such as brain region selective expression levels of FAAH (Egertova *et al*, 2003). As elevated AEA (by FAAH inhibition or deletion) accelerates MWM extinction rates (Varvel *et al*, 2007), reducing hippocampal and cerebellum AEA might therefore be predicted to impair MWM extinction learning; however, this outcome was not observed. Furthermore, FAAH inhibition does not reverse fear extinction deficits in DAGL-$\alpha^{-/-}$ mice (Cavener *et al*, 2018). Therefore, while AEA was lowered in hippocampus and cerebellum, it was not sufficient to alter extinction vehicle-control level performance of DAGL-α inhibitor treated mice.

The cerebellum specifically showed modest basal differences in cannabinoid related lipids as well as across both pharmacological and genetic manipulations. Basal levels of AA in control mice (DAGL-$\alpha^{+/+}$ and veh-treated mice) were lower in cerebellum than the other brain areas tested. Also, elevations of cerebellar SAG in DAGL-$\alpha^{-/-}$ and DO34-treated mice were modest in comparison to hippocampal, PFC, and striatal elevations. The understanding of the cerebellar role in spatial memory has progressed

from simple motor learning to considerations about goal directed navigation specifically through distinguishing between self- and externally-generated vestibular signals (Rochefort *et al*, 2013). Furthermore, destruction of cerebellar Purkinje cells produce impaired MWM acquisition (Gandhi *et al*, 2000), and MWM reversal task deficits (Leggio *et al*, 1999). The reduction in cerebellar basal AA tone and modest SAG elevations after DAGL-α disruption might indicate a spatially dependent role for these upstream and downstream bioactive lipids of DAGL-α in the presently disrupted tasks of MWM spatial memory.

The finding that DAGL-α is important for the integration of new spatial information in the healthy mouse brain, may point to DAGL-α dysregulation as a target for disease states where learning is impaired. Given that DAGL-α expression decreases with age (Piyanova *et al*, 2015), one such example of DAGL-α-related pathology could exist in the form of age-related cognitive decline. Future experiments evaluating if age-related MWM performance deficits in C57BLB6/J mice correlate with lowered DAGL-α expression/activity would be of interest. Furthermore, I would predict that mice showing age-related MWM performance deficits would be more vulnerable to the learning and memory impairing effects of DAGL-α inhibitors than young C57BL6/J mice. Finally, investigation into the mechanisms of how DAGL-α is impacting memory would valuable, specifically in identifying which lipid, upstream or downstream of DAGL-α, is responsible for the presently observed effects. To evaluate if lowered 2-AG is responsible for the learning and memory impairing effects of DO34, co-administration of a MAGL inhibitor could be used to assess if rescue of memory impairing effects is possible through elevation of 2-AG in the presence of DAGL-α inhibition.

Future Directions

While the hypothesis that DAGL-β disruption would protect against TBI-induced cognitive impairments was not supported, the evaluation of perturbations to neurochemical lipid correlates of DAGL-β deletion, and downstream pro-inflammatory mediators, to assess their relationship to the survival protective phenotype of DAGL-$\beta^{-/-}$ mice will be important. Changes in whole brain 2-AG levels are however not evident in DAGL-$\beta^{-/-}$ mice (Tanimura *et al*, 2010; and data not shown) perhaps a result of the cell specific location of DAGL-β on microglia, which make up only 5-12% of total CNS cells depending on brain area (Lawson *et al*, 1990). Yet *in vitro* DAGL-β regulates the levels of 2-AG, AA, and prostaglandins in primary cultured microglia (Viader *et al*, 2015b). As such, development of a procedure to measure *ex vivo* levels of endocannabinoids and their related lipids specifically in microglia from adult mouse brain collected following a TBI would be a valuable addition to the present work. Such a procedure could be established using cell sorting by magnetic immunoprecipitation. Magnetic cell sorting uses a magnetic antibody which when incubated with cells from CNS tissue and passed over a magnetic column, produces isolation of a microglial positive fraction. The use of a magnetic CD11b+ antibody has previously produced CD11b+ fractions with low expression of astrocytic, oligodendrocyte, and neuronal mRNA, and enrichment of microglial protein expression (Holt and Olsen, 2016). As such, I predict that microglial 2-AG and AA would be lower in DAGL-$\beta^{-/-}$ mice compared to DAGL-$\beta^{+/+}$ mice. Also I would predict that TBI might yield increased microglial 2-AG and AA in DAGL-$\beta^{+/+}$ mice, whereas TBI DAGL-$\beta^{-/-}$ mice might show no change in 2-AG and AA compared to their sham controls, and also possible protection from increased AA metabolites. However, if

ex vivo mouse brain tissue is collected at the 2 min acute mortality cut off time, elevations of AA metabolites (e.g. prostaglandins) may not yet be present. Future adaptation of this procedure to evaluate endocannabinoid and related lipids in aveolar macrophage from mouse lung tissue (using a magnetic CD11C antibody) would also be a useful endeavor. A correlation of blunted lipid level changes in lung resident macrophages of TBI DAGL-$\beta^{-/-}$ mice to survival protection might connect this survival effect to acute lung injury protection following TBI.

The conclusions made about the role of DAGL-α in mouse spatial learning and memory might be further strengthened through the use of a second hippocampal-dependent learning and memory task. Specifically, a single trial spatial learning and memory task such as the Object Location assay, a hippocampal dependent adaptation of the Object Recognition task (Assini *et al*, 2009). The Object Recognition task consists of 2 identical objects which are explored in sample phase, then during choice phase (3 h later) one object is moved to a new location, the novelty of which being sufficient to produce increased exploration of the moved object in naïve C57BL6/J mice. Comparable deficits in two distinct hippocampal learning and memory tasks would add weight to the present conclusions that DAGL-α is an important mediator in the regulation of hippocampal learning and memory. Given anandamide (AEA) was also lowered following DAGL-α deletion, inclusion of a future experiment where a FAAH inhibitor is administered to DAGL-$\alpha^{-/-}$ mice to evaluate if the return of AEA levels to baseline would reverse the behavioral impairment would be a useful inquiry to rule out any effect of AEA.

The dissertation data presented suggest that DAGL-α, but not DAGL-β, is an important contributor to the neurobiology of learning and memory, whereas DAGL-β contributes to TBI-induced acute mortality. Knowledge of the differential contributions of these enzymes to the normal regulation of memory, and memory following disease states such as TBI are invaluable as the search for effective treatments for memory pathology continues.

List of References

Adams, J.H., Doyle, D., Ford, I., Gennarelli, T.A., Graham, D.I., McLellan DR (1989). Diffuse axonal injury in head injury: definition, diagnosis and grading. *Histopathology* **15**: 49–59.

Ahn K, Johnson DS, Mileni M, Beidler D, Long JZ, McKinney MK, *et al* (2009). Discovery and characterization of a highly selective FAAH inhibitor that reduces inflammatory pain. *Chem Biol* **16**: 411–20.

Albert-WeiBenberger C, Varrallyay C, Raslan F, Kleinschnitz C, Siren AL (2012). An experimental protocol for mimicking pathomechanisms of traumatic brain injury in mice. *Exp Transl Stroke Med* **4**: 1–5.

Alger BE, Kim J (2011). Supply and demand for endocannabinoids. *Trends Neurosci* **34**: 304–315.

Allen A, Gammon C, Ousley A, McCarthy K, Morell P (1992). Bradykinin stimulates arachidonic acid release through the sequential actions of an sn-1 diacylglycerol lipase and a monoacylglycerol lipase. *J Neurochem* **58**: 1130–1139.

Altman J, Das GD (1965). Post-natal origin of microneurones in the rat brain. *Nature* **207**: 953–956.

Alvarez J, Quevedo O, Furelos L, Gonzalez I, Llapur E, Valeron M, *et al* (2015). Pulmonary Complications in Patients with Severe Brain Injury. *Pulm Res Respir Med* **2**: 69–74.

Amenta PS, Jallo JI, Tuma RF, Elliott MB (2012). A cannabinoid type 2 receptor agonist attenuates blood-brain barrier damage and neurodegeneration in a murine model of traumatic brain injury. *J Neurosci Res* **90**: 2293–2305.

Arai K, Lo EH (2009). Experimental models for analysis of oligodendrocyte pathophysiology in stroke. *Exp Transl Stroke Med* **1**: 6.

Assaf F, Fishbein M, Gafni M, Keren O, Sarne Y (2011). Pre- and post-conditioning treatment with an ultra-low dose of Δ9-tetrahydrocannabinol (THC) protects against pentylenetetrazole (PTZ)-induced cognitive damage. *Behav Brain Res* **220**: 194–201.

Assini FL, Duzzioni M, Takahashi RN (2009). Object location memory in mice: pharmacological validation and further evidence of hippocampal CA1 participation. *Behav Brain Res* **204**: 206–211.

Atkinson JLD, Anderson RE, Murray MJ (1998). The early critical phase of severe head injury: importance of apnea and dysfunctional respiration. *J Trauma Inj Infect Crit Care* **45**: 941–945.

Atwood BK, MacKie K (2010). CB 2: A cannabinoid receptor with an identity crisis. *Br J Pharmacol* **160**: 467–479.

Avraham Y, Magen I, Zolotarev O, Vorobiav L, Nachmias A, Pappo O, *et al* (2008). Prostaglandins , Leukotrienes and Essential Fatty Acids in various rat tissues during the evolution of experimental cholestatic liver disease. **79**: 35–40.

Baggelaar MP, Esbroeck ACM van, Rooden EJ van, Florea BI, Overkleeft HS, Marsicano G, *et al* (2017). Chemical proteomics maps brain region specific activity of endocannabinoid hydrolases. *ACS Chem Biol* **12**: 852–861.

Baguley IJ, Nott MT, Howle AA, Simpson GK, Browne S, King AC, *et al* (2012). Late mortality after severe traumatic brain injury in New South Wales: a multicentre study. *Med J Aust* **196**: 40–5.

Balsinde J, Diez E, Mollinedo F (1991). Arachidonic acid release from diacylglycerol in human neutrophils. Translocation of diacylglycerol-deacylating enzyme activities from an intracellular pool to plasma membrane upon cell activation. *J Biol Chem* **266**: 15638–15643.

Barbacci DC, Roux A, Muller L, Jackson SN, Post J, Baldwin K, *et al* (2017). Mass spectrometric imaging of ceramide biomarkers tracks therapeutic response in traumatic brain injury. *ACS Chem Neurosci* **8**: 2266–2274.

Basavarajappa BS, Nagre NN, Subbanna S (2014). Elevation of endogenous anandamide impairs LTP, learning, and memory through CB1 receptor signaling in mice. *Hippocampus* **24**: 808–818.

Başkaya MK, Rao a M, Doğan a, Donaldson D, Dempsey RJ (1997). The biphasic opening of the blood-brain barrier in the cortex and hippocampus after traumatic brain injury in rats. *Neurosci Lett* **226**: 33–36.

Bell RL, Kennerly DA, Stanford N, Majerus PW (1979). Diglyceride lipase: a pathway for arachidonate release from human platelets. *Proc Natl Acad Sci U S A* **76**: 3238–3241.

Ben-Shabat S, Fride E, Sheskin T, Tamiri T, Rhee MH, Vogel Z, *et al* (1998). An entourage effect: inactive endogenous fatty acid glycerol esters enhance 2-arachidonoyl-glycerol cannabinoid activity. *Eur J Pharmacol* **353**: 23–31.

Beni-Adani L, Gozes I, Cohen Y, Assaf Y, Steingart R a, Brenneman DE, *et al* (2001). A peptide derived from activity-dependent neuroprotective protein (ADNP) ameliorates injury response in closed head injury in mice. *J Pharmacol Exp Ther* **296**: 57–63.

Béquet, F., Uzabiaga, F., Desbazeille, M., Ludwiczak, P., Maftouh, M., Picard, C., Scatton, B., Le Fur G (2007). CB1 receptor-mediated control of the release of endocannabinoids (as assessed by microdialysis coupled with LC/MS) in the rat hypothalamus. *Eur J Neurosci* **26**: 3458–3464.

Bernasconi-Guastalla S, Wolfer DP, Lipp HP (1994). Hippocampal mossy fibers and swimming navigation in mice: Correlations with size and left-right asymmetries. *Hippocampus* **4**: 53–63.

Berry C, Ley EJ, Tillou A, Cryer G, Margulies DR, Salim A (2009). The effect of gender on patients with moderate to severe head injuries. *J Trauma* **67**: 950–953.

Bilkei-Gorzo A, Albayram O, Draffehn A, Michel K, Piyanova A, Oppenheimer H, *et al* (2017). A chronic low dose of . ∆9-tetrahydrocannabinol (THC) restores cognitive function in old mice. *Nat Med* **23**: 782–787.

Bioque M, Cabrera B, Garcia-Bueno B, Mac-Dowell KS, Torrent C, Saiz PA, *et al* (2016). Dysregulated peripheral endocannabinoid system signaling is associated with cognitive deficits in first-episode psychosis. *J Psychiatr Res* **75**: 14–21.

Bisogno T, Howell F, Williams G, Minassi A, Cascio M, Ligresti A, *et al* (2003a). Cloning of the first sn1-DAG lipases points to the spatial and temporal regulation of endocannabinoid signaling in the brain. *J Cell Biol* **163**: 463–468.

Bisogno T, Howell F, Williams G, Minassi A, Cascio MG, Ligresti A, *et al* (2003b). Cloning of the first sn1-DAG lipases points to the spatial and temporal regulation of endocannabinoid signaling in the brain. *J Cell Biol* **163**: 463–468.

Blankman JL, Cravatt BF (2013). Chemical probes of endocannabinoid metabolism. *Pharmacol Rev* **65**: 849–71.

Blankman JL, Simon GM, Cravatt BF (2007). A Comprehensive Profile of Brain Enzymes that Hydrolyze the Endocannabinoid 2-Arachidonoylglycerol. *Chem Biol* **14**: 1347–1356.

Bliss T V., Lomo T (1973). Long lasting potentiation of synaptic transmission in the dentate area of the anaesthetized rabbit following stimulation of the perforant path. *J Physiol* **232**: 331–356.

Boger D, Fecik R, Patterson J (2000). Fatty acid amide hydrolase substrate specificity. *Bioorg Med Chem Lett* **10**: 2613–2616.

Bolkvadze T, Pitkanen A (2012). Development of Post-Traumatic Epilepsy after Controlled Cortical Impact and Lateral Fluid-Percussion-Induced Brain Injury in the Mouse. *J Neurotrauma2* **29**: 789–812.

Bonini JS, Silva WC Da, Bevilaqua LR, Medina JH, Izquierdo I (2007). On the participation of hippocampal PKC in acquisition, consolidation and reconsolidation of spatial memory. *Neuroscience* **147**: 37–45.

Booth M (St. Martin's Press: New York, 2003). *Cannabis: a history*. .

Brambrink, A.M., Dick WF (1997). Neurogenic pulmonary edema. Pathogenesis, clinical picture and therapy. *Anaesthesist* **46**: 953–963.

Brash AR (2001). Arachidonic acid as a bioactive molecule. *J Clin Invest* **107**: 1339–1345.

Bratton SL, Chestnut RM, Ghajar J, McConnell Hammond FF, Harris O a., Hartl R, *et al* (2007). VIII. Intracranial Pressure Thresholds. *J Neurotrauma* **24**: S-55-S-58.

Braun M, Khan ZT, Khan MB, Kumar M, Ward A, Achyut BR, *et al* (2018). Selective activation of cannabinoid receptor-2 reduces neuroinflammation after traumatic

brain injury via alternative macrophage polarization. *Brain, Behav Immun* **68**: 224–237.

Brittis P, Silver J, Walsh F, Doherty P (1996). Fibroblast growth factor receptor function is required for the orderly projection of ganglion cell axons in the developing mamalian retina. *Mol Cell Neurosci* 120–128.

Brown KD, Iwata A, Putt ME, Smith DH (2006). Chronic ibuprofen administration worsens cognitive outcome following traumatic brain injury in rats. *Exp Neurol* **201**: 301–307.

Buczynski MW, Dumlao DS, Dennis EA (2009). Thematic Review Series: Proteomics. An integrated omics analysis of eicosanoid biology. *J Lipid Res* **50**: 1015–38.

Bullock, R., Chestnut, R., Ghajar, J., Gordon, D., Hartl, R., Newell, D. W., Servadei, F., Walters, B. C., Wilberger JE (2006). Guidelines for the surgical management of traumatic brain injury. *Neurosurgery* **58**: S2-62.

Bullock R, Zauner A, Woodward JJ, Myseros J, Choi SC, Ward JD, *et al* (1998). Factors affecting excitatory amino acid release following severe human head injury. *J Neurosurg* **89**: 507–518.

Cabral GA, Raborn ES, Griffin L, Dennis J, Marciano-Cabral F (2008). CB2 receptors in the brain: role in central immune function. *Br J Pharmacol* **153**: 240–51.

Carbonell WS, Maris DO, McCall T, Grady MS (1998). Adaptation of the fluid percussion injury model to the mouse. *J Neurotrauma* **15**: 217–229.

Carlesimo GA, Sabbadini M, Loasses A, Caltagirone C (1997). Forgetting from long-term memory in severe closed-head injury patients: Effect of retrieval conditions and semantic organization. *Cortex* **33**: 131–142.

Carlson G, Wang Y, Alger BE (2002). Endocannabinoids facilitate the induction of LTP in the hippocampus. *Nat Neurosci* **5**: 723–724.

Carrier EJ, Auchampach J a, Hillard CJ (2006). Inhibition of an equilibrative nucleoside transporter by cannabidiol: a mechanism of cannabinoid immunosuppression. *Proc Natl Acad Sci U S A* **103**: 7895–7900.

Carrier EJ, Kearn CS, Barkmeier AJ, Breese NM, Yang W, Nithipatikom K, *et al* (2004). Cultured rat microglial cells synthesize the endocannabinoid 2-arachidonylglycerol, which increases proliferation via a CB2 receptor-dependent mechanism. *Mol Pharmacol* **65**: 999–1007.

Casarejos MJ, Perucho J, Gomez A, Mu??oz MP, Fernandez-Estevez M, Sagredo O, *et al* (2013). Natural cannabinoids improve dopamine neurotransmission and tau and amyloid pathology in a mouse model of tauopathy. *J Alzheimer's Dis* **35**: 525–539.

Cavener VS, Gaulden A, Pennipede D, Jagasia P, Uddin J, Marnett LJ, *et al* (2018). Inhibition of diacylglycerol lipase impairs fear extinction in mice. *Front Neurosci* **12**: eCollection.

Centonze D, Rossi S, Cavasinni F, Chiara V De, Bergami A, Musella A, *et al* (2009). Inflammation triggers synaptic alteration and degeneration in experimental autoimmune encephalomyelitis. *J Neurosci* **29**: 3442–3452.

Cernak I, O'Connor C, Vink R (2002). Inhibition of cyclooxygenase 2 by nimesulide improves cognitive outcome more than motor outcome following diffuse traumatic brain injury in rats. *Exp Brain Res* **147**: 193–199.

Chakraborty S, Skolnick B, Narayan RK (2016). Neuroprotection trials in traumatic brain injury. *Curr Neurol Neurosci Rep* **16**: 29.

Chau L, Tai H (1981). Release of arachidonate from diglyceride in human platelets requires the sequential action of a diglyceride lipase and a monoglyceride lipase. *Biochem Biophys Res Commun* **100**: 1688–1695.

Chen F, Sugiura Y, Myers KG, Liu Y, Lin W (2010a). Ubiquitin carboxyl-terminal hydrolase L1 is required for maintaining the structure and function of the neuromuscular junction. *Proc Natl Acad Sci U S A* **107**: 1636–1641.

Chen JK, Chen J, Imig JD, Wei S, Hachey DL, Guthi JS, *et al* (2008). Identification of novel endogenous cytochrome p450 arachidonate metabolites with high affinity for cannabinoid receptors. *J Biol Chem* **283**: 24515–24524.

Chen X, Lin YP, Wang D, Zhang JN (2010b). Dexamthosone exacerbates spatial acquisition deficits after traumatic brain injury in rats. *Neurol Res* **32**: 1097–1102.

Chen X, Zhang KL, Yang SY, Dong JF, Zhang JN (2009). Glucocorticoids aggravate retrograde emmory deficiency associated with traumatic brain injury. *J Neurotrauma* **26**: 253–260.

Chen Y, Shohami E, Constantini S, Weinstock M (1998). Rivastigmine, a brain-selective acetylcholinesterase inhibitor, ameliorates cognitive and motor deficits induced by closed-head injury in the mouse. *J Neurotrauma* **15**: 231–237.

Chevaleyre V, Castillo PE (2004). Endocannabinoid-mediated metaplasticity in the hippocampus. *Neuron* **43**: 871–881.

Chodobski A, Zink BJ, Szmydynger-chodobska J (2012). *Blood-brain barrier pathophysiology in traumatic brain injury*. *Transl Stroke Res* **2**: .

Christodoulou C, DeLuca J, Ricker JH, Madigan NK, Bly BM, Lange G, *et al* (2001). Functional magnetic resonance imaging of working memory impairment after

traumatic brain injury. *J Neurol Neurosurg Psychiatry* **71**: 161–168.

Chu CJ, Huang SM, Petrocellis L De, Bisogno T, Ewing SA, Miller JD, *et al* (2003). N-oleoyldopamine, a novel endogenous capsaicin-like lipid that produces hyperalgesia. *J Biol Chem* **278**: 13633–13639.

Cipolotti L, Shallice T, Chan D, Fox N, Scahill R, Harrison G, *et al* (2001). Long-term retrograde amnesia...the crucial role of the hippocampus. *Neuropsychologia* **39**: 151–172.

Corcoran L, Roche M, Finn DP (Elsevier Inc.: 2015). *The Role of the Brain's Endocannabinoid System in Pain and Its Modulation by Stress*. *Int Rev Neurobiol* **125**: .

Corrigan, John D; Selassie, Anbesaw W; Orman JA (2010). The Epidemiology of Traumatic Brain Injury. *J Head Trauma Rehabil* **25**: 72–80.

Costa B, Comelli F, Bettoni I, Colleoni M, Giagnoni G (2008). The endogenous fatty acid amide, palmitoylethanolamide, has anti-allodynic and anti-hyperalgesic effects in a murine model of neuropathic pain: involvement of CB1, TRPV1 and PPAR?? receptors and neurotrophic factors. *Pain* **139**: 541–550.

Costola-de-Souza C, Ribeiro A, Ferraz-de-Paula V, Calefi AS, Aloia TPA, Gimenes-Júnior JA, *et al* (2013). Monoacylglycerol Lipase (MAGL) Inhibition Attenuates Acute Lung Injury in Mice. *PLoS One* **8**: 1–15.

Cravatt BF, Demarest K, Patricelli MP, Bracey MH, Giang DK, Martin BR, *et al* (2001). Supersensitivity to anandamide and enhanced endogenous cannabinoid signaling in mice lacking fatty acid amide hydrolase. *Proc Natl Acad Sci U S A* **98**: 9371–6.

Cravatt BF, Giang DK, Mayfield SP, Boger DL, Lerner R a, Gilula NB (1996). Molecular

characterization of an enzyme that degrades neuromodulatory fatty-acid amides. *Nature* **384**: 83–87.

Dash PK, Mach SA, Moore AN (2000). Regional expression and role of cyclooxygenase-2 following experimental traumatic brain injury. *J Neurotrauma* **17**: 69–81.

Dash PK, Orsi S a., Zhang M, Grill RJ, Pati S, Zhao J, *et al* (2010). Valproate administered after traumatic brain injury provides neuroprotection and improves cognitive function in rats. *PLoS One* **5**: .

Davalos D, Grutzendler J, Yang G, Kim J V., Zuo Y, Jung S, *et al* (2005). ATP mediates rapid microglial response to local brain injury in vivo. *Nat Neurosci* **8**: 752–758.

Davis DP, Douglas DJ, Smith W, Sise MJ, Vilke GM, Holbrook TL, *et al* (2006). Traumatic brain injury outcomes in pre- and post-menopausal females versus age-matched males. *J Neurotrauma* **23**: 140–148.

Deacon E, Pettitt T, Webb P, Cross T, Chahal H, Wakelam M, *et al* (2001). Generation of diacylglycerol molecular species through the cell cycle: a role for 1-stearoyl, 2-arachidonyl glycerol in the activation of nuclear protein kinase C-βII at G2/M. *J Cell Sci* **115**: 983–989.

Deng W, Aimone J, Gage F (2010a). New neurons and new memories: how does adult hippocampal neurogenesis affect learning and memory? *Nat Rev Neurosci* **11**: 339–350.

Deng Y, Theken KN, Lee CR (2010b). Cytochrome P450 epoxygenases, soluble epoxide hydrolase, and the regulation of cardiovascular inflammation. *J Mol Cell Cardiol* **48**: 331–341.

Deutsch D, Chin S (1993). Enzymatic synthesis and degradation of anandamide, a cannabinoid receptor agonist. *Biochem Pharmacol* **46**: 791–6.

Deutsch DG, Goligorsky MS, Schmid PC, Krebsbach RJ, Schmid HHO, Das SK, *et al* (1997). Production and physiological actions of anandamide in the vasculature of the rat kidney. *J Clin Invest* **100**: 1538–1546.

Devane, W.A., Hanus, L., Breuer, A., Pertwee, R.G., Stevenson, L.A., Griffin, G., Gibson, D., Mandelbaum, A., Etinger, A., Mechoulam R (1992). Isolation and Structure of a Brain Constituent That Binds to the Cannabinoid Receptor. *Science (80-)* **258**: 1946–1949.

Devane WA, Dysarz III FA, Johnson MR, Melvin LS, Howlett AC (1988). Determination and Characterization of a Cannabinoid Receptor in Rat Brain. *Mol Pharmacol* **34**: 605–613.

Dinh TP, Carpenter D, Leslie FM, Freund TF, Katona I, Sensi SL, *et al* (2002). Brain monoglyceride lipase participating in endocannabinoid inactivation. *Proc Natl Acad Sci U S A* **99**: 10819–24.

Dirnagl U, Simon RP, Hallenbeck JM (2003). Ischemic tolerance and endogenous neuroprotection. *Trends Neurosci* **26**: 248–254.

Dixon CE, Lyeth BG, Povlishock JT, Findling RL, Hamm RJ, Marmarou a, *et al* (1987). A fluid percussion model of experimental brain injury in the rat. *J Neurosurg* **67**: 110–119.

Donat CK, Scott G, Gentleman SM, Sastre M (2017). Microglial activation in traumatic brain injury. *Front Aging Neurosci* **9**: 208.

Dragoi G, Tonegawa S (2012). Preplay of future place cell sequences by hippocampal

cellular assemblies. *Nature* **469**: 397–401.

Dragoi G, Tonegawa S (2014). Selection of preconfigured cell assemblies for representation of novel spatial experiences. *Philos Trans R Soc Lond B Biol Sci* **369**: 20120522.

Duggan KC, Hermanson DJ, Musee J, Prusakiewicz JJ, Scheib JL, Carter BD, *et al* (2011). (R)-Profens are substrate-selective inhibitors of endocannabinoid oxygenation by COX-2. *Nat Chem Biol* **7**: 803–809.

Egan KM, Lawson JA, Fries S, Koller B, Rader DJ, Smyth EM, *et al* (2004). COX-2-derived prostacyclin confers atheroprotection on female mice. *Science (80-)* **306**: .

Egertova M, Cravatt BF, Elphick MR (2003). Comparative analysis of fatty acid amide hydrolase and CB1 cannabinoid receptor expression in the mouse brain: evidence of a widespread role for fatty acid amide hydrolase in regulation of endocannabinoid signaling. *Neuroscience* **119**: 481–496.

Egertová M, Giang DK, Cravatt BF, Elphick MR (1998). A new perspective on cannabinoid signalling: complementary localization of fatty acid amide hydrolase and the CB1 receptor in rat brain. *Proc Biol Sci* **265**: 2081–5.

Eichenbaum H, Stewart C, Morris RG (1990). Hippocampal representation in place learning. *J Neurosci* **10**: 3531–3542.

El-Gaby M, Shipton O a., Paulsen O (2014). Synaptic Plasticity and Memory: New Insights from Hippocampal Left-Right Asymmetries. *Neurosci* **21**: 490–502.

Elphick M, Egertova M (2005). The phylogenetic distribution and evolutionary origins of endocannabinoid signalling. *Handb Exp Pharmacol* **168**: 283–297.

Elsohly MA, Radwan MM, Gul W, Chandra S, Galal A (2017). *Phytochemistry of*

Cannabis sativa L. **103**: .

Faul F, Erdfelder E, Lang AG, Buchner A (2007a). G*Power 3: A flexible statistical power analysis program for the social, behavioral, and biomedical sciences. *Behav Res Methods* **39**: 175–191.

Faul M, Wald MM, Rutland-Brown W, Sullivent EE, Sattin RW (2007b). Using a cost-benefit analysis to estimate outcomes of a clinical treatment guideline: testing theBrain Trauma Foundation guidelines for the treatment of severe traumatic brain injury. *J Trauma* **63**: 1271–1278.

Feigenbaum JJ, Bergmann F, Richmond SA, Mechoulam R, Nadler V, Kloog Y, *et al* (1989). Nonpsychotropic cannabinoid acts as a functional N-methyl-D-aspartate receptor blocker. *Proc Natl Acad Sci U S A* **86**: 9584–7.

Ferguson S, Mouzon B, Paris D, Aponte D, Abdullah L, Stewart W, *et al* (2017). Acute or delayed treatment with anatabine improves spatial memory and reduces pathological sequelae at late time-points after repetitive mild traumatic brain injury. *J Neurotrauma* **34**: 1676–1691.

Ferraro FR (1996). Cognitive slowing in closed-head injury. *Brain Cogn* **32**: 429–440.

Floyd CL, Golden KM, Black RT, Hamm RJ, Lyeth BG (2002). Craniectomy position affects morris water maze performance and hippocampal cell loss after parasagittal fluid percussion. *J Neurotrauma* **19**: 303–316.

Floyd CL, Gorin FA, Lyeth BG (2010). Mechanical Strain Injury Increases Intracellular Sodium and Reverses Na+ /Ca2+ Exchange in Cortical Astrocytes. *Glia* **51**: 35–46.

Fox GB, LeVasseur RA, Faden AI (1999). Behavioral responses of C57BL/6, FVB/N, and 129/SvEMS mouse strains to traumatic brain injury: implications for gene

targeting approaches to neurotrauma. *J Neurotrauma* **16**: 377–389.

Furtado JC, Mazurek MF (1996). Behavioral characterization of quinolinate-induced lesions of the medial striatum: relevance for Huntington's disease. *Exp Neurol* **138**: 158–168.

Gaetz M (2004). The neurophysiology of brain injury. *Clin Neurophysiol* **115**: 4–18.

Gage FH (2000). Mammalian neural stem cells. *Science (80-)* **287**: 1433–1438.

Gandhi CC, Kelly RM, Wiley RG, Walsh TJ (2000). Impaired acquisition of a Morris water maze task following selective destruction of cerebellar purkinje cells with OX7-saporin. *Behav Brain Res* **109**: 37–47.

Gao Y, Vasilyev D, Goncalves M, Howell F, Hobbs C, Reisenberg M, *et al* (2010). Loss of retrograde endocannabinoid signaling and reduced neurogenesis in diacylglycerol lipase knock-out mice. *J Neurosci* **30**: 2017–2024.

Gazzaniga MS, Sperry RW (1967). Language after section of the cerebral commissures. *Brain* **90**: 131–148.

Gerlai RT, McNamara A, Williams S, Phillips HS (2002). Hippocampal dysfunction and behavioral deficit in the water maze in mice: An unresolved issue? *Brain Res Bull* **57**: 3–9.

Gertsch J, Pertwee RG, Marzo V Di (2010). Phytocannabinoids beyond the Cannabis plant - Do they exist? *Br J Pharmacol* **160**: 523–529.

Gidday JM (2006). Cerebral preconditioning and ischaemic tolerance. *Nat Rev Neurosci* **7**: 437–448.

Girgis H, Palmier B, Croci N, Soustrat M, Plotkine M, Marchand-Leroux C (2013). Effects of selective and non-selective cyclooxygenase inhibition against

neurological deficit and brain oedema following closed head injury in mice. *Brain Res* **1491**: 78–87.

Goldstein LE, Fisher a. M, Tagge C a., Zhang X-L, Velisek L, Sullivan J a., *et al* (2012). Chronic Traumatic Encephalopathy in Blast-Exposed Military Veterans and a Blast Neurotrauma Mouse Model. *Sci Transl Med* **4**: 134ra60-134ra60.

Gomez-Gonzalo M, Navarrete M, Perea G, Covelo A, Martin-Fernandez M, Shigemoto R, *et al* (2015). Endocannabinoids induce lateral long-term potentiation of transmitter release by stimulation of gliotransmission. *Cereb Cortex* **25**: 3699–3712.

Goncalves M, Suetterlin P, Yip P, Molina-Holgado F, Walker D, Oudin M, *et al* (2008). A diacylglycerol lipase-CB2 cannabinoid pathway regulates adult subventricular zone neurogenesis in an age-dependent manner. *Mol Cell Neurosci* **38**: 526–536.

Goto K, Kurashima R, Gokan H, Inoue N, Ito I, Watanabe S (2010). Left-right asymmetry defect in the hippocampal circuitry impairs spatial learning and working memory in IV mice. *PLoS One* **5**: 1–7.

Gotts SJ, Jo HJ, Wallace GL, Saad ZS, Cox RW, Martin A (2013). Two distinct forms of functional lateralization in the human brain. *Proc Natl Acad Sci U S A* **110**: E3435–E3444.

Graeber MB (2010). Changing face of microglia. *Science (80-)* **330**: 783–788.

Graham DI, McIntosh TK, Maxwell WL, Nicoll JA (2000). Recent advances in neurotrauma. *J Neuropathol Exp Neurol* **59**: 641–651.

Gregus AM, Buczynski MW, Dumlao DS, Norris PC, Rai G, Simeonov A, *et al* (2018). Inhibition of Spinal 15-LOX-1 Attenuates TLR4-Dependent, NSAID-Unresponsive Hyperalgesia in Male Rats. *Pain* in publication.

Gregus AM, Doolen S, Dumlao DS, Buczynski MW, Takasusuki T, Fitzsimmons BL, *et al* (2012). Spinal 12-lipoxygenase-derived hepoxilin A3 contributes to inflammatory hyperalgesia via activation of TRPV1 and TRPA1 receptors. *Proc Natl Acad Sci U S A* **109**: 6721–6726.

Groot YCT, Wilson BA, Evans J, Watson P (2002). Prospective memory functioning in people with and without brain injury. *J Int Neuropsychol Soc* **8**: 645–654.

Gulyas AI, Cravatt BF, Bracey MH, Dinh TP, Piomelli D, Boscia F, *et al* (2004). Segregation of two endocannabinoid-hydrolyzing enzymes into pre- and postsynaptic compartments in the rat hippocampus, cerebellum and amygdala. *Eur J Neurosci* **20**: 441–458.

Gutiérrez H, Hernández-Echeagaray E, Ramírez-Amaya V, Bermúdez-Rattoni F (1999). Blockade of N-methyl-D-aspartate receptors in the insular cortex disrupts taste aversion and spatial memory formation. *Neuroscience* **89**: 751–758.

GW Research Ltd A Randomized Controlled Trial of Cannabidiol (GWP42003-P, CBD) for Seizures in Tuberous Sclerosis Complex (GWPCARE6). *Clin Bethesda Natl Libr Med* at <https://clinicaltrials.gov/show/NCT02544763>.

Halpern ME, Gunturkun O, Hopkins WD, Rogers LJ (2005). Lateralization of the vertebrate brain: taking the side of model systems. *J Neurosci* **25**: 10351–10357.

Hama H, Hara C, Yamaquchi K, Miyawaki A (2004). PKC signaling mediates global enhancement of excitatory synaptogenesis in neurons triggered by local contact with astrocytes. *Neuron* **41**: 405–415.

Hamm RJ (2001). Neurobehavioral assessment of outcome following traumatic brain injury in rats: an evaluation of selected measures. *J Neurotrauma* **18**: 1207–16.

Hamm RJ, Pike BR, O'Dell DM, Lyeth BG, Jenkins LW (1994). The rotarod test: an evaluation of its effectiveness in assessing motor deficits following traumatic brain injury. *J Neurotrauma* **11**: 187–196.

Hansen HH, Schmid PC, Bittigau P, Lastres-Becker I, Berrendero F, Manzanares J, *et al* (2002). Anandamide, but not 2-arachidonoylglycerol, accumulates during in vivo neurodegeneration. 1415–1427.

Hartl R, Medary M, Ruge M, Arfors KE, Ghajar J (1997). Blood brain barrier breakdown occurs early after traumatic brain injury and is not related to white blood cell adherence. *Acta Neurochir Suppl* **70**: 240–242.

Hasko G, Pacher P (2008). A2A receptors in inflammation and injury: lessons learned from transgenic animals. *J Leukoc Biol* **83**: 447–455.

Haut MW, Petros T V, Frank RG (1990). The recall of prose as a function of importance following closed head injury. *Brain Inj* **4**: .

Hayes RL, Stalhammar D, Povlishock JT, Allen AM, Galinat BJ, Becker DP, *et al* (1987). A new model of condussive brain injury in the cat produced by extradural fluid volume loading: II. Physiological and neuorpathological observations. *Brain Inj* **1**: 93–112.

Heimann AS, Gomes I, Dale CS, Pagano RL, Gupta A, Souza LL de, *et al* (2007). Hemopressin is an inverse agonist of CB1 cannabinoid receptors. *Proc Natl Acad Sci U S A* **104**: 20588–20593.

Herkenham M, Lynn a B, Johnson MR, Melvin LS, Costa BR de, Rice KC (1991). Characterization and localization of cannabinoid receptors in rat brain: a quantitative in vitro autoradiographic study. *J Neurosci* **11**: 563–583.

Hicks R, Soares H, Smith D, McIntosh T (1996). Temporal and spatial characterization of neuronal injury following lateral fluid-percussion brain injury in the rat. *Acta Neuropathol* **91**: 236–246.

Higgs HN, Glomset JA (1994). Identification of a phosphatidic acid-preferring phospholipase A1 from bovine brain and testis. *Proc Natl Acad Sci U S A* **91**: 9574–9578.

Hill AJ, Jones NA, Smith I, Hill CL, Williams CM, Stephens GJ, *et al* (2014). Voltage-gated sodium (NaV) channel blockade by plant cannabinoids does not confer anticonvulsant effects per se. *Neurosci Lett* **566**: 269–274.

Hillard CJ (2000a). Biochemistry and pharmacology of the endocannabinoids arachidonylethanolamide and 2-arachidonylglycerol. *Prostaglandins Other Lipid Mediat* **61**: 3–18.

Hillard CJ (2000b). Endocannabinoids and Vascular Function 1. *Pharmacology* **294**: 27–32.

Hind WH, Tufarelli C, Neophytou M, Anderson SI, England TJ, O'Sullivan SE (2015). Endocannabinoids modulate human blood-brain barrier permeability in vitro. *Br J Pharmacol* **172**: 3015–3027.

Hindenes JO, Nerdal W, Guo W, Di L, Small DM, Holmsen H (2000). Physical Properties of the Transmembrane Signal Molecule, sn-1-Stearoyl 2-Arachidonoylglycerol. *J Biol Chem* **275**: 6857–6867.

Holland MC, Mackersie RC, Morabito D, Campbell AR, Kivett VA, Patel R, *et al* (2003). The development of acute lung injury is associated with worse neurologic outcome in patients with severe traumatic brain injury. *J Trauma* **55**: 106–111.

Hollup S a, Molden S, Donnett JG, Moser MB, Moser EI (2001). Accumulation of hippocampal place fields at the goal location in an annular watermaze task. *J Neurosci* **21**: 1635–1644.

Holmin S, Mathiesen T (1999). Long-term intracerebral inflammatory response after experimental focal brain injury in rat. *Neuroreport* **10**: 1889–1891.

Holt LM, Olsen ML (2016). Novel applications of magnetic cell sorting to analyze cell-type specific gene and protein expression in the central nervous system. *PLoS One* **11**: 1–18.

Hsu K-L, Tsuboi K, Adibekian A, Pugh H, Masuda K, Cravatt BF (2012). DAGLβ inhibition perturbs a lipid network involved in macrophage inflammatory responses. *Nat Chem Biol* **8**: 999–1007.

Hu D-E, Easton AS, Fraser P a (2005). TRPV1 activation results in disruption of the blood-brain barrier in the rat. *Br J Pharmacol* **146**: 576–584.

Hu SS, Bradshaw HB, Chen JS, Tan B, Walker JM (2008). Prostaglandin E2 glycerol ester, an endogenous COX-2 metabolite of 2-arachidonoylglycerol, induces hyperalgesia and modulates NFkappaB activity. *Br J Pharmacol* **153**: 1538–1549.

Huestis M (2007). Human cannabinoid pharmacokinetics. *Chem Biodivers* **4**: 1770–1804.

Hughes V (2012). Microglia: the constant gardeners. *Nature* **485**: 570–572.

Hutsler J, Galuske R a W (2003). Hemispheric asymmetries in cerebral cortical networks. *Trends Neurosci* **26**: 429–435.

Iglói K, Doeller CF, Berthoz A, Rondi-Reig L, Burgess N (2010). Lateralized human hippocampal activity predicts navigation based on sequence or place memory. *Proc*

Natl Acad Sci U S A **107**: 14466–14471.

Izzo AA, Deutsch DG (2011). Unique pathway for anandamide synthesis and liver regeneration. *Proc Natl Acad Sci U S A* **108**: 6339–6340.

Janssen FJ, Stelt M van der (2016). Inhibitors of diacyglycerol lipases in neurodegenerative and metabolic disorders. *Bioorg Med Chem Lett* **26**: 3831–3837.

Jenniches I, Ternes S, Albayram O, Otte DM, Bach K, Bindila L, *et al* (2016). Anxiety, Stress, and Fear Response in Mice with Reduced Endocannabinoid Levels. *Biol Psychiatry* **79**: 858–868.

Johnson VE, Stewart JE, Begbie FD, Trojanowski JQ, Smith DH, Stewart W (2013). Inflammation and white matter degeneration persist for years after a single traumatic brain injury. *Brain* **136**: 28–42.

Johnson VE, Stewart W, Smith DH (2010). Traumatic brain injury and amyloid-β pathology: a link to Alzheimer's disease? *Nat Rev Neurosci* **11**: 361–70.

Jones BJ, Roberts DJ (1968). The quantiative measurement of motor inco-ordination in naive mice using an acelerating rotarod. *J Pharmacol Pharmacother* **20**: 302–304.

Jung KM, Astarita G, Zhu C, Wallace M, Mackie K, Piomelli D (2007). A key role for diacylglycerol lipase-α in metabotropic glutamate receptor-dependent endocannabinoid mobilization. *Mol Pharmacol* **72**: 612–621.

Jung MW, McNaughton BL (1993). Spatial selectivity of unit activity in the hippocampal granular cell layer. *Hippocampus1* **3**: .

Kalsotra A, Zhao J, Anakk S, Dash PK, Strobel HW (2007). Brain trauma leads to enhanced lung inflammation and injury: evidence for role of P4504Fs in resolution.

J Cereb Blood Flow Metab **27**: 963–974.

Kano M, Ohno-Shosaku T, Hashimotodani Y, Uchigashima M, Watanabe M (2009). Endocannabinoid-mediated control of synaptic transmission. *Physiol Rev* **89**: 309–380.

Katona I, Urban G, Wallace M, Ledent C, Jung K, Piomelli D, *et al* (2006). Molecular composition of the endocannabinoid system at glutamatergic synapses. *J Neurosci* **26**: 5628–5637.

Katz PS, Sulzer JK, Impastato RA, Teng SX, Rogers EK, Molina PE (2015). Endocannabinoid degradation inhibition improves neurobehavioral function, blood-brain barrier integrity, and neuroinflammation following mild traumatic brain injury. *J Neurotrauma* **32**: 297–306.

Kawakami R, Shinohara Y, Kato Y, Sugiyama H, Shigemoto R, Ito I (2003). Asymmetrical allocation of NMDA recetpro epsilon 2 subunits in hippocampal circuitry. *Science (80-)* **300**: 900–994.

Kelly DF, Martin NA, Kordestani R, Counelis G, Hovda DA, Bergsneider M, *et al* (1997). Cerebral blood flow as a predictor of outcome following traumatic brain injury. *J Neurosurg April* **86**: 633–641.

Kigerl KA, Gensel JC, Ankeny DP, Alexander JK, Donnelly DJ, Popovich PG (2009). Identification of two distinct macrophage subsets with divergent effects causing either neurotoxicity or regeneration in the injured mouse spinal cord. *J Neurosci* **29**: 13435–44.

Kitagawa, K., Matsumoto, M., Kuwabara, K., Tagaya, M., Ohtsuki, T., Hata, R., Ueda, H., Handa, N., Kimura, K., Kamada T (1991). “Ischemic tolerance” phenomenon

detected in various brain regions. *Brain Res* **561**: 203–211.

Knoller N, Levi L, Shoshan I, Reichenthal E, Razon N, Rappaport ZH, *et al* (2002). Dexanabinol (HU-211) in the treatment of severe closed head injury: a randomized, placebo-controlled, phase II clinical trial. *Crit Care Med* **30**: 548–554.

Knoth R, Singec I, Ditter M, Pantazis G, Capetian P, Meyer R, *et al* (2010). Murine features of neurogenesis in the human hippocampus across the lifespan from 0 to 100 years. *PLoS One* **5**: e8809.

Kohl MM, Shipton OA, Deacon RM, Rawlins JNP, Deisseroth K, Paulsen O (2011). Hemisphere-specific optogenetic stimulation reveals left-right asymmetry of hippocampal plasticity. *Nat Neurosci* **14**: 1413–1415.

Kolesnick RN, Kronke M (1998). Regulation of ceramide production and apoptosis. *Annu Rev Physiol* **60**: 643–665.

Kosaki Y, Watanabe S (2012). Dissociable roles of the medial prefrontal cortex, the anterior cingulate cortex, and the hippocampus in behavioural flexibility revealed by serial reversal of three-choice discrimination in rats. *Behav Brain Res* **227**: 81–90.

Koutsoukou A, Katsiari M, Orfanos SE, Kotanidou A, Daganou M, Kyriakopoulou M, *et al* (2016). Respiratory mechanics in brain injury: A review. *World J Crit Care Med* **5**: 65–73.

Kozak KR, Crews BC, Morrow JD, Wang LH, Ma YH, Weinander R, *et al* (2002). Metabolism of the endocannabinoids, 2-arachidonylglycerol and anandamide, into prostaglandin, thromboxane, and prostacyclin glycerol esters and ethanolamides. *J Biol Chem* **277**: 44877–44885.

Kozak KR, Rowlinson SW, Marnett LJ (2000). Oxygenation of the endocannabinoid, 2-

arachidonylglycerol, to glyceryl prostaglandins by cyclooxygenase-2. *J Biol Chem* **275**: 33744–33749.

Kwiatkoski M, Guimaraes FS, Del-Bel E (2012). Cannabidiol-treated rats exhibited higher motor score after cryogenic spinal cord injury. *Neurotox Res* **21**: 271–280.

Kwilasz AJ, Abdullah RA, Poklis JL, Lichtman AH, Negus SS (2015). Effects of the fatty acid amide hydrolase (FAAH) inhibitor URB597 on pain-stimulated and pain-depressed behavior in rats. *Behav Pharmacol* **25**: 119–129.

Lafourcade M, Elezgarai I, Mato S, Bakiri Y, Grandes P, Manzoni O (2007). Molecular components and functions of the endocannabinoid system in mouse prefrontal cortex. *PLoS One* **2**: .

Lalonde R (1994). Cerebellar contributions to instrumental learning. *Neurosci Biobehav Rev* **18**: 161–170.

Lambert, D. M., Di Marzo V (1999). The palmitoylethanolamide and oleamide enigmas : are these two fatty acid amides cannabimimetic? *Curr Med Chem* **6**: 757–773.

Langlois JA, Rutland-Brown W, Wald MM (2006). The epidemiology and impact of traumatic brain injury: a brief overview. *J Head Trauma Rehabil* **21**: 375–378.

Lapchak PA, Araujo DM, Song D, Zivin JA (2001). Neuroprotection by the selective cyclooxygenase-2 inhibitor SC-236 results in improvements in behavioral deficits induced by reversible spinal cord ischemia. *Stroke* **32**: 1220–1225.

Larson J, Wong D, Lynch G (1986). Patterned stimulation at the theta frequency is optimal for the induction of hippocampal long-term potentiation. *Brain Res* **368**: 347–350.

Laskowitz DT, Mckenna SE, Song P, Wang H, Durham L, Yeung N, *et al* (2007).

COG1410, a novel apolipoprotein E-based peptide improves functional recovery in a murine model of traumatic brain injury. *J Neurotrauma* **24**: 1093–1107.

Lawson LJ, Perry VH, Dri P, Gordon S (1990). Heterogeneity in the distribution and morphology of microglia in the normal adult mouse brain. *Neuroscience* **39**: 151–170.

Leggio MG, Neri P, Graziano A, Mandolesi L, Molinari M, Petrosini L (1999). Cerebellar contribution to spatial event processing: characterization of procedural learning. *Exp Brain Res* **127**: 1–11.

Leutgeb JK, Leutgeb S, Moser M, Moser EI, Moser I (2007). Pattern Gyms in the Dentate Separation and CA3 of the Hippocampus. *Science (80-)* **315**: 961–966.

Leutgeb S, Leutgeb JK, Barnes C a, Moser EI, McNaughton BL, Moser M-B (2005). Independent codes for spatial and episodic memory in hippocampal neuronal ensembles. *Science (80-)* **309**: 619–623.

Ley EJ, Short SS, Liou DZ, Singer MB, Mirocha J, Melo N, *et al* (2013). Gender impacts mortality after traumatic brain injury in teenagers. *J Trauma Acute Care Surg* **75**: 682–686.

Lichtman AH, Hawkins EG, Griffin G, Cravatt BF (2002). Pharmacological Activity of Fatty Acid Amides Is Regulated, but Not Mediated, by Fatty Acid Amide Hydrolase in Vivo. *J Pharmacol Exp Ther* **302**: 73–79.

Lieberwirth C, Pan Y, Liu Y, Zhang Z, Wang Z (2016). Hippocampal adult neurogenesis: its regulation and potential role in spatial learning and memory. *Brain Res* **1644**: 127–140.

Liu J, Batkai S, Pacher P, Harvey-White J, Wagner JA, Cravatt BF, *et al* (2003).

Lipopolysaccharide induces anandamide synthesis in macrophages via CD14/MAPK/phosphoinositide 3-kinase/NF-_B independently of platelet-activating factor. *J Biol Chem* **278**: 45034–45039.

Long JZ, Nomura DK, Vann RE, Walentiny DM, Booker L, Jin X, *et al* (2009). Dual blockade of FAAH and MAGL identifies behavioral processes regulated by endocannabinoid crosstalk in vivo. *Proc Natl Acad Sci U S A* **106**: 20270–5.

Lopez-Rodriguez AB, Acaz-Fonseca E, Giatti S, Caruso D, Viveros MP, Melcangi RC, *et al* (2015). Correlation of brain levels of progesterone and dhydroepiandrosterone with neurological recovery after traumatic brain injury in female mice. *Psychoneuroendocrinology* **56**: 1–11.

Lopez Rodriguez A, Belen B, Romero-Zerbo SY, Rodriguez-Rodriguez N, Bellini MJ, Rodriguez De Fonseca F, *et al* (2011). Estradiol decreases cortical reactive astrogliosis after brain injury by a mechanism involving cannabinoid receptors. *Cereb Cortex* **21**: 2046–2055.

Lu C, Liu Y, Sun B, Sun Y, Hou B, Zhang Y, *et al* (2015). Intrathecal Injection of JWH-015 Attenuates Bone Cancer Pain Via Time-Dependent Modification of Pro-inflammatory Cytokines Expression and Astrocytes Activity in Spinal Cord. *Inflammation* **38**: 1880–1890.

Lu D, Qu C, Goussev A, Jiang H, Lu C, Schallert T, *et al* (2007). Statins increase neurogenesis in the dentate gyrus, reduce delayed neuronal death in the hippocampal CA3 region, and improve spatial learning in rat after traumatic brain injury. *J Neurotrauma* **24**: 1132–1146.

Maas AIR, Murray G, Henney H, Kassem N, Legrand V, Mangelus M, *et al* (2006).

Efficacy and safety of dexanabinol in severe traumatic brain injury: Results of a phase III randomised, placebo-controlled, clinical trial. *Lancet Neurol* **5**: 38–45.

Maccarrone M, Salvati S, Bari M, Finazzi A (2000). Anandamide and 2-arachidonoylglycerol inhibit fatty acid amide hydrolase by activating the lipoxygenase pathway of arachidonate cascade. *Biochem Biophys Res Commun* **278**: 576–583.

MacDonald PL, Gardner RC (2000). Type I error rate comparisons of post hoc procedures for IxJ Chi-square tables. *Eductional Psychol Meas* **60**: 735–754.

Mackie K (2006). Mechanisms of CB1 receptor signaling: endocannabinoid modulation of synaptic strength. *Int J Obes* **30 Suppl 1**: S19-23.

Mantovani A, Biswas SK, Galdiero MR, Sica A, Locati M (2013). Macrophage plasticity and polarization in tissue repair and remodeling. *J Pathol* **229**: 176–185.

Maresz K, Carrier EJ, Ponomarev ED, Hillard CJ, Dittel BN (2005). Modulation of the cannabinoid CB2 receptor in microglial cells in response to inflammatory stimuli. *J Neurochem* **95**: 437–445.

Marklund N, Clausen F, Lewander T, Hillered L (2001). Monitoring of reactive oxygen species production after traumatic brain injury in rats with microdialysis and the 4-hydroxybenzoic acid trapping method. *J Neurotrauma* **18**: 1217–1227.

Marsicano, G., Goodenough, S., Monory, K., Hermann, H., Eder M., Cannich, A., Azad, S. C., Cascio, M. G., Gutierrez, S. O., van der Stelt, M., Lopez-Rodriguez, M. L., Casanova, E., Schutz, G., Zieglgansberger, W., Di Marzo, V., Behl, C., Lutz B (2003). CB1 Cannabinoid Receptors and On-Demand Defense. *Science (80-)* **84**: 84–88.

Martinez-Vargas M, Morales-Gomez J, Gonzalez-Rivera R, Hernandez-Enriquez C, Perez-Arredondo A, Estrada-Rojo F, *et al* (2013). Does the neuroprotective role of anandamide display diurnal variations? *Int J Mol Sci* **14**: 23341–23355.

Martinez FO, Gordon S (2014). The M1 and M2 paradigm of macrophage activation: time for reassessment. *F1000Prime Rep* **6**: 13.

Marzo V Di (2008). Targeting the endocannabinoid system: to enhance or reduce? *Nat Rev Drug Discov* **7**: 438–55.

Mayer, S.A., Badjatia N (Wolters Kluwer Lippincott Williams & Wilkins: Philadelphia, 2010). *Merritt's Neurology*. .

Mayeux JP, Katz PS, Edwards S, Middleton J, Molina P (2016). Inhibition of Endocannabinoid Degradation Improves Outcomes from Mild Traumatic Brain Injury: A Mechanistic Role for Synaptic Hyperexcitability. *J Neurotrauma* **8**: neu.2016.4452.

Mazarati A (2006). Is posttraumatic epilepsy the best model of posttraumatic epilepsy? *Epilepsy Curr* **6**: 213–4.

Mazzeo AT, Brophy GM, Gilman CB, Alves OL, Robles JR, Hayes RL, *et al* (2009). Safety and tolerability of cyclosporin a in severe traumatic brain injury patients: Results from a prospective randomized trial. *J Neurotrauma* **26**: 2195–2206.

Mbye LHAN, Singh IN, Carrico KM, Saatman KE, Hall ED (2009). Comparative neuroprotective effects of cyclosporin A and NIM811, a nonimmunosuppressive cyclosporin A analog, following traumatic brain injury. *J Cereb Blood Flow Metab* **29**: 87–97.

McIntosh TK, Vink R, Noble L, Yamakami I, Fernyak S, Soares H, *et al* (1989).

Traumatic brain injury in the rat: characterization of a lateral fluid-percussion model. *Neuroscience* **28**: 233–244.

Mecha M, Carrillo-Salinas FJ, Feliu A, Guaza C (2016). Microglia activation states and cannabinoid system: therapeutic implications. *Pharmacol Ther* **166**: 40–55.

Mecha M, Feliu A, Carrillo-Salinas FJ, Rueda-Zubiaurre A, Ortega-Gutierrez S, Sola RG De, *et al* (2015). Endocannabinoids drive the acquisition of an alternative phenotype in microglia. *Brain, Behav Immun* **49**: 233–245.

Mechoulam, R., Goani Y (1967). Recent advances in the chemistry of hashish. *Fortschritte der Chemie Org Naurstoffe* **25**: 175–213.

Mechoulam, R., Lichtman AH (2003). Stout guards of the central nervous system. *Science (80-)* **302**: 65–67.

Mechoulam R, Ben-Shabat S, Hanus L, Ligumsky M, Kaminski NE, Schatz AR, *et al* (1995). Identification of an endogenous 2-monoglyceride, present in canine gut, that binds to cannabinoid receptors. *Biochem Pharmacol* **50**: 83–90.

Mechoulam R, Parker L a. (2011). The Endocannabinoid System and the Brain. *Annu Rev Psychol* **64**: 120717165617008.

Melck D, Bisogno T, Petrocellis L De, Chuang H, Julius D, Bifulco M, *et al* (1999). Unsaturated long-chain N-acyl-vanillyl-amides (N-AVAMs): vanilloid receptor ligands that inhibit anandamide-facilitated transport and bind to CB1 cannabinoid receptors. *Biochem Biophys Res Commun* **262**: 275–284.

Meltser I, Tahera Y, Simpson E, Hultcrantz M, Charitidi K, Gustafsson JA (2008). Estrogen receptor beta protects against acoustic trauma in mice. *J Clin Invest* **118**: 1563–1570.

Mestre L, Correa F, Ar??valo-Mart??n A, Molina-Holgado E, Valenti M, Ortar G, *et al* (2005). Pharmacological modulation of the endocannabinoid system in a viral model of multiple sclerosis. *J Neurochem* **92**: 1327–1339.

Meyer MJ, Megyesi J, Meythaler J, Murie-Fernandez M, Aubut J-A, Foley N, *et al* (2010). Acute management of acquired brain injury part II: An evidence-based review of pharmacological interventions. *Brain Inj* **24**: 706–721.

Mills B, Yepes A, Nugent K (2015). Synthetic cannabinoids. *Can Med Assoc J* **350**: 59–62.

Milner B (Academic Press: New York, 1970). *Memory and the medial temporal lobe regions of the brain*. *Biol Mem* .

Mitchnick KA, Creighton SD, Cloke JM, Wolter M, Zaika O, Christen B, *et al* (2016). Dissociable roles for histone acetyltransferases p300 and PCAF in hippocampus and perirhinal cortex-mediated object memory. *Genes, Brain Behav* **15**: 542–557.

Morad SA, Cabot MC (2013). Ceramide-orchestrated signalling in cancer cells. *Nat Rev Cancer* **13**: 51–65.

Morgan AJ, Kingsley PJ, Mitchener MM, Altemus M, Patrick TA, Gaulden AD, *et al* (2018). Detection of Cyclooxygenase-2-Derived Oxygenation Products of the Endogenous Cannabinoid 2-Arachidonoylglycerol in Mouse Brain. *ACS Chem Neurosci* **9**: 1552–1559.

Morris RGM (1981). Spatial localization does not require the presence of local cues. *Learn Motiv* **12**: 239–260.

Morris RGM (1984). Developments of a water-maze procedure for studying spatial learning in the rat. *J Neurosci Methods* **11**: 47–60.

Motley SE, Kirwan CB (2012). A Parametric Investigation of Pattern Separation Processes in the Medial Temporal Lobe. *J Neurosci* **32**: 13076–13084.

Mukherjee S, Zeitouni S, Cavarsan CF, Shapiro LA (2013). Increased seizure susceptibility in mice 30 days after fluid percussion injury. *Front Neurol* **4**: 1–11.

Mukhopadhyay P, Pan H, Rajesh M, Bátkai S, Patel V, Harvey-White J, *et al* (2010a). CB 1 cannabinoid receptors promote oxidative/nitrosative stress, inflammation and cell death in a murine nephropathy model. *Br J Pharmacol* **160**: 657–668.

Mukhopadhyay P, Rajesh M, B??tkai S, Patel V, Kashiwaya Y, Liaudet L, *et al* (2010b). CB1 cannabinoid receptors promote oxidative stress and cell death in murine models of doxorubicin-induced cardiomyopathy and in human cardiomyocytes. *Cardiovasc Res* **85**: 773–784.

Mumby DG, Cameli L, Glenn MJ (1999). Impaired allocentric spatial working memory and intact retrograde memory after thalamic damage caused by thiamine deficiency in rats. *Behav Neurosci* **113**: 42–50.

Munro S, Thomas KL, Abu-Shaar M (1993). Molecular characterization of a peripheral receptor for cannabinoids. *Nature* **365**: 61–65.

Murray CA, Lynch MA (1998). Evidence that increased hippocampal expression of the cytokine interleukin-1 beta is a common trigger for age- and stress-induced impairments in long-term potentiation. *J Neurosci* **18**: 2974–2981.

Naito M, Takahashi K, Nishikawa S (1990). Development, differentiatio, and maturation of macrophages in the fetal mouse liver. *J Leukoc Biol* **48**: 27–37.

Nakane S, Oka S, Arai S, Waku K, Ishima Y, Tokumura A, *et al* (2002). 2-Arachidonoyl-sn-glycero-3-phosphate, an arachidonic acid-containing lysophosphatidic acid:

occurrence and rapid enzymatic conversion to 2-arachidonoyl-sn-glycerol, a cannabinoid receptor ligand, in rat brain. *Arch Biochem Biophys* **402**: 51–58.

Nakashiba T, Young JZ, McHugh TJ, Buhl DL, Tonegawa S (2008). Transgenic inhibition of synaptic transmission reveals role of CA3 output in hippocampal learning. *Science* **319**: 1260–1264.

Nanry KP, Mundy WR, Tilson HA (1989). Colchicine-induced alterations of reference memory in rats: role of spatial versus non-spatial task components. *Behav Brain Res* **35**: 45–53.

Narayan RK, Michel ME, Ansell B, Baethmann A, Biegon A, Bracken MB, *et al* (2002). Clinical trials in head injury. *J Neurotrauma* **19**: 503–557.

Neese SL, Clough RW, Banz WJ, Smith DC (2010). Bisdehydrodoisynolic acid (Z-BDDA): an estrogenic seco-steroid that enhances behavioral recovery following moderate fluid percussion brain injury in male rats. *Brain Res* **1362**: 93–101.

Nguyen BM, Kim D, Bricker S, Bongard F, Neville A, Putnam B, *et al* (2014a). Effect of marijuana use on outcomes in traumatic brain injury. *Am Surg* **80**: 979–983.

Nguyen BM, Kim D, Bricker S, Bongard F, Neville A, Putnam B, *et al* (2014b). Effect of marijuana use on outcomes in traumatic brain injury. *Am Coll Surg* **80**: 979–983.

Nicolls MR, Laubach VE (2014). Traumatic brain injury: lungs in a RAGE. *Sci Transl Med* **6**: 252fs234.

Nilsson P, Hillered L, Ponten U, Ungerstedt D (1990). Changes in cortical extracellular levels of energy-related metabolites and amino acids following concussive brain injury in rats. *Jounal Cereb Blood Flow Metab* **10**: 631–637.

Niogi SN, Mukherjee P, Ghajar J, Johnson C, Kolster RA, Sarkar R, *et al* (2008). Extent

of microstructural white matter injury in postconcussive syndrome correlates with impaired cognitive reaction time: A 3T diffusion tensor imaging study of mild traumatic brain injury. *Am J Neuroradiol* **29**: 967–973.

Niphakis MJ, Johnson DS, Ballard TE, Stiff C, Cravatt BF (2012). *O* -Hydroxyacetamide Carbamates as a Highly Potent and Selective Class of Endocannabinoid Hydrolase Inhibitors. *ACS Chem Neurosci* **3**: 418–426.

Noda M, Kariura Y, Pannasch U, Nishikawa K, Wang L, Seike T, *et al* (2007). Neuroprotective role of bradykinin because of the attenuation of pro-inflammatory cytokine release from activated microglia. *J Neurochem* **101**: 397–410.

Nomura DK, Hudak CSS, Ward AM, Burston JJ, Issa RS, Fisher KJ, *et al* (2008). Monoacylglycerol lipase regulates 2-arachidonoylglycerol action and arachidonic acid levels. *Bioorganic Med Chem Lett* **18**: 5875–5878.

Nomura DK, Morrison BE, Blankman JL, Jonathan Z, Kinsey SG, Marcondes MCG, *et al* (2011). Endocannabinoid hydrolysis generates brain prostaglandins that promote neuroinflammation. *Science (80-)* **334**: 809–813.

Novgorodov SA, Voltin JR, Gooz MA, Li L, Lemasters JJ, Gudz TI (2018). Acid sphingomyelinase promotes mitochondrial dysfunction due to glutamate-induced regulated necrosis. *J Lipid Res* **59**: 312–329.

Oddo M, Nduom E, Frangos S, MacKenzie L, Chen I, Maloney-Wilensky E, *et al* (2010). Acute lung injury is an independent risk factor for brain hypoxia after severe traumatic brain injury. *Neurosurgery* **67**: 338–344.

Oddy M, Coughlan T, Tyerman A, Jenkins D (1985). Social adjustment after closed head injury: A further follow-up seven years after injury. *J Neurol Neurosurg*

Psychiatry **48**: 564–568.

Ogasawara D, Deng H, Viader A, Baggelaar MP, Breman A, Dulk H den, *et al* (2016). Rapid and profound rewiring of brain lipid signaling networks by acute diacylglycerol lipase inhibition. *Proc Natl Acad Sci U S A* **113**: 26–33.

Ohno-Shosaku T, Kano M (2014). Endocannabinoid-mediated retrograde modulation of synaptic transmission. *Curr Opin Neurobiol* **29**: 1–8.

Ohta A, Sitkovsky M (2001). Role of G-protein-coupled adenosine receptors in downregulation of inflammation and protection from tissue damage. *Nature* **414**: 916–920.

Oka S, Wakui J, Ikeda S, Yanagimoto S, Kishimoto S, Gokoh M, *et al* (2006). Involvement of the cannabinoid CB2 receptor and its endogenous ligand 2-arachidonoylglycerol in oxazolone-induced contact dermatitis in mice. *J Immunol* **177**: 8796–805.

Okada, M., Urae, A., Mine, K., Shoyama, Y., Iwasaki, K., Fujiwara M (1992). The facilitating and suppressing effects of delta 9-tetrahydrocannabinol on the rise in intrasynaptosomal Ca2+ concentration in rats. *Neurosci Lett* **140**: 55–58.

Okazaki T, Sagawa N, Okita J, Bleasdale J, MacDonald P, Johnston J (1981). Diacylglycerol metabolism and arachidonic acid release in human fetal membranes and decidua vera. *J Biol Chem* **256**: 7316–7321.

Oudin M, Hobbs C, Doherty P (2011). DAGL-dependent endocannabinoid signalling: roles in axonal pathfinding, synaptic plasticity and adult neurogenesis. *Eur J Neurosci* **34**: 1634–1646.

Pan B, Wang W, Long J, Sun D, Hillard CJ, Cravatt BF, *et al* (2009). Blockade of 2-

arachidonoylglycerol hydrolysis by selective monoacylglycerol lipase inhibitor 4-nitrophenyl 4-(dibenzo[d][1,3]dioxol-5-yl(hydroxy)methyl)piperidine-1-carboxylate (JZL184) Enhances retrograde endocannabinoid signaling. *J Pharmacol Exp Ther* **331**: 591–597.

Pan B, Wang W, Zhong P, Blankman JL, Cravatt BF, Liu QS (2011). Alterations of endocannabinoid signaling, synaptic plasticity, learning, and memory in monoacylglycerol lipase knock-out mice. *J Neurosci* **31**: 13420–13430.

Panikashvili D, Mechoulam R, Beni SM, Alexandrovich A, Shohami E (2005). CB1 cannabinoid receptors are involved in neuroprotection via NF-kappa B inhibition. *J Cereb Blood Flow Metab* **25**: 477–484.

Panikashvili D, Shein NA, Mechoulam R, Trembovler V, Kohen R, Alexandrovich A, *et al* (2006). The endocannabinoid 2-AG protects the blood-brain barrier after closed head injury and inhibits mRNA expression of proinflammatory cytokines. *Neurobiol Dis* **22**: 257–264.

Panikashvili D, Simeonidou C, Ben-Shabat S, Hanus L, Breuer a, Mechoulam R, *et al* (2001). An endogenous cannabinoid (2-AG) is neuroprotective after brain injury. *Nature* **413**: 527–531.

Pascual JL, Murcy MA, Li S, Gong W, Eisenstadt R, Kumasaka K, *et al* (2013). Neuroprotective effects of progesterone in traumatic brain injury: blunted in vivo neutrophil activation at the blood-brain barrier. *Am J Surg* **206**: 840–845.

Pelosi P, Severgnini P, Chiaranda M (2005). An integrated approach to prevent and treat respiratory failure in brain-injured patients. *Curr Opin Crit Care* **11**: 37–42.

Perez M, Benitez SU, Cartarozzi LP, Bel E del, Guimarães FS, Oliveira ALR (2013).

Neuroprotection and reduction of glial reaction by cannabidiol treatment after sciatic nerve transection in neonatal rats. *Eur J Neurosci* **38**: 3424–3434.

Perry VH, Hume DA, Gordon S (1985). Immunohistochemical localization of macrophages and microglia in the adult and developing mouse brain. *Neuroscience* **15**: 313–326.

Pertwee RG, Ross RA (2002). Cannabinoid receptors and their ligands. *Prostaglandins Leukot Essent Fat Acids* **66**: 101–121.

Ping X, Jin X (2016). Chronic posttraumatic epilepsy following neocortical undercut lesion in mice. *PLoS One* **11**: 1–12.

Piomelli D (R.G. Landes Company: Georgetown, Texas, 1996). *Arachidonic acid in cell signaling*. .

Piyanova A, Lomazzo E, Bindila L, Lerner R, Albayram O, Ruhl T, *et al* (2015). Age-related changes in the endocannabinoid system in the mouse hippocampus. *Mech Ageing Dev* **150**: 55–64.

Plassman BL, Havlik RJ, Steffens DC, Helms MJ, Newman TN, Drosdick D, *et al* (2000). Documented head injury in early adulthood and risk of Alzheimer's disease and other dementias. *Neurology* **55**: 1158–1166.

Ponomarev ED, Maresz K, Tan Y, Dittel BN (2007). CNS-derived interleukin-4 is essential for the regulation of autoimmune inflammation and induces a state of alternative activation in microglial cells. *J Neurosci* **27**: 10714–10721.

Porter, A. C., Sauer, J. M., Knierman, M. D., Becker, G. W., Berna, M. J., Bao, J., Nomikos, G. G., Carter P., Bymaster, F. P., Baker Leese, A., Felder CC (2002). Characterization of a Novel Endocannabinoid, Virodhamine, with Antagonist

Activity at the CB1 Receptor. *J Pharmacol Exp Ther* **301**: 1020–1024.

Powell DR, Gay JP, Wilganowski N, Doree D, Savelieva K V., Lanthorn TH, *et al* (2015). Diacylglycerol Lipase α Knockout Mice Demonstrate Metabolic and Behavioral Phenotypes Similar to Those of Cannabinoid Receptor 1 Knockout Mice. *Front Endocrinol (Lausanne)* **6**: eCollection.

Radin NS (2004). Poly-drug cancer therapy based on ceramide. *Eksp Onkol* **26**: 3–10.

Raghupathi R (2004). Cell death mechanisms following traumatic brain injury. *Brain Pathol* **14**: 215–222.

Ramlackhansingh AF, Brooks DJ, Greenwood RJ, Bose SK, Turkheimer FE, Kinnunen KM, *et al* (2011). Inflammation after trauma: microglial activation and traumatic brain injury. *Annu Neurol* **70**: 374–383.

Reeves TM, Trimmer PA, Colley BS, Phillips LL (2016). Targeting Kv1 . 3 channels to reduce white matter pathology after traumatic brain injury. *Exp Neurol* **283**: 188–203.

Reggio PH (2002). Endocannabinoid structure-activity relationships for interaction at the cannabinoid receptors. *Prostaglandins Leukot Essent Fatty Acids* **66**: 143–160.

Reilly PL (2001). Brain injury: the pathophysiology of the first hours.'Talk and Die revisited'. *J Clin Neurosci* **8**: 398–403.

Reisenberg M, Singh PK, Williams G, Doherty P (2012). The diacylglycerol lipases: structure, regulation and roles in and beyond endocannabinoid signalling. *Philos Trans R Soc Lond B Biol Sci* **367**: 3264–3275.

Ribeiro R, Wen J, Li S, Zhang Y (2013). Involvement of ERK1/2, cPLA2 and NF-κB in microglia suppression by cannabinoid receptor agonists and antagonists.

Prostaglandins Other Lipid Mediat **100**: 1–14.

Ribot TH (Kegan Paul, Trench and Co.: London, 1882). *Diseases of memory.* .

Ricciotti E, FitzGerald GA (2011). Prostaglandins and inflammation. *Arterioscler Thromb Vasc Biol* **31**: 986–1000.

Río-Hortega P Del (Paul B. Hoeber, New York: 1932). *Cytology and cellular pathology of the nervous system.* .

Rocchetta AI della (1986). Classification and recall of pictures after unilateral frontal or temporal lobectomy. *Cortex* **22**: 189–211.

Rochefort C, Lefort JM, Rondi-Reig L (2013). The cerebellum: a new key structure in the navigation system. *Front Neural Circuits* **7**: 35.

Rossi S, Studer V, Motta C, Chiara V De, Barbieri F, Bernardi G, *et al* (2012). Inflammation inhibits GABA transmission in multiple sclerosis. *Mult Scler J* **18**: 1633–1635.

Roux A, Muller L, Jackson SN, Post J, Baldwin K, Hoffer B, *et al* (2016). Mass spectrometry imaging of rat brain lipid profile changes over time following traumatic brain injury. *J Neurosci Methods* **272**: 19–32.

Rubovitch V, Ten-Bosch M, Zohar O, Harrison CR, Tempel-Brami C, Stein E, *et al* (2011). A mouse model of blast-induced mild traumatic brain injury. *Exp Neurol* **232**: 280–289.

Rudy JW (Sinauer Associates, Inc.: Sunderland, MA, 2014). *The neurobiology of learning and memory*. .

Ryberg E, Larsson N, Sjögren S, Hjorth S, Hermansson N-O, Leonova J, *et al* (2007). The orphan receptor GPR55 is a novel cannabinoid receptor. *Br J Pharmacol* **152**:

1092–101.

Saab BJ, Georgiou J, Nath A, Lee FJ, Wang M, Michalon A, *et al* (2009). NCS-1 in the dentate gyrus promotes exploration, synaptic plasticity, and rapid acquisition of spatial memory. *Neuron* **63**: 643–656.

Sahay A, Scobie K, Hill A, O'Carroll C, Kheirbek M, Burghardt N, *et al* (2011). Increasing adult hippocampal neurogenesis is sufficient to improve pattern separation. *Nature* **472**: 466–470.

Sahuquillo J, Arikan F (2006). Decompressive craniectomy for the treatment of refractory high intracranial pressure in traumatic brain injury. *Cochrane database Syst Rev* CD003983doi:10.1002/14651858.CD003983.pub2.

Sang N, Zhang J, Chen C (2007). COX-2 oxidative metabolite of endocannabinoid 2-AG enhances excitatory glutamatergic synaptic transmission and induces neurotoxicity. *Jounal Neurochem* **102**: 1966–1977.

Sarne Y, Asaf F, Fishbein M, Gafni M, Keren O (2011). The dual neuroprotective-neurotoxic profile of cannabinoid drugs. *Br J Pharmacol* **163**: 1391–1401.

Schaible E V., Windschugl J, Bobkiewicz W, Kaburov Y, Dangel L, Kramer T, *et al* (2014). 2-Methoxyestradiol confers neuroprotection and inhibits a maladaptive HIF-1α response after traumatic brain injury in mice. *J Neurochem* **129**: 940–954.

Schmitt U, Tanimoto N, Seeliger M, Schaeffel F, Leube RE (2009). Detection of behavioral alterations and learning deficits in mice lacking synaptophysin. *Neuroscience* **162**: 234–243.

Schmitter-Edgecombe M, Nissley HM (2000). Effects of divided attention on automatic and controlled components of memory after severe closed-head injury.

Neuropsychology **14**: 559–569.

Schöpke R, Wolfer DP, Lipp HP, Leisinger-Trigona MC (1991). Swimming navigation and structural variations of the infrapyramidal mossy fibers in the hippocampus of the mouse. *Hippocampus* **1**: 315–328.

Schurman LD, Smith TL, Morales AJ, Lee NN, Reeves TM, Phillips LL, *et al* (2017). Investigation of left and right lateral fluid percussion injury in C57BL6/J mice: in vivo functional consequences. *Neurosci Lett* **653**: 31–38.

Scoville WB, Milner B (1957). Loss of recent memory after bilateral hippocampal lesions. *J Neurol Neurosurg Psychiatry* **20**: 11–12.

Sen AP, Gulati A (2010). Use of Magnesium in Traumatic Brain Injury. *Neurotherapeutics* **7**: 91–99.

Shah S, Yallampalli R, Merkley TL, McCauley SR, Bigler ED, Macleod M, *et al* (2012). Diffusion tensor imaging and volumetric analysis of the ventral striatum in adults with traumatic brain injury. *Brain Inj* **26**: 201–10.

Shang JL, Cheng Q, Yang WF, Zhang M, Cui Y, Wang YF (2014). Possible roles of COX-1 in learning and memory impairment induced by traumatic brain injuryn in mice. *Brazilion J Med Biol Res* **47**: 1050–1056.

Shiina G, Onuma T, Kameyama M, Shimosegawa Y, Ishii K, Shirane R, *et al* (1998). Sequential assessment of cerebral blood flow in diffuse brain injury by 123I-iodoamphetamine single-photon emission CT. *Am J Neuroradiol* **19**: 297–302.

Shinohara Y, Hirase H (2009). Size and Receptor Density of Glutamatergic Synapses: A Viewpoint from Left-Right Asymmetry of CA3-CA1 Connections. *Front Neuroanat* **3**: 10.

Shinohara Y, Hirase H, Watanabe M, Itakura M, Takahashi M, Shigemoto R (2008). Left-right asymmetry of the hippocampal synapses with differential subunit allocation of glutamate receptors. *Proc Natl Acad Sci U S A* **105**: 19498–19503.

Shinohara Y, Hosoya A, Yamasaki N, Ahmed H, Hattori S, Eguchi M, *et al* (2012). Right-hemispheric dominance of spatial memory in split-brain mice. *Hippocampus* **22**: 117–121.

Shipton O, El-Gaby M, Apergis-Schoute J, Karl D, Bannerman DM, Paulsen O, *et al* (2014). Left-right dissociation of hippocampal memory processes in mice. *Proc Natl Acad Sci U S A* **111**: 15238–15243.

Shitaka Y, Tran HT, Bennett RE, Sanchez L, Levy MA, Dikranian K, *et al* (2012). Repetitive closed-skull traumatic brain injury in mice causes persistent multifocal axonal injury and microglial reactivity. *J Neuropathol Exp Neurol* **70**: 551–567.

Shohami E, Novikov M, Bass R (1995). Long-Term Effect of Hu-211, a Novel Noncompetitive Nmda Antagonist, on Motor and Memory Functions after Closed-Head Injury in the Rat. *Brain Res* **674**: 55–62.

Shonesy BC, Bluett RJ, Ramikie T, Baldi R, Hermanson DJ, Kingsley PJ, *et al* (2014). Genetic disruption of 2-arachidonoylglycerol synthesis reveals a key role for endocannbinoid signaling in anxiety modulation. *Cell Rep* **9**: 1644–1653.

Shonesy BC, Parrish WP, Haddad HK, Stephenson JR, Baldi R, Bluett RJ, *et al* (2018). Role of striatal direct pathway 2-arachidonoylglycerol signaling in sociability and repetitive behavior. *Biol Psychiatry* **84**: 304–315.

Sica A, Mantovani A (2012). Macrophage plasticity and polarization: in vivo veritas. *J Clin Investig* **122**: 787–795.

Siegel GJ (Lippincott-Raven: Philadelphia, 1999). *Basic Neurochemistry*. .

Sieger D, Moritz C, Ziegenhals T, Prykhozhij S, Peri F (2012). Long range Ca2+ waves transmit brain-damage signals to microglia. *Dev Cell* **22**: 1138–1148.

Sigel E, Baur R, Rácz I, Marazzi J, Smart TG, Zimmer A, *et al* (2011). The major central endocannabinoid directly acts at GABA(A) receptors. *Proc Natl Acad Sci U S A* **108**: 18150–5.

Silva-Cruz A, Carlstrom M, Ribeiro JA, Sebastiao AM (2017). Dual influence of endocannabinoids on long-term potentiation of synaptic transmission. *Front Pharmacol* **8**: .

Singh IN, Sullivan PG, Deng Y, Mbye LH, Hall ED (2006). Time course of post-traumatic mitochondrial oxidative damage and dysfunction in a mouse model of focal traumatic brain injury: implications for neuroprotective therapy. *J Cereb Blood Flow Metab Metab* **26**: 1407–1418.

Siopi E, Llufriu-Daben G, Fanucchi F, Poltkine M, Marchand-Leroux C, Jafarian-Tehrani M (2012). Evaluation of late cognitive impairment and anxiety states following traumatic brain injury in mice: the effect of minocycline. *Neurosci Lett* **511**: 110–115.

Skolnick BE, Maas AI, Narayan RK, Hoop RG van der, MacAllister T, Ward JD, *et al* (2014). A clinical trial of progesterone for severe traumatic brain injury. *N Engl J Med* **371**: 2467–2476.

Smart D, Gunthorpe MJ, Jerman JC, Nasir S, Gray J, Muir AI, *et al* (2000). The endogenous lipid anandamide is a full agonist at the human vanilloid receptor (hVR1). *Br J Pharmacol* **129**: 227–30.

Smith, D.H., Chen, X., Nonaka, M., Trojanowski, J.Q., Lee, V.M., Saatman, K.E., Leoni, M.J., Xu, B.N., Wolf, J.A., Meaney DF (1999). Accumulation of amyloid β and tau and the formation of neurofilament inclusions following diffuse brain injury in the pig. *J Neuropathol Exp Neurol* **58**: 982–992.

Snyder J, Hong N, McDonald R, Wojtowicz J (2005). A role for adult neurogenesis in spatial long-term memory. *Neuroscience* **130**: 843–852.

Sorrells SF, Paredes MF, Cebrian-Silla A, Sandoval K, Qi D, Kelley KW, *et al* (2018). Human hippocampal neurogenesis drops sharply in children to undetectable levels in adults. *Nature* **555**: 377–381.

Spain A, Daumas S, Lifshitz J, Rhodes J, Andrews PJD, Horsburgh K, *et al* (2010). Mild fluid percussion injury in mice produces evolving selective axonal pathology and cognitive deficits relevant to human brain injury. *J Neurotrauma* **27**: 1429–1438.

Stablum F, Leonardi G, Mazzoldi M, Umilta C, Morra S (1994). Attention and control deficits following closed head injury. *Cortex* **30**: 603–618.

Staiano RI, Loffredo S, Borriello F, Iannotti FA, Piscitelli F, Orlando P, *et al* (2015). Human lung-resident macrophages express CB1 and CB2 receptors whose activation inhibits the release of angiogenic and lymphangiogenic factors. *J Leukoc Biol* **99**: jlb.3HI1214-584R-.

Stéfan A, Mathé JF, Dhenain M, Blanchard P, Blondet E, Mathé JF, *et al* (2016). What are the disruptive symptoms of behavioral disorders after traumatic brain injury? A systematic review leading to recommendations for good practices. *Ann Phys Rehabil Med* **59**: 5–17.

Stein SC, Georgoff P, Meghan S, Mizra K, Sonnad SS (2010). 150 Years of Treating

Severe Traumatic Brain Injury: a Systematic Review of Progress in Mortality. *J Neurotrauma* **27**: 1343–53.

Stellwagen D, Beattie EC, Seo JY, Malenka RC (2005). Differential regulation of AMPA receptor and GABA receptor trafficking by tumor necrosis factor-alpha. *J Neurosci* **25**: 3219–3228.

Stence N, Waite M, Dailey ME (2001). Dynamics of microglial activation: a confocal time-lapse analysis in hippocampal slices. *Glia* **33**: 256–266.

Sticht MA, Limebeer CL, Rafla BR, Abdullah RA, Poklis JL, Ho W, *et al* (2016). Endocannabinoid regulation of nausea is mediated by 2-arachidonoylglycerol (2-AG) in the rat visceral insular cortex. *Neuropharmacology* **102**: 92–102.

Stiver SI (2009). Complications of decompressive craniectomy for traumatic brain injury. *Neurosurg Focus* **26**: E7.

Straiker A, Wager-Miller J, Hu SS, Blankman JL, Cravatt BF, Mackie K (2011). COX-2 and fatty acid amide hydrolase can regulate the time course of depolarization-induced suppression of excitation. *Br J Pharmacol* **164**: 1672–1683.

Stranahan A (2011). Similarities and differences in spatial learning and object recognition between young male C57Bl/6J mice and Sprague-Dawley rats. *Behav Neurosci* **125**: 791–795.

Sugaya Y, Cagniard B, Yamazaki M, Sakimura K, Kano M (2013). The endocannabinoid 2-arachidonoylglycerol negatively regulates habituation by suppressing excitatory recurrent network activity and reducing long-term potentiation in the dentate gyrus. *J Neurosci* **33**: 3588–3601.

Sugaya Y, Yamazaki M, Uchigashima M, Kobayashi K, Watanabe M, Sakimura K, *et al*

(2016). Crucial roles of the endocannabinoid 2-arachidonoylglycerol in the suppression of epileptic seizures. *Cell Rep* **16**: 1405–1415.

Sugiura T, Kondo S, Sukagawa A, Nakane S, Shinoda A, Itoh K, *et al* (1995). 2-Arachidonoylglycerol: a possible endogenous cannabinoid receptor ligand in brain. *Biochem Biophys Res Commun* **215**: 89–97.

Surgeons. BTFAA of NSC of N (2007). Guidelines for the Management of Severe Traumatic Brain Injury 3rd Edition. *J Neurosurg* **24**, **Suppl**: S1-106.

Tanimura A, Uchigashima M, Yamazaki M, Uesaka N, Mikuni T, Abe M, *et al* (2012). Synapse type-independent degradation of the endocannabinoid 2-arachidonoylglycerol after retrograde synaptic suppression. *Proc Natl Acad Sci U S A* **109**: 12195–12200.

Tanimura A, Yamazaki M, Hashimotodani Y, Uchigashima M, Kawata S, Abe M, *et al* (2010). The endocannabinoid 2-arachidonoylglycerol produced by diacylglycerol lipase alpha mediates retrograde suppression of synaptic transmission. *Neuron* **65**: 320–327.

Tapia-Perez JH, Sanchez-Aguilar M, Torres-Corzo JG, Gordillo-Moscoso A, Martinez-Perez P, Madeville P, *et al* (2008). Effect of rosuvastatin on amnesia and disorientation after traumatic brain injury (NCT003229758). *J Neurotrauma* **25**: 1011–7.

Tchantchou F, Tucker LB, Fu AH, Bluett RJ, McCabe JT, Patel S, *et al* (2014). The fatty acid amide hydrolase inhibitor PF-3845 promotes neuronal survival, attenuates inflammation and improves functional recovery in mice with traumatic brain injury. *Neuropharmacology* **85**: 427–439.

Tchantchou F, Zhang Y (2013). Selective inhibition of alpha/beta-hydrolase domain 6 attenuates neurodegeneration, alleviates blood brain barrier breakdown, and improves functional recovery in a mouse model of traumatic brain injury. *J Neurotrauma* **30**: 565–79.

Temkin NR, Anderson GD, Winn HR, Ellenbogen RG, Britz GW, Schuster J, *et al* (2007). Magnesium sulfate for neuroprotection after traumatic brain injury: a randomised controlled trial. *Lancet Neurol* **6**: 29–38.

Teyler TJ, DiScenna P (1986). The hippocampal memory indexing theory. *Behav Neurosci* **100**: 147–152.

Teyler TJ, Rudy JW (2007). The hippocampus indexing theory of episodic memory: updating the index. *Hippocampus* **17**: 1158–1169.

Thompson HJ, McCormick WC, Kagan SH (2006). Traumatic brain injury in older adults: epidemiology, outcomes, and future implications. *J Am Geriatr Soc* **54**: 1590–1595.

Tilley SL, Coffman TM, Koller BH (2001). Mixed messages: modulation of inflammation and immune responses by protaglandins and thromboxanes. *J Clin Invest* **108**: 15–23.

Titomanlio L, Fern??ndez-L??pez D, Manganozzi L, Moretti R, Vexler ZS, Gressens P (2015). Pathophysiology and neuroprotection of global and focal perinatal brain injury: Lessons from animal models. *Pediatr Neurol* **52**: 566–584.

Tolon RM, Nunez E, Pazos MR, Benito C, Castillo AI, Martinez-Orgado JA, *et al* (2009). The activation of cannabinoid CB2 receptors stimulates in situ and in vitro beta-amyloid removal by human macrophages. *Brain Res* **1283**: 148–154.

Townend J (John Wiley & Sons Ltd: Chichester, West Sussex, England, 2013).

Practical Statistics for Environmental and Biological Scientists. .

Tsenter J, Beni-Adani L, Assaf Y, Alexandrovich AG, Trembovler V, Shohami E (2008). Dynamic changes in the recovery after traumatic brain injury in mice: effect of injury severity on T2-weighted MRI abnormalities, and motor and cognitive functions. *J Neurotrauma* **25**: 324–333.

Tucker LB, Burke JF, Fu AH, McCabe JT (2016). Neuropsychiatric Symptom Modeling in Male and Female C57BL/6J Mice after Experimental Traumatic Brain Injury. *J Neurotrauma* **16**: neu.2016.4508.

Umeano O, Wang H, Dawson H, Lei B, Umeano A, Kernagis D, *et al* (2017). Female gonadal hormone effects on microglia activation and functional outcomes in a mouse model of moderate traumatic brain injury. *World J Crit Care Med* **6**: 107–115.

Vakil E (2005). The effect of moderate to severe traumatic brain injury (TBI) on different aspects of memory: a selective review. *J Clin Exp Neuropsychol* **27**: 977–1021.

Van KC, Lyeth BG (2016). Lateral (Parasagittal) Fluid Percussion Model of Traumatic Brain Injury. *Methods Mol Biol* **1462**: 231–251.

Varga R, Wagner JA, Bridgen DT, Kunos G (1998). Platelet- and macrophage-derived endogenous cannabinoids are involved in endotoxin-induced hypotension. *FASEB* **12**: 1035–1044.

Varvel SA, Anum EA, Lichtman AH (2005). Disruption of CB(1) receptor signaling impairs extinction of spatial memory in mice. *Psychopharmacology (Berl)* **179**: 863–872.

Varvel SA, Lichtman AH (2002). Evaluation of CB1 receptor knockout mice in the Morris

water maze. *J Pharmacol Exp Ther* **301**: 915–924.

Varvel SA, Wise LE, Niyuhire F, Cravatt BF, Lichtman AH (2007). Inhibition of fatty-acid amide hydrolase accelerates acquisition and extinction rates in a spatial memory task. *Neuropsychopharmacology* **23**: 1032–1041.

Viader A, Ogasawara D, Joslyn C, Sanchez-Alavez M, Mori S, Nguyen W, *et al* (2015a). A chemical proteomic atlas of brain serine hydrolases identifies cell type-specific pathways regulating neuroinflammation. *Elife* **5**: 1–24.

Viader A, Ogasawara D, Joslyn C, Sanchez-Alavez M, Mori S, Nguyen W, *et al* (2015b). A chemical proteomic atlas of brain serine hydrolases identifies cell type-specific pathways regulating neuroinflammation. *Elife* **5**: e12345.

Villapol S, Loane DJ, Burns MP (2017). Sexual dimorphism in the inflammatory response to traumatic brain injury. *Glia* **65**: 1423–1438.

Vink R, Mullins PG, Temple MD, Bao W, Faden AI (2001). Small shifts in craniotomy position in the lateral fluid percussion injury model are associated with differential lesion development. *J Neurotrauma* **18**: 839–847.

Viviani B, Bartesaghi S, Gardoni F, Vezzani A, Behrens MM, Bartfai T, *et al* (2003). Interleukin-1beta enhances NMDA receptor-mediated intracellular calcium increase through activation of the Src family of kinases. *J Neurosci* **23**: 8692–8700.

Vorhees C V, Williams MT (2006). Morris water maze: procedures for assessing spatial and related forms of learning and memory. *Nat Protoc* **1**: 848–858.

Wagner AK, Brayer SW, Hurwitz M, Niyonkuru C, Zou H, Failla M, *et al* (2013). Non-spatial pre-training in the water maze as a clinically relevant model for evaluating learning and memory in experimental TBI. *Neurobiol Learn Mem* **106**: .

Waite JJ, Chen AD, Wardlow ML, Thal LJ (1994). Behavioral and biochemical consequences of combined lesions of the medial septum/diagonal band and nucleus basalis in the rat when ibotenic acid, quisqualic acid, and AMPA are used. *Exp Neurol* **130**: 214–229.

Walker WC, Pickett TC (2007). Motor impairment after severe traumatic brain injury: A longitudinal multicenter study. *J Rehabil Res Dev* **44**: 975–82.

Wallace MJ, Wiley JL, Martin BR, DeLorenzo RJ (2001). Assessment of the role of CB1 receptors in cannabinoid anticonvulsant effects. *Eur J Pharmacol* **428**: 51–57.

Walter L, Franklin A, Witting A, Wade C, Xie Y, Kunos G, *et al* (2003). Non-psychotropic cannabinoid receptors regulate microglial cell migration. *J Neurosci* **23**: 1398–1405.

Wang K, Liu BY, Ma J (2014). Research progress in traumatic brain penumbra. *Chin Med J (Engl)* **127**: 1964–1968.

Wang Q, Peng Y, Chen S, Gou X, Hu B, Du J, *et al* (2009). Pretreatment With Electroacupuncture Induces Rapid Tolerance to Focal Cerebral Ischemia Through Regulation of Endocannabinoid System. *Stroke* **40**: 2157–2164.

Wang X, Wang Y, Zhang C, Liu C, Zhao B, Wei N, *et al* (2016). CB1 receptor antagonism prevents long-term hyperexcitability after head injury by regulation of dynorphin-KOR system and mGluR5 in rat hippocampus. *Brain Res* **1646**: 174–181.

Whishaw IQ, Mittleman G, Bunch ST, Dunnett SB (1987). Impairments in the acquisition, retention and selection of spatial navigation strategies after medial caudate-putamen lesions in rats. *Behav Brain Res* **24**: 125–138.

Wiley JL, Marusich JA, Huffman JW (2014). Moving around the molecule: Relationship

between chemical structure and in vivo activity of synthetic cannabinoids. *Life Sci* **97**: 55–63.

Wilkerson JL, Donvito G, Grim TW, Abdullah RA, Ogasawara D, Cravatt BF, *et al* (2017). Investigation of Diacylglycerol Lipase Alpha Inhibition in the Mouse Lipopolysaccharide Inflammatory Pain Model. *J Pharmacol Exp Ther* **363**: 394–401.

Wilkerson JL, Ghosh S, Bagdas D, Mason BL, Crowe MS, Hsu KL, *et al* (2016). Diacylglycerol lipase β inhibition reverses nociceptive behaviour in mouse models of inflammatory and neuropathic pain. *Br J Pharmacol* **173**: 1678–1692.

Williams EJ, Walsh F, Doherty P (1994). The production of arachidonic acid can account for calcium channel activation in the second messenger pathway underlying neurite outgrowth stimulated by NCAM, N-cadherin, and L1. *J Neurochem* **62**: 1231–1234.

Williams EJ, Walsh FS, Doherty P (2003). The FGF receptor uses the endocannabinoid signaling system to couple to an axonal growth response. *J Cell Biol* **160**: 481–486.

Wirz L, Reuter M, Felten A, Schwabe L (2017). A haplotype associated with enhanced mineralocorticoid receptor expression facilitates the stress-induced shift from “cognitive” to “habit” learning. *eNeuro* **4**: 1–16.

Woodcock T, Morganti-Kossmann MC (2013). The role of markers of inflammation in traumatic brain injury. *Front Neurol* **4**: 1–18.

Wright DW, Yeatts SD, Silbergleit R, Palesch YY, Hertzberg VS, Frankel M, *et al* (2014). Very early administration of progesterone for acute traumatic brain injury. *N Engl J Med* **371**: 2457–2466.

Wu Y, Kawakami R, Shinohara Y, Fukaya M, Sakimura K, Mishina M, *et al* (2005). Target-cell-specific left-right asymmetry of NMDA receptor content in schaffer collateral synapses in epsilon1/NR2A knock-out mice. *J Neurosci* **25**: 9213–9226.

Xie WL, Chipman JG, Robertson DL, Erikson RL, Simmons DL (1991). Expression of a mitogen-responsive gene encoding prostaglandin synthase is regulated by mRNA splicing. *Proc Natl Acad Sci U S A* **88**: 2692–2696.

Xu J-Y, Zhang J, Chen C (2012). Long-lasting potentiation of hippocampal synaptic transmission by direct cortical input is mediated via endocannabinoids. *J Physiol* **590**: 2305–2315.

Yoshida T, Fukaya M, Uchigashima M, Miura E, Kamiya H, Kano M, *et al* (2006). Localization of diacyglycerol lipase-alpha around postsynaptic spine suggests close proximity between production site of an endocannabinoid, 2-arachidonoyl-glycerol, and presynaptic cannabinoid CB1 receptor. *J Neurosci* **26**: 4740–4751.

Yoshida T, Uchigashima M, Yamasaki M, Katona I, Yamazaki M, Sakimura K, *et al* (2011). Unique inhibitory synapse with particularly rich endocannabinoid signaling machinery on pyramidal neurons in basal amygdaloid nucleus. *Proc Natl Acad Sci U S A* **108**: 3059–3064.

Yoshino H, Miyamae T, Hansen G, Zambrowicz B, Flynn M, Pedicord D, *et al* (2011). Post-synaptic diacylglycerol lipase mediates retrograde endocannabinoid suppression of inhibition in mouse prefrontal cortex. *J Physiol* **589**: 4857–4884.

Zec RF, Zellers D, Belman J, Miller J, Matthews J, Femeau-Belman D, *et al* (2001). Long-term consequences of severe closed head injury on episodic memory. *J Clin Exp Neuropsychol* **23**: 671–91.

Zhang J, Teng Z, Song Y, Hu M, Chen C (2014). Inhibition of monoacylglycerol lipase prevents chronic traumatic encephalopathy-like neuropathology in a mouse model of repetitive mild closed head injury. *J Cereb Blood Flow Metab* **35**: 443–453.

Zhang J, Yang Y, Li H, Cao J, Xu L (2005). Amplitude/frequency of spontaneous mEPSC correlates to the degree of long-term depression in the CA1 region of the hippocampal slice. *Brain Res* **1050**: 110–117.

Zhang L, Wang M, Bisogno T, Marzo V Di, Alger BE (2011). Endocannabinoids generated by Ca2+ or by metabotropic glutamate receptors appear to arise from different pools of diacylglycerol lipase. *PLoS One* **6**: e16305.

Zhang Z, Wang W, Zhong P, Liu SJ, Long JZ, Zhao L, *et al* (2015). Blockade of 2-arachidonoylglycerol hydrolysis produces antidepressant-like effects and enhances adult hippocampal neurogenesis and synaptic plasticity. *Hippocampus2* **25**: 16–26.

Zhao Z, Loane DJ, Murray MG, Stoica B a., Faden AI (2012). Comparing the Predictive Value of Multiple Cognitive, Affective, and Motor Tasks after Rodent Traumatic Brain Injury. *J Neurotrauma* **29**: 2475–2489.

Zhao ZC, Li F, Maiese K (2005). Oxidative stress in the brain: Novel cellular targets that govern survival during neurodegenerative disease. *Prog Neurobiol* **75**: 207–246.

Zola-Morgan S, Squire LR, Amaral DG (1986). Human amnesia and the medial temporal region: enduring memory impairment following a bilateral lesion limited to field CA1 of the hippocampus. *J Neurosci* **6**: 2950–2967.

Zucker RS, Regehr WG (2002). Short-term synaptic plasticity. *Annu Rev Physiol* **64**: 355–405.

Zygmunt PM, Petersson J, Andersson D a, Chuang H, Sørgård M, Marzo V Di, *et al*

(1999). Vanilloid receptors on sensory nerves mediate the vasodilator action of anandamide. *Nature* **400**: 452–457.

Vita

Lesley Denise Schurman (née O'Brien) was born in Crewe, England, on June 9th, 1977. After leaving The Grange Grammar school in 1994, she returned to higher education in 2008 to read Psychology at the University of Guelph, Ontario, Canada, where she earned her Bachelor of Science with Honors in 2012. In 2013 she earned her Master of Science in Neuroscience, also from the University of Guelph, Ontario, Canada.